2015

Developing a Grid-Based Surrogate Reservoir Model Using Artificial Intelligence

Shohreh Amini

Developing A Grid-Based Surrogate Reservoir Model Using Artificial Intelligence

Shohreh Amini

Dissertation submitted
to the College of Engineering and Mineral Resources
at West Virginia University
in partial fulfillment of the requirements for the degree of

Doctor of Philosophy in
Petroleum and Natural Gas Engineering

Approved By
Shahab D. Mohaghegh, Ph.D., Chair
Samuel Ameri, M.S., P.E.
Khashayar Aminian, Ph.D.
Nigel Clark, Ph.D.
Behrooz Fattahi, Ph.D.

Department of Petroleum and Natural Gas Engineering

Morgantown, West Virginia
2014

Keywords: Surrogate Reservoir Modeling, Proxy Modeling in Reservoir Engineering, Artificial Intelligence, Neural Network, CO_2 sequestration

ABSTRACT

Developing A Grid-Based Surrogate Reservoir Model Using Artificial Intelligence

Shohreh Amini

Reservoir simulation models are the major tools for studying fluid flow behavior in hydrocarbon reservoirs. They are now being used extensively in performing any kind of studies related to fluid production/injection in hydrocarbon bearing formations. Reservoir simulation models are constructed based on geological models, which are developed by integrating data from geology, geophysics, and petro-physics. This data comes from observation, measurements, and interpretations.

Integration of maximum data from geology, geophysics, and petro-physics, contributes to building geologically complex and more realistic models. As the complexity of a reservoir simulation model increases, so does the computation time. Therefore, to perform any comprehensive study which involves thousands of simulation runs (such as uncertainty analysis), a massive amount of time is needed to complete all the required simulation runs. On many occasions, the sheer number of required simulation runs, makes the accomplishment of a project's objectives impractical.

In order to address this problem, several efforts have been made to develop proxy models which can be used as a substitute for complex reservoir simulation models. These proxy models aim to reproduce the outputs of the reservoir models in a very short amount of time. In this study, a Grid-Based Surrogate Reservoir Model (SRM) is developed to be used as a proxy model for a complex reservoir simulation model. SRM is a customized model based on Artificial Intelligent (AI) and Data Mining (DM) techniques and consists of several neural networks, which are trained, calibrated, and validated before being used online.

In this research, a numerical reservoir simulation model is developed and history matched for a CO_2 sequestration project, which was performed in Otway basin, Australia where CO_2 is injected into a depleted gas reservoir through one injection well. In order to develop SRM, a handful of appropriate simulation scenarios for different operational constraints and/or geological realizations are designed and run. A comprehensive spatio-temporal data set is generated by integrating data from the conducted simulation runs and it is used to train, calibrate, and verify several neural networks which are further combined to make the surrogate model.

This model is able to generate pressure, saturation, and CO_2 mole fraction at each grid block of the reservoir with a significantly less computational effort compared to the numerical reservoir simulation model.

*This dissertation is dedicated to my **loving husband** and my **wonderful parents** for their endless love, enormous support and constant encouragement.*

ACKNOWLEDGEMENT

During the past five years I have gone through many ups and downs to accomplish this work. My success would not have been possible without the help and support of many individuals who contributed to this journey.

First and foremost, I would like to express my sincere thanks and appreciation to my advisor, **Dr. Shahab Mohaghegh**, for all his support and guidance throughout my PhD studies. I am truly grateful for all opportunities that I was given as a research assistant and a teaching assistant, which not only helped me to extend my technical knowledge and insight but also to develop my personal and interpersonal skills in different ways.

I would like to express my appreciation and gratitude to my examination committee, **Professor Sam Ameri**, **Dr. Kashy Aminian**, **Dr. Nigel Clark** and **Dr. Behrooz Fattahi** for their time and valuable comments and suggestions on my research and dissertation. I would also like to acknowledge Dr. Grant Bromhal for his comments and remarks during the course of this work.

I would like to thank Intelligent Solutions, Inc. and Computer Modeling Group (CMG) for providing the software packages that were used throughout this research.

I would like to greatly thank my loving husband, Razi Gaskari, for his patience, unconditional love and endless support throughout this journey. Thanks for believing in me and my abilities. Thanks for being there for me through every single complication that I experienced during the last few years. Each statement of encouragement that I received from you was a step forward for me to accomplish this work.

I am deeply grateful to all my family members whose love and support, sent from thousands of miles away, was always a driving force for me to accomplish this work. I would like to give my special thanks and appreciation to my wonderful mom and dad, Farideh Gorji and Abbas Amini, whose unlimited love and support throughout my life provided me with whatever I needed to get to the point that I am today. I am so grateful to my older brother, Shahram Amini, for being a role model for me in pursuing an advanced degree. Your significant academic achievements were always an inspiration for me. Thanks for all your guidance and support in my life. My heartfelt thanks go to my twin sister Shahla Amini, who has been a part of my soul, my entire life. Thanks for always being my best classmate, my best friend, and my best companion. Your love and emotional support gave me the power to overcome the most difficult problems I encountered during the last five years.

I would like to express my especial thanks to my best friends in different corners of this world especially, Azadeh Keshtgar whose love and care helped me to keep a positive spirit during my PhD studies while I was far away from my family.

I am also grateful to all PEARL (Petroleum Engineering & Analytics Research Lab) group members here at WVU for all their friendship and support during the last few years. I especially would like to thank my latest officemates, Vida Gholami and Faegheh Javadi, who made the office a warm, friendly and quiet environment for me to finalize my research and write my dissertation. I am also very grateful to Vida Gholami for her pleasant collaboration in studying and contemplating several technical materials related to this research.

Last but not least, I would like to thank all my great friends in Morgantown, including Vida Gholami, Mohammad Maysami, Mehrdad Zamirian, Neda Nasiriani, Alireza Haghighat, Alireza Shahkarami and Shirin Akbari, whose friendship and support made all these tough years a pleasant and memorable interval of my life.

Table of Contents

List of Figures

List of Tables

CHAPTER 1.
INTRODUCTION

1.1 Motivation and Problem Statement

In a geological carbon sequestration once the CO_2 is injected underground there is no direct method which is able to exactly determine the CO_2 flow path in the porous media. Numerical reservoir simulation models are the major tools through which the CO_2 fate can be studied after being injected underground. These models are constructed based on the geological studies and interpretations, field observation, and measurements, and therefore are essentially uncertain. In each specific sequestration project, different operational practices will have different sequestration outcomes. Consequently, any practical uncertainty analysis and risk assessment technique should address both geological and operational uncertainties.

Developing a reservoir simulation model and conducting that for thousands of different scenarios ultimately provides us with a solution space which can be practically used for an extensive uncertainty analysis. The most widely used techniques for this purpose is Monte Carlo simulation. However, this method will be essentially impractical for a geologically complex reservoir simulation model, which requires even few hours for a single run to be accomplished.

On one hand, adding complexity to the reservoir simulation model is inevitable since integrating all the observations and measurements is the sensible way to reduce the uncertainty. On the other hand, the more complex the simulation model, the higher the run time. Therefore, any study which involves thousands of simulation runs such as uncertainty analysis, optimization study, or history matching can become prohibitive due to the massive required run time and computational effort.

Encountering such a problem motivates the quest to find an alternative approach through which we can utilize the complex numerical reservoir model to develop a surrogate model, which can significantly lower the computational cost while it approximates the results of the complex model with an acceptable accuracy.

In order to address this problem, several efforts have been made to develop proxy models which can be used as a substitute for a complex reservoir simulation model. What is sought in the area of proxy or surrogate modeling is generating a meaningful representation of the existing complex system which can be performed in a computationally efficient way.

The existing proxy models, which have been applied in petroleum engineering, can be generally categorized into four different groups based on their development approach. These four groups are: statistics-based approach, reduced physics approach, reduced order modeling approach, and data driven or artificial intelligence-based technique. Although all the developed proxy models are trying to address the problem of expensive numerical reservoir simulation models, these proxy models still have many drawbacks and limitations to be used as a practical tool.

The statistical methods, such as response surfaces, are trying to generate a function which can capture the input-output relationship of the involved parameters. In order to be practical, hundreds of simulation runs must be conducted in order to generate sufficient data to cover all the input space and that is due to the statistical nature of the approach.

In proxy models based on reduced physics, the physics of the process is simplified by applying several assumptions. The formulations which are used in petroleum engineering, and particularly the ones related to the fluid flow in porous media, are developed based on some simplifying assumptions and the results we obtain by applying these formulations is already an estimation of what is actually happening and can be even very far from the reality. Therefore, simplifying the existing formulation and generating proxies based on these simplified formulations make a large amount of limitations in their application.

The reduced order modeling approach is used to reduce the computational effort of solving the system of non-linear equations pertaining to the fluid flow in porous media and some of the techniques in this category are able to decrease the run time for a numerical reservoir model by several orders of magnitude. However, the development procedure of this type of reduced order model is computationally expensive and therefore construction of such a surrogate model can only be justified if thousands of simulation cases are to be conducted for a comprehensive study.

Finally, proxy models can be constructed using Artificial intelligence. Artificial intelligence and in particular artificial neural networks (ANN) have proven to be powerful data processing tools and can be applied to a wide variety of problems in different areas such as medical, engineering, financial, business, etc. Artificial neural network is a virtual intelligence technique which is an efficient tool for detecting and approximating the highly non-linear relationship between inputs and outputs of a system. During the last three decades this technique has been employed in petroleum engineering in different areas as an efficient tool to predict reservoir characteristics such as porosity and permeability, synthetic log generation, well production performance, etc. However, this technique has not been used to develop a surrogate model which is able to predict the dynamic variables of the reservoir at the grid block level.

1.2 Research Objective

The principle objective of this research is to develop a surrogate reservoir model by using artificial neural networks, which do not have the draw backs and shortcomings of the existing surrogate or proxy modeling techniques.

In this research the goal is to develop a grid-based surrogate reservoir model as a proxy for a numerical reservoir simulation model. The numerical reservoir model is developed for the purpose of investigating the outcomes of different injection scenarios and/or geological realizations, for a CO_2 sequestration project, in terms of pressure, gas saturation, and CO_2 mole fraction distribution throughout the reservoir.

The surrogate reservoir model must be capable of generating pressure, gas saturation, and CO_2 mole fraction at each grid block of the reservoir at the desired time step when the uncertain input parameters are changed within a specific range (range of data by which the SRM is trained).

This surrogate model is constructed based on the data extracted from a handful of numerical reservoir simulation scenarios and it is able to generate the results of the numerical reservoir model at the gird block within a few seconds.

1.3 Dissertation Outline

This dissertation includes nine chapters, which are organized as follows:

Chapter 1 presents the background, motivations, and objective of this research.

Chapter 2 includes a brief overview of CO_2 sequestration, which is the process based on which the surrogate model is developed in this work. Further in this chapter a thorough study and evaluation of the previous works that have been done in the area of proxy/surrogate modeling is presented and the advantages of the approach used in this research against other methods are discussed.

Chapter 3 introduces the artificial intelligence background as the methodology that is deployed in this research for grid-based surrogate reservoir model development. This chapter specifically includes a detailed description of the artificial neural network structure, formulation, and training process as applied in this study.

Chapter 4 presents the workflow that was followed to develop and history match a numerical reservoir simulation model for a CO_2 sequestration process.

Chapter 5 includes detailed description of different steps to develop a surrogate reservoir model for the first layer of the reservoir. This part of the SRM development is considered as proof of concept for the proposed methodology.

Chapter 6 covers some studies related to data sampling as a data reduction technique for reducing the dimensionality of the under study system.

Chapter 7 presents a full-field SRM development that is applied for two different grid resolutions of the numerical reservoir simulation model. This section includes the results of SRM and a comparison between the SRM output and numerical reservoir model output, as well as a general error evaluation.

Chapter 8 comprises two sections of lessons learned and conclusion of this study which highlights the key findings and the learned lessons through performing the current research followed by a list of concluding remarks of this study.

Chapter 9 presents the possible further studies that can be performed in the future in order to improve the current research or extend its application.

CHAPTER 2.
LITERATURE REVIEW

2.1 Overview of Geological Carbon Sequestration

A viable means of CO_2 reduction in the atmosphere is to capture and concentrate CO_2 from large point sources, such as power plants and petroleum refineries, and store it by underground injection. This process is called Geological Carbon Sequestration (GCS).

There are several options to store CO_2 in an underground geological structure which are: depleted oil and gas reservoirs, saline aquifers, and unmineable coal-beds. Each of these geological structures has its own characteristics which must be extensively studied before any CO_2 is injected underground and stored for a long time (Bachu 2000).

The injected CO_2 can be stored through different trapping mechanisms (Kaldi and Gibson-Poole 2008), such as:

- Physical trapping that happens in structural or stratigraphic traps, where the free-phase CO_2 is physically trapped by the geometric structure of the reservoir and its caprock. This type of trapping is similar to hydrocarbon accumulations in the reservoir.
- Residual trapping, where the CO_2 is trapped in the pore spaces due to the capillary pressure forces.
- Solubility trapping, which takes place when the injected CO_2 dissolves into the formation water.
- Mineral trapping through which CO_2 precipitates as new carbonate minerals and therefore becomes immobile.
- Adsorption trapping, which happens when CO_2 is injected in to the coal-beds, where the CO_2 adsorbs onto the surface of the coal.

Although carbon sequestration seems to be a sensible way of reducing the ever increasing level of CO_2 in the atmosphere, the risk involved in this process is always a matter of concern. A safe sequestration is achieved when it is ensured that once the CO_2 is injected underground it will remain safely in the structure over a long geological time (thousands of years). In general the risk involved in CO_2 sequestration in geological formations decreases as time passes. The risk associated with any geological sequestration is directly related to the geological uncertainties of the structure and operational practices, and therefore these items are required to be comprehensively studied for any CO_2 sequestration plan.

Reservoir simulation models are the major tools used to perform principal studies related to uncertainty analysis of CO_2 sequestration. They provide us with a means to predict the performance of this process under different geological realizations and different injection scenarios. The outcome of any realization can be studied from different aspects such as:

- Distribution of CO_2 though the pore spaces of the formation and CO_2 front prediction
- Displacement of water, oil, or gas caused by CO_2 injection
- Pressure build-up due to injection

In order to comprehensively study and quantify the risk associated with a sequestration project, thousands of simulation runs are required to take into account the variability of the uncertain parameters in the project, which can be practically used for an extensive uncertainty analysis.

2.2 Surrogate/Proxy Models: Applications and Previous works

Due to the advancement of technology and software improvements, the developed models for simulating different processes in different science and engineering areas are becoming more and more complex and computationally expensive to perform. On some occasions these complex models are required to be performed hundreds or thousands of times, which requires a massive amount of time and computational effort to be completed. Sometimes these runs are just required to answer some questions about the behavior of the system or some general evaluation of the system response to the change of involved variables. Therefore, engineers are looking for a way which enables them to make use of the complex models and generate a surrogate or proxy model, which can provide them with the information they are looking for with less computational effort.

The basic idea of surrogate modeling is to avoid investing on computational time and effort to answer the questions in hand, and instead, investing in the development of models which can approximate the long running simulation models in a significantly shorter time. These approximations can answer many questions and can provide many insights of the under study process more efficiently (Forrester, Sobester and Keane 2008).

What we are looking for in the area of proxy or surrogate modeling is generating a meaningful representation of the existing complex system, which can be performed in a computationally efficient fashion. The surrogate acts as a function which relates the inputs of the system to its outputs, and therefore it is able to approximate the system response without using the primary expensive simulation source. Generally, the approach is based on the assumption that once the surrogate model is developed it can be run significantly faster than the primary complex model while it offers an acceptable accuracy of the predicted results.

During the last decade, in the petroleum industry, many proxy models or surrogate models have been developed with the purpose of replicating the functionality of numerical simulation models with different objectives such as optimization, history matching, uncertainty analysis, risk assessment, etc.

The proxy models that have been developed in petroleum engineering area can generally be categorized into four different groups based on their development approach. These four categories are:

1. Statistical method
2. Simplified analytical (reduced physics) approach
3. Reduced order modeling approach
4. Data driven or artificial intelligence-based technique

The following sections provide an extensive description of the background, previous works, and application of the aforementioned proxy modeling techniques. Furthermore, proxy modeling capabilities and limitations of their application to develop a surrogate model for a numerical reservoir model are evaluated.

2.2.1 Statistics-Based or Response Surface Method (RSM)

Response Surface Methodology is a combination of mathematical and statistical techniques. This methodology is used for modeling and analysis of problems in which the output is influenced by several input variables (Montgomery 2005).

In the area of petroleum engineering, this technique has been applied in several types of studies such as history matching (Slotte and Smorgrav 2008), upscaling geological models (Narayanan, et al. 1999), field development planning (Carreras, Turner and Wilkinson 2006), optimization (Purwar, Jablonowski and Nguyen 2010), and many other studies. However, the most common area where this methodology has been applied is in uncertainty analysis of a particular process such as oil production (Ahmed, et al. 2013) (Al Salhi, et al. 2005) and CO_2 sequestration (Yeten, Castellini, et al., A Comparison Study on Experimental Design and Response Surface Methodologies 2005).

Uncertainty analysis requires identification of the involved uncertain parameters that affect the desired output of a system and evaluation of their degree of influence. Ideally, all possible combinations of these parameters should be tested in order to capture and evaluate the relationship between the behavior of the system and uncertain parameters. However, due to limited computational power, evaluation of all combinations of the uncertain parameter is

practically impossible for a complex model which requires a huge amount of time for a single run to be accomplished.

A response surface is a mathematical function that is capable of representing the behavior of a system, either real or simulated, by approximating the relationship between the inputs and outputs of the system. In the field of reservoir engineering, the system is a reservoir flow simulator, the inputs are the uncertain parameters such as reservoir characteristics or operational constraints, and the output can be production or injection variables such as oil/water rates or the wells' pressure (Fetel and Caumon 2007) or other parameters based on the objective of the study.

In order to develop a response surface, the first step is to generate a number of simulation runs which can provide a maximum amount of information from the system. This process is called design of experiment, which aims at finding the minimum number of simulation runs by selecting the best combination of uncertain parameters. The combination of experimental design and response surface is a statistical approach for uncertainty assessment which has some advantages as well as shortcomings. The earlier application of this methodology in petroleum engineering can be found in studies conducted by Chu (Chu 1990) and Damsleth (Damsleth, Hage and Volden 1992).

The linear multivariate regression and interpolation methods are amongst the most popular response surface methods (Yeten, Castellini, et al., A comparison study on experimental design and response surface methodology 2005). Linear multivariate regression is a parametric approach which aims at fitting a given priori model to a set of data points.

Interpolation is a non-parametric mathematical procedure through which the system response is estimated at a given location based on the nearby known value. The results of the research performed by Fetel et al. show that response surfaces developed based on linear regression methods are generally unable to capture the non-linearity of the actual reservoir flow behavior. Therefore, they suggest applying interpolation methods such as Discrete Smooth Interpolation (DSI) or Kriging method combined with an external drift (KED), which results in a lower amount of error when applied for developing a model to estimate production rate (Fetel and Caumon 2007).

Other regression methods such as Gaussian Process regression (GP) can also be applied to develop a response surface. This method was used by Zhang et al. to develop a proxy model for risk assessment of a geological CO_2 sequestration in a brine reservoir (Zhang and Pau 2012). This proxy model was developed for a numerical reservoir simulation model, which consists of 470,573 non-uniform grid blocks in 77 layers. The model was developed to approximate the

desired output of the system (pressure at a specific time and specific location of the reservoir) for different values of the uncertain input parameters and consequently the constructed model was used for uncertainty quantification. However, due to the substantial limitations of the applied methodology for this proxy development, in practice the model is just able to make a prediction in a certain time and at a certain location of the reservoir. Therefore, the developed proxy model is not applicable for a comprehensive uncertainty analysis purpose.

The research that has been conducted by Zhang et al. is another attempt of using response surface methodology or, in particular Polynomial Chaos Expansion (PCE) method to develop a proxy model for a numerical reservoir simulation model with the objective of approximating pressure and saturation of each grid block of the reservoir (Zhang and Sahinidis 2012).
This work is the only one, among several response surface approaches, that have been applied in reservoir engineering with the objective of approximating pressure and saturation of the grid blocks of the reservoir under uncertain input parameters.

Due to the similarity of the objective of the work performed by Zhang et al. with the objective of the current research, the PCE method and its specific application in this area is described in more detail in the following section.

Polynomial Chaos Expansion (PCE)

PCE has been applied as a method for analyzing uncertain behavior of complex systems in different areas such as oceanology (Webster and Tatang 1996), aerospace (Eldred and Burkardt 2009), risk assessment of CO_2 storage (Oladyshkin, et al. 2011), and history matching (Bazargan and Christie 2012).
Zhang et al. developed a surrogate model using the PCE method to approximate the outputs of a numerical reservoir simulation model of a CO_2 sequestration process as polynomial functions of the uncertain parameters (porosity and permeability). In this work, the developed surrogate model has been used for geological uncertainty analysis and consequently optimizing the amount of CO_2 injection into a saline aquifer (Zhang and Sahinidis 2012).

In order to develop a PCE-based model, it is assumed that the model output (y) is a function of uncertain parameters (x) and can be represented by a polynomial chaos expansion as formulated below.

$$y = M(x) = \propto_0 B_0 + \sum_{j=1}^{M} \propto_j B_1(x_j) + \sum_{j=1}^{M}\sum_{k=1}^{j} \propto_{jk} B_2(x_j, x_k) + \sum_{j=1}^{M}\sum_{k=1}^{j}\sum_{h=1}^{k} \propto_{jkh} B_3(x_j, x_k, x_h) + \cdots$$

Equation 1

Where the α's are coefficients and the B's are multivariate polynomial basis functions that are orthogonal to the joint Probability Distribution Function (PDF) of x.

The PCE, in practice, is truncated to a finite number of terms which can be calculated as follows:

$$N_t = \frac{(M+d)!}{M!\,d!}$$

Equation 2

Where, M is the number of model inputs and d is the degree of expansion which is the highest degree of the polynomial basis function.

Each x is a single random variable and the orthogonal polynomials for this variable are defined as:

$$\int_{\Omega} \varphi_d\, \varphi_c f(x) dx = 0, d \neq c$$

Equation 3

Where, $\{\varphi_d = x^d + lower\ degree\ terms, d = 0,1,2,\dots\}$ are polynomial functions of x and orthogonal to polynomial φ_c and $f(x)$ is the PDF of x. Ω is the support of the random variable x. If x can be characterized with one of the most commonly known PDFs, such as a normal or uniform distribution, then the corresponding orthogonal polynomials can be chosen through some known methods. If x has an arbitrary PDF, the orthogonal polynomials should be generated numerically. These orthogonal polynomials are optimal with respect to the PDF of x, since the error computed as a difference between the exact value of a model output y and the value approximated by Equation 1 with $\{B_i = \varphi_i, i = 0, \dots, d\}$ converges to zero exponentially as d increases linearly.

For the case where input vector x contains M random variables, Equation 3 can be applied to define the multidimensional orthogonal polynomials. If x_i's are independent of each other, then the joint PDF of x is a product of the marginal distributions of each x_i. Therefore, B_d which is the

multidimensional orthogonal polynomial of degree d can be calculated by multiplying the corresponding individual orthogonal polynomial for each x_i, as shown in Equation 4.

$$B_d(x) = \prod_{i=1}^{M} \varphi_{m_i}(x_i)$$

Equation 4

In this equation:

$\sum_{i=1}^{M} m_i = d$ and $\varphi_0(x_i) = 1, i = 1, \dots, M$

The next step is to estimate the coefficient vector α in Equation 1. N_p points are selected for x and the coefficients are calculated by solving the following linear equation:

$$B\alpha = y$$

Equation 5

In order to calculate α′s, the error between the real and estimated output is minimized by minimizing the training error of $\|B \propto -y\|^2$.

Therefore, to build a PCE, an initial value is assumed for the degree of expansion ($d = 0$) then the coefficients are calculated through a minimization procedure where the error is monitored and if it is within an acceptable range then d is considered as the best degree of expansion. If not, the value of d is increased and the same procedure is followed so that it meets the condition (in this work the calculated degree of expansion has been reported as 3 or 4).

In this research, a PCE-based surrogate model was developed for a numerical reservoir simulation model of a CO_2 sequestration process to approximate the pressure and saturation of the model during CO_2 injection as a function of two uncertain parameters of porosity and permeability.
The numerical reservoir simulation model is a 2D vertical model which consists of 1972 non-uniform grid blocks; however, the PCE was developed for half of this model which contains 986 grid blocks. By using Latin Hyper Cube Sampling (LHS) method, and based on the uncertain parameters, 100 simulation runs were performed and PCE was developed for each grid block of the reservoir.

The limitations of the developed proxy model can be listed as follows:

- The computation time for generating a single PCE is relatively small; however, the fact that this method is an iterative method that requires PCE generation for each single grid block of the reservoir at each single time step, implies that the proxy model development

time will increase dramatically if this method is to be developed for a numerical reservoir model with a huge number of grid blocks and for a large number of time steps.

- The same argument can be applied to the deployment of the method to estimate the output parameters for a new scenario. The method calculates the output for each single grid block at each time step by evaluating the obtained polynomial with the uncertain parameter value at each specific grid block and specific time step.
- In this study, the results of pressure and gas saturation distribution have been presented for a very short time interval (30 days of CO_2 injection), which is not a realistic injection duration for a CO_2 injection process.
- Although different distribution functions was considered for porosity and permeability of the reservoir, the study has actually been conducted on a homogenous reservoir, which is another shortcoming of this method.

The aforementioned limitations of the application of the PCE methodology endorse that this technique is not practical to be used for grid-based surrogate modeling of a complex reservoir model.

2.2.2 Reduced Physics Models

Developing a simulation model of a system in order to investigate its behavior under different conditions is a common practice in the field of engineering. These models are developed based on the formulations through which a physical phenomenon is described. The complexity of these models can be dramatically increased in an attempt to develop a more realistic model by including several parameters in the model for the purpose of obtaining more reliable results.

Reduced physics proxy models are the models which are developed through simplifying a physics-based formulation of a process or by disregarding some parameters which are responsible for representing a particular phenomenon that is taking place in the process.

In reservoir engineering, the reduced physics proxy modeling technique has most commonly been used in modeling thermal recovery processes such as SAGD (Steam Assisted Gravity Drainage) and Vapex (Vapor extraction), and also Shale gas production.

Using this approach, several proxies have been developed based on analytical formulations for modeling SAGD processes. Azad et al. used an analytical physics-based proxy model and the Extended Kalman Filter method for the purpose of reservoir characterization (Azad, Chalaturnyk and Movaghati 2011).

Vanegas et al. (Vanegas, Deutsch and Cunha 2008) developed a proxy model based on Butler's formulation (Butler, A New Approach to the Modeling of Steam-Assisted Gravity Drainage 1987) for predicting oil flow rate, cumulative oil production, and cumulative steam injection under some uncertain parameters of porosity, horizontal permeability, vertical permeability, oil saturation, and rock type (shale or sand). This model was developed for a 2D heterogeneous reservoir with 5796 grid blocks ($161 \times 36 \times 1$) for a single SAGD well pairs. They performed 100 simulation runs in order to generate the required data to develop the proxy model. Making some simplifying assumptions to the general formulation a proxy model was developed, which includes four tuning factors to adjust the proxy behavior for different parameters with respect to the full model. The tuning process is implemented through an error minimization procedure.

Jindong Shi and Juliana Leung built a physics-based proxy model for a Vapex process in a heterogeneous reservoir which allows the prediction of total drainage rate, drainage rate change with time, and the change of solvent chamber boundary position during the spreading chamber period (Shi and Leung 2013). In this study, they proposed a formulation based on Butler's analytical solution developed for the conditions applicable for typical Hele-Shaw cell experiments (Butler and Mokrys, Solvent Analog Model of Steam Assisted Gravity Drainage 1989), and therefore certain modifications were made in order to model the Vapex process in porous media.

A sequence of explicit calculation of the analytical equations was performed to predict the solvent-oil interface position and producing oil rate as a function of time. They applied the analytical proxy model to three case studies and compared the obtained results with the constructed numerical simulation model for all cases. All the numerical reservoir models are 2D models; the first one consists of 108 grid blocks ($12 \times 9 \times 1$) and the second and third cases comprise 3600 grid blocks ($120 \times 30 \times 1$).

The results of applying the proposed proxy model in different case studies demonstrates that as the complexity of the system increases the efficiency of the proxy model in terms of run time decreases. According to their study, the proxy model developed for the first case, which is a small case, aims at simulating the experiments of Butler and Mokrys (Butler and Mokrys, Solvent Analog Model of Steam Assisted Gravity Drainage 1989). In this case, the total run time was decreased from 67 hours of numerical simulation to 2 seconds through the proxy model application. In the second case, which is a compositional flow simulation of the Vapex process in a homogeneous reservoir, the computational time was reported as 9 hours, which was decreased to 3 seconds by using the developed proxy model. The last case is the same as case 2 where the reservoir model is a heterogeneous model, and therefore it is the most complex case in this study. The total simulation

run time for the numerical model was about 5 hours, which could be reduced to 3 seconds (Shi and Leung 2013).

The study of shale production is another area in which reduced physics approach has been used to develop proxy model as a substitute for a numerical reservoir simulation model.

In the research performed by Wilson et al. (Wilson and Durlofsky 2012) the objective is to develop a much simpler and faster reduced-physics surrogate model that can be used for optimization of shale gas production (K. C. Wilson 2012). In this study, a full-physics 2D numerical simulation model was developed, which comprises 50,000 to 250,000 grid blocks in different cases. The fluid flow is considered as non-Darcy flow and was modeled through Fourchhemeire modification to Darcy's law. This model is considered as the reference model, that includes highly-resolved fracture networks, dual-porosity, dual-permeability regions, and gas desorption. The objective is to determine well spacing, well length, and the number of fractures for each horizontal well in order to optimize gas production from a shale reservoir.

The developed reduced-physics surrogate is a simplified model that not only considers fewer physical effects, but also contains fewer grid blocks than the full-physics model. In order to determine the required level of physics, and also the degree of reduction in grid resolution, some numerical experiments were performed. According to this study, a single-porosity model, without desorption or grid refinement, could provide results close to the full-physics model outputs. Another simplification assumption is that each fracture in the reduced-physics model was represented through an additional perforation along the wellbore in the stimulated region instead of explicitly being modeled. The reduced-physics model contains only 5618 grid blocks, which is a factor of 10 (or more) fewer than a typical full-physics model.

The simplified model must then be tuned with the results of the reference model. The tuning parameters are the porosity and permeability of the surrogate model. An optimization procedure was applied to minimize the error of the gas production resulted from the full-physics models and the proxy model when the models are conducted for a variety of scenarios. These scenarios are designed based on changes in parameters such as well lengths, well spacing, and fracture spacing which are the key parameters for gas production optimization, for the under study shale reservoir.

The surrogate model was implemented in two different cases. The results for the first case, with long well length and high density fracture, and the second case, with short well length and low density fracture, demonstrate that the surrogate model was able to generate the results within 4 seconds for both cases while the two full-physics models were run in 2100 and 560 seconds respectively.

According to the research that has been performed on the development of proxy models through reduced physics approach, the following can be concluded:

- From the studies related to proxy modeling for thermal recovery processes using simplified physics, it can be inferred that although in some cases the results demonstrate the capability and efficiency of these proxy models in predicting the required output parameters, the application of these proxy models is significantly limited.
- These proxy models have never been applied to a complex 3D reservoir with a large number of grid blocks in order to evaluate their range of capabilities when the size of the reservoir grows dramatically. In this case the tuning process of the simplified model can be significantly difficult due to the high dimensionality.
- The argument for the case where the proxy was developed for shale is that since a single value for porosity and permeability was used it cannot be considered as a realistic assumption and therefore it seems impractical due to the over simplification.

Based on the applications of this approach for proxy model development (as it appears in the literature), it can be generally concluded that reduced physics models are efficient when they are applied for very complex processes such as thermal recovery or production from shale reservoirs. That is due to the fact that there are many unknown complexities pertaining to such processes that can be represented as a simplified format; however, for a non-complex process which is happening in a complex reservoir (can be complex structure/geology) the mathematical formulation of the physical phenomenon is already simplified through several assumptions. Therefore, further simplification either results in a very unrealistic representation of the system or it will not be efficient in terms of reducing the computational effort.

Consequently, this methodology cannot be considered as a universal approach which can be effectively applied to variety of problems associated with fluid flow in porous media.

2.2.3 Reduced Order Models

Reduced order modeling is an approach through which the high-dimensional models are transformed into lower dimensional models that can be performed more efficiently with less computational costs. The low order model should be a meaningful representation of the high dimensional model.

Reduced order modeling has been applied in different areas for several purposes of simulation, classification, visualization, and compression of high-dimensional data. The application of this

methodology in subsurface fluid flow modeling is relatively new, and is mostly based on Krylov subspace, balanced truncation, and proper orthogonal decomposition (POD) techniques. All of these approaches are using projection methods to transform the high-dimensional state space of the original model into a low-dimensional subspace (M. a. Cardoso 2009). Proper orthogonal decomposition is probably the most commonly used method for the reduced order modeling of nonlinear systems.

The reduced order models are beneficial in several types of problems such as optimization and uncertainty analysis where a large number of high order models are required to be performed. In reservoir engineering, POD has been vastly used as an approach to develop fast running proxy models for variety of numerical reservoir simulation models. However, many researchers have modified POD methodology in an attempt to enhance the results or the efficiency of POD through integrating some other techniques. For example Cardoso et al. (Cardoso and Durlofsky 2010) have used clustering technique to optimize the snapshots for the eigen-decomposition problem and missing point estimation (MPE) procedure to reduce the dimension of the POD basis vectors. Other techniques include the application of POD-TPWL (Trajectory Piecewise Linearization) and POD-DEIM (Discrete Empirical Interpolation Method) which are elaborated further in this chapter.

Since POD is the most commonly used approach in reduced order model (ROM) development in reservoir engineering, this methodology is described in more details in the next section, followed by presenting other studies through which some modifications have been performed on this methodology.

Proper Orthogonal Decomposition (POD)

Proper Orthogonal Decomposition (POD), also known as principal component analysis, Karhunen-Loeve decomposition or the method of empirical orthogonal function is a model reduction technique through which a low-order model is generated using snap shots from a high-order simulation model.

POD was first introduced by Lumley (Lumley 1967) where it was employed to identify coherent structures in dynamic systems then it was applied in fluid mechanics (Holmes, Lumley and Berkooz 1996), (Sirovich 1987) and has been frequently used in reduced-order model development for several physical processes (Ly and Tran 2001); however, its application in the area of reservoir modeling has been introduced in the past two decades (Hejin, Markovinovic and Jansen 2003), (Heijn, Markovinovic and Jansen, Generation of Low-Order Reservoir Models Using System-Theoretical Concepts 2006), (Van Doren, Markovinovic and Jansen 2006).

There are several works in which POD-based reduced order models have been developed for subsurface flow modeling. Vermeulen has applied this technique to simulate the long-term effect of change in precipitation/evaporation and also the effects of different well production rates for a heterogeneous aquifer (Vermeulen, Heemink and Te Stroet, Reduced models for linear ground water flow models using empirical orthogonal function n.d.). This model includes 33,000 active nodes. The reduced order model can achieve a 625 run time speed up, which is due to the linearity of the system.

However, several other researchers have used the same technique for non-linear two-phase subsurface flow. Van Doren et al. (Van Doren, Markovinovic and Jansen 2006) developed an adjoint-based optimal control methodology for water-flooding of a heterogeneous two-dimensional model which contains 2,025 grid blocks and two horizontal wells, one producer, and one injector. Proper orthogonal decomposition was used to compute reduced order models, which resulted in reducing the number of unknowns from 4,050 in the high-order model to 20-100. Finally, they applied this method to optimize the net present value (NPV). The run time speedups they achieved were only about a factor of 1.5.

In other work, Markovinovic and Jansen (Markovinovic and Jansen, Accelerating iterative solution methods using reduced-order models as solution predictors 2006) proposed the use of POD to accelerate the iterative linear solver used for the high-order model, which consists of 93,500 grid blocks. Generating a reduced order model, based on POD, they achieved up to a factor of 3 in speedup.

The outcomes of all these works in the development of reduced order models by using POD, illustrate the challenges pertaining to using this method for problems with significant nonlinearity. It should be noted that even though the ROMs can be used for nonlinear problems, their performance generally reduces considerably compared to the linear cases (Astrid 2004) (Rewienski and White 2003).

The following section is a summary on applications of POD in reduced order model development for numerical simulation reservoir models. Introducing the application of this methodology as an approach to reduce the order of the high dimensional subsurface flow necessitates the description of the formulations of fluid flow in porous media as used to develop full order reservoir models. Therefore, the first part in the following section presents the related formulations.

Full order Reservoir Model

To develop a reduced order model for a reservoir simulation model, first the full order model must be run in order to generate several snapshots, which are representative of the dynamic system.

Considering a two-dimensional reservoir with $\bar{m} \times \bar{n}$ grid blocks, the fluid flow in porous media can be formulated as a set of partial differential equations resulted from material balance for oil and water and Darcy's law (Aziz and Settari 1979). Assuming a two phase flow in an iso-thermal condition, and disregarding the gravity forces, the governing fluid flow equation for oil and water phases can be written as:

$$-\nabla.\left\{\frac{\alpha\rho_w k_{rw}}{\mu_w} K\left(\nabla p_w - \frac{\partial p_c}{\partial S_w}\,\nabla S_w\right)\right\} + \alpha\frac{\partial(\rho_w \varphi S_w)}{\partial t} - \alpha\rho_w q_w = 0$$

Equation 6

$$-\nabla.\left\{\frac{\alpha\rho_o k_{ro}}{\mu_o} K\left(\nabla p_o - \frac{\partial p_c}{\partial S_o}\,\nabla S_o\right)\right\} + \alpha\frac{\partial(\rho_o \varphi S_o)}{\partial t} - \alpha\rho_o q_o = 0$$

Equation 7

Where, α is geometrical factor, ρ_w and ρ_o are water and oil densities, K is permeability and k_{rw} and k_{ro} are water and oil relative permeability, respectively.

Sw is water saturation, So is oil saturation, and $p_c = p_o - p_w$ (where p_c is capillary pressure, p_o is pressure in the oil phase, and p_w is pressure in the water phase).

Discretizing the above equations in space using a five-point block-centered grid will result in the following system of non-linear first order differential equations:

$$\begin{bmatrix} V_{wp}(s) & V_{ws} \\ V_{op}(s) & V_{os} \end{bmatrix}\begin{bmatrix}\dot{p}\\ \dot{s}\end{bmatrix} + \begin{bmatrix} T_w(s) & D \\ T_o(s) & 0 \end{bmatrix}\begin{bmatrix} p \\ s \end{bmatrix} = \begin{bmatrix} q_w \\ q_o \end{bmatrix}$$

Equation 8

Where $\boldsymbol{s}$ is the vector of water saturation, $\boldsymbol{V}$ and $\boldsymbol{T}$ are matrices containing accumulation and transmissibility term respectively, which are the function of $\boldsymbol{s}$, and $\boldsymbol{D}$ is a matrix with entries containing diffusion coefficient (Jansen and Markovinovic 2004).

Equation 8 can be rearranged in the form of state variable representation as a non-linear ordinary differential equation (Heijn, Markovinovic and Jansen, Generation of Low-Order Reservoir Models Using System-Theoretical Concepts 2006).

$$\dot{x}\,(t) = f\big(x(t), u(t)\big) = A_c x(t) + B_c u(t)\,,\; y(t) = C_c x(t)$$

Equation 9

Where, $\boldsymbol{x}$ is the state vector containing oil pressures (p_o) and water saturations (S_w) for each grid block. The order *n* of the state space system in Equation 9 is equal to the total number of state variables, which in this case will be $n = 2\bar{m}\bar{n}$.

A_c is the *system matrix*, and B_c is the *input matrix*, and their parameters are functions of x**.**
y is the *output vector*, which is represented by *output matrix* $\boldsymbol{C_c}$**,** times the state variable of the system. Here, x is the *n-dimensional* state vector.

First, Equation 9 is linearized around point x=x*:

$$\dot{x}\,(t) = [f]_{x^*} + \left[\frac{\partial f}{\partial x}\right]_{x^*}(x(t) - x_0) + \cdots \approx \left[\frac{\partial f}{\partial x}\right]_{x^*} x(t) + [B_c]_{x^*}\, u(t) + \left[A_c - \frac{\partial f}{\partial x}\right]_{x^*} x^*$$

Equation 10

$$y(t) = C_c x(t)$$

Equation 11

In the case that $\left[\frac{\partial f}{\partial x}\right]_{x^*}$ exists, $\bar{x} = x + \left[\frac{\partial f}{\partial x}\right]_{x^*}^{-1}\left[A_c - \frac{\partial f}{\partial x}\right]_{x^*} x^*$ and $\bar{y} = y + C_c\left[\frac{\partial f}{\partial x}\right]_{x^*}^{-1}\left[A_c - \frac{\partial f}{\partial x}\right]_{x^*} x^*$. In general state space notation in continuous time (Equation 9) can be rewritten as:

$$\dot{\bar{x}}\,(t) = \bar{A}_c \bar{x}(t) + \bar{B}_c \bar{u}(t)\,, \bar{y}(t) = \overline{C_c} x(t)$$

Equation 12

Where:

$$\bar{A}_c = \left[\frac{\partial f}{\partial x}\right]_{x^*}\;,\quad \bar{B}_c = [B_c]_{x^*}\; and\; \overline{C_c} = \boldsymbol{K^T}$$

$\boldsymbol{K}$ is a matrix selecting only the elements that contain a well segment. Using semi-implicit Euler discretization of Equation 12 by treating the state vector $x(t)$ implicitly and the input vector $u(t)$ explicitly results in:

$$x(k+1) = [\boldsymbol{I} - \Delta t\, \bar{A}_c\,]^{-1}[x(k) + \Delta t\, \bar{B}_c\, u(k)] \qquad , \qquad y(k) = \overline{C_d} x(k)$$

Equation 13

In this equation k represents the discrete time. Now, by defining $\bar{A}_d = [\boldsymbol{I} - \Delta t\, \bar{A}_c\,]^{-1}$ and $\bar{B}_d = [\boldsymbol{I} - \Delta t\, \bar{A}_c\,]^{-1}\Delta t\, \bar{B}_c$, and $\bar{C}_d = \bar{C}_c$, the general state space system in discrete time is expressed as followed:

$$x(k+1) = \bar{A}_d x(k) + \bar{B}_d u(k) \quad , \quad y(k) = \overline{C_d} x(k)$$

Equation 14

It should be noted that in order to simplify the notations, the over-bar sign will be omitted during the rest of this section.

Reduction of the High-Order Reservoir Model

The POD technique uses a transformation matrix of the non-linear high-order model in order to reduce the order of the system. In other words, POD can be described as an orthogonal linear transformation that transforms a set of data to a new coordinate system, such that the greatest variance lies in the first coordinate, the second greatest variance in the second coordinate, and so on. This theory exits for both infinite and finite dimensional systems; however, it is more generally applied to the latter.

Suppose the original system has a n-dimensional state space, the objective is to lower the dimension of the system by projecting the state space into a lower dimensional space. Therefore, first the n-dimensional reservoir model is run and a total number of M snapshots of the state variables are generated $\{x_i\}_{i=1}^{M}$. Note that n is much larger than M (i.e. $n \gg M$).

$$X := [x_1 \;\; x_2 \;\; \ldots \;\; x_M]$$

Equation 15

Given the data matrix $\boldsymbol{X}$, which comprises of the state vectors (x), it is desired to find a transformation so that:

$$x \simeq \phi_l z$$

Equation 16

Where, ϕ is an $n \times l$ transformation matrix and z is a reduced state vector of length l. Therefore, based on Equation 14 and Equation 16, the reduced state vector is calculated as follows:

$$z(k+1) = \phi^T[\bar{A}_d x(k) + \bar{B}_d u(k)], \;\; y(k) = \overline{C_d}\phi z(k)$$

Equation 17

The objective of using POD is to find l orthogonal eigenvectors ($l \leq M \ll n$), represented by $\{\phi_i\}_{i=1}^{l}$ such that the total square distance between the snapshots and its projections on the subspace defined by the $n \times l$ matrix is minimized for any l.

$$Q(\Phi) := \frac{1}{M}\sum_{i=1}^{M} \|x_i - \Phi\, \Phi^T x_i\|^2$$

Equation 18

$$\Phi := [\phi_1 \;\; \phi_2 \;\; \ldots \;\; \phi_M]$$

Equation 19

In summary, the POD method characterizes the states of the system by a set of orthonormal basis functions, which correspond to the leading eigenvectors of a covariance matrix constructed from a set of computed solutions. These solutions are generated by using some snapshots of the high-fidelity (high-dimensional) simulation runs which are considered as training. The method of snapshot was introduced by Sirovich (Sirovich 1987) to identify the POD basis functions for large systems.

Singular Value Decomposition (SVD) can be used in order to more efficiently generate the basis function and obtain the transformation matrix (Markovinovic, System-Theoretical Model Reduction for Reservoir Simulation and Optimization 2009).

Consequently, a reduced-order model is generated by projecting the original governing equations onto the POD basis functions, which significantly reduces the number of unknowns that must be computed. Since the error between the original data (snapshots from the high-order reservoir model) and the reconstructed data for any given number of basis functions is minimized, the obtained basis is considered to be optimum. Consequently, the full state vector (x) is reconstructed using φ (M. A. Cardoso 2009).

Summary of POD-Based ROM Using SVD

In order to develop a reduced order model for a numerical reservoir model using POD method, the reservoir simulation model is run and solution snapshots of the state variables (pressure and saturation) of the system is stored. In the next step the singular value decomposition (SVD) is performed on the resulting data matrix that generates a reduced basis, which is used to project the solution into a lower dimensional subspace. Consequently, the equations are only solved for a reduced set of unknowns.

The POD procedure requires performing the following steps (N_c represents the number of grid blocks):

1. The full reservoir simulation model is run one time or more with prescribed sequences of the control u. These runs are called training simulations.
2. The state variables of the system (pressure and saturation) at each time step are saved as solution snapshots and the data matrix is generated (individually for pressure and saturation). If k is the number of snapshots, the matrix X is of dimensions $N_c \times k$ (typically$k \ll N_c$).
3. The eigen functions of XX^T(with a dimension of $N_c \times N_c$) generates the POD basis matrix. Since N_c is large the eigen-decomposition is very expensive, instead the Singular Value Decomposition (SVD) is used.
4. l most significant eigenvectors encompass the energy of $E_l = \sum_{i=1}^{l} \lambda_i$. The total energy of the system (E_t) can be calculated by setting $l = k$. Based on the amount of energy which is desired to be captured in ϕ**,** a fraction of total energy is specified through which a value for $l \ll k$ can be determined.
5. Following the above steps, ϕ_P(of dimensions $N_c \times l_p$) and ϕ_s(of dimension $N_c \times l_s$) are obtained and are combined to produce the basis matrix ϕ.
6. Since ϕ is orthonormal, z is calculated through. $z = \phi^T x$.
7. At each iteration of each time step, the full Jacobian matrix ***J*** must be evaluated. This part of the POD procedure makes it a costly computation since this calculation is performed at each iteration.

Combination of POD and TPWL

The application of POD for solving a non-linear subsurface flow problem provides a run time speed up of about three or less, which can be significantly improved if used in combination with other methods. Trajectory piecewise linearization (TPWL) and Discrete Empirical Interpolation Method (DEIM) are the two methodologies that have been used in conjunction with the POD technique in order to make this method more efficient (M. A. Cardoso 2009) (Rousset, et al. 2013) (Gildin, et al. 2013) (He and Durlofsky, Reduced-Order Modeling for Compositional Simulation by use of Trajectory Piecewise Linearization 2014). The application of these two

methodologies in ROM development for reservoir simulation model is discussed in the following sections.

Trajectory piecewise linearization method was introduced by Rewienski (Rewienski and White 2003). In this methodology, a nonlinear system is presented as a weighted combination of a piecewise linear system and each linear system is projected into a low-dimensional space through a ROM procedure. New state variables of the system are represented in terms of piecewise linear expansions around previously simulated (and saved) states and Jacobian matrices.

Based on this method, Cardoso et al. have used a reduced-order modeling technique to reduce the computational time of numerical model of two-phase fluid flow in porous media (M. a. Cardoso 2009) (Cardoso and Durlofsky 2010). In this study, in order to achieve a significantly greater speed up, Trajectory Piecewise Linearization Method was used, which represents new pressure and saturation states using linear expansions around the states previously simulated and saved. This linearized representation is then projected into a lower dimensional space using POD procedure.

As stated before, the governing equation of fluid flow in porous media can be represented through the following partial differential equation:

$$\frac{\partial}{\partial t}\left(\varphi \rho_j S_j\right) - \nabla.\left[\rho_j \lambda_j \boldsymbol{k}\left(\nabla p_j - \rho_j g \nabla D\right)\right] + q_j^w = 0$$

Equation 20

Where j designates component/phase ($j = o$ for oil and w for water), $\boldsymbol{k}$ stands for the (diagonal) absolute permeability tensor, $\lambda_j = k_{rj}/\mu_j$ is the phase mobility in which k_{rj} is the relative permeability to phase j, and μ is the phase viscosity, p_j is phase pressure, $\rho_j$is the phase density, g is gravitational acceleration, D is depth, t is time, φ is porosity, S_j is saturation, and q_j^w is the source/sink term.

Equation 20 is a non-linear system of equations, which comprises four equations and four unknowns (p_o, p_w, S_o, S_w). In a two phase fluid system (water and oil), the constraint of $So + Sw = 1$, and also the capillary pressure relationship $p_c(Sw) = p_o - p_w$ are the two other equations which are used to solve the equations. This system of equation can be solved through a fully implicit approach. Based on the finite volume scheme, the non-linear equation can be discretized. The discretized system for fully-implicit formulation can be presented as follows (Aziz and Settari 1986):

$$g(x^{n+1}, u^{n+1}) = A(x^{n+1}, x^n) + F(x^{n+1}) + Q(x^{n+1}, u^{n+1}) = 0$$

Equation 21

In this equation, g is the residual vector aimed to drive to zero and $x = [p_o, S_w]$ is the state vector, u represents the (specified) well control parameters (e.g. bottom-hole pressure), n and $n + 1$ identify time level, A and F are the discretized accumulation, and Q represents the flux and source/sink terms.

Equation 21 represents a fully implicit non-linear system, which is solved through application of Newton's method with the Jacobian matrix of $J = {\partial g}/{\partial x}$. This is an iterative procedure which requires a huge amount of computational effort especially when the numerical reservoir simulation model comprises a large number of grid blocks (in the order of 10^6). Therefore, in order to address this problem, Cardoso et al. have utilized TPWL technique to linearize Equation 21. This linearization is performed by expanding the governing equation around a particular state (here is the previously saved state x^{sv}) which correspond to a set of controls (u^{sv}). The expansion of Equation 21 will result in:

$$g(x^{n+1}, u^{n+1}) = g(x^{sv}, u^{sv}) + \left(\frac{\partial g}{\partial x}\right)_{sv} (x^{n+1} - u^{sv}) + \left(\frac{\partial g}{\partial u}\right)_{sv} (u^{n+1} - u^{sv}) + \cdots$$

Equation 22

Where u^{n+1}, is the new set of controls, x^{n+1} is the new state to be determined. Both terms of $(\frac{\partial g}{\partial x})_{sv}$ and $(\frac{\partial g}{\partial u})_{sv}$ are matrices evaluated at (x^{sv}, u^{sv}).

The goal is to represent x^{n+1} in the form of Equation 22 when the solution at time step n (x^n) is known. When information about the higher-order derivatives is not available, error will be minimized by expanding around the saved state that is the closest to x^{n+1}. The state that is closest to x^n is designated as x^i. It is assumed that the closest saved state to x^{n+1} (the unknown state) is x^{i+1}, which is the saved state that follows x^i.

The coressponding Jacobian matirx of the system is defined as:

$$j^{i+1} = \frac{\partial F^{i+1}}{\partial x^{i+1}} + \frac{\partial A^{i+1}}{\partial x^{i+1}} + \frac{\partial Q^{i+1}}{\partial x^{i+1}}$$

Equation 23

Applying the expansion in the form of Equation 22, for each single term of Equation 21, and using the Jacobian matrix will result in the following equation assuming that the residual term at the new state is set to zero ($g(x^{n+1}, u^{n+1}) = 0$).

$$\boldsymbol{J}^{i+1}\left(x^{n+1}-x^{i+1}\right)=-[\boldsymbol{F}^{i+1}+\boldsymbol{A}^{i+1}+\frac{\partial A^{i+1}}{\partial x^{i}}\left(x^{n}-x^{i}\right)+\boldsymbol{Q}\left(x^{i+1},u^{n+1}\right)]$$

Equation 24

If the number of grid blocks in the numercial reservoir simulation model is denoted as N_c, then the dimension of the matrices $\boldsymbol{J}^{i+1}$ and $\frac{\partial A^{i+1}}{\partial x^{i}}$ are $2N_c \times 2N_c$. Still the high dimensionality of the problem makes it computationlly expensive to solve the system of equations. Therefore, a reduced-order modeling technique can be applied in conjunction with TPWL to project the high-dimensional linearized model into lower-dimension space. Propoer Orthogonal Decomposition, Krylov subspace (Gratton and Willcox 2004), and balanced truncation method (Markovinovic and Jansen, Accelerating iterative solution methods using reduced-order models as solution predictors 2006) (Heijn, Markovinovic and Jansen, Generation of low-order reservoir models using system-theoretical concepts 2004) are among the possible reduced order techniques that can be used.

For solving this problem through POD procedure a basis matrix (ϕ) is sought so that:

$$x=\begin{bmatrix}P\\S_w\end{bmatrix}\simeq \phi z=\begin{bmatrix}\phi_P & 0\\0 & \phi_s\end{bmatrix}\begin{bmatrix}z_p\\z_s\end{bmatrix}$$

Equation 25

Where ϕ relates the high dimensional state x to the reduced state z, which is of dimension l. Since ϕ is orthonormal, z is calculated through $z=\phi^T x$. The full Jacobian matrix $\boldsymbol{J}$ is projected to reduced Jacobian J_r by using $J_r=\phi^T J\phi$.

Using ϕ and the reduced Jacobian, Equation 24 can be solved directly for z^{n+1}. Therefore, the TPWL-POD formulation can be represented as follows:

$$\boldsymbol{z}^{n+1}=\boldsymbol{z}^{i+1}-\left(\boldsymbol{J}_r^{i+1}\right)^{-1}[\left(\frac{\partial \boldsymbol{A}^{i+1}}{\partial \boldsymbol{x}^{i}}\right)_r\left(z^{n}-z^{i}\right)+\left(\frac{\partial \boldsymbol{Q}^{i+1}}{\partial \boldsymbol{u}^{i+1}}\right)_r\left(u^{n+1}-u^{i+1}\right)]$$

Equation 26

Cardoso et al. have applied this methodology to two reservoir models (Cardoso and Durlofsky 2010). The first one is a three dimensional model which contains 24,000 grid blocks $(60\times 80\times 5)$, including 4 production and two water injection wells. The second one consists of 79,000 grid blocks $(60\times 220\times 6)$. They used a different bottom hole pressure scheme for the production wells in two training sets while the bottom hole pressure of the injection wells are kept constant. The models were run for a time interval of 5000 days. The two models are similar in all

properties except for the oil and water densities, which are assumed to be equal in the second model. The results of the test runs to predict the production and injection rates show a very good agreement with the reservoir model output. They ultimately used the constructed ROM for a multi-objective optimization study. The run time speed up reported as 500 to 2000 using this methodology when the mass balance error was not evaluated.

Although in this study the pressure and saturation of each grid block is calculated at each time step, since the objective is to obtain the production and injection rates through the ROM, the calculated pressure and saturation at the grid block level were not compared to those of the high dimensional reservoir model.

In a similar work, the same methodology was used to construct a ROM for a simplified though non-linear thermal recovery (SAGD) problem (Rousset, et al. 2013) (M. Rousset 2010). Three high dimensional reservoir models were constructed. The first one consists of 75,000 $(50 \times 50 \times 30)$ grid blocks, which was used for simulating the primary production where permeability field follows a log-normal distribution. The second and third are both two dimensional models (in Y-Z direction) with 3,751 and 6,050 grid blocks respectively and they simulate idealized SAGD process. The permeability field is considered as homogeneous in the second model and heterogeneous for the third one.

The result of the ROM in estimating the oil and water production, as well as water injection, was compared to those of the high fidelity reservoir model, which shows some discrepancies between the two outputs when applied for the most complex model. The run time speed up is reported as 200-500 in the test cases.

In this study, the oil saturation distribution map has also been generated for different time of the simulation for the second and third models, which shows more accuracy in the case of homogeneous permeability field. However, the pressure distribution maps were not generated in this study.

A similar work was done by Jincong He (He, Enhanced Linearized Reduced-order Models For Subsurface Flow Simulation 2010) on the application of POD-TPWL method for subsurface flow simulation.

According to the latest study, which was conducted by Jincong He (He and Durlofsky, Reduced-Order Modeling for Compositional Simulation by use of Trajectory Piecewise Linearization 2014), a reduced order model was developed for a compositional numerical reservoir model, which at the maximum consists of 52,800 grid blocks.

Summary of POD-TPWL Procedure

Development of POD-TPWL requires two different steps of offline and inline calculations.

The offline calculation includes the following steps:

1. The controls are set and the high-dimensional reservoir simulation (training run) is performed.
2. The snapshots of $\boldsymbol{X_p}$and $\boldsymbol{X_s}$ are saved.
3. The matrix ϕ is constructed (by combining ϕ_P and ϕ_s).
4. All the reduced order items that are required in Equation 26 are generated.

The inline calculation consists of the steps below:

1. The control u is prescribed.
2. At each time step, the closest z^i to z^n is computed.
3. The linearized model (Equation 26) is solved to obtain z^{n+1} (the new state).
4. The full order state is constructed through $x^{n+1} \approx \phi z^{n+1}$.

There are two major sources of error when POD-TPWL is used to develop a proxy model. The first one is disregarding the higher terms in linearization step, and the second is projection into reduced space and reconstruction of the parameters into actual space.

Combination of POD and DEIM

As mentioned in the previous section, the objective of integrating TPWL with POD is to achieve a significant run time speed up with respect to POD by linearizing the system of non-linear equations. However, TPWL suffers from some instability problems when the fluids have high density difference. In order to avoid such a problem another method was introduced by Gildin et al. which uses Discrete Empirical Interpolation Method (DEIM). The objective of using DEIM is to approximate the nonlinear term of the system of equations through some form of interpolations (Gildin, et al. 2013).

Through DEIM procedure an interpolation function is constructed, which is used for evaluation of the nonlinear terms in the partial differential equations by selecting an optimal subset of indexes. Consequently, the nonlinear function only needs to be evaluated at this greatly reduced set of component functions.

If the nonlinear part of the flow equation is represented by $g(x)$, then it can be projected into a sub-space spanned by a basis $\{u_1, \dots, u_m\} \subset R^N$ with dimension $m < n$ and the approximation is given as follows:

$$g(x) \approx Uc(x)$$

Equation 27

In this equation, columns of U are the projection basis, which are obtained through applying singular value decomposition to the nonlinear function snapshots, and c(x) is the corresponding coefficient vector. To determine $c(.)$, m rows of the overdetermined system in Equation 27 which cover the largest range of solution is selected.

$$c(x) = (P^T U)^{-1} P^T g(x)$$

Equation 28

Where, P is the output of a DEIM function. This function gets the U_m as input and finds the coefficient so that the solution range is maximized. The complexity reduction lies in the fact that each of these components only depend on a small subset of the state variables.

In the study performed by Gildin (Gildin, et al. 2013), the POD-DEIM methodology was applied to a two dimensional, heterogeneous numerical reservoir simulation model, which consists of 2,025 grid blocks ($45 \times 45 \times 1$). This model simulated oil production under a 5-spot water flood process for an interval of 1,000 days. Applying the POD-DEIM method, the production rate of four producing wells, in addition to the pressure and saturation at each grid block, were estimated. As reported, the error for the pressure and saturation estimation is of order 10^{-3}, and the results show a close agreement between the production rate from high dimensional reservoir simulation and the POD-DEIM reduced model results.

POD-DEIM methodology has also been used in a study by Han Chen (Chen, Klie and Wang 2013) to predict the space-time pressure solution by using a non-intrusive reduced order model. In this work, a simplified equation was assumed for the pressure (Laplacian Model), which is supposed to give the real solution for pressure if an error term is added to this equation ($P_{Real} = P_{simplified} + Error$). The simplified pressure equation was solved through an implicit scheme. The reservoir is a 2D space, which consists of 30×30 grid blocks, and is run for 500 time steps. Chen et al. tried to develop a surrogate model which is able to approximate the error with respect to the actual flow equation. To generate the input-output samples for training, 18 simulations were run. The ROM result was compared to the true physics model results, and the error was computed.

Limitations of POD-based reduced order models

- The proxy models developed based on POD does not provide a significant run time speed up, which is due to the fact that the nonlinear function must still be evaluated at the full order number of states, and this consequently makes this approach computationally expensive and inefficient.
- In order to generate the Jacobian matrix, the source code of the high-dimensional reservoir model must be accessible. However, using the common commercial reservoir simulators does not provide the access to the source code, and therefore generating the Jacobian matrix as an output at each iteration is not generally possible.
- The computational time required for constructing the basis and generating the required reduced matrices are comparable to the run time of the training simulation. The overall processing overhead for building TPWL is about the time required to simulate four high-fidelity models (Cardoso and Durlofsky 2010). Therefore, the application of this method is only practical when many simulation runs are required for a specific study.
- The generated output files are also significantly large which requires a large amount of space to be stored.
- One of the most important draw backs of this method is that when the system includes fluids with strong density differences, the accuracy of the estimated parameters is deteriorated, especially when applied to a model with a large number of grid blocks. This issue is related to the stability of the linearized representation. In the study conducted by Cardoso et al. (Cardoso and Durlofsky 2010), the inaccuracy in the estimated parameters was reported when the two fluids (oil and water) with different densities are used, and the reason of the result inaccuracy is said to be related to the more complex physics due to unequal densities. The understudy systems did not include a gas phase, which obviously have a huge density difference with the oil and water. Therefore, it can be concluded that using TPWL is not practical when it comes to a three phase fluid flow system.

2.2.4 Data driven or Artificial Intelligence-based Models

Data-driven proxy models are developed based on comprehensive analysis of all the existing data, which are extracted or become available from an understudy system.

In the approach based on Artificial Intelligence, employing machine learning techniques enables us to construct a model that can learn the behavior of the system through the provided data and perform a forecast of the system outputs when new data is introduced to the model.

In data-driven models, virtual intelligence techniques can be employed, which includes neural networks, fuzzy logic, and genetic algorithm. Pattern recognition and learning capability of artificial intelligence are the key characteristics of the AI-based surrogate reservoir models, which make it a unique and efficient approach for proxy model development.

Some of the advantages of AI-based surrogate reservoir models are low development cost and fast track analysis (S. Mohaghegh, Reservoir Simulation and Modeling Based on Pattern Recognition 2011).

CHAPTER 3.
SURROGATE RESERVOIR MODELING BASED ON ARTIFICIAL INTELLIGENCE

3.1 Surrogate Reservoir Model (SRM)

The Artificial Intelligence-based modeling approach can be viewed as finding the complex relationships between the input-output parameters involved in fluid flow in porous media, and it is the most flexible technique, which can be used for variety of problems in petroleum and reservoir engineering areas such as field development planning, uncertainty analysis, production optimization, formation evaluation, history matching, etc.

In some instances, although the mathematical representation of the physical phenomenon is considered to be accurate enough for the analysis purposes, due to the required computational effort for performing the analysis, using the mathematical formulations may become impractical. Therefore, the AI-based modeling approach in which the relationship between the inputs and outputs are learned through the provided data seems to be an efficient way of performing the required analysis.

Surrogate Reservoir Model (SRM) is a reasonably accurate replica of a reservoir simulation model that runs in a very short period of time. SRM was first developed and introduced in 2006 (S. D. Mohaghegh 2006). Originally, the SRM only dealt with pressure and production profiles at the well, and therefore was later named Well-Based SRM.

In reservoir engineering, the pressure and gas saturation of the reservoir are among the key factors for decision making and consequently affects the operational practices. Therefore, a proxy model, which can generate the outputs of a reservoir simulation model at the grid block level in a short time, is desired. The Grid-based Surrogate Reservoir Model was developed for the first time for a CO_2 sequestration project (Amini, et al. 2012).

There are a few number of proxy models that aimed at predicting the pressure and gas saturation of the reservoir at the grid block level. However, the limitations and shortcomings of these approaches make them have a limited application, and in some occasions are even impractical to be used in real cases.

The following section presents the capabilities and advantages of using Grid-Based SRM against the other techniques which have been used for the same objective.

3.2 SRM versus other Proxy Modeling Techniques

The choice of the best technique for the purpose of proxy modeling must be driven considering the capability as well as the applicability of the technique.

In the statistics-based proxy modeling a specific function of $y = f(x_1, x_2, \dots x_n)$ is generated to predict the system output (y) when the inputs $(x_1, x_2, \dots x_n)$ are changed. The number of inputs is limited to the uncertain parameters of the system. Even with this limited number of inputs, this approach requires hundreds of simulation runs to properly cover the input-output space.
However, in AI-based surrogate modeling, a variety of inputs can be used. These inputs not only include the uncertain parameters of interest, but also many other parameters which can provide more information regarding the entire system. With the large number of inputs that can be integrated into the model, still the number of runs required for developing a surrogate model remains considerably lower than the statistics-based modeling technique. This characteristic of the AI-based approach makes it remarkably flexible and significantly less dependent to the complexity of the high fidelity reservoir model.

The reduced-physics modeling approach is claimed to be more accurate due to the fact that the physics of the phenomenon is taken into account, and therefore the developed proxy model honors the involved physics. However, it should be noted that even in the source model (the numerical reservoir simulation model), which is believed to perform based on the physics of the process, a large number of assumptions are made. Consequently, these detailed, complex numerical reservoir models are just a significantly simplified mathematical formulations of the physical phenomenon that is actually taking place in reality. As a result, the proxy model, which is developed based on further simplification of the involved formula, barely represents the actual physics of the process. Calibrating or tuning the reduced-physics model against the full-physics model, based on a limited number of runs, does not guarantee proper generalization ability for the model that can be applicable in a variety of cases.

In the AI-based approach, no simplifying assumptions are made, and instead, the hidden complex relationship between the inputs of the model and the outputs is sought based on pattern recognition ability of this technique. Consequently, the behavior of the system under several conditions is taught to the surrogate model through provided data, which enables the surrogate model to predict the outputs when new inputs are introduced to the system.

The reduced order modeling technique is basically based on partial differential equations of the fluid flow in porous media. In the ROM types of proxy modeling, we are still bounded to the entire physics-based mathematical formulations of fluid flow, and therefore this method suffers

from the problems that engineers encounter when they are dealing with solving a system of non-linear equations. In order to overcome this problem, in some occasions further simplifications of the problem is required. For instance, in the study based on POD-TPWL, which was conducted by Cardoso et al. (Cardoso and Durlofsky 2010), in the cases with high difference in density of the existing fluids they experienced some instability problems. Even if we assume that the stability and convergence problem can be solved, the size of the problem still can be a significant obstacle for this type of approach.

The reduced order modeling technique reduces the computational effort of solving the huge system of partial differential equations by projecting the high-dimensional system matrix into a lower-dimension matrix through a method of transformation, and consequently the system of equations can be solved faster. However, this procedure still needs to be performed on the full reservoir, and therefore it would not be as efficient when it is applied to a reservoir with a large number of grid blocks (over 10^6). That is due to fact that in this approach, generating a low order model requires generating a system of partial differential equations for a million grid blocks. The question is that to what extent the order of the system matrix can be reduced? There is no doubt that in order to achieve a certain amount of accuracy, the order reduction cannot exceed a certain amount, and therefore, in practice, the reduced order model development for such a large number of grids becomes inefficient if not impossible. Consequently, there are many limitations associated with the reduced order modeling based on fluid flow formulations. Still this type of modeling has not been successfully applied on a large (more than 10^5 grids) and complex reservoir model with no simplifying assumptions.

On the other hand, the AI-based surrogate reservoir modeling provides a significant amount of flexibility in so many aspects that are listed below:

- There is no limitation regarding the involved parameters, such as the number of phases involved in the reservoir model, geological complexity, number of grid blocks, number of injection and production wells, rock-fluid properties, etc.
- The physics of the phenomenon is not simplified.
- It can be developed with a relatively low computational effort.

All the mentioned characteristics and the amount of flexibility of the AI-based technique makes it a prominent and distinctive approach in the area of proxy modeling, which is much more applicable and practical for a variety of problems with different degrees of complexity.

3.3 Artificial Intelligence (AI)

Artificial Intelligence is a universal field which encompasses a huge variety of subfields, from more general areas such as learning and perception to more specific tasks such as playing chess, writing poetry, and diagnosing diseases (Russell and Norvig 2003).

McCarthy was the first one to introduce AI as a new field in 1955. Afterwards McCarthy and some other researchers resumed their research in this field in spite of all the difficulties they encountered. Three decades later, AI became a science and a revolution that occurred both in its content and methodology (Russell and Norvig 2003).

There are several definitions for AI according to different researchers; however, it can generally be defined as "the study and design of intelligent agents." An intelligent agent is something that acts intelligently in an environment according to the circumstances and its goal. This agent is flexible to the change of environments and goals. it learns from experience, and, within a certain limitation, it is able to make appropriate choices (Poole, Mackworth and Goebel 1998).

Artificial Neural Network (ANN), Fuzzy Logic (FL), and Genetic Algorithms (GA) are among the most popular artificial intelligence techniques that are used to solve engineering problems. Incorporation of several virtual or artificial intelligence tools in a hybrid manner can generate a successful intelligent application. Virtual intelligence tools are able to complement each other by amplifying each other's effectiveness (S. Mohaghegh, Virtual-Intelligence Applications in Petroleum Engineering: Part 2-Evolutionary Computing 2000).

As one of the sub-categories of the artificial intelligence method, Artificial Neural Networks (ANNs) have a great potential for performing accurate analysis and predictions from historical data. The ANNs are particularly useful where mathematical modeling cannot be considered as a practical option. This can be due to the fact that all the parameters involved in the process are not known and/or there is a very complex relationship between the parameters of the system, which is too complicated to be presented through mathematical formulations (Holdaway 2014).

The artificial neural network is a powerful tool that has been successfully used in a wide variety of problems in different areas such as medical, engineering, financial, business, etc. However, in different industries, many cases of unsuccessful neural network implementations have been reported, which can be traced back to inappropriate neural network design and general misconceptions about how they work (Reid 2014).

In the current research, the artificial neural network method is employed to develop a surrogate reservoir model. This technique is explained in detail throughout the upcoming sections.

3.3.1 Artificial Neural Network Overview

Artificial Neural Network is an information-processing paradigm that was inspired by the biological nervous system. This inspiration comes from the way information is processed through the interconnected structure of the nervous system (Basu, Bhattacharyya and Kim 2010).

The most attractive characteristics of artificial neural networks are their ability to learn complex nonlinear input-output relationships, use sequential training procedures, and adapt themselves to the data. Therefore, ANN has been used as a powerful data processing tools in a wide variety of problems in different areas such as medical, engineering, financial, business, etc.

The first artificial neural network were introduced and modeled by McCulloch and Pitts in 1943 (McCulloch and Pitts 1988). There is a wide variety of neural networks used in solving different engineering and science complex problems, some of which can be named as feed-forward neural network, radial basis function network, recurrent network, modular neural network, etc.

ANN can be considered as generalizations of mathematical models of biological neurons. It consists of a large number of simple processing elements called neurons where the information processing occurs. Each neuron is connected to other neurons by means of communication link any of which has an associated weight. The weights represent information being used by the net to reach the solution (S. D. Mohaghegh, Virtual-Intelligence Applications in Petroleum Engineering: Part 1-Artificial Neural Networks 2000).

Generally a neural network is characterized by three items which are:

1. Pattern of connections between the neurons (network architecture)
2. Method of determining the weights on the connections (training or learning algorithm)
3. Activation function that converts the neuron's weighted input into the output activation

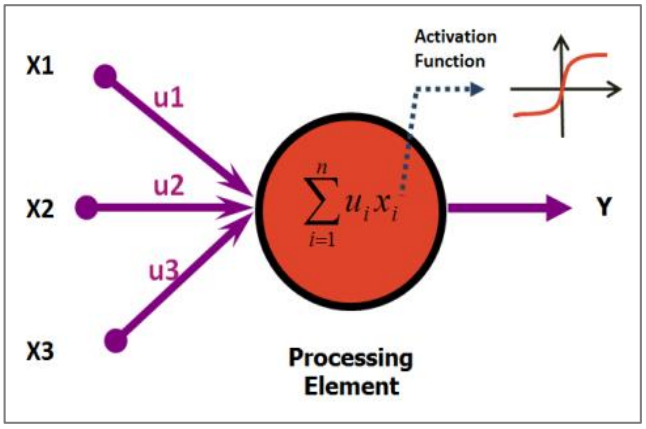

Figure 1. An artificial neuron (a single processing element of a Neural Network)

illustrates the process that occurs in an artificial neuron as an example. Several inputs are weighted and received by a single neuron and are summed up and subsequently applied to the activation function which results in the neuron output.

Three different methods can be used as learning or training strategies which are: supervised, unsupervised, or reinforcement learning.

In supervised learning, the network is trained by providing a set of inputs and their corresponding outputs (training set). At each training iteration, the error between the network output and provided output is computed, and based on the error signal the network parameters are adjusted. At each iteration, the network is applied to a set of inputs without their expected output to verify the performance of the trained network. This procedure is repeated until some criteria are met.

Unsupervised learning is a method through which a hidden structure in input data is sought when the output is not provided. Since no output is available there is no error signal to lead the network to the solution. This method is used to cluster data, find, summarize, and explain the key features of the data.

In the reinforcement learning method, the agent is rewarded when it makes a good move and is punished for a bad move, and consequently it learns from its success and failure (C. M. Bishop 2006).

In this study, the purpose of using neural networks is to develop a proxy model which is able to mimic the outputs of a reservoir simulation model, and therefore the neural networks are trained through the supervised learning strategy.

The feed-forward neural network method is the type of neural network used in this research. Therefore, this specific class of neural network is presented in detail in the following sections.

3.3.2 Feed-forward Neural Network Model

Among all the different types of neural networks, the feed-forward neural network is the first and one of the most widely used types of the artificial neural network in which the information flows in one direction from input toward output.

The simplest feed-forward artificial neural network consists of a single perceptron that is only capable of learning linear separable problems. A simple multi-layer feed-forward artificial neural network is used to solve more complex problems.

The basic neural network model can be described as a series of functional transformations. Neural networks use basis functions in the form of Equation 29 (C. M. Bishop 2006).

$$y(x, w) = f(\sum_{j=1}^{M} \omega_j \phi_j(x))$$

Equation 29

Each basis function, itself, is a nonlinear function of a linear combination of the inputs. Considering $x_1, x_2, \dots, x_D$ as inputs, in order to develop the neural network, M linear combinations of the input variables are constructed through the following formulation.

$$a_j = \sum_{i=1}^{D} \omega_{ji}{}^{(1)} x_i + \omega_{j0}{}^{(1)}$$

Equation 30

Where, a_j is known as activation, $j = 1,2, \dots, M$, and subscript (1) is the representative of the first layer of the network. The parameters $\omega_{ji}{}^{(1)}$ are referred to as weights, and $\omega_{j0}{}^{(1)}$'s are called the biases.

Each activation is transformed by using a nonlinear activation function $h(.)$ which then gives:

$$z_j = h(a_j)$$

Equation 31

These quantities correspond to the hidden units. The nonlinear function of $h(.)$ can be a sigmoidal function or the $'tanh'$ function. In order to obtain the output unit activation, these values are again linearly combined.

$$a_k = \sum_{j=1}^{M} \omega_{kj}{}^{(2)} z_j + \omega_{k0}{}^{(2)}$$

Equation 32

Equation 32 is the transformation related to the second layer of the network in which, $k = 1,2, \dots, K$ and K is the number of outputs. The same as Equation 30, the $\omega_{j0}{}^{(1)}$'s are the bias parameters.

Finally, in order to calculate the network output, y_k the output unit activations, are transformed through an appropriate activation function. Several activation functions are available for different

systems. The linear, unit step, ramp, logistic sigmoid, hyperbolic tangent, and Gaussian transfer function are the most commonly used. The diagram below shows the schematics of the six

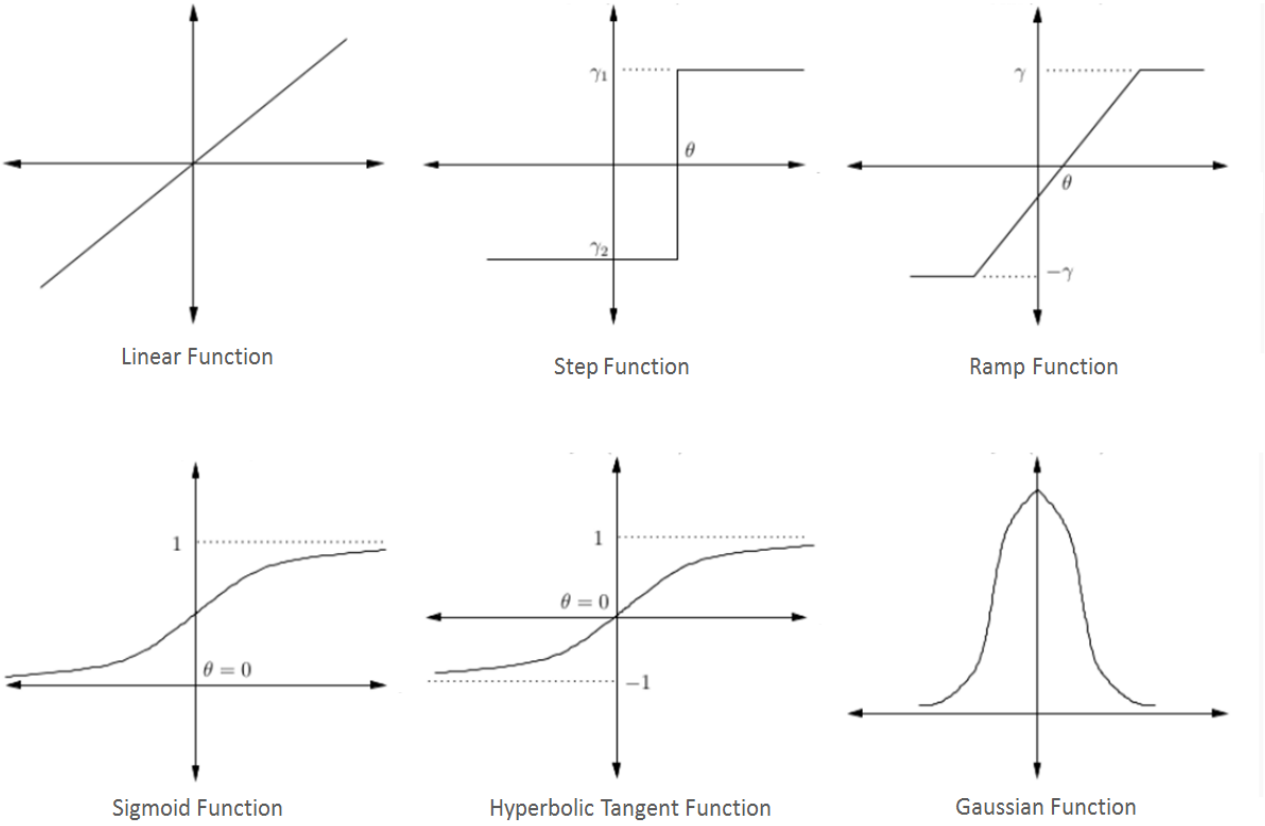

activation functions.

Figure 2. Six most popular activation functions used in neural network models (Reid 2014)

The choice of activation function is determined based on the nature of the data and also the type of problem (C. M. Bishop 2006). The logistic sigmoid function, δ which is the activation function used in this work, is defined as:

$$\delta(a) = \frac{1}{1 + \exp(-a)}$$

Equation 33

Considering the sigmoid function as the activation function, each output unit is transformed through $y_k = \delta(a_k)$ formula.

By combining the various stages mentioned above (Equation 30 to Equation 32), the overall neural network function can be represented in the following form.

$$y_k(x,w) = \delta\left(\sum_{j=1}^{M} \omega_{kj}{}^{(2)}\, h\left(\sum_{i=1}^{D} \omega_{ji}{}^{(1)} x_i + \omega_{j0}{}^{(1)}\right) + \omega_{k0}{}^{(2)}\right)$$

Equation 34

As indicated in Equation 34 the neural network model is a nonlinear function of a set of input $\{x_i\}$ to a set of output $\{y_i\}$, and it is controlled by a set of adjustable parameters which are the weights.

Figure 3 demonstrates the network diagram, which represents the input-output relationship corresponding to Equation 34. In this diagram, the input, hidden, and output variables are denoted by nodes. The weights are indicated by links between the nodes. The bias parameters are the additional nodes in input and hidden layers x_0, z_0 respectively. The green arrows show the direction of flow of information through the network during forward propagation.

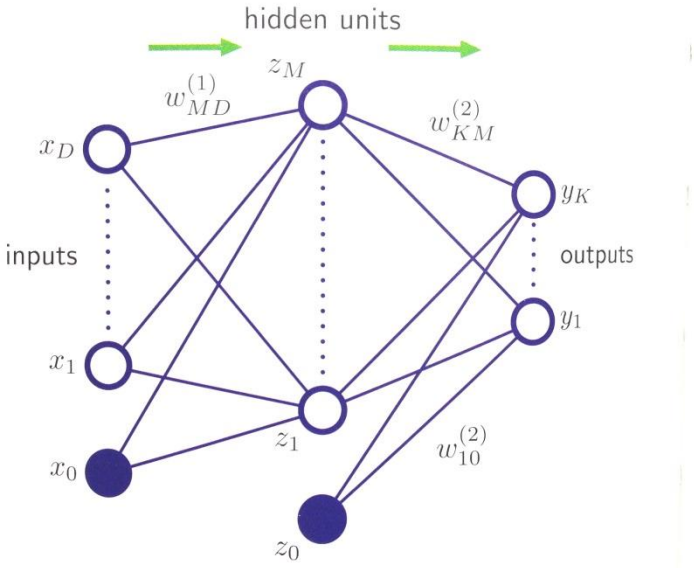

Figure 3. Diagram of a Two-layer Feed-forward Neural Network (C. M. Bishop 2006)

3.3.3 Neural Network Training

Neural network training will be performed once the network structure is determined. In general, neural network is considered as a class of non-linear parametric function. The neural network training process comprises several steps that lead to the determination of the involved network parameters. A simple analogy to this process is curve fitting through which a sum of squares of

the error function is minimized. Therefore, in a neural network, given a set of input vectors $\{x_n\}$, $n = 1,2, \dots, N$, and the corresponding set of target vectors $\{t_n\}$, the goal is to minimize the error function which can be denoted as follows.

$$E(w) = \frac{1}{2}\sum_{n=1}^{N} \|y(x_n, w) - t_n\|^2$$

Equation 35

The next step is to find the weight vector such that the error function is minimized. In most techniques, an initial value is chosen for the weight vector ($w^{(0)}$), and in subsequent steps the weights are updated through:

$$w^{(\tau+1)} = w^{(\tau)} + \Delta w^{(\tau)}$$

Equation 36

Where, τ is an indicator for the iteration step. Different algorithms use different choices for updating the weight vector. However, many of them apply gradient information, and therefore the value of $\nabla E(w)$ should be evaluated at the new iteration step (C. M. Bishop 2006).
Back propagation technique is applied as the neural network training method in this research.

Back Propagation Technique

Back propagation is found to be an efficient technique for evaluating the gradient of an error function for a feed-forward neural network. In this method, the calculated error is sent backward through the network and the weights are updated accordingly.

Assuming a particular input pattern n, the error function takes the following form.

$$E_n = \frac{1}{2}\sum_{k} (y_{nk} - t_{nk})^2$$

Equation 37

Where, $y_{nk} = y_k(x_n, w)$. The gradient of this error function is calculated with respect to a weight w_{ij} through Equation 38.

$$\frac{\partial E_n}{\partial w_{ij}} = \left(y_{nj} - t_{nj}\right)x_{ni}$$

Equation 38

In general feed-forward network, each unit calculates the weighted some of its inputs as denoted below:

$$a_j = \sum_i w_{ij}\, z_i$$

Equation 39

In this equation, z_i represents the activation of a unit, or an input that has a connection to unit j, and w_{ij} is the weight associated with that connection. The summation in Equation 39 is transformed through a nonlinear activation function to generate the activation z_j of unit j.

$$z_j = h(a_j)$$

Equation 40

The forward propagation is the process through which the input vectors are supplied to the network, and the activations of the hidden and output units are calculated by successive application of Equation 39 and Equation 40.

Applying the chain rule to the gradient of the error function, the partial derivative can be rewritten as:

$$\frac{\partial E_n}{\partial w_{ij}} = \frac{\partial E_n}{\partial a_j}\frac{\partial a_j}{\partial w_{ij}}$$

Equation 41

Now, a new notation is introduced as $\delta_j \equiv \frac{\partial E_n}{\partial a_j}$.

Using Equation 39, the second term can be written as $\frac{\partial a_j}{\partial w_{ij}} = z_i$.

By substituting these two terms into Equation 41, the derivative can be obtained by multiplying the value of δ for the unit at the output end of the weight by the value of z for the unit at the input end of the weight.

$$\frac{\partial E_n}{\partial w_{ij}} = \delta_j z_i$$

Equation 42

For the output layer we have:

$$\delta_k = y_k - t_k$$

Equation 43

For the hidden layer, again making use of chain rule, results in:

$$\delta_j = \sum_k \frac{\partial E_n}{\partial a_k} \frac{\partial a_k}{\partial a_j}$$

Equation 44

Where, the sum applies on all of unit k to which unit j sends connections. The schematic of the units and how the error is back propagated is illustrated in the figure below, where the purple arrow indicates the direction of information flow through the network in forward propagation, and the red arrows show the direction of the backward propagation of the error information.

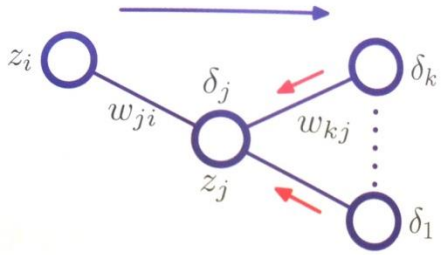

Figure 4. Backward propagation of error information from the output layer to hidden layer (C. M. Bishop 2006)

Using the definition of δ, and making use of Equation 39 and Equation 40, the back propagation formula can be represented as follows.

$$\delta_j = h'(a_j) \sum_k w_{kj} \delta_k$$

Equation 45

The procedure to apply the back propagation method can be summarized in the following steps (C. M. Bishop 2006).

1. The input vector is applied to the network and it is propagated forward through the network using Equation 39 and Equation 40. This results in finding the activations for all the hidden and output units.
2. δ_k's are evaluated for all the output units using Equation 43.

3. The δ's are back propagated using Equation 40 to obtain δ_j's for each hidden unit in the network.
4. Equation 42 is applied to evaluate the required derivatives.
5. The weights are updated and the same procedure is repeated until the stopping condition is met.

3.4 Application of Neural Network in Petroleum Engineering

In the past three decades, neural networks have become of interest to petroleum engineers and geoscientists. In petroleum engineering, the supervised training algorithms are commonly used. In this method both the inputs and outputs are presented to the network and the learning process takes place based on error feedback to the network (S. D. Mohaghegh, Virtual-Intelligence Applications in Petroleum Engineering: Part 1-Artificial Neural Networks 2000).

Artificial neural network has been used for a variety of problems in petroleum engineering. The earlier applications of this method are well test interpretation (Al-Kaabi and Lee 1993), prediction of formation permeability (S. Mohaghegh, R. Arefi, et al. 1995) (Mohaghegh, Ameri and Arefi, Virtual Measurement of Heterogeneous Formation Premeability Using Geophysical Well Log Responses 1996), prediction of formation damage due to injection into low permeability reservoirs (Nikravesh, Kovscek and Patzek 1996) and reservoir characterization (Mohaghegh, Arefi and Ameri, Petroleum Reservoir Characterization with the Aid of Artificial Neural Network 1996).

Later, applications of neural networks in several areas of petroleum engineering became more common. Gorucu et al. applied this methodology to construct a tool which was named a "Neurosimulation Tool", with the objective of predicting the performance of CO_2 sequestration process for enhanced coalbed methane (Gorucu, et al. 2005). In order to perform an optimization study for this process, thousands of numerical reservoir simulation runs were required to evaluate the effect of several operational conditions. This would require a massive amount of time. However, the AI-based proxy model was able to generate the required results in a few seconds.

Alajmi et al. developed a pressure transient analysis tool which was able to predict the desired unknown properties of a double-porosity reservoir system such as permeability of the matrix, porosity of the matrix, and fracture by training a neural network. In the training process they used the known properties of the reservoir, fluid properties, and well parameters as the neural network input (Alajmi and Ertekin 2007).

In another study performed by Mohaghegh et al. a well-based surrogate reservoir model was developed for a giant oil field in the Middle-East in order to identify the wells that are prime candidates for rate relaxation with the objective of higher oil production. The field production after more than two years confirmed the results predicted by developed SRM, which demonstrates the capability of the reservoir models developed based on neural network in real field operation (Mohaghegh, Modavi, et al. 2009).

Shahkarami et al. have used the AI-based approach to develop an assisted history matching technique for a synthetic oil field with 24 production wells and 30 years of production. The history matching process in this study is based on three uncertain parameters of the reservoir which are porosity, permeability and thickness. The results of this study showed that neural networks can be used as a fast and efficient tool for assisted history matching process (Shahkarami 2014).

In the study performed by Esmaili (Esmaili 2013) an AI-based model was developed for a Marcellus Shale asset which includes 135 horizontal wells from 43 pads. The full field AI-based shale model was used to predict the well/reservoir performance and also forecast the behavior of the new wells. Moreover, based on the developed model the impact of design and native parameters on gas production was investigated. This work demonstrated that application of artificial intelligence, and in particular neural network, can be significantly advantageous in shale modeling where development of a numerical reservoir simulation models is substantially costly due to the massive amount of time and effort required. In the occasions where the field involves a large number of wells, modeling through conventional reservoir simulators is impractical if not impossible.

In general, according to the existing literature, artificial intelligence techniques have been mostly used to develop proxy models, which aim at computing well related parameters such as production/injection rather than dynamic parameters of the reservoir such as pressure and gas saturation. The well-based models are constructed for a variety of problems including well performance analysis, optimization, history matching, etc.

There are only a few studies that have been conducted using artificial neural networks for the purpose of pressure and gas saturation calculation at the reservoir grid block level. In a study performed Klie, POD and DEIM methodology and Radial Basis Function (RBF) networks were used to develop a proxy model with two objectives. The first objective is to generate the well oil and gas production rate under uncertain permeability. The second objective is to predict the pressure and gas saturation distribution under uncertain permeability and varying injection rate.

This study was performed on two very simple reservoir simulation models. The first model is a 2D-2phase reservoir with a maximum of 100 grid blocks and the second model is a 3D black oil reservoir with 300 grid blocks ($10 \times 10 \times 3$). In this study, POD and DEIM were used as a tool to reduce the dimensionality of the generated matrices which are going to be used as inputs for the RBF network (Klie 2013). Therefore, they need to go through all the complications of the POD methodology, which was discussed in the previous chapter, before they can use the RBF network to develop the proxy model.

In the research performed by Chen et al. (Chen, Klie and Wang 2013) a proxy model was developed for a 2D reservoir model with 900 grid blocks (30×30) and a heterogeneous permeability distribution and a constant porosity. They assumed that saturation is known and tried to predict the pressure at each grid block by using the simplified developed proxy model using artificial neural networks. In this work a very simplified formulation and reservoir model has been used which does not demonstrate the ability of the model to be applied for a more realistic case.

The existing studies on the application of artificial neural network for developing a grid-based surrogate reservoir model have many limitations and deficiencies, and therefore, they fail to generate acceptable models that can be used as a practical tool for a complex numerical reservoir simulation model.

The current research uses a novel approach to develop a surrogate reservoir model by using artificial neural networks. The capability of the developed model is demonstrated by applying the technique to a real case 3D heterogeneous reservoir with 100,000 active blocks which is used for a CO_2 sequestration study.

CHAPTER 4.
NUMERICAL RESERVOIR MODEL DEVELOPMENT

A numerical reservoir simulation model is developed based on a CO_2 injection and sequestration project which was implemented in Australia. In this work all the available filed data was integrated to develop the model. The following sections present more details regarding the field background and the operations performed in this field for the purpose of CO_2 sequestration. Later, the process through which the numerical reservoir simulation model was developed will be explained.

4.1 Field Background

The understudy field is a depleted gas reservoir located in Otway Basin in Victoria, Australia (Figure 5). This field was identified as a proper option for CO_2 sequestration since the site is well characterized due to its natural gas production history. Furthermore, having previously stored natural gas for millions of years it obviously has a proven storage capacity in which CO_2 can be safely stored (CSIRO 2008).

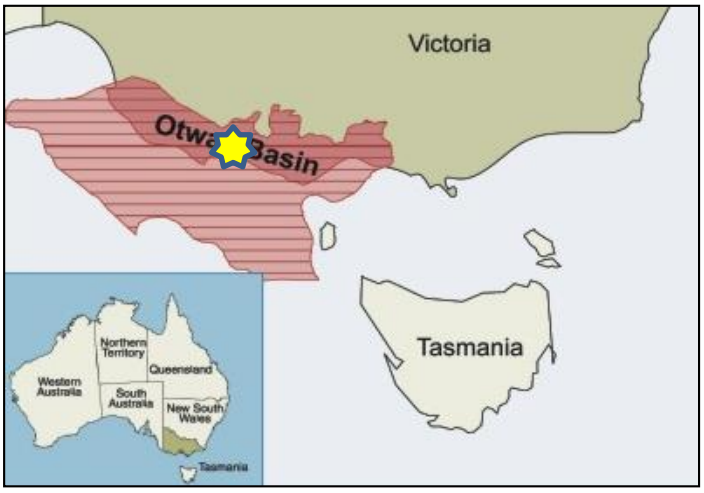

Figure 5. Otway Field Location in Victoria, Australia
(Reference: IEA Greenhouse gas R&D program website)

The target reservoir for injecting CO_2 is Waarre-C formation, which is a sandstone reservoir approximately 100 ft thick and located 6561 ft underground with an area of about 500 acres. The reservoir is overlain by a caprock of mudstones (Flaxman and Belfast Formations). The structure is bound with three major sealing faults and two aquifers which are connected to the reservoir

from south-east and west side. The reservoir has an average porosity and permeability of 15% and 1,000 md respectively (Dancea, Spencera and Xua 2008). The stratigraphy column of the reservoir is depicted in Figure 6.

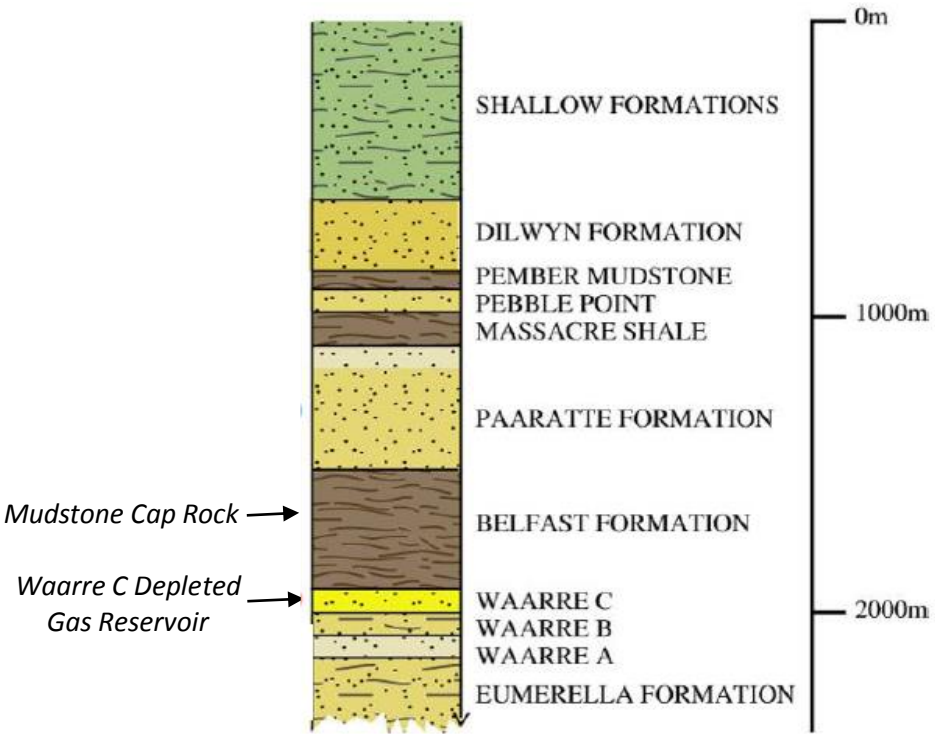

Figure 6. Stratigraphy column of the Otway field

Two wells exist in this reservoir. The first one is Naylor-1 which was a natural gas production well, producing from May 2002 to October 2003 and later it was converted to a monitoring well in 2007. The second one is CRC-1 through which the CO_2 is injected underground. It was drilled in 2007 and is located approximately 980 ft away from Naylor-1 well.

In this pilot project, CO_2-rich gas that contains about 80% CO_2 and 20% methane is produced from a nearby gas field then compressed, transported, and injected into the depleted gas reservoir.

CO_2 injection through CRC-1 started at March 2008 (Dancea, Spencera and Xua 2008). Figure below shows the injection and monitoring wells and how CO_2 is transported and injected into the reservoir for long-term storage.

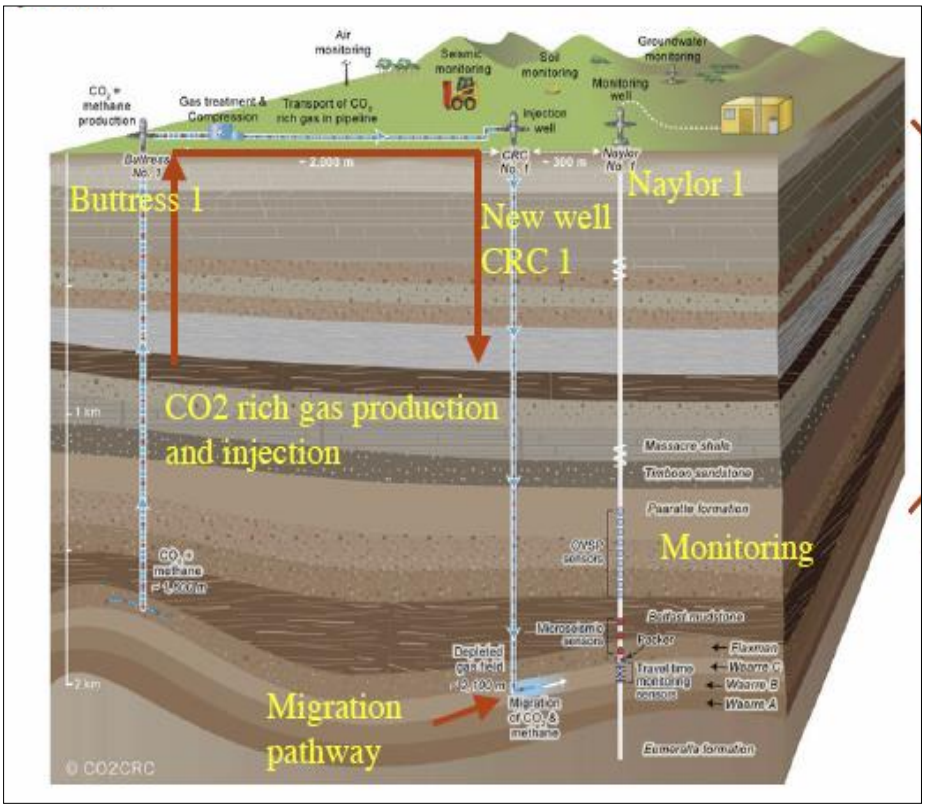

Figure 7. Schematic of the Otway CO_2 injection project (Source: CO_2CRC)

4.2 Reservoir Model Development

In this research a numerical reservoir simulation model was constructed to simulate the natural gas production as well as the CO_2 injection processes which were performed in this reservoir. However, further studies were performed based on the CO_2 injection process. The reservoir model was developed in CMG-GEM (Compositional Modeling module) using the available field data.

The structure of the reservoir was generated by making use of a contour map available from the geological information of the field. This model includes 100×100 grid blocks in x-y direction and consists of 10 layers. The reservoir structure and well locations are depicted in Figure 8. The production well was completed in layers 5 and 6; however, the injection well was completed in 5 layers from layer 3 to layer 7.

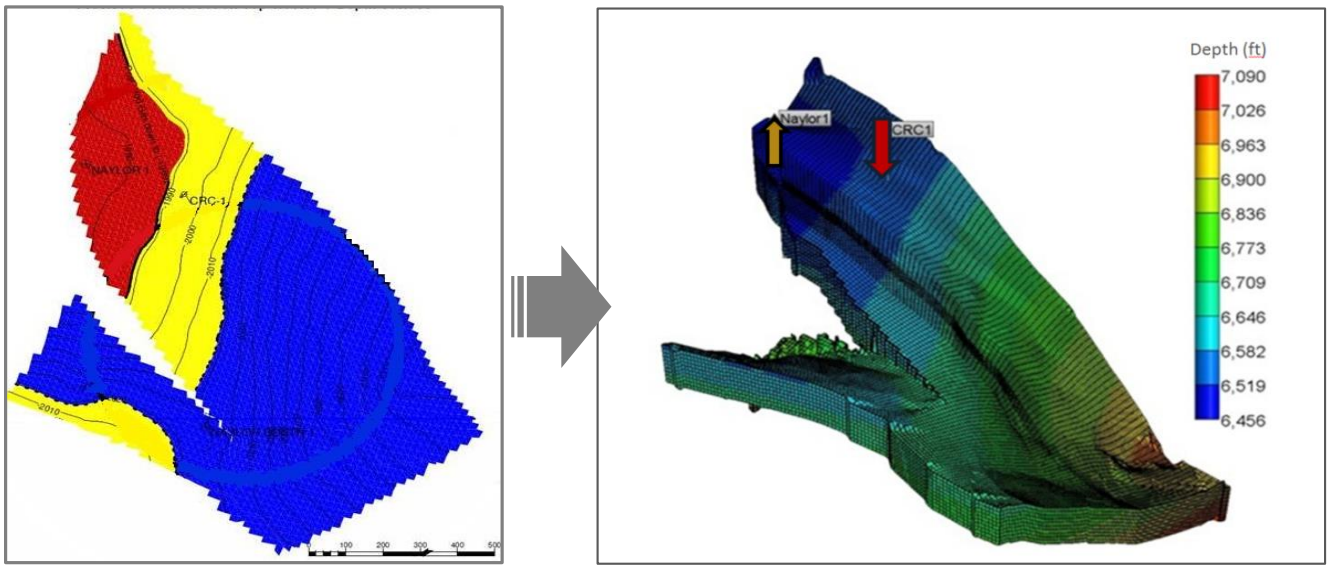

Figure 8. Left: Available contour map of the reservoir, Right: Reservoir model structure and well locations

Reservoir parameter distribution (porosity and permeability) was generated through statistical method using the CRC-1 core and log data (Figure 9) and using average values of porosity and permeability at each layer of the reservoir.

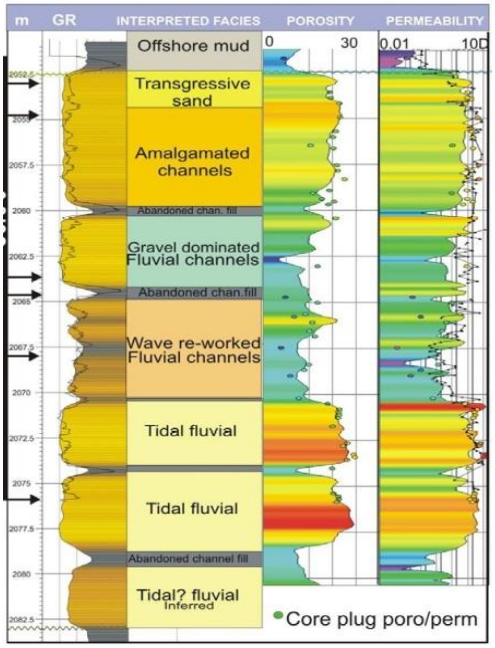

Figure 9. Porosity and Permeability values from core and log data

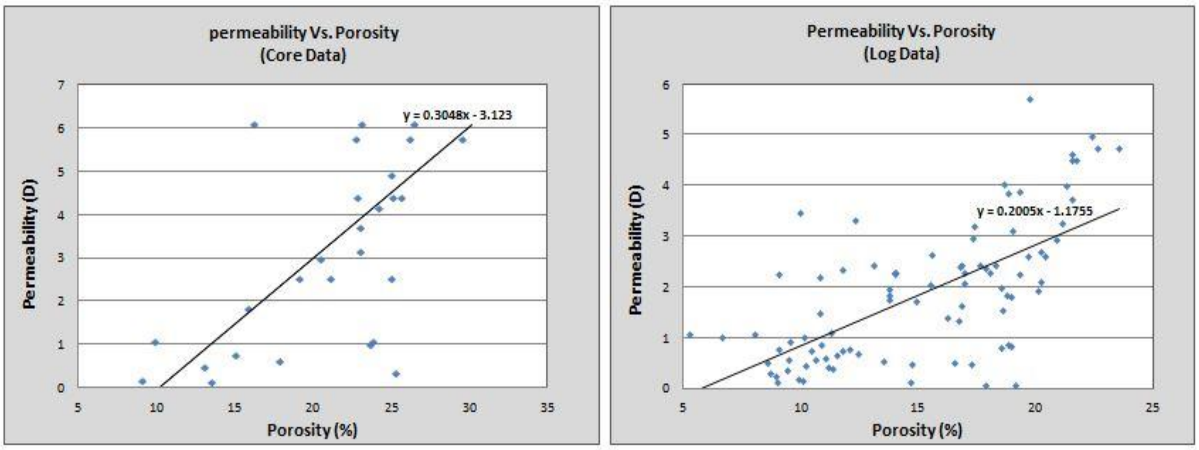

Figure 10. Correlation between porosity and permeability using log and core data

The composition of the original natural gas was assigned according to the following table as reported in the available data.

Table 1. Natural gas composition of the reservoir

Composition	Mole Percentage
C1	84.35
C2	4.62
C3	2.01
C4+	1.48
N2	6.52
CO_2	1.02

When injection takes place in the reservoir, hysteresis phenomenon plays a significant role on fluid flow behavior. In the early injection period, drainage is the dominant process; however, imbibition takes place when the CO_2 plume starts migrating. Hysteresis affects the CO_2 mobility as well as the gas water contact. In order to include the hysteresis effect, the following relative permeability curves were used, which were generated based on the laboratory measurement on a core from CRC-1 well.

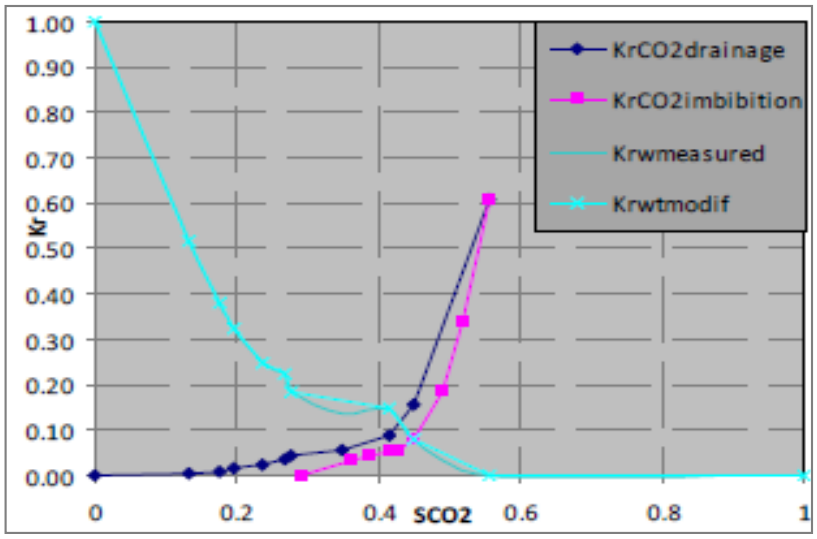

Figure 11. Relative permeability curves including hysteresis effect

Due to the existence of an active aquifer system, a fraction of the injected CO_2 is dissolved into the water phase and therefore in this model the CO_2 solubility in water was also taken into account.

4.3 History Matching

The developed reservoir model was history matched based on the available field data both in the natural gas production phase and the CO_2 injection phase. During the history matching process the monthly natural gas production rate for 18 months and the monthly CO_2 injection rate for 8 months were considered as the constraint in the model and the well bottom-hole pressure was matched for the production and injection wells by changing the reservoir parameters. The thickness of the reservoir layers was assumed to be a constant value equal to 11 feet. Therefore, during the history matching process, the porosity and permeability of the reservoir were used as the major tuning parameters.

Figure 12 demonstrates the result of history matching (matched BHP) for both production and injection wells.

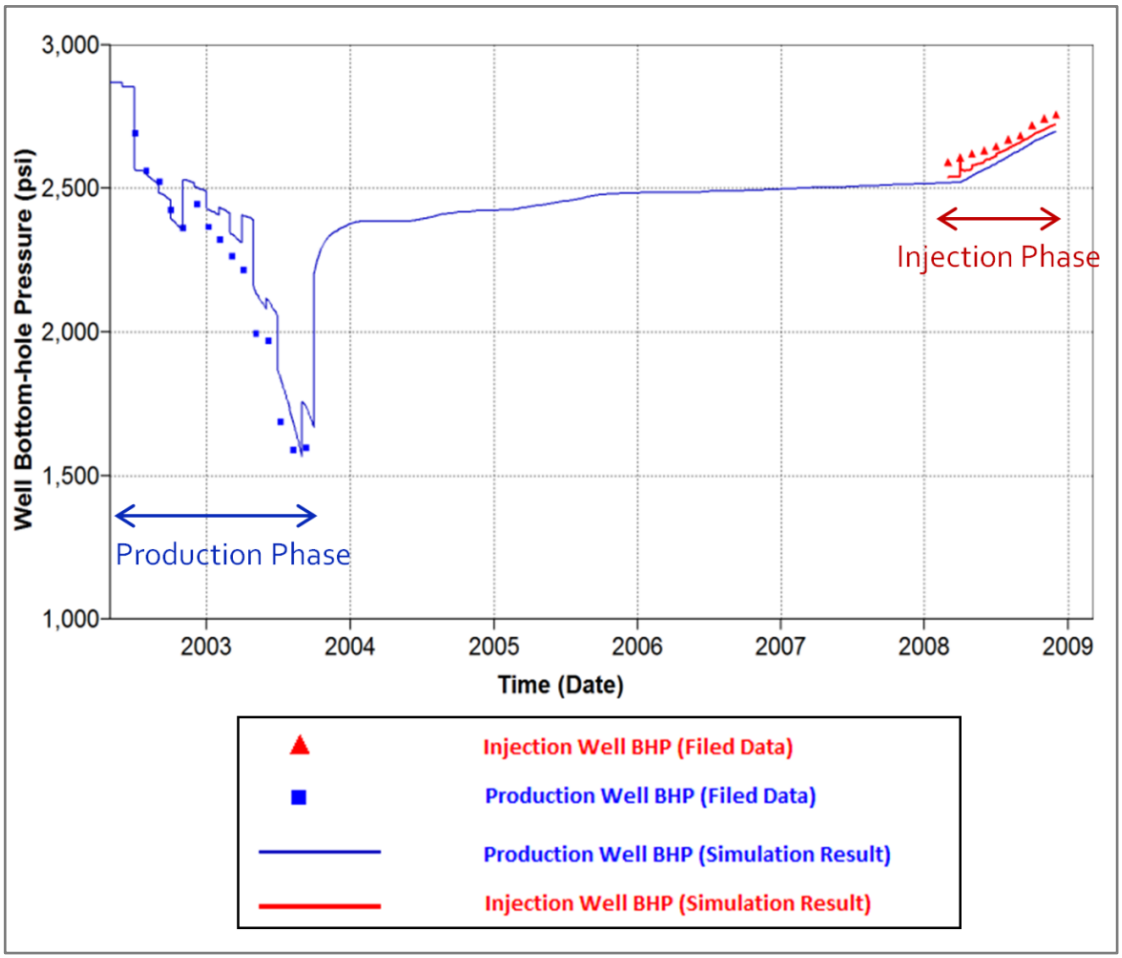

Figure 12. History Matched BHP for production and injection well

The history matched model was used as a base model to generate the grid-based surrogate reservoir model for the injection interval when the model was run for several injection scenarios and multiple geological realizations.

CHAPTER 5.
SURROGATE RESERVOIR MODEL (SRM) DEVELOPMENT

Surrogate reservoir modeling is an artificial-intelligence-based approach to construct a proxy model which can be used to generate the output of a complex numerical reservoir simulation model. In this context SRM can be defined as a customized model comprised of a collection of neural networks which are trained, calibrated, and verified for a specific problem.

Once developed for a particular problem it can generate the outputs of the numerical reservoir simulation model when the inputs are changed within a specific range which the networks have been trained with. Details regarding the structure of the neural network, type of the neural network, and its training process for the purpose of proxy modeling have been thoroughly explained in Chapter 3.

The workflow demonstrated in Figure 13 was followed in the current research to develop a SRM for the particular problem of CO_2 injection and sequestration.

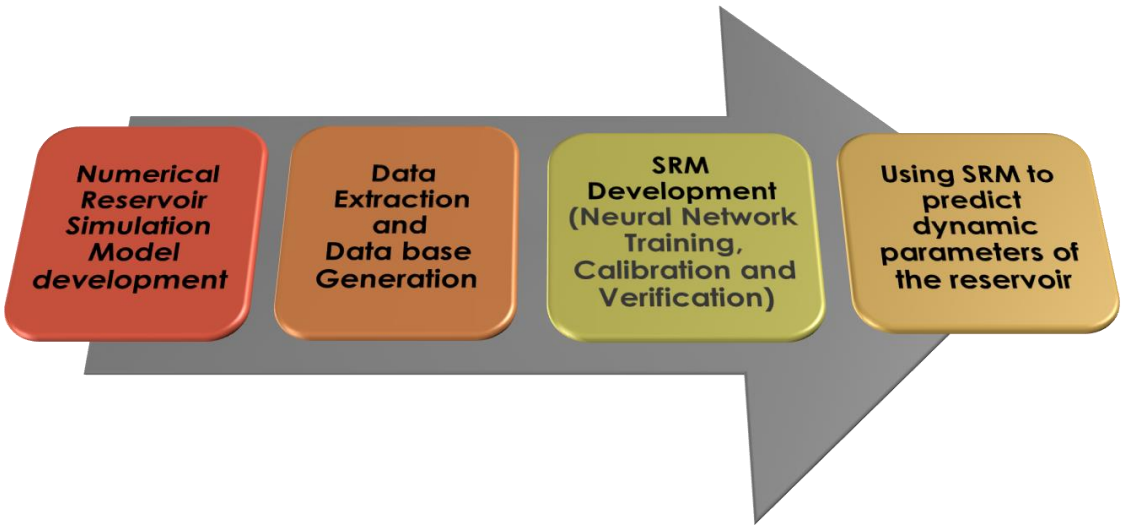

Figure 13. General workflow for SRM development

5.1 Proof of Concept

Artificial intelligence approach can be applied to develop a proxy model for a numerical reservoir simulation model with a large number of grid blocks (greater than 10^5); however, applying this methodology to fewer number of grid blocks reduces the complexity of the generated data set and therefore enables us to fully understand different aspects of this approach before applying it to a significantly larger number of grid blocks.

Consequently, the initial goal is set to construct an SRM for the top layer of the reservoir which enables us to observe and study the distribution of the dynamic parameters of the reservoir at the first layer, located just below the caprock, under different injection scenarios. Practically, the results of this study would be useful to evaluate the risk of CO_2 leakage through the reservoir caprock under the change of uncertain parameters. Therefore, as a proof of concept the SRM was primarily developed for the first layer only. This SRM is referred to as Layer-1 SRM further in this study.

It should be mentioned that this approach does not assume the first layer as an isolated layer through which some changes are taking place. Instead, the methodology for this SRM development is based on the fact that whatever changes are happening in the first layer are directly related to the changes in the layers beneath due to the CO_2 injection.

In the following sections the procedure of Layer-1 SRM construction is elaborated.

5.1.1 Reservoir Partitioning

As mentioned in the previous chapter, the reservoir model comprises 10 layers. A simplified schematic of the reservoir layers is depicted in Figure 14. Different colors in this figure demonstrate the classification of the reservoir layers in four distinct layers which contribute to data set generation.

In the top layer SRM, the first layer (Layer 1) and the second layer (Layer A) were considered individually. Layer 3 to layer 7, are the perforated layers in which CO_2 injection takes place. These three layers were lumped as Layer B. Similarly, the last three layers of the reservoir were grouped as Layer C.

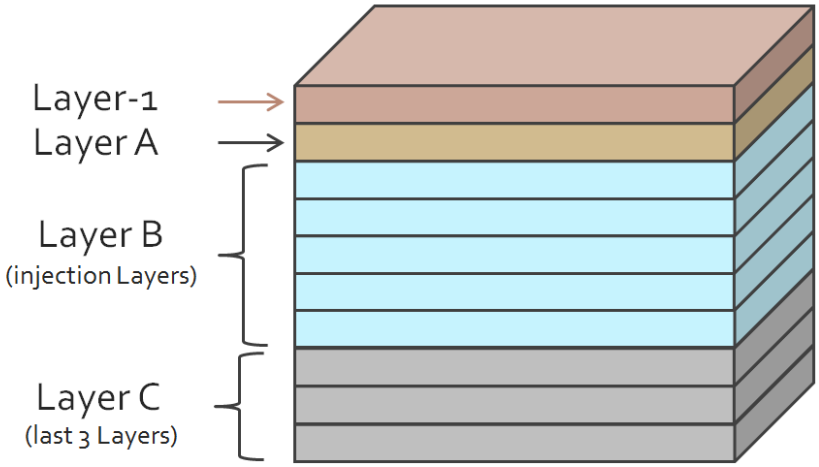

Figure 14. Schematic of the reservoir layers as contributing to the data set generation

5.1.2 SRM Development Procedure

SRM development comprises four major stages which can be listed as follows:

1. Based on the objective of the study a handful of reservoir simulation scenarios are conducted.
2. The required static and dynamic data are extracted and organized in order to generate a comprehensive spatio-temporal dataset which is further used to generate input data set for training neural network.
3. Several neural networks are designed and trained.
4. The neural network models are validated by applying them to a set of blind scenarios.

SRM development for the top layer of the reservoir is described in detail in the following sections.

5.1.3 Simulation Scenario Design

The training simulation runs are the simulation scenarios which provide the sample space of model input-output relationships for the neural network training purpose. Since the surrogate reservoir model is developed to observe the CO_2 injection under different operational constraints and different geological realizations, the training simulation runs were designed so that they take into account both areas of concern.

Considering the real case CO_2 injection scenario (the history matched model) as the base model, five other injection scenarios were designed. In two of them, the behavior of the system was investigated when higher amounts of CO_2 were injected over the same injection interval (with respect to the base model) and in others, the impact of CO_2 injection over longer injection periods were observed.

For the purpose of providing multiple geological realizations, two other realizations were generated. Considering the history matched model as the base case, in the first realization the porosity and permeability was non-uniformly increased in all ten layers of the reservoir to generate high porosity-high permeability case. In the second realization, the porosity and permeability of all layers of the reservoir was non-uniformly decreased through which the low porosity-low permeability case was generated.

According to the available field data for CO_2 injection in Otway CO_2 sequestration process, a total amount of about 593 MMSCF of CO_2 is injected into the reservoir during 8 months.

Considering "*G*" as the total amount of gas injected in real case injection scenario and "*L*" as the real case injection length, different injection scenarios were defined based on combination of these two parameters according to the table presented below.

Table 2. Six injection scenario schedule based on the amount of CO_2 and the injection duration

Total CO2 \ inj Length	1L	3L	5L
1G			
1.5G			
3G			

Consequently, 18 different simulation cases (three geological realizations under six injection schedules) were designed and conducted in CMG-GEM as the training scenarios.

5.1.4 Data Base Generation

Surrogate reservoir modeling process used in this study is a data driven approach and therefore the type and the amount of data provided for the training phase plays a crucial role in the success of the developed model.

The philosophy behind this type of proxy modeling is to represent the entire reservoir system and also the process which is taking place in the reservoir through data. Therefore data from multiple

domains is required to properly introduce the whole system and to represent the input-output relationship.

For this purpose two types of data were generally collected, which are static data and dynamic data.

The static data does not change over time and provides information related to the reservoir structure such as the location of the grid blocks, reservoir parameters such as porosity and permeability. The static data also includes other types of data which need to be calculated such as distance of the grid blocks to the injection well, relative grid distance to the boundaries of the reservoir, etc. Some other parameters, such as the initial values of pressure, phase saturation and CO_2 model fraction of each grid block, are also considered as constant variables with respect to time.

Dynamic data consists of the parameters in the well domain and the grid block domain. The parameters at the well domain are related to the well constraints which generally include production/injection rates or well bottom-hole pressures that are changing over time. Dynamic parameters at the grid blocks are the state variables of the systems (pressure, gas saturation and CO_2 mole fraction) which are changing over time.

The entire data, which is used in SRM development, is listed in the following diagram.

Table 3. List of data collected for SRM database generation

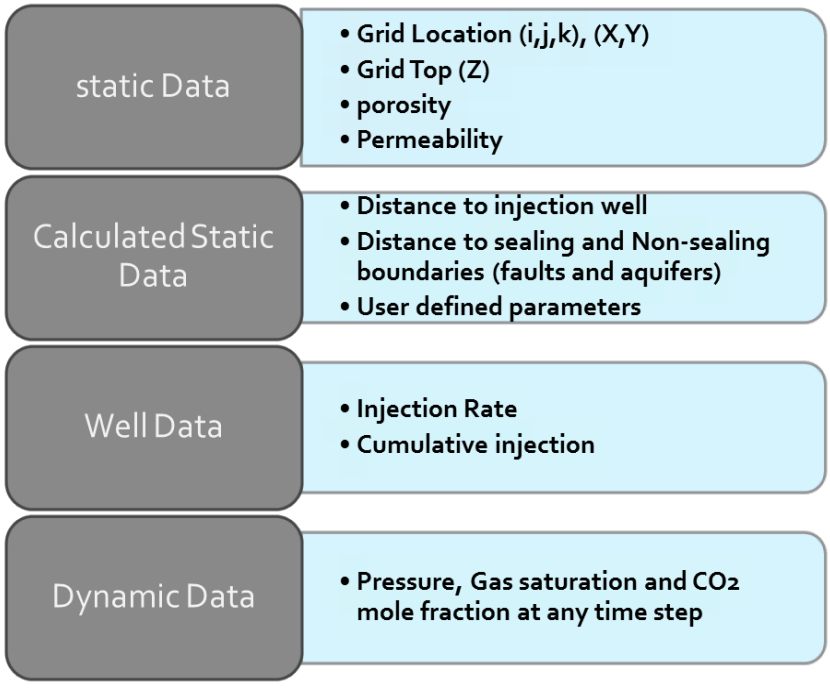

For some parameters such as porosity, permeability, pressure, saturation and CO_2 model fraction, data from both the main grid block and from the neighboring grid blocks is included in the data set. The surrounding blocks are identified in different ways known as "Tier System." The tier system which was used in this part of the study includes the four grid blocks around the main block.

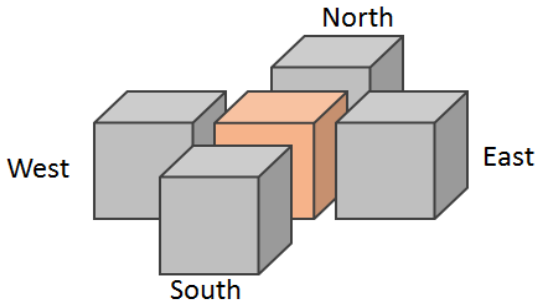

Figure 15. The tier system of each grid block used in Layer-1 SRM

Static Parameter Averaging

As mentioned earlier in this chapter, the data from layers beneath the first layer of the reservoir is also integrated into the data set. Data related to the lumped layers are averaged through different methods based on the type of the parameter.

The X and Y of each grid block remain the same and the average depth of each grid block is calculated through:

$$Z_{avg} = (Z_1 + Z_2 + \cdots .. + Z_n)/n$$

To obtain the average value of permeability and porosity, the geometric average and arithmetic average is used respectively.

$k_{avg} = \sum_{j=1}^{n} L_j \,/\, \sum_{j=1}^{n} \frac{L_j}{k_j}$ (L_j: layer depth, k_j : grid absolute permeability)

$$\Phi_{avg} = (\,\Phi_1 + \,\Phi_2 + \cdots \ldots + \,\Phi_n)/n$$

Dynamic Parameter Averaging

All the dynamic parameters including pressure, gas saturation, CO_2 mole fraction in gas phase, CO_2 mole fraction in water phase and global CO_2 mole fraction at different time steps for each

grid block of the new layers have been calculated through arithmetic averaging method, through following equations.

$$P_{avg} = (P_1 + P_2 + \cdots + P_n)/n$$

$$S_{avg} = (S_1 + S_2 + \cdots + S_n)/n$$

$$m_{avg} = (m_1 + m_2 + \cdots + m_n)/n$$

Distance Calculation

The distance of each grid block to the injection well is calculated based on the location of the grid and the location of the middle perforation of the well through the following formula.

$$D = \sqrt{(x_1 - x_2)^2 + (y_1 - y_2)^2 + (z_1 - z_2)^2}$$

In order to include the distance of the grid block to each boundary of the reservoir the distance of each grid block to every grid on the boundary is calculated through the above equation and then the minimum distance value is considered as the minimum distance to the boundary.

For all 18 scenarios, the required data was individually extracted from each CMG simulation scenario. Generating a data set which includes all the data listed in Table 3 required a software which is able to organize the CMG output files with a specific CMG format into the desired format, and furthermore to perform the required calculations for some of the parameters. This software was developed in Visual Basic and it is capable of transforming the CMG output files and other data files format to a comprehensive spatio-temporal data set which includes all the required data for neural network training input file.

5.1.5 Data Selection and SRM Input Generation

As mentioned in Table 2, data from different simulation cases, which have different injection duration, are integrated to develop the SRM. Therefore, in order to make use of all scenarios, the SRM was developed for three time steps during the injection interval, which are at the end of the first month of injection (Time-1), in the middle of the injection interval (Time-Mid), and at the end of injection interval (Time-End).

For SRM development, the input data were arranged so that besides the static and well data, the value of the dynamic parameters at time-0 (before injection takes place), is considered as the input. The output is the value of dynamic parameter of interest (pressure, gas saturation, and CO_2 mole fraction) at each grid block and at each time step of interest.

Adding Additional data

One of the advantages of using artificial intelligence to develop SRM is that any type of parameter that seems to provide additional information about the system can be integrated as an input and therefore it is not limited to a specific type of data.

In this part of the study as mentioned before, data are collected from multiple scenarios with different geological realizations and different amounts of total CO_2 injected, as well as different injection intervals. In order to identify different scenarios used in the data set, a new parameter was added to the data set, which is presented as "Scenario Index" and it is calculated as follows.

$$Scenario\ Index\ =\ Injection\ index\ \times\ Geological\ Index$$

where,

$$Injection\ index\ =\ G\ (MMMScf)\ \times\ L\ (Month)$$

Where, G is the total CO_2 injected in each simulation case and L is the total injection length.

Since the different geological realization is related to the different porosity and permeability value, the geological index is calculated through the following formula:

$$Geological\ Index = \varphi_{index} \times k_{index}$$

where,

$$\varphi_{\text{index}} = \frac{(\varphi_{max} - \varphi_{min})}{STD(\varphi)}$$

$$k_{\text{index}} = \frac{(k_{max} - k_{min})}{STD(k)}$$

Adding all the customized data, for all gird blocks at the time step of interest, SRM input generation is accomplished.

5.1.6 Neural network Construction and Training

The generated input file was used to construct several artificial neural networks which include the networks for pressure, gas saturation, and CO_2 mole fraction at each time slice.

"Back Propagation" algorithm was used as the training method. In this method the error is fed back to the network by the end of each training epoch (C. M. Bishop 1995). All the networks contain one hidden layer and one output. A typical neural network architecture used in this work is depicted in Figure 16.

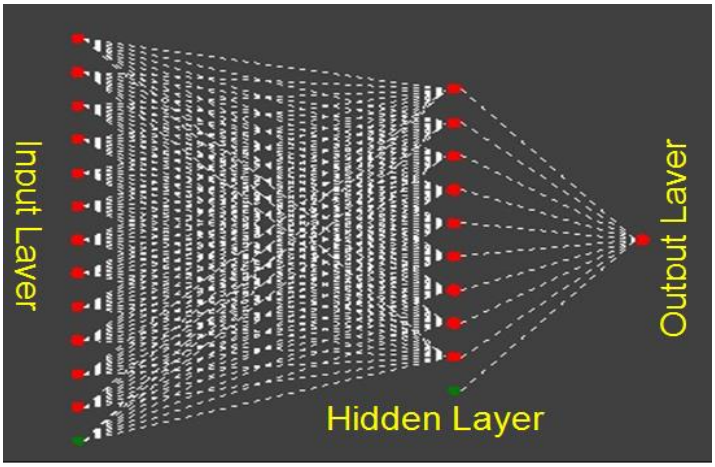

Figure 16. Typical NN architecture for the current SRM

Previous similar works on SRM development for several subjects in petroleum engineering have shown that adding more hidden layers to the network architecture does not significantly affect the accuracy of the results, and therefore in this research the number of hidden layers remains unchanged. For the purpose of adding more complexity to the network structure, the number of neurons in the hidden layer can be increased.

During the training process, performance of the neural networks in predicting the output parameter can be investigated by observing the cross plots of the predicted versus simulation output data, scatter plot which shows the predicted and actual value of the parameter and the calculated R-squared value.

5.1.7 Validation with Blind Scenario

The last step in the SRM development process is to verify the result of the constructed SRM when it is applied to a blind case. A blind case is defined as a simulation scenario which has not been used in neural network training.

Therefore, a blind simulation scenario was defined and run in which 2G (1.187 BCF) total amount of CO_2 is injected into the reservoir (history matched model) within 2L (16 Months). The figure below demonstrates the blind injection scenario selection based on the amount of CO_2 injection and the injection duration.

Table 4. Blind set injection scenario for Layer-1 SRM

inj Length / Total CO2	1L	2L	3L	5L
1G				
1.5G				
2G				
3G				

The required data was extracted and SRM input was generated for Time-1, Time-mid, and Time-end, as well as post injection time intervals of 100 and 500 years after injection. The corresponding SRM was applied to this blind scenario and results are generated.

5.1.8 Post Injection Scenario

In any CO_2 sequestration project in order to insure that the injected CO_2 will remain safely within the reservoir structure for a long time, the CO_2 movement in reservoir layers must be studied for a long interval of time. Therefore, all the reservoir simulation scenarios in this part of the study were performed for 500 years after injection and SRM is developed for the post injection interval to investigate the dynamic parameter distribution throughout the reservoir after a long time under different injection scenarios.

5.2 Layer-1 SRM Results

In this section, the developed SRM is first applied to a scenario which was included in the training set and then the results of SRM is presented when it is applied to a blind scenario.

5.2.1 Training Set Results

The constructed neural networks for pressure, gas saturation, and CO_2 mole fraction at the three time steps of interest were individually applied to scenario#6 data set (as an example). In this scenario, the amount of CO_2 injected is 1.78 BCF and this amount is injected into the reservoir during 40 Months.

In the following sections, the 2D distribution maps of pressure, gas saturation, and CO_2 mole fraction in the first layer of the reservoir are presented for the three time intervals during the injection period. In each of them, SRM result is compared to the CMG output and the error distribution is depicted for each parameter.

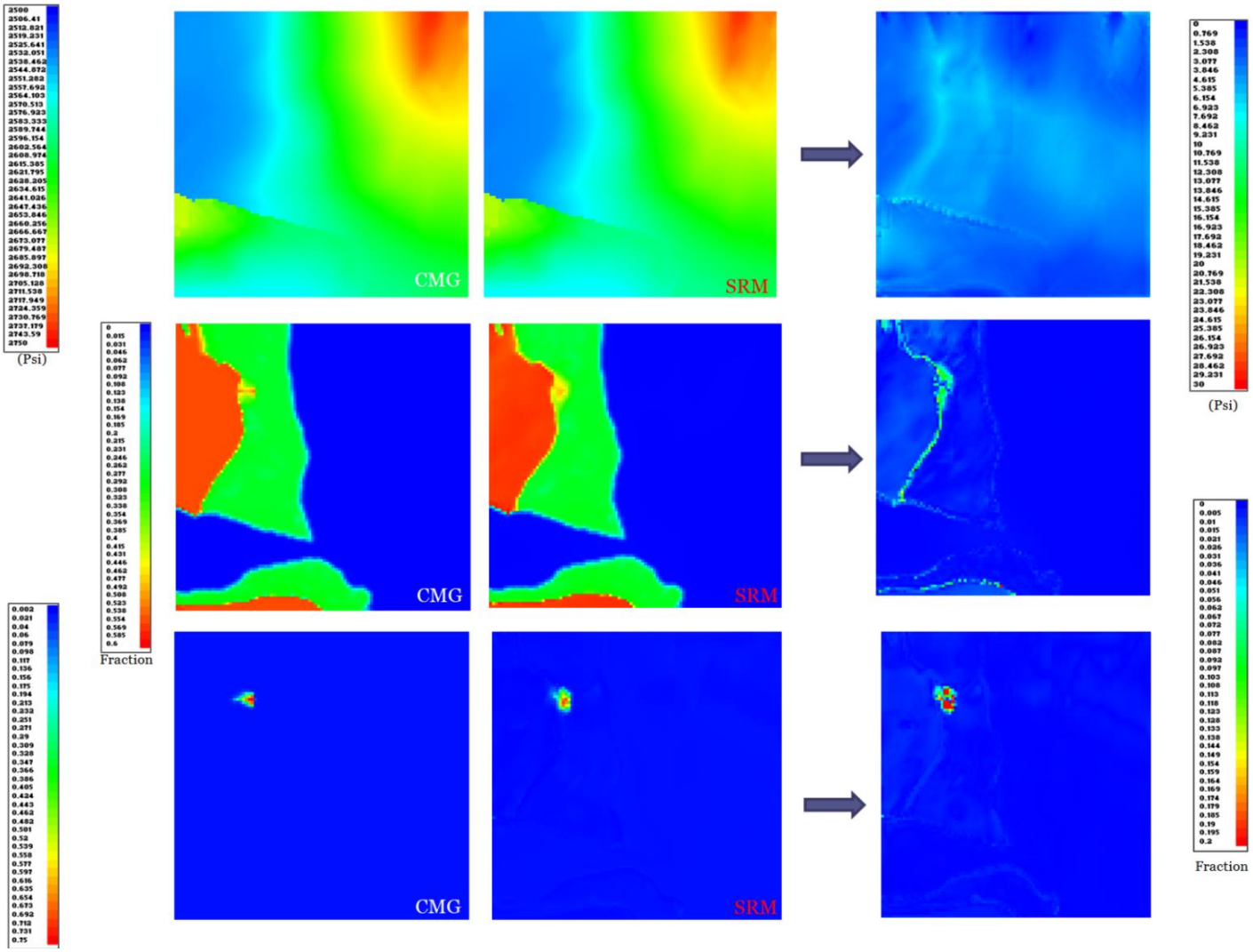

Figure 17. Distribution maps of Pressure, Gas saturation and CO_2 mole fraction (top to bottom) in the first layer of the reservoir (left to right: CMG output, SRM result and Error)-After 1 month of injection

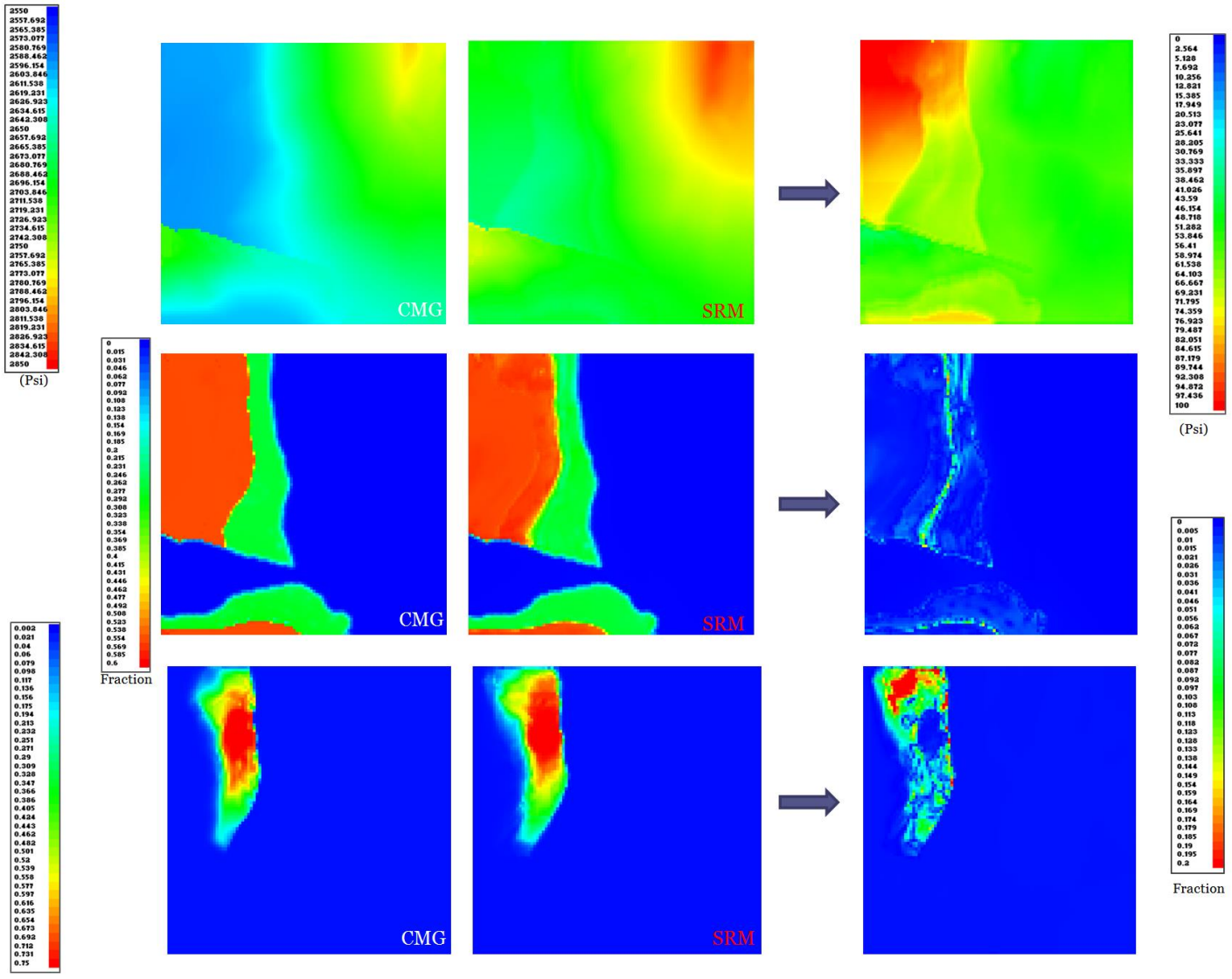

Figure 18. Distribution maps of Pressure, Gas saturation and CO_2 mole fraction (top to bottom) in the first layer of the reservoir (left to right: CMG output, SRM result and Error)-After 20 months of injection

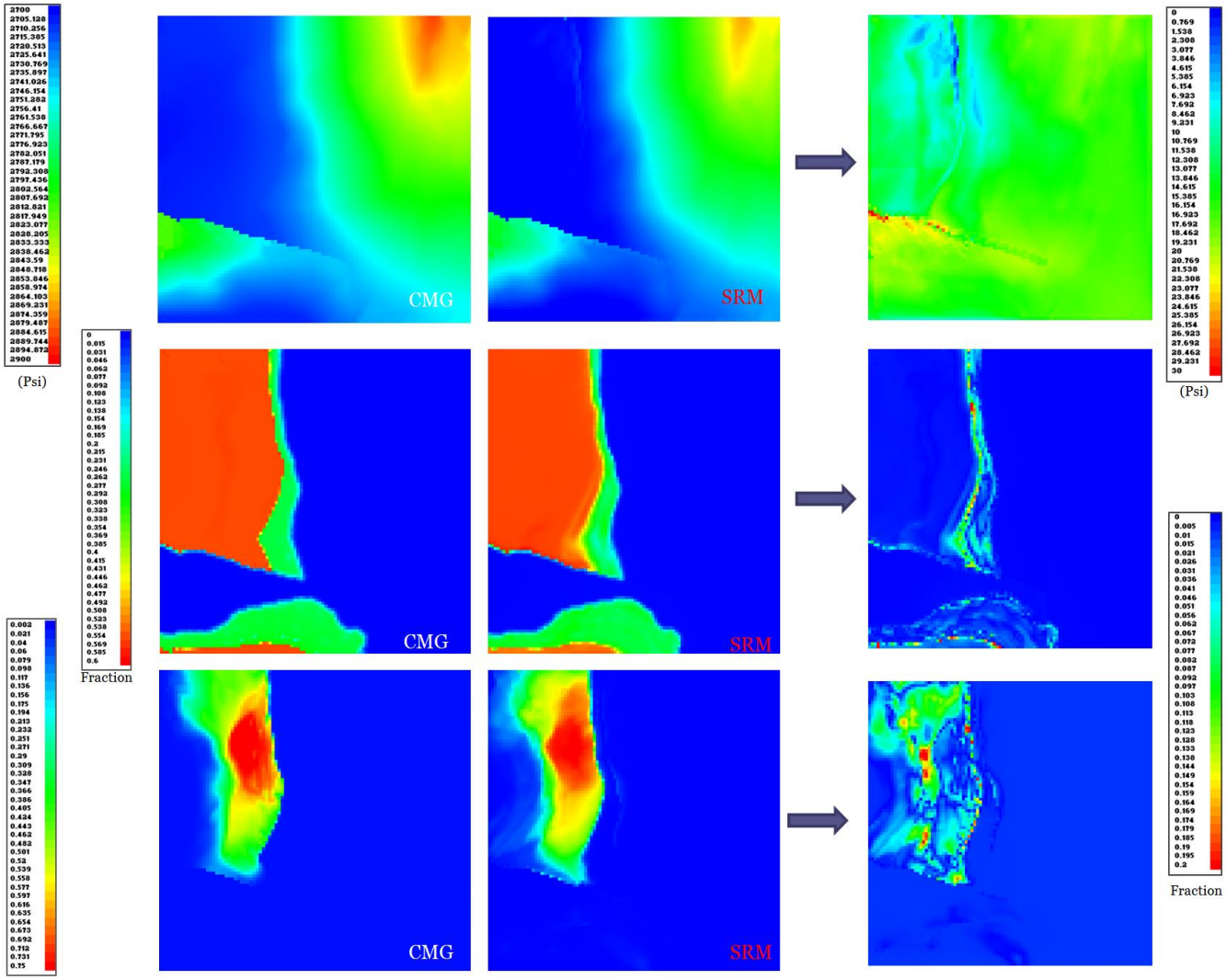

Figure 19. Distribution maps of Pressure, Gas saturation and CO_2 mole fraction (top to bottom) in the first layer of the reservoir (left to right: CMG output, SRM result and Error)-After 40 months of injection

5.2.2 Blind Set Results

In order to validate the results of SRM in generating the dynamic parameter distribution the same networks were applied to the blind case which was presented in the previous section and distribution maps were generated.

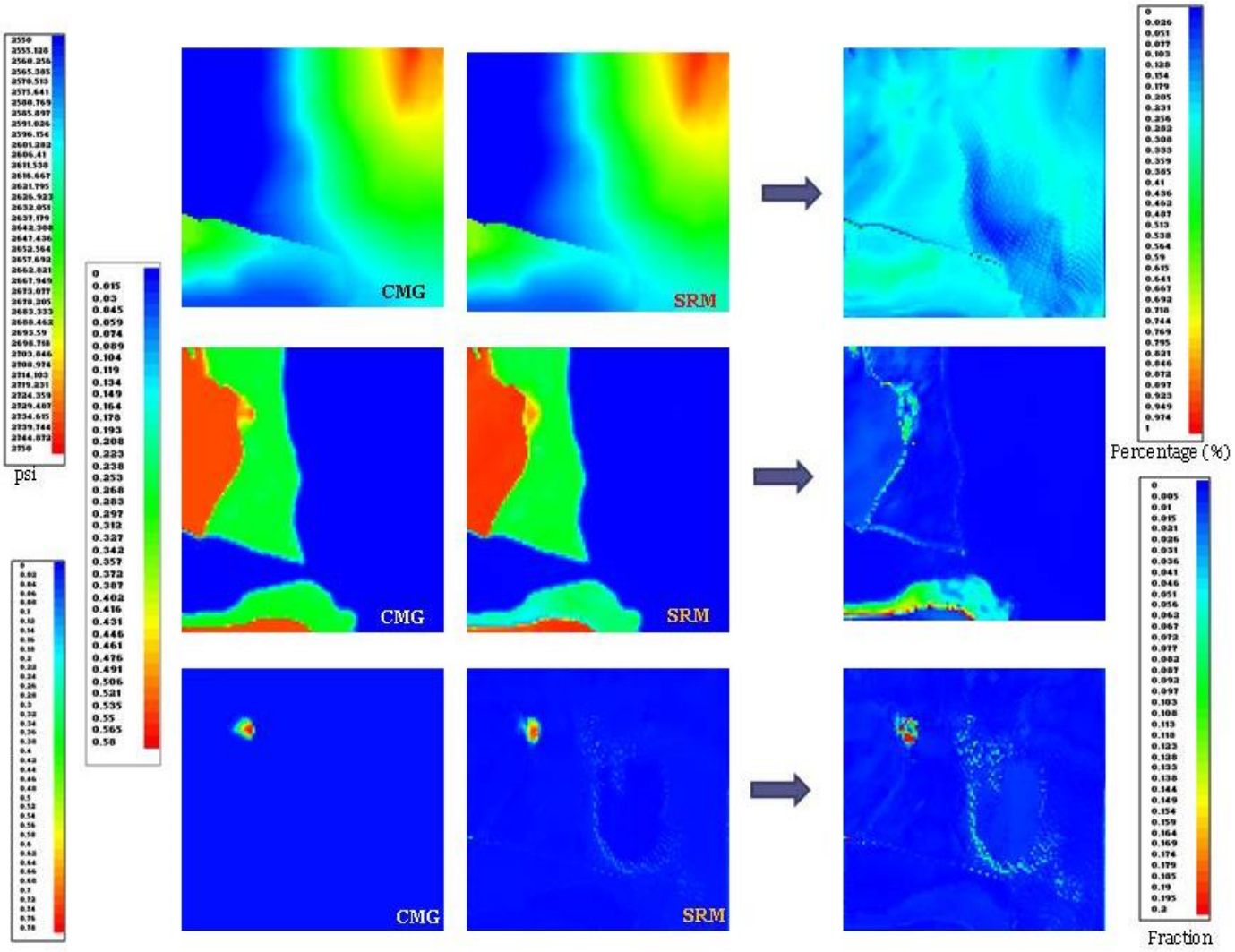

Figure 20. Distribution maps of Pressure, Gas saturation and CO_2 mole fraction (top to bottom) in the first layer of the reservoir (left to right: CMG output, SRM result and Error)-After 1 month of injection

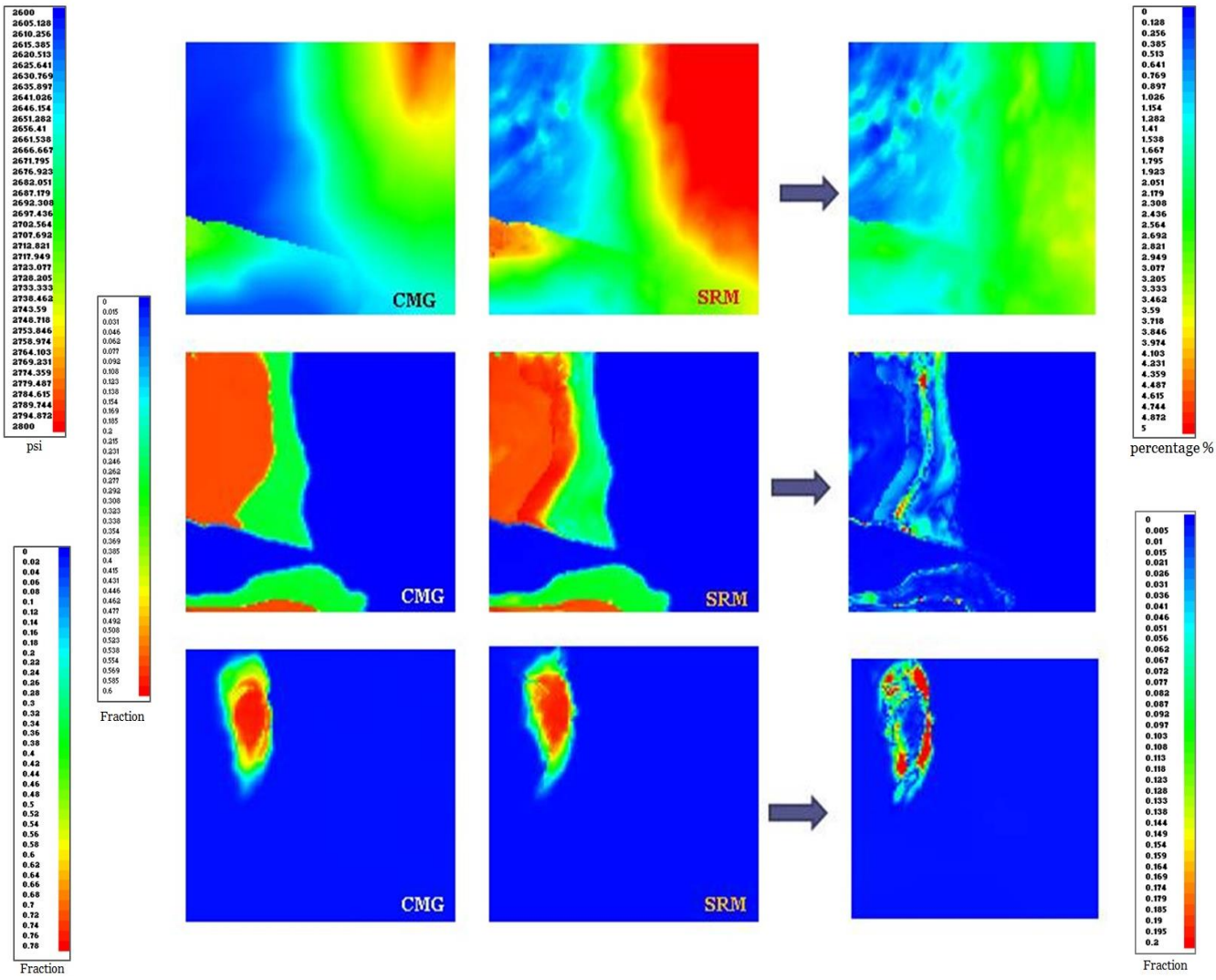

Figure 21. Distribution maps of Pressure, Gas saturation and CO_2 mole fraction in the first layer of the reservoir ((left to right: CMG output, SRM result and Error)-After 8 months of injection

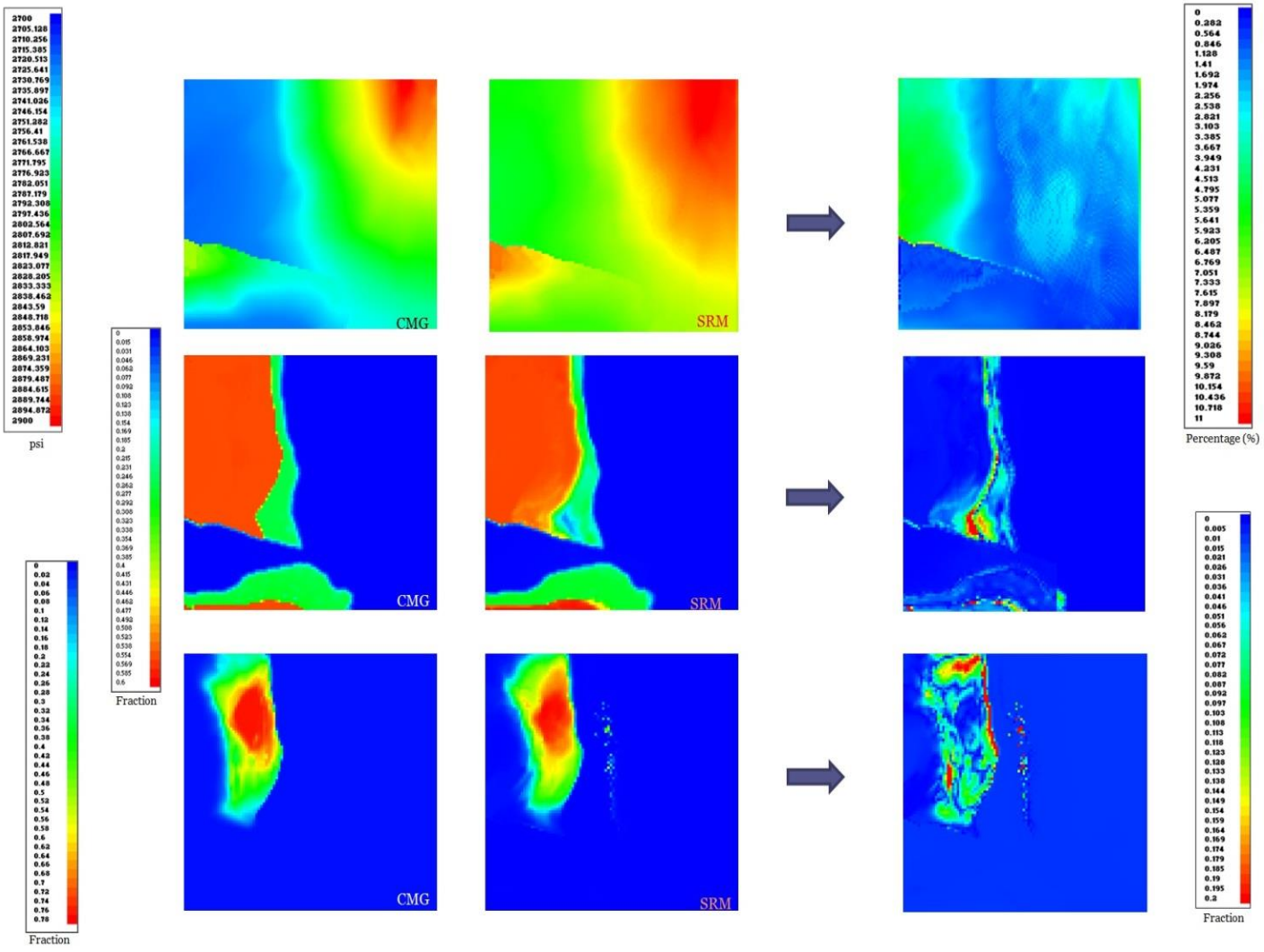

Figure 22. Distribution maps of Pressure, Gas saturation and CO_2 mole fraction (top to bottom) in the first layer of the reservoir (left to right: CMG output, SRM result and Error)-After 16 months of injection

5.2.3 Post Injection Results

The developed SRM for pressure, gas saturation and CO_2 mole fraction in 100 and 500 years after injection was stopped were applied to scenario#6 data and the SRM result is compared to the CMG output and the error distribution is depicted for each parameter in the mentioned post injection times.

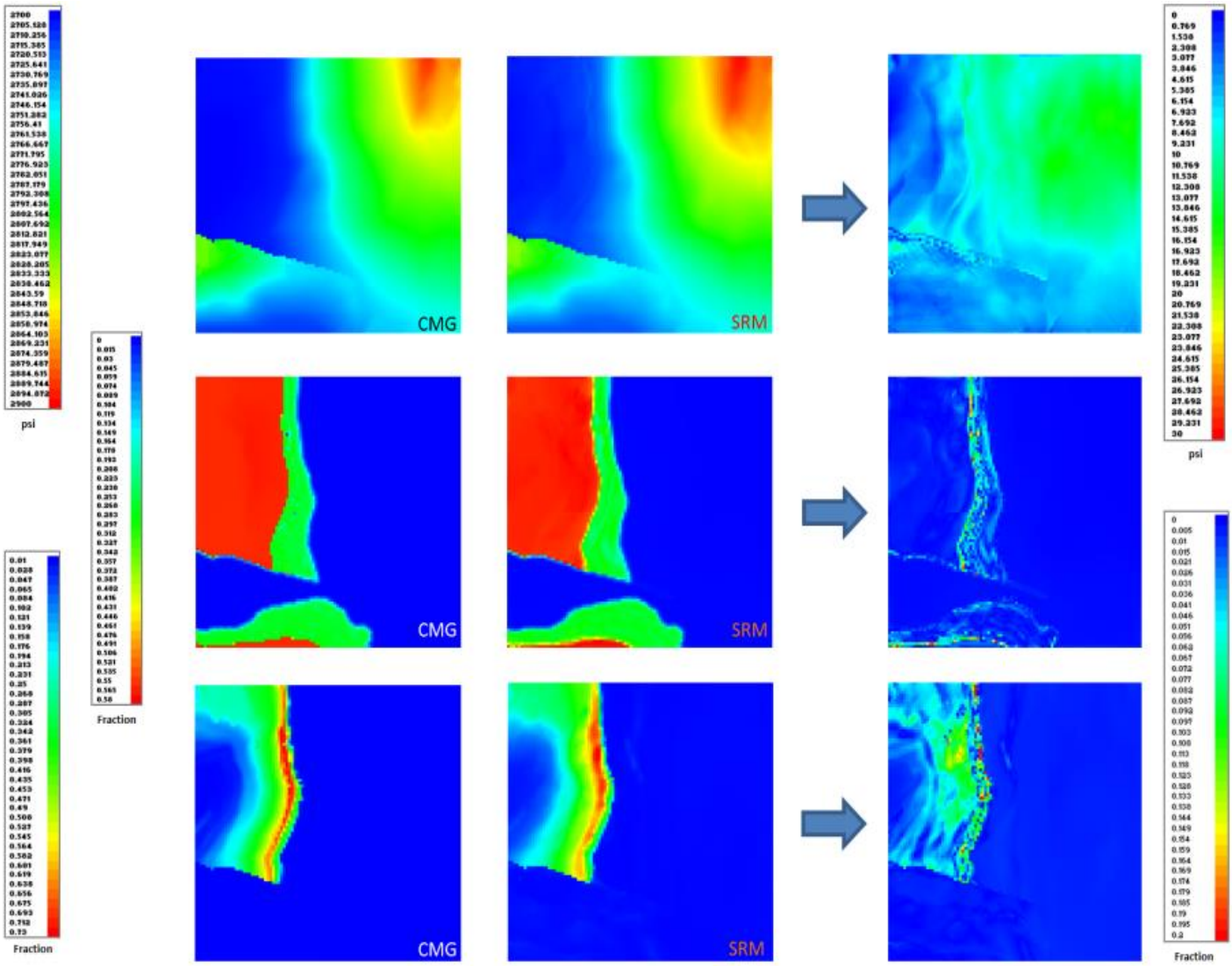

Figure 23. Distribution maps of Pressure, Gas saturation and CO_2 mole fraction (top to bottom) in the first layer of the reservoir (left to right: CMG output, SRM result and Error)-100 years after end of injection

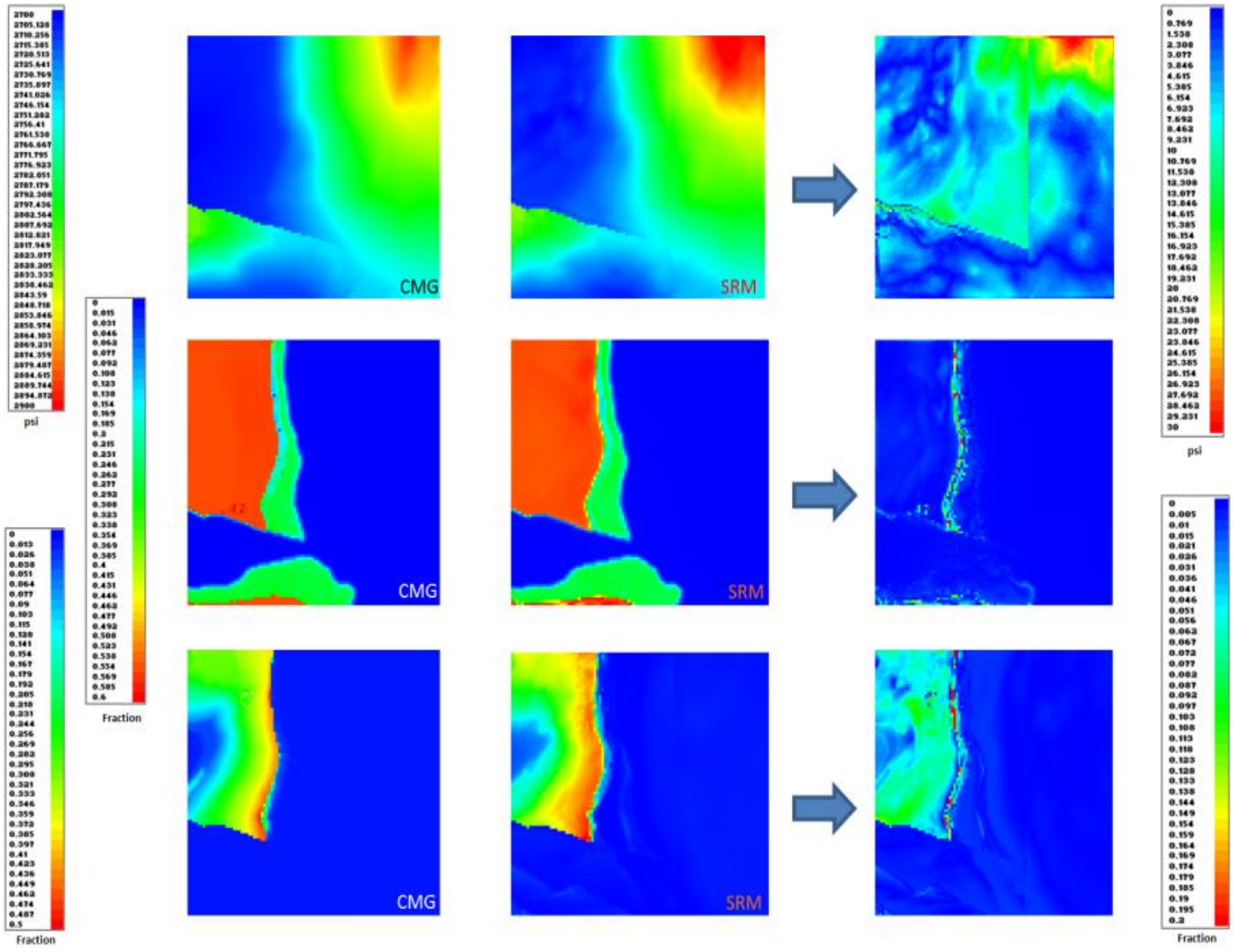

Figure 24. Distribution maps of Pressure, Gas saturation and CO_2 mole fraction (top to bottom) in the first layer of the reservoir (left to right: CMG output, SRM result and Error)-500 years after end of injection

5.3 Layer-1 SRM Discussion

The result of the developed SRM for the first layer of the reservoir demonstrates the capability of the SRM to generate the output of the numerical reservoir simulation model at the grid block level. However, the result which is obtained so far does not reflect the ultimate SRM accuracy as a proxy model, and therefore some modifications are required to improve the results. Some of the factors that could be responsible for the large amount of time required for SRM development or the amount of errors in the presented SRM results are as follows:

1. Although this SRM was developed for the first layer of the reservoir, the data set included a huge amount of data (180,000 data records). Including this amount of data makes the training process significantly time consuming and thus considerably inefficient. This process can become more efficient by reducing the dimensionality of the data set.
2. This SRM was developed based on the data extracted from three different geological realizations as well as different injection scenarios. The result of SRM might be improved if these two contexts are studied separately.
3. The accuracy of the SRM to predict the dynamic parameters' distribution might be improved by including more injection scenarios in the training process.
4. To develop the current SRM the CO_2 injection scenarios have different injection intervals, and therefore the SRM was developed only for three specific time steps during the injection interval. Using this scheme for SRM development may not be as efficient as the SRM that is developed for a constant injection interval which includes consecutive time steps.

The upcoming chapters address the aforementioned issues through different SRM development approaches.

Since in developing grid-based SRM we are dealing with a massive amount of data which represents all the grid blocks of a numerical reservoir model, the first issue mentioned above regarding the efficiency of the SRM development becomes a significantly important issue for any grid-based surrogate reservoir modeling. As a possible solution to this problem a "Data Sampling" approach is proposed.

Due to the importance of this subject and the fact that further in this work, data sampling will be used as an approach for data reduction, an individual chapter is devoted to this subject. In this chapter, two different sampling techniques are presented and their performance is investigated when both of them are applied as a data reduction tool for SRM development.

CHAPTER 6.
DATA SAMPLING AS A DATA REDUCTION TOOL

Data sampling refers to the practice of selection of a sub set from the entire population. Sampling should be performed in such a way to ensure that the selected data are a proper representation of the whole system, and therefore the analysis that is performed on the selected portion of data can be generalized or applied to the entire data set. However, the approximation models are generally generating the results more accurately for the points in the vicinity of the sampled points (Forrester, Sobester and Keane 2008).

In grid-based surrogate reservoir development we are dealing with an enormous amount of data. As the reservoir simulation tools, and also the computer hardwares are advancing, the number of grid blocks that can be used in the numerical reservoir models is significantly increasing. If all the data from all grid blocks of the reservoir are included in the training process, a massive amount of time would be required to develop and train a neural network that is able to predict the outputs of the system. This problem is referred to as the so called "curse of dimensionality."

A solution to address this problem is "Data Sampling," which enables us to make use of a portion of data that are a proper representation of the entire system. This process makes the neural network training process significantly more efficient.

In this work, two different techniques are used for data sampling. The two approaches are described below in details. The first is based on spatial parameter distribution at each time step and the second one is based on the changes of parameters at each time step with respect to time zero. The efficiency of two methods were verified when they were applied to the same data set based on which the layer-1 SRM was developed.

6.1 Data Sampling Based on Parameter Distribution

In this approach, a data sampling method was used which samples data based on distribution of a parameter versus one or more other parameters. A Visual Basic computer code was developed to sample the data and generate the SRM input files for each parameter of pressure, gas saturation, and CO_2 mole fraction at each time step.

In this part of the study, the same simulation runs as used in previous chapters were used to generate a comprehensive data set.

In order to sample data for pressure models, a plot of pressure versus depth at the desired time step was generated. Based on a user defined number of segments between the minimum and maximum value of each parameter, gridding was performed on the plot.

For the purpose of data sampling for gas saturation and CO_2 mole fraction, these parameters were plotted versus location (X and Y) and the same procedure was followed for gridding the plot.

In the next step, a portion of data (10% in this case) was randomly selected out of each generated grid (2D for pressure plot and 3D for gas saturation and CO_2 mole fraction).

6.1.1 SRM Based on First Approach Sampling

Using the sampled data through the above procedure, SRM input was generated for each parameter individually at each time step.

The input files were used to develop and train 3 neural networks at each time step (one month after the start of injection, in the middle of the injection, and at the end of injection).

The constructed networks were applied to all grid blocks of the first layer of the reservoir and the results were visualized in 2D distribution maps of pressure, gas saturation, and CO_2 mole fraction.

Comparing the SRM results with the simulation output (for scenario 1, as an example) generally shows a very poor prediction of the parameters especially for the CO_2 mole fraction.

The 2D distribution maps of the three parameters are depicted in the following figures for the middle and the last time steps.

It should be mentioned that the color bar scale chosen in this section differs from those presented in the previous chapter. The same scale (as used in this section) will be applied to present the further results throughout this study.

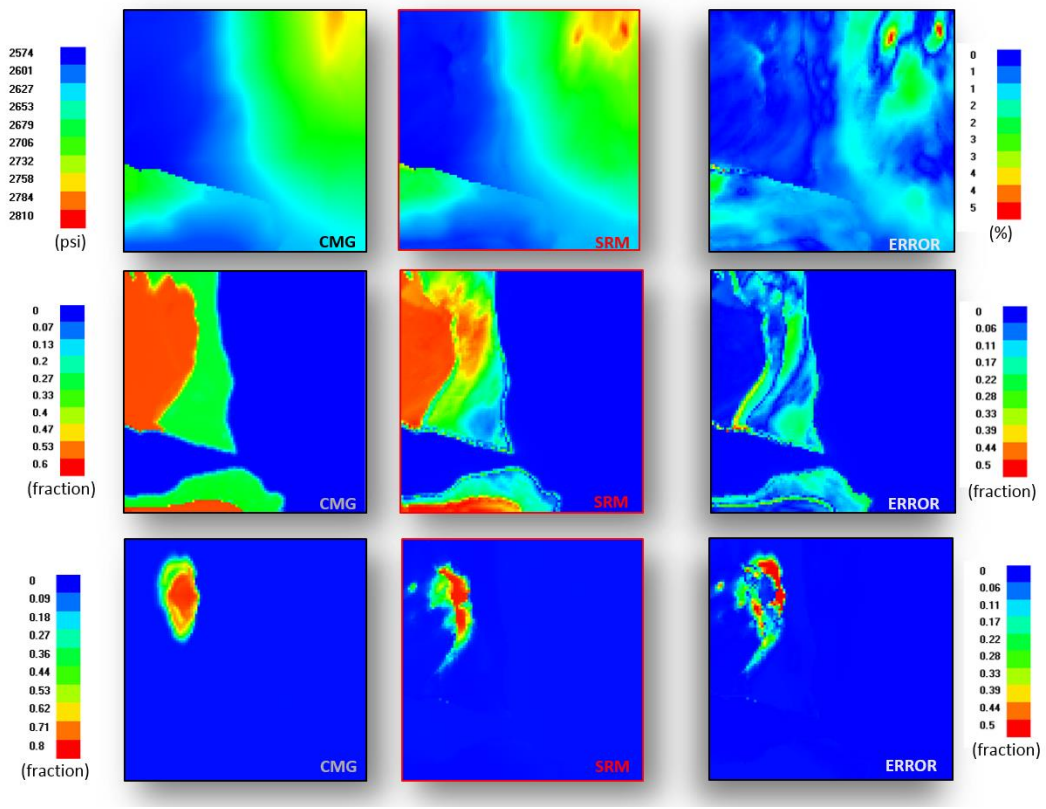

Figure 25. Distribution maps of Pressure, Gas saturation and CO_2 mole fraction (top to bottom) in the first layer of the reservoir (left to right: CMG output, SRM result and Error)-4 months after injection (using sampling approach 1)

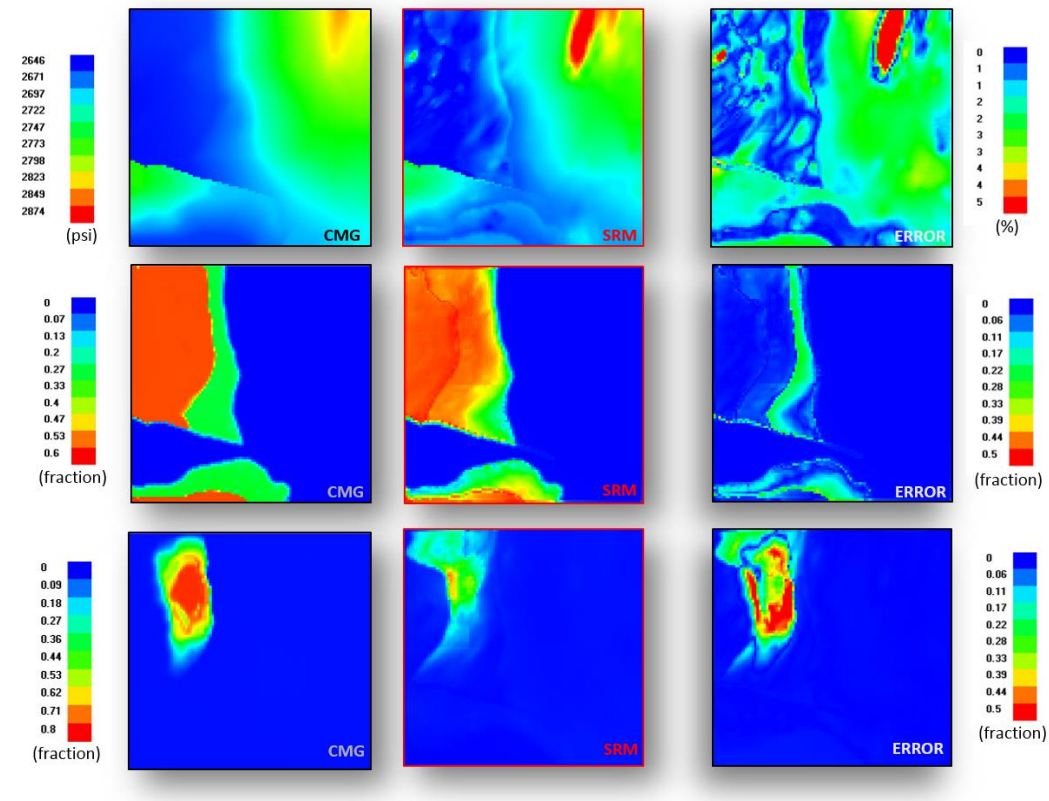

Figure 26. Distribution maps of Pressure, Gas saturation and CO_2 mole fraction (top to bottom) in the first layer of the reservoir (left to right: CMG output, SRM result and Error)-8 months after injection (using sampling approach 1)

6.2 Data Sampling Based on Change of Dynamic Parameters

Since in numerical simulation models we are dealing with the changes in dynamic parameters at each time step, the second proposed sampling method is based on the changes in dynamic parameters of the reservoir at each time step rather than the parameter distribution.
Prior to sampling, some analyses were performed on the extent of changes of dynamic parameters at different time steps during the injection.

In this study the difference between each parameter of pressure, gas saturation and CO_2 mole fraction at each time step with respect to time-0 was calculated. For each parameter at the desired time step a histogram was generated individually based on minimum and maximum change of parameter to observe how many gird blocks are changed to which extend.

As an example, the histograms of all the existing data which was generated for individual parameters at the mid time step (middle of the injection) are presented in Figure 27.

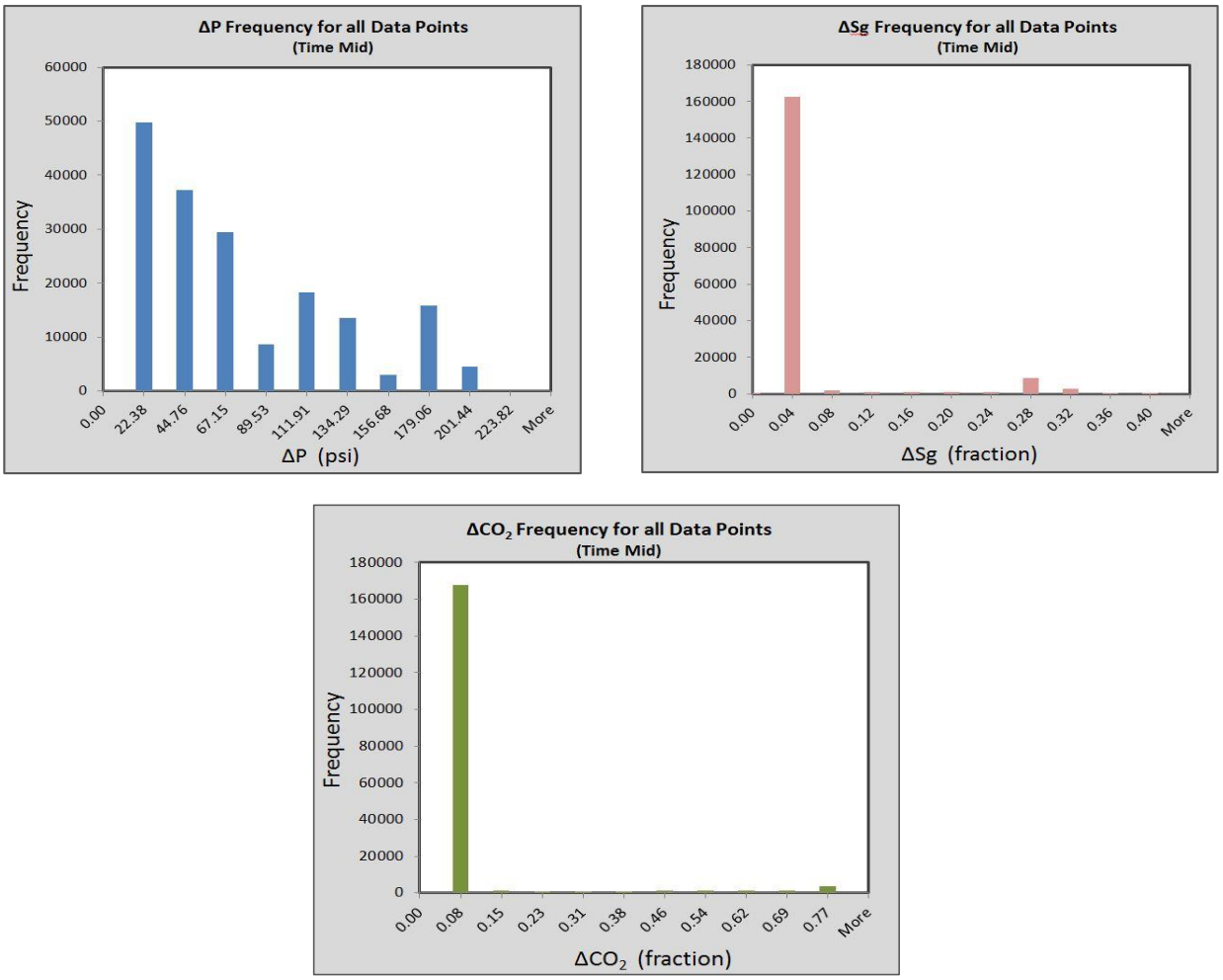

Figure 27. Histograms of ΔP, ΔSg and ΔCO_2 at the middle of injection

As demonstrated in the above histograms, the majority of the grid blocks are exposed to lower amounts of changes during injection. Therefore, it can be concluded that sampling will be more efficient if it is performed by taking into account where the higher amount of change takes place. This process results in a smarter data sampling for SRM development since the change of dynamic parameters are one of the most important items that we are looking for in reservoir modeling.

Using this concept, a Visual Basic computer code was developed to take the comprehensive dataset at each time step as input and generate the histograms based on the changes of the data. This code provides the facility for the user to choose the percentage of the data which is desired to be selected. The identified number of data is selected and SRM input is generated individually for each parameter of pressure, gas saturation, and CO_2 mole fraction at the time step of interest.

6.2.1 SRM Based on Second Approach Sampling

Using the generated input files, 9 neural networks were trained and applied to all grid blocks of the reservoir top layer for all scenarios. The results of this SRM in generating the dynamic parameter distribution, when applied to scenario 1, at two time steps are demonstrated in the following sections.

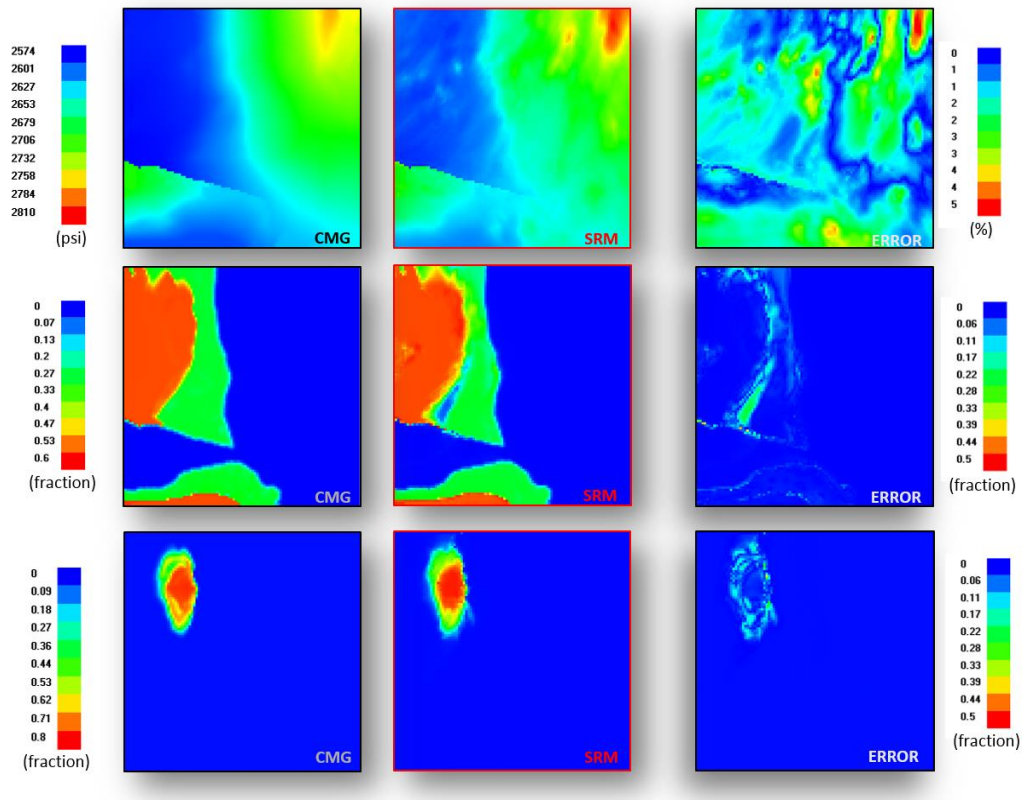

Figure 28. Distribution maps of Pressure, Gas saturation and CO_2 mole fraction (top to bottom) in the first layer of the reservoir (left to right: CMG output, SRM result and Error)-4 months after injection (using sampling approach 2)

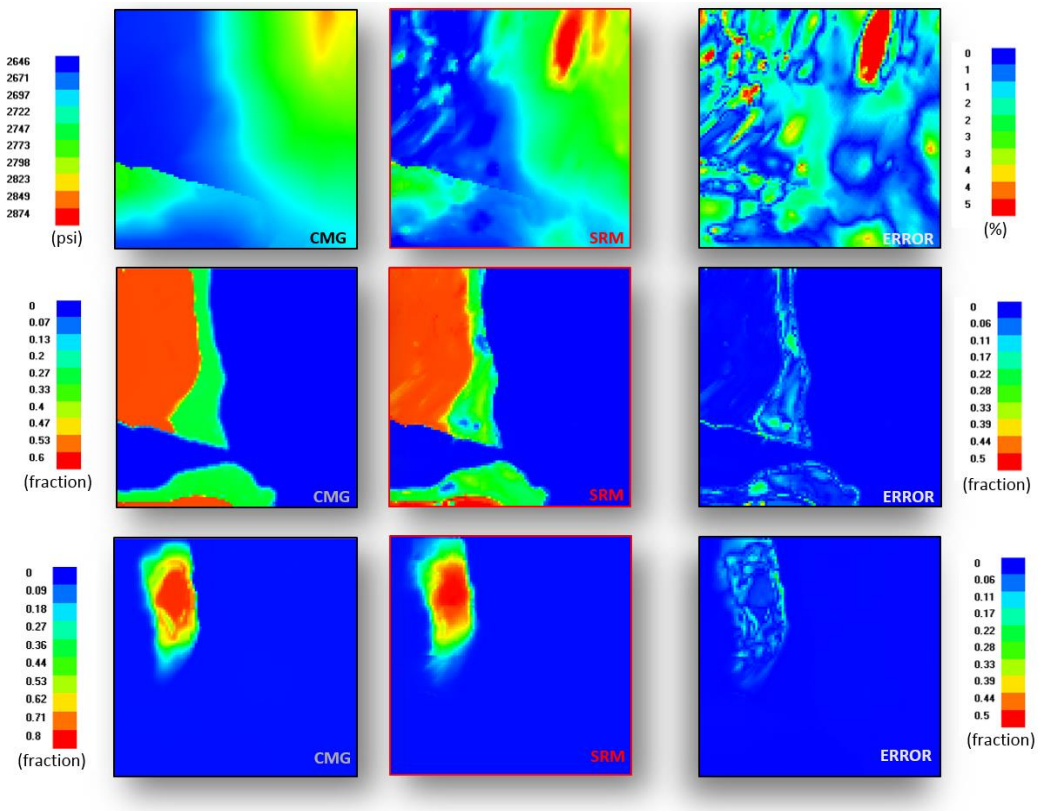

Figure 29. Distribution maps of Pressure, Gas saturation and CO_2 mole fraction (top to bottom) in the first layer of the reservoir (left to right: CMG output, SRM result and Error)-8 months after injection (using sampling approach 2)

The results of SRM prediction using the second approach sampling show a significant improvement compared to those of the first approach; especially for the gas saturation and CO2 mole fraction distribution. Therefore, the second sampling method will be applied further in this work.

6.3 Application of Data Sampling on New Simulation Runs

In Chapter 5, SRM was developed using three geological realizations of the reservoir each of which was conducted under six injection scenarios. In this section, we would like to investigate the result of SRM when it is developed using a single geological model and several injection scenarios.

As mentioned before, the injection scenarios are defined based on the changes in the amount of injected CO_2 as well as the injection duration. In the developed SRM no specific procedure was followed to select the six combinations of these two parameters, and therefore the injection scenarios were defined based on the values presented in Table 2. In this part of the study, 10 new numerical reservoir simulation scenarios are designed based on a more systematic approach

which is called “design of experiment” and is commonly used when more than one parameter is involved in defining different scenarios.

6.31. Design of Experiment (Latin Hyper Cube Sampling Method)

Assuming that the maximum CO_2 injection that is going to be performed in this sequestration project reaches to 3 times the real case, and the maximum injection interval can be extended up to 5 times the real case, 10 different injection scenarios are designed based on these two parameters using Latin Hypercube Sampling method (LHS).

To ensure that the constructed SRM is able to generate the results between minimum and maximum boundaries of the involved parameters, the four combinations of the minimum and maximum amount of total CO_2 injected (denoted as G) and injection duration (denoted as L) are manually selected to be included in the simulation runs (shown in red stars with circle, in Figure 30). The other six remaining combinations are selected by using LHS method through a computer code which was developed in MATLAB. There are four types of LHS that can be used to generate the desired combinations. In this work the “LHS-Correlation” type was used through which correlation between the generated combinations is minimized.

The following figure shows all combinations of G and L, which are used to design the simulation scenarios.

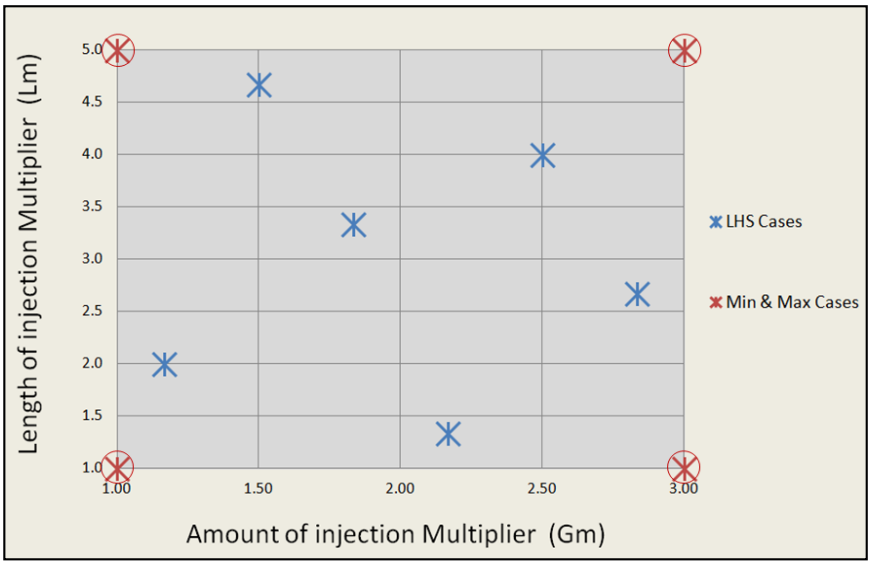

Figure 30. Final G-L multiplier combination obtained through LHS Method (Blue) and the min-max value of G and L multipliers (Red)

Having the generated G and L multipliers for 10 scenarios, the amount of CO_2 and the injection duration was calculated for each scenario and presented in Table 5.

Table 5. The calculated amount and length of injection for 10 simulation scenarios

G (MMScf)	L (Month)
1.68E+03	21
8.90E+02	37
1.48E+03	32
6.92E+02	16
1.29E+03	11
1.09E+03	27
5.93E+02	8
1.78E+03	8
5.93E+02	40
1.78E+03	40

A computer code was developed in MATLAB to generate the injection schedule for 10 scenarios based on the table above and also considering the base case monthly injection rate. The following plot demonstrates the generated CO_2 injection schedule for the 10 scenarios.

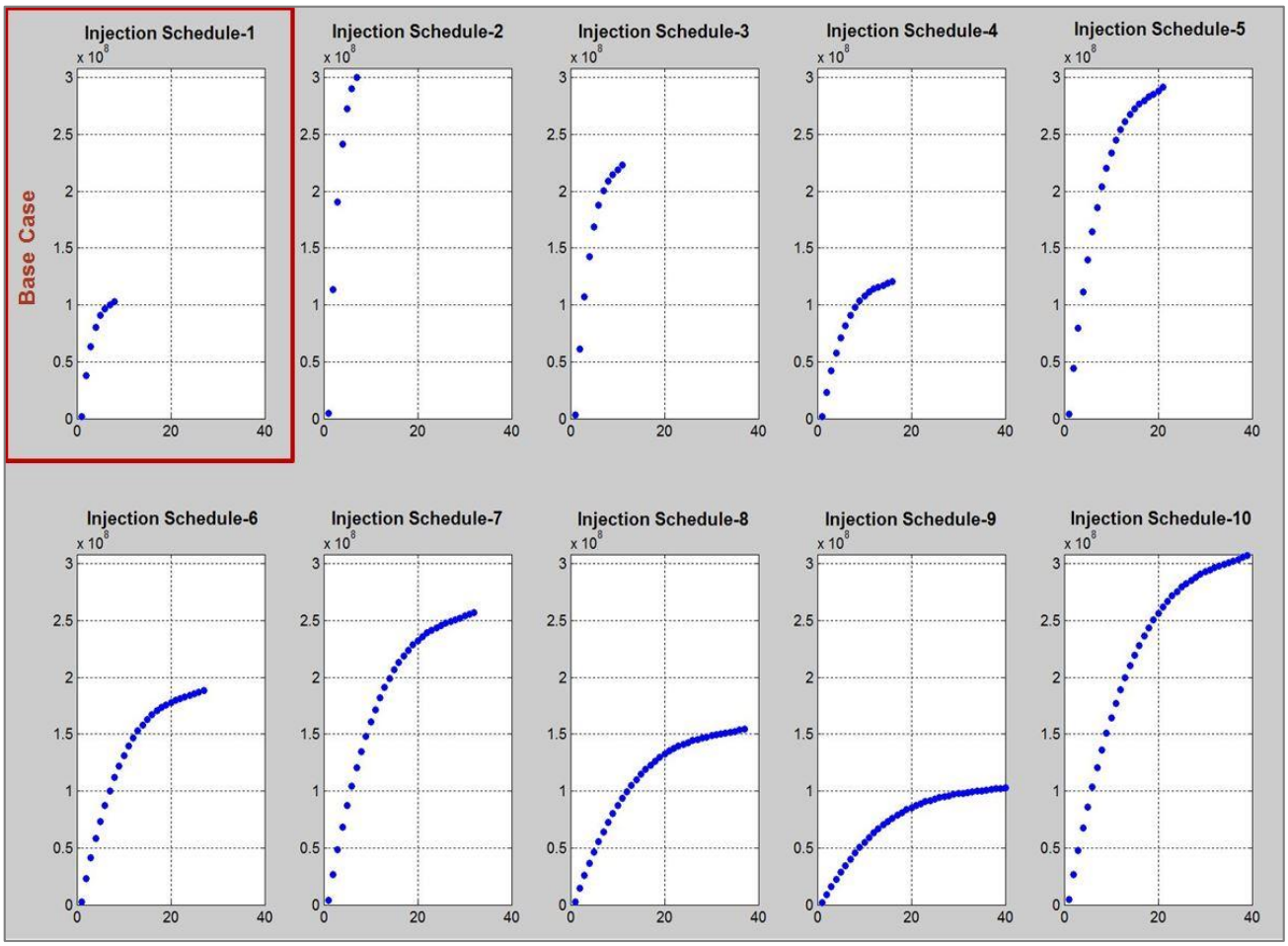

Figure 31. Injection schedule generated for 10 simulation scenarios

6.3.2 Dataset Generation and Data Sampling

A comprehensive spatio-temporal data set was generated to properly introduce the entire system as well as the changes which are taking place within this system. The data set again includes several types of data such as reservoir structure and properties, initial distribution of dynamic parameters, well data, and dynamic data from the time step of interest.

Due to the large dimensionality of the data set, when all the data are incorporated, a computer code was developed in Visual Basic to arrange the extracted data from CMG reservoir simulation scenarios into the desired dataset format. Next it performs the required calculations for some parameters such as distance of each grid block to the boundaries, average value of the parameters in the adjacent grid blocks, and etc.

Integrating data from 100,000 grid blocks of each simulation scenario, results in a huge data matrix of 1,000,000 rows and some tens of columns. This amount of data is far more than the limit which can be utilized to develop and train a neural network. Therefore, in order to be able to properly use the available data, a portion of data should be selected. The sampled data must carry the most important information regarding the changes that are taking place in the system.

Using the second sampling approach, which was presented earlier in this chapter, 10% of the data (100,000) was selected to be used for neural network training process.

6.3.3 Neural Network Development and Training

In order to develop the SRM for this study, data from different simulation cases were integrated which have different injection durations. Therefore, neural network input was generated for three time steps during the injection interval similar to the previous models. The networks were developed and trained individually for pressure, gas saturation and CO_2 mole fraction at three time slices.

6.3.4 Result of the Neural Network Deployment

In order to generate the dynamic parameter distribution in the entire grid blocks of the reservoir, the developed neural networks were applied to one of the scenarios (scenario#4, in which a total of 0.687 BCF of CO_2 was injected into the reservoir within 16 months).

As an example, the 2D distribution maps of the three parameters at the first layer of the reservoir at two time steps (in the middle of injection and at the end of injection) are presented below. In each of them, SRM result is compared to its corresponding CMG output.

Observing the results presented in Figure 32 and Figure 33 and comparing them to the results shown in Figure 28 and Figure 29, it is concluded that the prediction accuracy is improved significantly when the number of numerical reservoir models is increased reasonably through a systematic approach. Therefore, in a data driven approach it is not just the methodology that can lead to a successful proxy model; the type and amount of data which are introduced to the model are of the same significance.

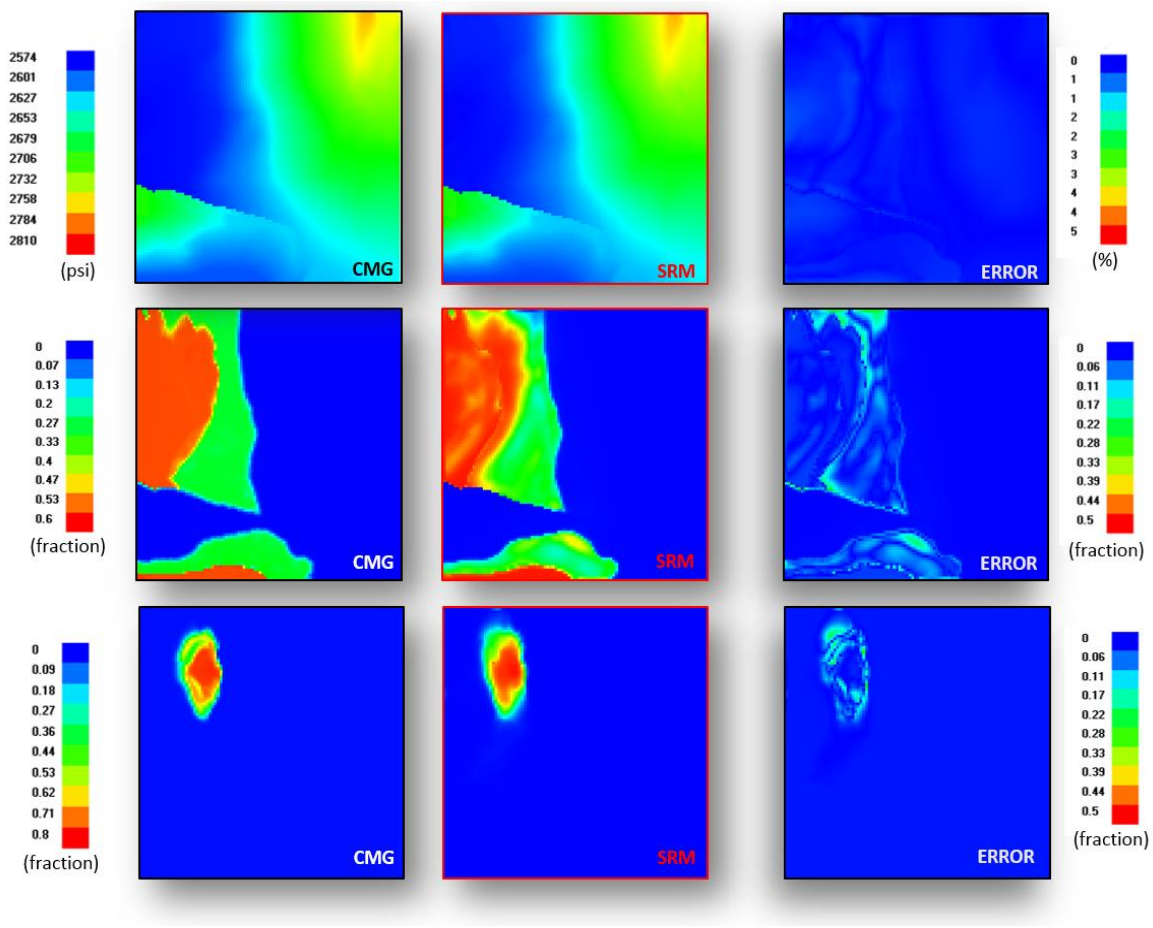

Figure 32. Distribution maps of Pressure, Gas saturation and CO_2 mole fraction (top to bottom) in the first layer of the reservoir (left to right: CMG output, SRM result and Error)-8 months after injection

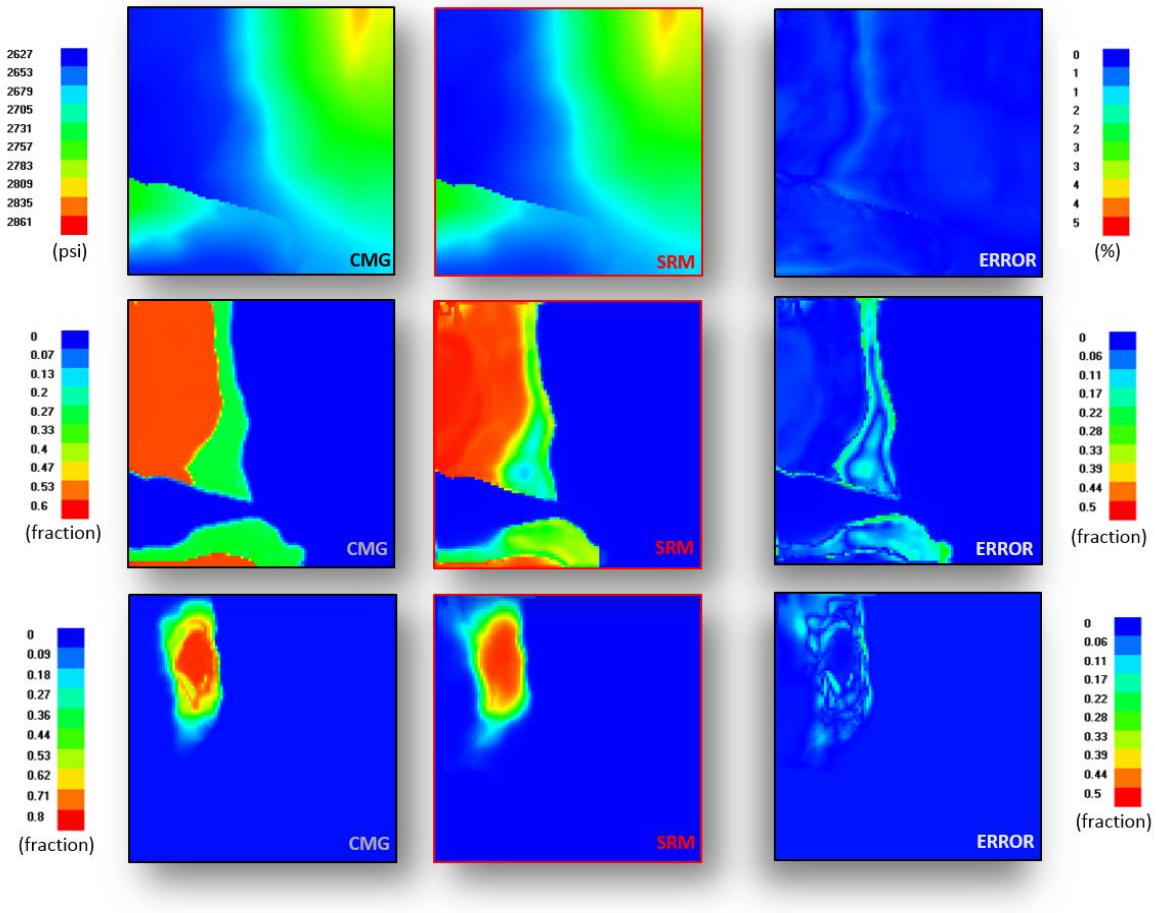

Figure 33. Distribution maps of Pressure, Gas saturation and CO_2 mole fraction (top to bottom) in the first layer of the reservoir (left to right: CMG output, SRM result and Error)-16 months after injection

CHAPTER 7.

FULL-FIELD SURROGATE RESERVOIR MODEL

In Chapter 5, SRM was developed for the first layer of the reservoir in order to prove the capability of artificial intelligence technique for proxy model development which aims at generating the output of a reservoir simulation model at the grid block level.

In this section, the application of this technique is extended to develop a proxy model for the three dimensional reservoir. For this purpose the 3D reservoir model of two different areal resolutions is used, both of which consist of 10 layers. The coarse-grid model comprises 20×20 grid blocks and the fine model includes 100×100 grid blocks in X-Y direction.

It should be mentioned that the same history matched numerical reservoir simulation model which was presented in chapter 4 is used as the base case model in this part of the study.

All the SRMs in this section and in the rest of the study are developed for each consecutive time step during the entire injection interval.

7.1 Coarse-Grid Numerical Reservoir Model

The original numerical reservoir simulation model consists of $100 \times 100 \times 10$ grid blocks in X, Y and Z direction. The reservoir structure was modified to decrease the number of grid blocks in X and Y direction while the grid blocks in Z direction (number of layers) remains the same. The new model has a total number of 4,000 grid blocks ($20 \times 20 \times 10$). Figure 34 shows the structure of the coarse-grid model.

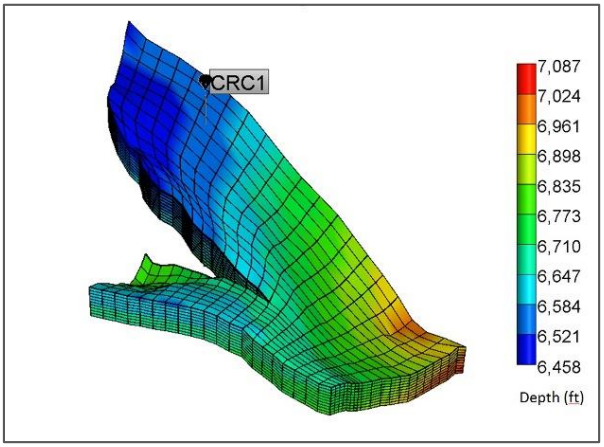

Figure 34. Reservoir structure of (20x20x10) grid block model

The porosity and permeability maps were imported from the original model to this model and the fluid properties, rock-fluid parameters, and the initial conditions are considered the same as the previously developed model.

7.2 SRM Development for Coarse-Grid Model

In the coarse-grid model, since the number of grid blocks for each case equals 4,000 we are not dealing with a huge number of data, and therefore SRM development does not require sampling which is used as a data reduction tool. In this part of the study all data from the training simulation cases are included in the neural network training process.

The previously developed SRM was based on the idea that in the training process, the dynamic parameters at the time before injection starts (Time 0) are introduced to the network as input in order to train the network to generate the dynamic parameters at the time step of interest, as output. However, according to the calculations which are performed in numerical reservoir simulation models, the results of the dynamic parameters of the system at the previous time step is used to compute the dynamic parameters at the current time step. This can be used as another approach to develop SRM which is called "Cascading SRM."

Therefore, in this part of the study, both of the mentioned approaches are used to develop the SRM and generate the result. Based on the result, one approach is used to move forward for the rest of the study.

7.2.1 Simulation Scenario Design

As mentioned above, the simulation runs used in this part of the study have a constant CO_2 injection interval. The minimum interval is considered as 8 months, and the maximum as 24 months. For each constant injection interval, 3 CO_2 injection scenarios are designed based on the amount of CO_2 injected into the reservoir. Assuming G as the total amount of CO_2 injected for the base case, in the 2 other scenarios, 2G and 3G total CO_2 is injected into the reservoir.

The plots of the monthly injection rates for 2 different injection intervals (which is used in this part of the study) are depicted in Figure 35 and Figure 36.

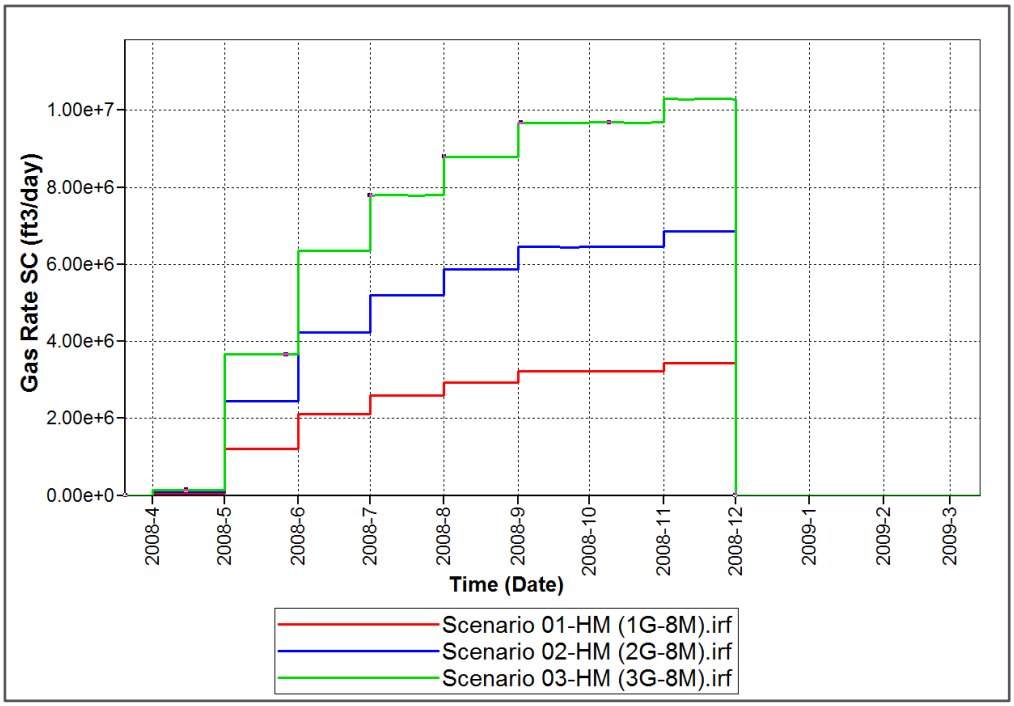

Figure 35. Three CO_2 injection scenarios within 8 months of injection

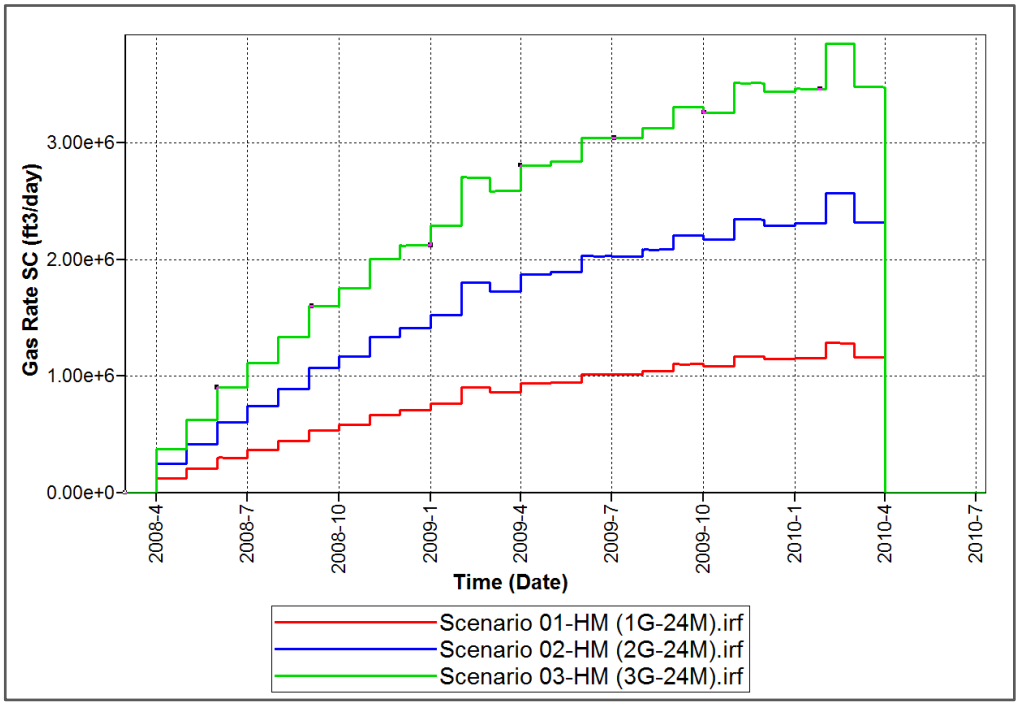

Figure 36. Three CO_2 injection scenarios within 24 months of injection

7.2.2 Data Set Generation

For each constant injection interval, all the required static and dynamic data are extracted and a comprehensive data set is generated for each injection scenario.

The only static parameter that has been changed to some extent, in this part of the study, is the calculation of the tier system through which the properties of the grid block around a single grid is introduced. In CO_2 injection and sequestration process, since CO_2 is migrating upward, CO_2 mole fraction, and as a result gas saturation changes, depend on the characteristics (such as porosity and permeability) of the lower and upper layer. It is not just a single grid block in the upper and lower layer that affect the dynamic parameter distribution, but rather a group of grid blocks. In other words, the degree of tightness of several grid blocks in the vicinity of the main grid can affect CO_2 movement and gas saturation distribution.

Therefore, in order to take into account the effect of this dependability, a new scheme is used for the tier system calculation which is depicted in Figure 37. To obtain the value of Tier-1, Tier-2, and Tier-3 the average value of the parameter is calculated over the grids which are included in the corresponding tier system. It should be mentioned that the number of grid blocks included at each tier system can be increased, in the case where reservoir grid blocks are smaller.

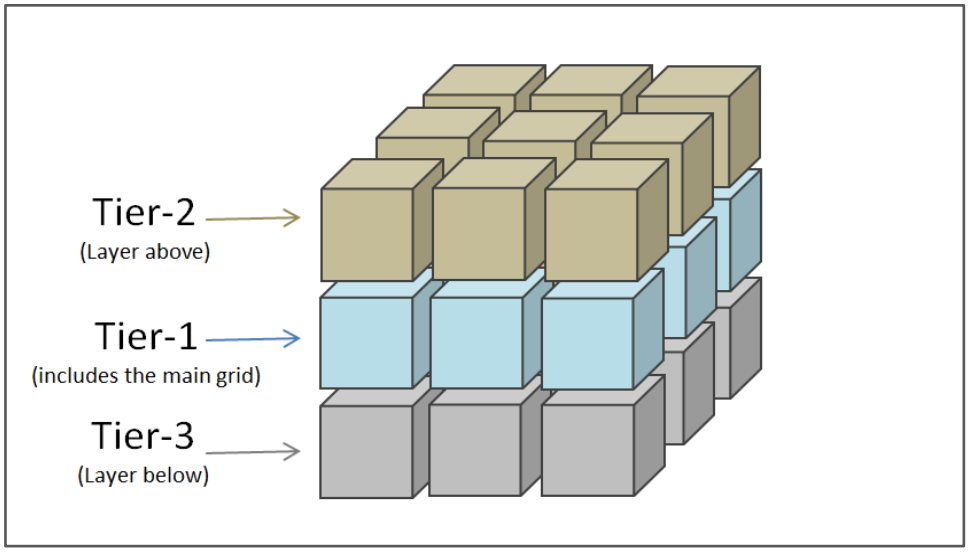

Figure 37. New scheme for Tier System calculation

As mentioned before, the data set includes all the dynamic parameters at each month of injection for the entire injection interval. In cascading SRM, two injection intervals of 8 months and 24 months are considered for model development. This is to investigate the capability of SRM in

generating the outputs of a numerical reservoir simulation when the injection interval is extended. The CO_2 injection schedule for 8 and 24 months of injection is demonstrated in Figure 35 and Figure 36 respectively.

7.2.3 Cascading SRM

As mentioned above, the organization of the SRM inputs in cascading SRM is different from the previously developed models. In this approach, the outputs of the system which were calculated at the previous time step are used to compute the outputs at the current time step, instead of using the dynamic parameters at the time 0.

Generating the appropriate inputs for the injection intervals of 8 and 24 months, neural networks are designed and trained for pressure, gas saturation, and CO_2 mole fraction at each month. Therefore, a total of 24 and 72 neural networks were trained for the two injection intervals of 8 months and 24 months respectively.

In order to implement the developed SRM, a computer code was developed through which at each time step (each month of injection), the neural network corresponding to each dynamic parameter (pressure, gas saturation and CO_2 mole fraction) is applied to one scenario data set. Then the results, which are the calculated dynamic parameters at each grid block, are saved. In the next step, the calculated outputs (pressure, gas saturation, and CO_2 mole fraction) are updated in the data set; these are in fact the inputs of the next time step neural networks. Therefore, using these new values the next time step networks are implemented. This procedure is continued for each consecutive injection month until it reaches the last time step.

The computer code mentioned above was implemented to deploy the SRM on Scenario#1 both for the 8 months of injection and 24 months of injection. The results of pressure, gas saturation and CO_2 mole fraction at each grid block were generated and the corresponding distribution maps were plotted. Figures 39 to 42 demonstrate the results.

Since at each time step, the 2D distribution maps are generated for each layer of the reservoir (number of layers equals to 10) for each of the dynamic parameters, the total number of generated maps is equal to 240 for the case with 8 months of injection, and 720 for the 24 months. Therefore, in the following section, as an example, the results are presented for layer 1 of the reservoir at two time steps only. The SRM results for some other layers of the reservoir are presented in the Appendix-B.

SRM Results for Training Case-8 Months of Injection

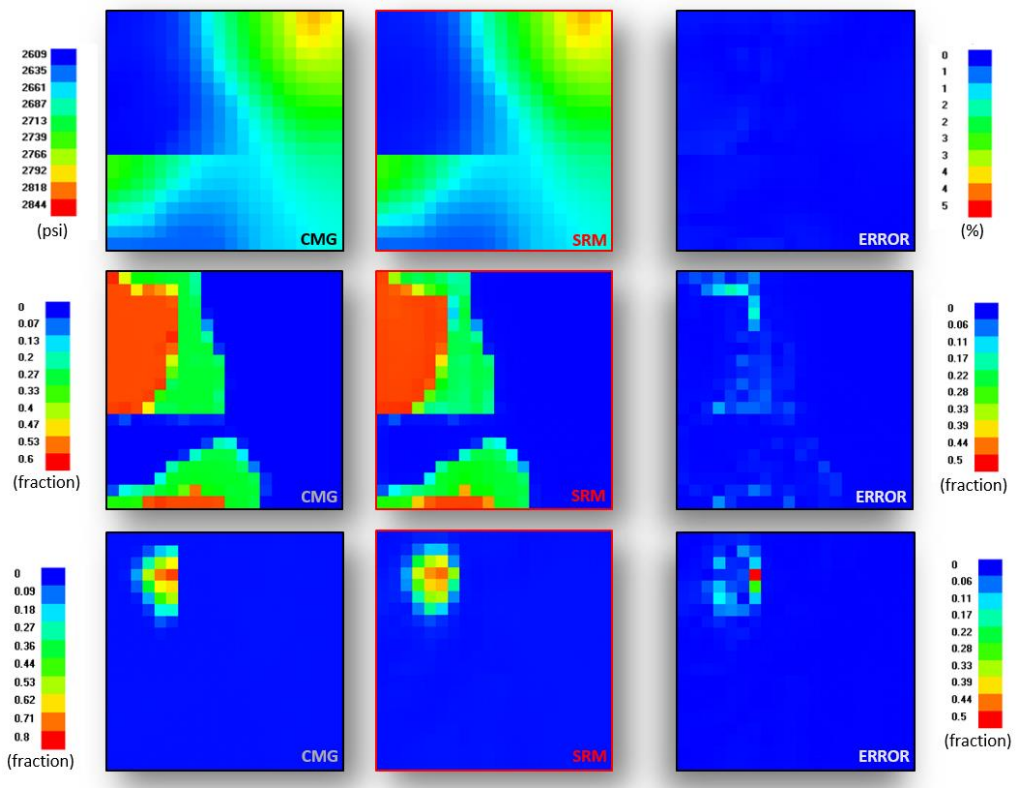

Figure 38. Distribution maps of Pressure, Gas saturation and CO_2 mole fraction in the first layer of the reservoir (from left: CMG output, SRM result and Error) – Training case- 4 Months after injection

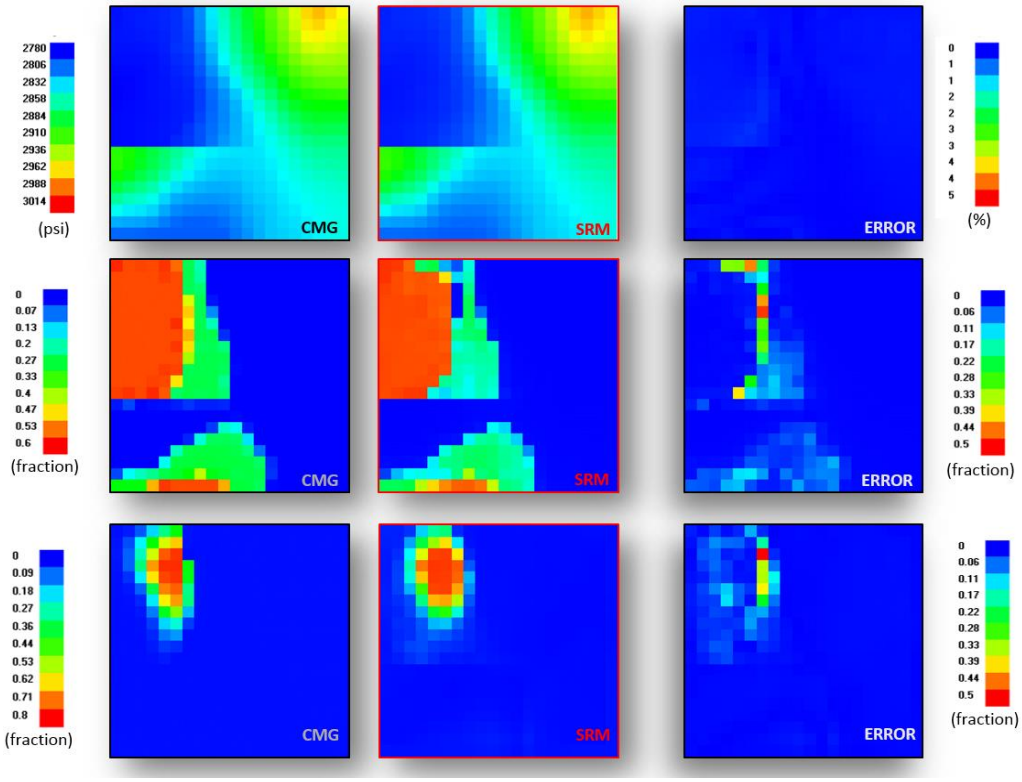

Figure 39. Distribution maps of Pressure, Gas saturation and CO_2 mole fraction in the first layer of the reservoir (from left: CMG output, SRM result and Error) – Training case- 8 Months after injection

SRM Results for Training Case-24 Months of Injection

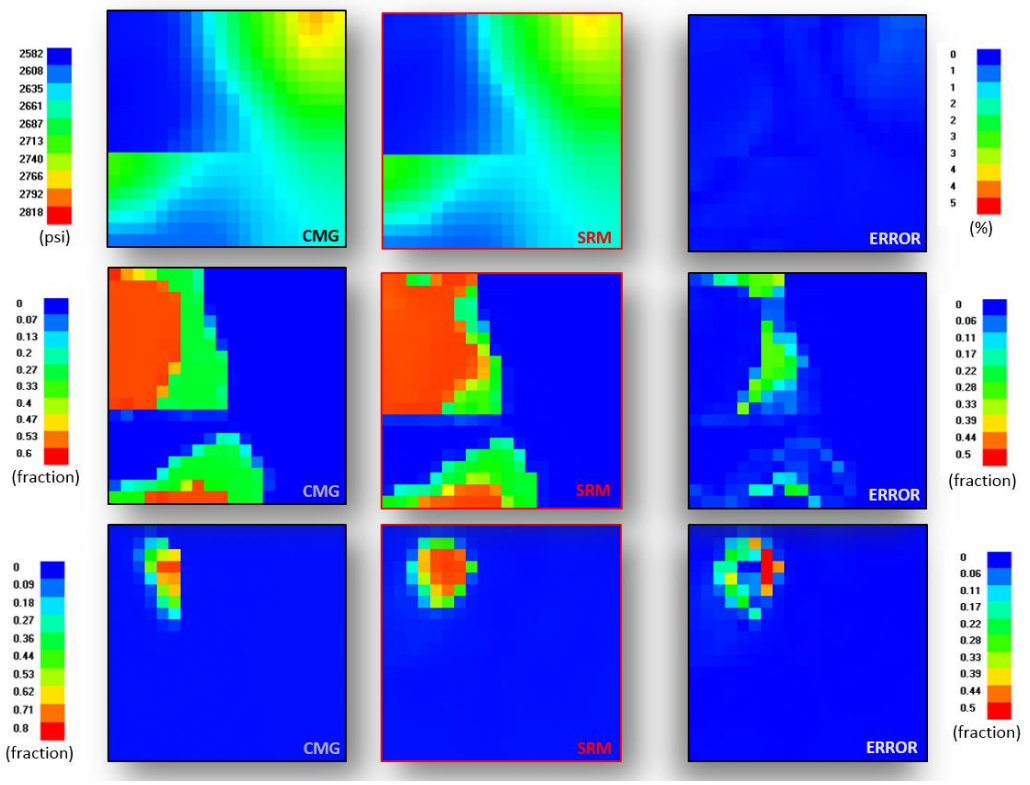

Figure 40. Distribution maps of Pressure, Gas saturation and CO_2 mole fraction in the first layer of the reservoir (from left: CMG output, SRM result and Error) – Training case- 12 Months after injection

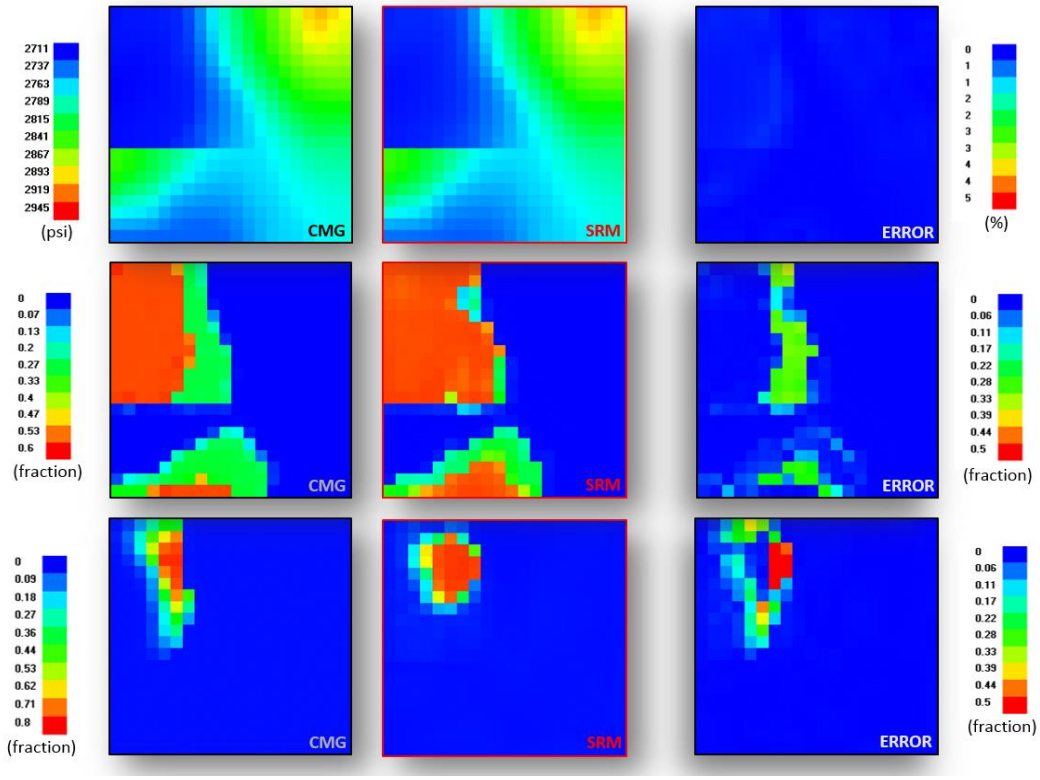

Figure 41. Distribution maps of Pressure, Gas saturation and CO_2mole fraction in the first layer of the reservoir (from left: CMG output, SRM result and Error) – Training case- 24 Months after injection

Cascading SRM discussion

The results which are obtained through the cascading approach shows that the calculated values of pressure, gas saturation, and CO_2 mole fraction at each grid block of the reservoir are of very high accuracy for the shorter injection interval or fewer number of time steps. However, as the number of time steps increases so does the amount of prediction error.

Generally, in the cascading SRM approach, the error of the predicted outputs is originated from two main sources. The first source of error is pertaining to the neural network training quality, which can be observed during the training process. The second comes from the fact that at each time step the predicted value of the previous time step is used as input to calculate the outputs of the current time step. This procedure results in an error accumulation that is responsible for a larger amount of error as time goes on and therefore poor predictions at the later times.

Therefore, in order to investigate the source of errors between the SRM calculated values and the CMG outputs, the two sources of error should be evaluated on developed SRM.

The IDEA software, through which the neural networks are developed, provides three different means for evaluating the quality of the neural network while it is being trained. The first parameter is the R-squared of error between the actual and virtual data. Cross plot of the actual verses predicted values and also the plot of error between these two are other ways of evaluating the network performance. Observing the cross plots and the R-squared of the error for all time steps during the 24 months, it can be concluded that all the networks' quality is almost the same and therefore deteriorating the results as time passes cannot be a result of network quality.

Consequently, the error accumulation at each time step can be considered as the major source of error which deteriorates the SRM output at the later times during injection.

More study on this issue was conducted which endorses the above claim regarding the source of errors which results in drawing the conclusion that cascading SRM is not a proper approach to be applied for this specific study (especially for a long duration of time). The result of this particular study is presented in the Appendix-B.

It should be mentioned that since SRM is a case-specific modeling technique, this conclusion may not be applicable if SRM is developed for a different system.

7.2.4 Non-Cascading SRM

To develop the non-cascading SRM two different injection intervals of 8 months, and 24 months were considered. The same comprehensive data set, as the one used in cascading SRM, was used to generate neural network input for non-Cascading approach.

Each input file includes data from three scenarios of similar injection interval. The input file is arranged so that besides the static parameters, the value of dynamic parameters for each grid block at time step 0 (before injection takes place) is considered as inputs. The output of each network is the pressure, gas saturation or CO_2 model fraction of each grid block at all monthly time steps during the injection interval.

7.2.4.1 Results of Non-Cascading SRM

In order to implement the developed SRM, a computer code was developed through which at each time step (each month of injection), the neural network corresponding to pressure, gas saturation and CO_2 mole fraction is applied to any scenario of interest.

The developed SRM for two different injection intervals were deployed to two cases. The first one is one of the scenarios which was included in the training process and the other one is a blind case which has not been used in training.

In order to make a comparison between the cascading and non-cascading SRM, the results of SRM for non-cascading approach is presented for the 8 months and 24 months of injection.

The output of SRM for the first layer of the reservoir is presented as 2D distribution maps in the following sections (Figure 43 to Figure 49) for a training case as well as a blind case. The maps demonstrate the pressure, gas saturation and CO_2 mole fraction distribution (first row, second row and third row respectively) generated by SRM (middle plot), its corresponding distribution map as CMG output (left plot) and also the error between these two (right plot). More distribution maps for other reservoir layers in different time steps are presented in Appendix-C.The results show that the accuracy of the SRM outputs based on non-cascading approach is significantly higher for gas saturation and CO_2 mole fraction predictions both for training case and blind case compared to that of the cascading approach (especially for the longer injection interval). However, observing the results for the pressure distribution generated through cascading approach shows a slight percentage increase in the error when applied to a blind case. This might be attributed to the problem of over training the pressure networks. Based on the results obtained in this part of the study, a non-cascading SRM scheme is chosen for the rest of this research.

SRM Results for Training Case-8 Months of Injection

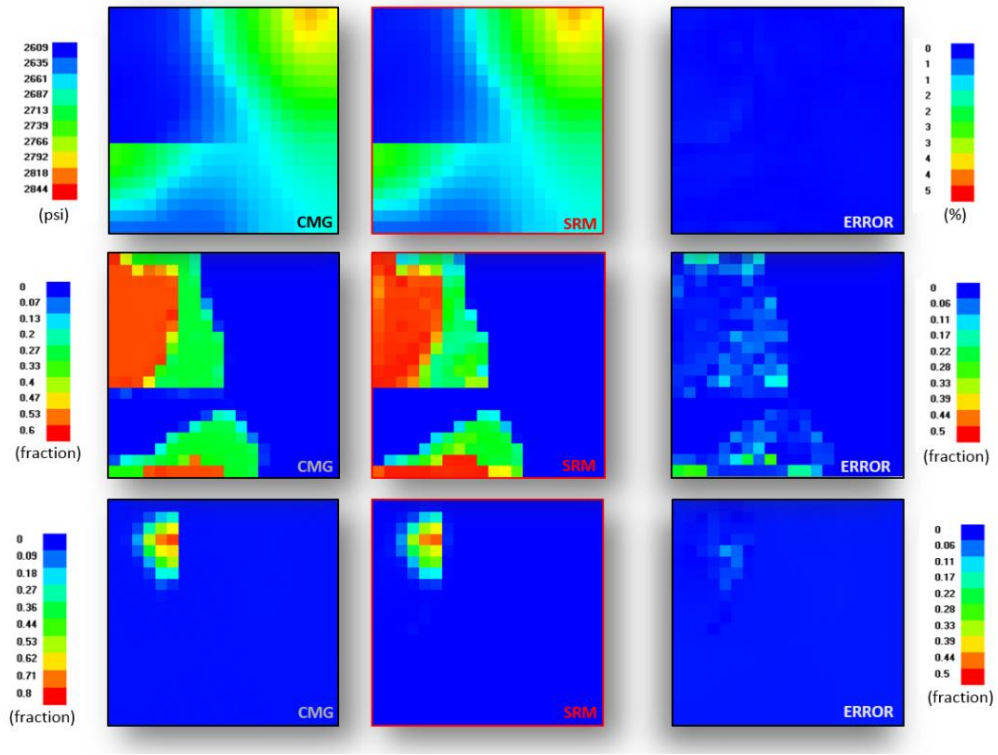

Figure 43. Distribution maps of Pressure, Gas saturation and CO_2mole fraction in the first layer of the reservoir (from left: CMG output, SRM result and Error) – Training case- 4 Months after injection

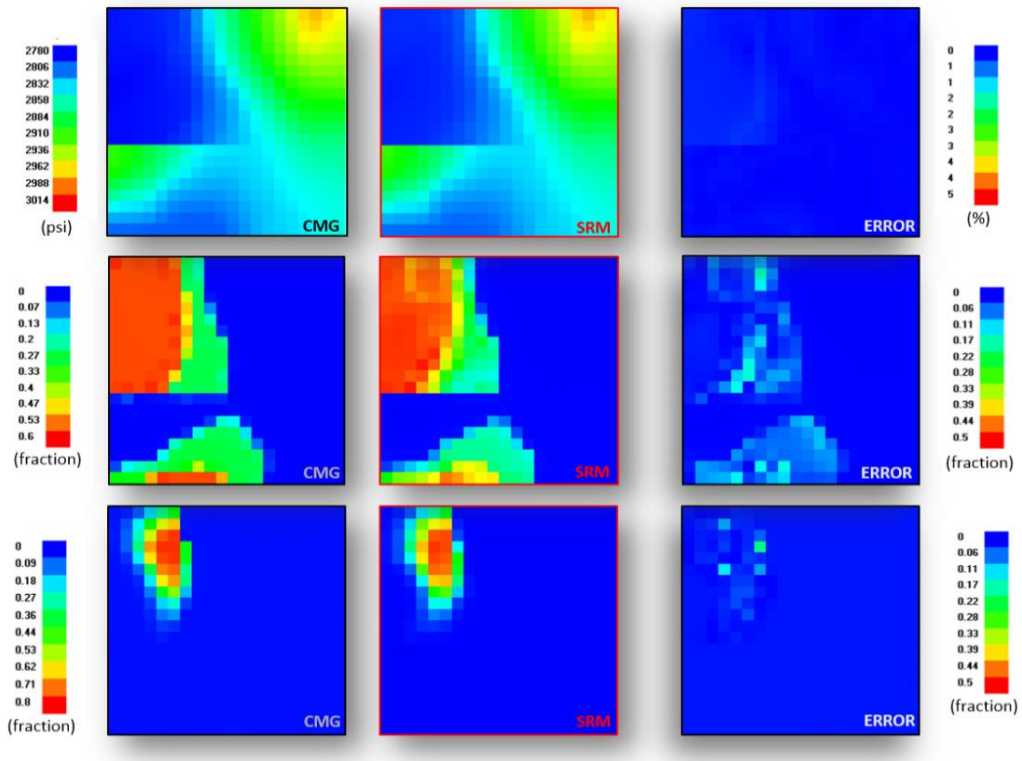

Figure 42. Distribution maps of Pressure, Gas saturation and CO_2mole fraction in the first layer of the reservoir (from left: CMG output, SRM result and Error) – Training case- 4 Months after injection

SRM Results for Blind Case-8 Months of Injection

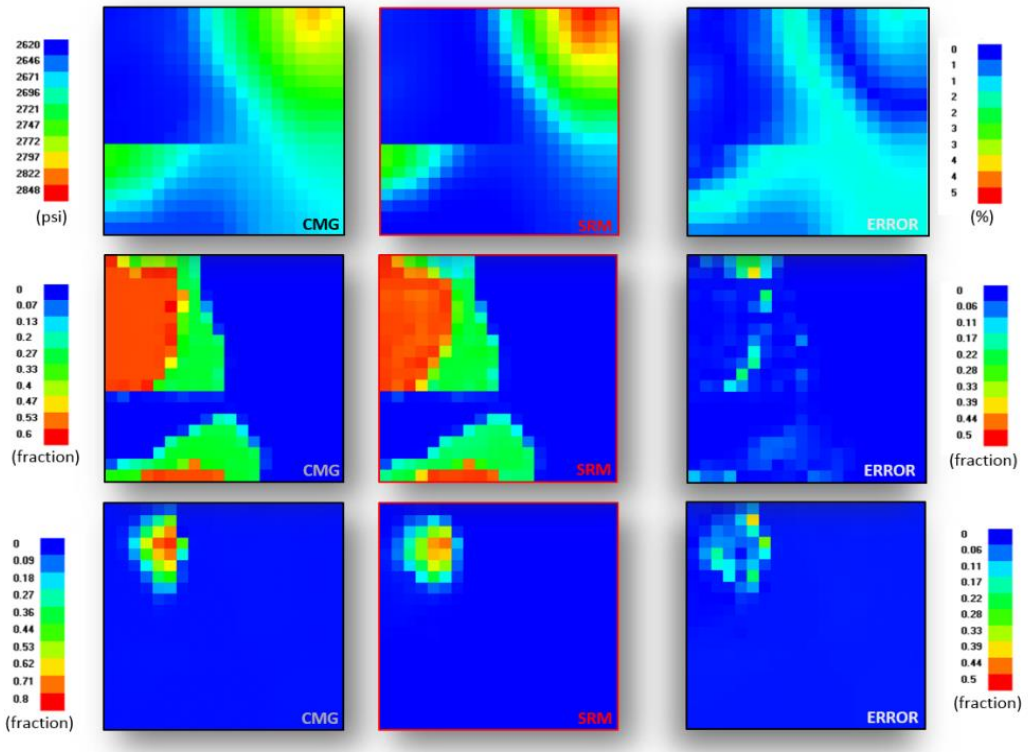

Figure 44. Distribution maps of Pressure, Gas saturation and CO_2 mole fraction in the first layer of the reservoir (from left: CMG output, SRM result and Error) – Blind case- 4 Months after injection

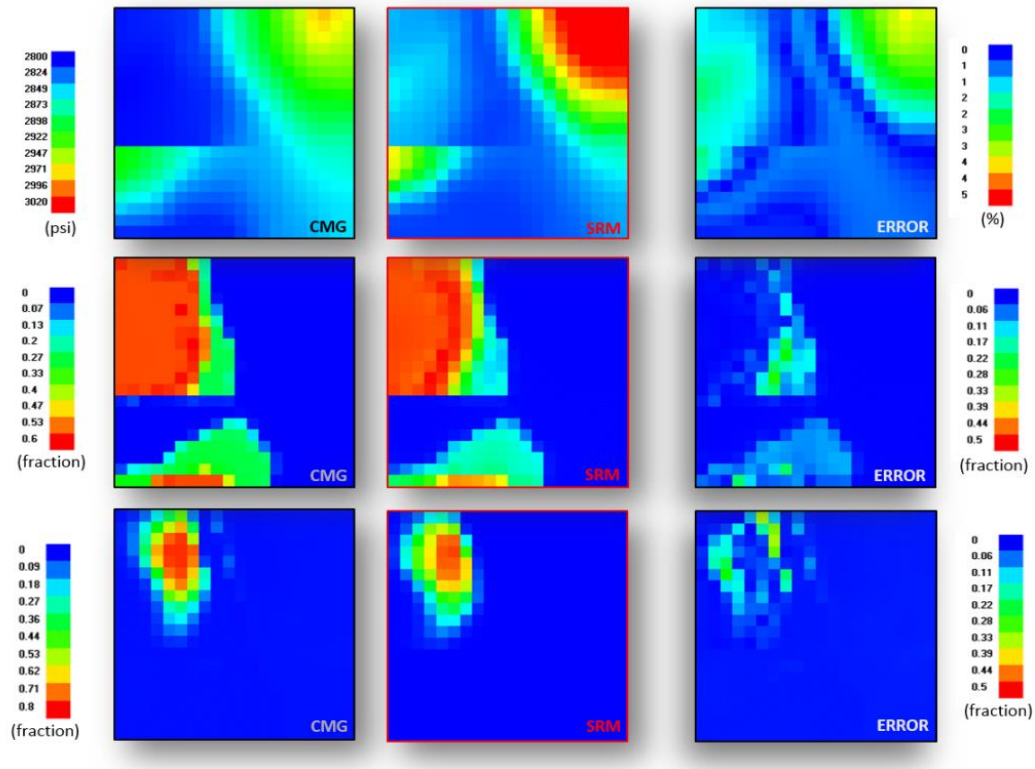

Figure 45. Distribution maps of Pressure, Gas saturation and CO_2 mole fraction in the first layer of the reservoir (from left: CMG output, SRM result and Error) – Blind case- 8 Months after injection

SRM Results for Training Case-24 Months of Injection

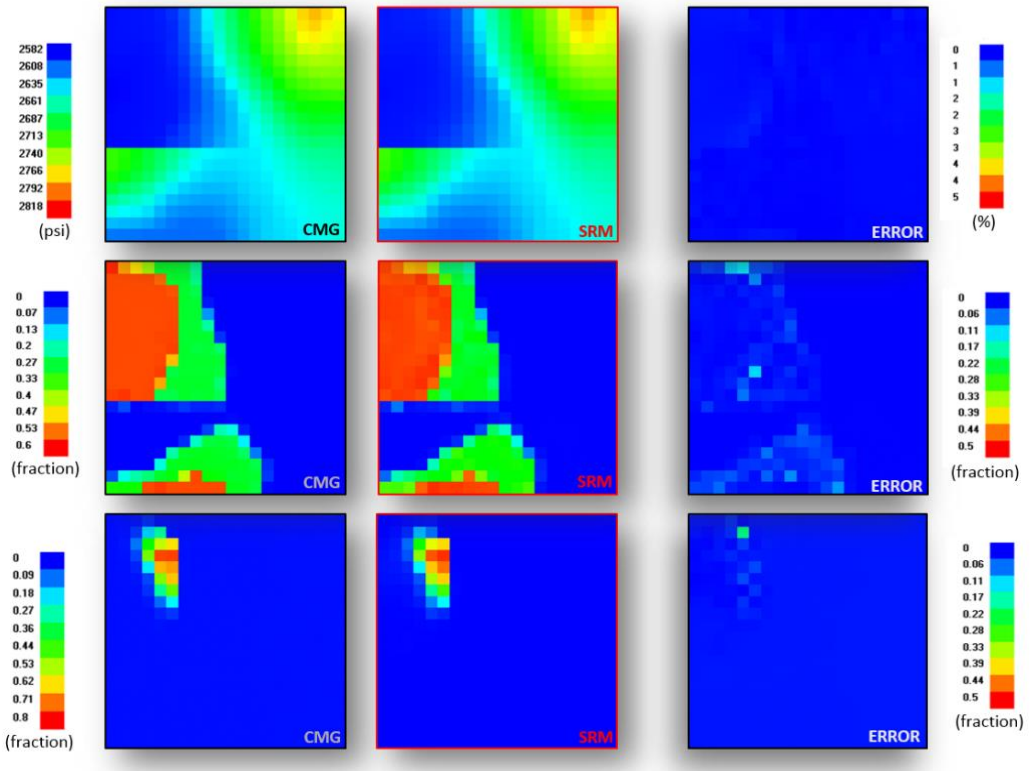

Figure 46. Distribution maps of Pressure, Gas saturation and CO_2 mole fraction in the first layer of the reservoir (from left: CMG output, SRM result and Error) – Training case- 12 Months after injection

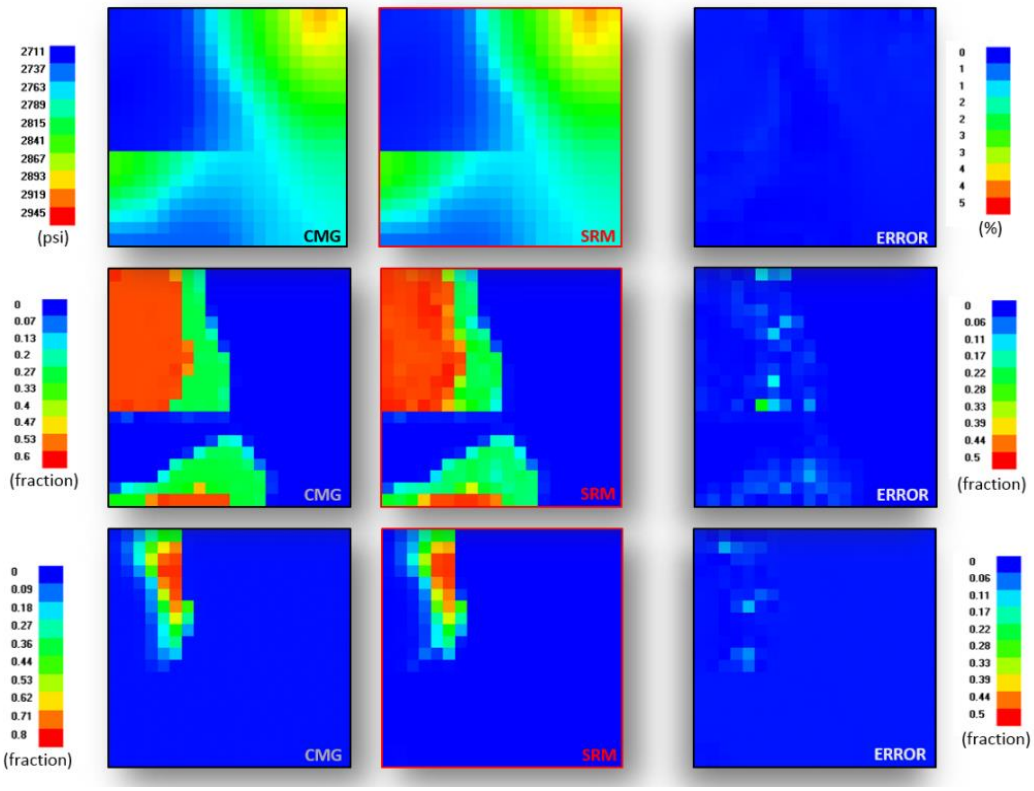

Figure 47. Distribution maps of Pressure, Gas saturation and CO_2 mole fraction in the first layer of the reservoir (from left: CMG output, SRM result and Error) – Training case- 24 Months after injection

SRM Results for Blind Case-24 Months of Injection

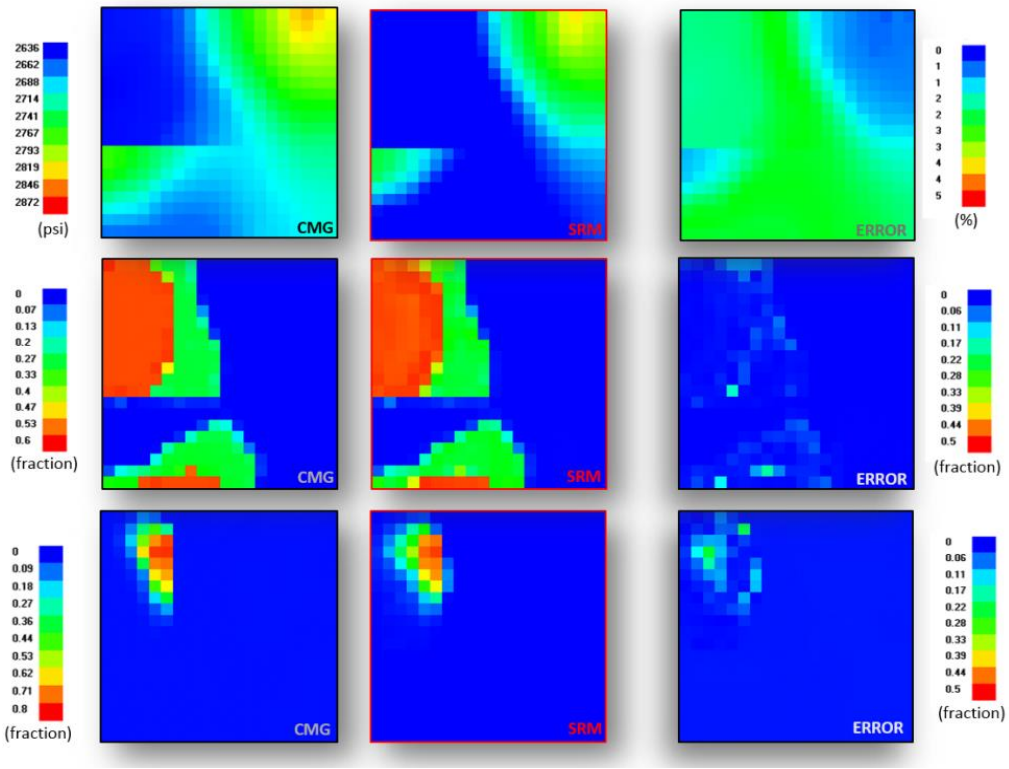

Figure 48. Distribution maps of Pressure, Gas saturation and CO_2 mole fraction in the first layer of the reservoir (from left: CMG output, SRM result and Error) – Blind case- 12 Months after injection

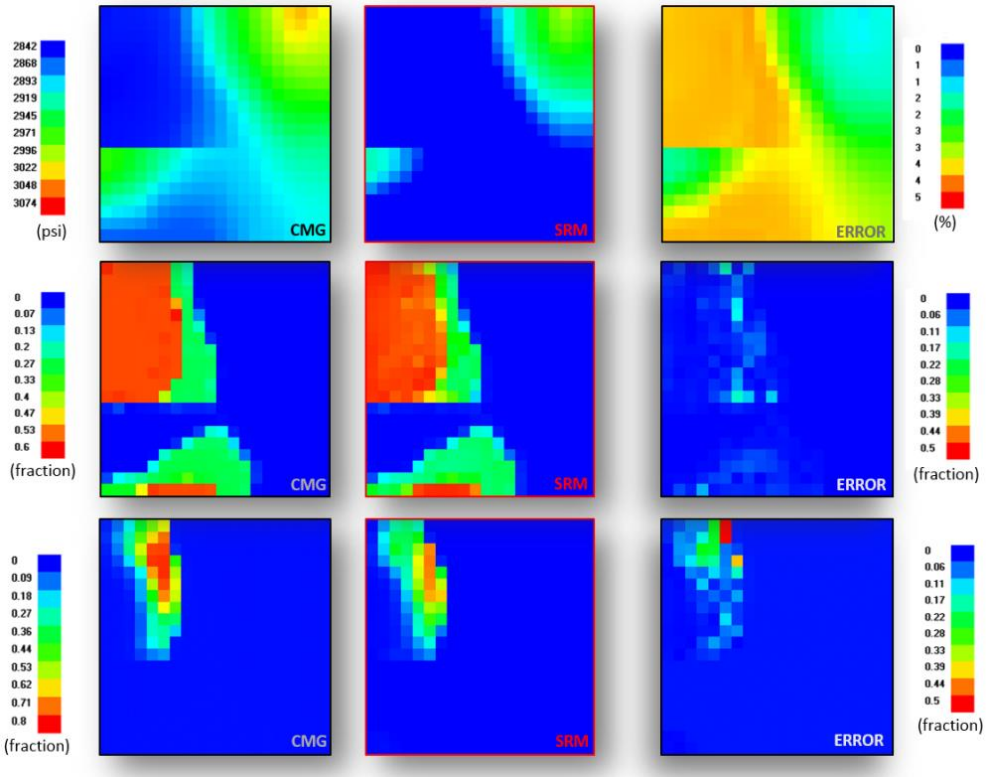

Figure 49. Distribution maps of Pressure, Gas saturation and CO_2 mole fraction in the first layer of the reservoir (from left: CMG output, SRM result and Error) – Blind case- 24 Months after injection

7.2.4.2 Coarse-Grid SRM Error Evaluation

The 2D distribution maps, which were presented in the previous sections, visualize the SRM result versus the CMG output for pressure, gas saturation and CO_2 mole fraction distribution in each layer of the reservoir. In this section the frequency error plots is presented in order to demonstrate the frequency distribution of the prediction error for all grid blocks of the reservoir.

The plots presented in Figure 50 to Figure 55 are generated for each parameter of pressure, gas saturation, and CO_2 mole fraction individually when neural networks are applied to two different scenarios with 24 months of injection (the training case and the blind case) at three time steps during the injection interval (as an example).

In general the frequency of the grid blocks with higher amount of error increases when the neural networks are applied to the blind case as opposed to the training case, especially in the later time steps. This is justified through the fact that the blind case scenario was not included in the neural network training process and therefore the prediction error for this case is generally higher.

The results show that the pressure networks have the highest acuracy in predicting the pressure distribution since for this parameter the amount of error for the blind case scenario after 24 months of injection does not exceed 5%.

The frequency error plot for gas saturation prediction for the same blind case after 24 months of injection shows that around 90% of the grid blocks have an error of less than 0.02.

The prediction results for the same case for CO_2 mole fraction show that more than 95% of the grid blocks have an error of less than or equal to 0.05.

Observing the amount of error presented in the frequency error plots it can be concluded that the developed SRM is a powerful tool to be used as a proxy model to generate the outputs of a numercial reservoir model at the grid block level.

Pressure Error Frequency Distribution plots-Training Case

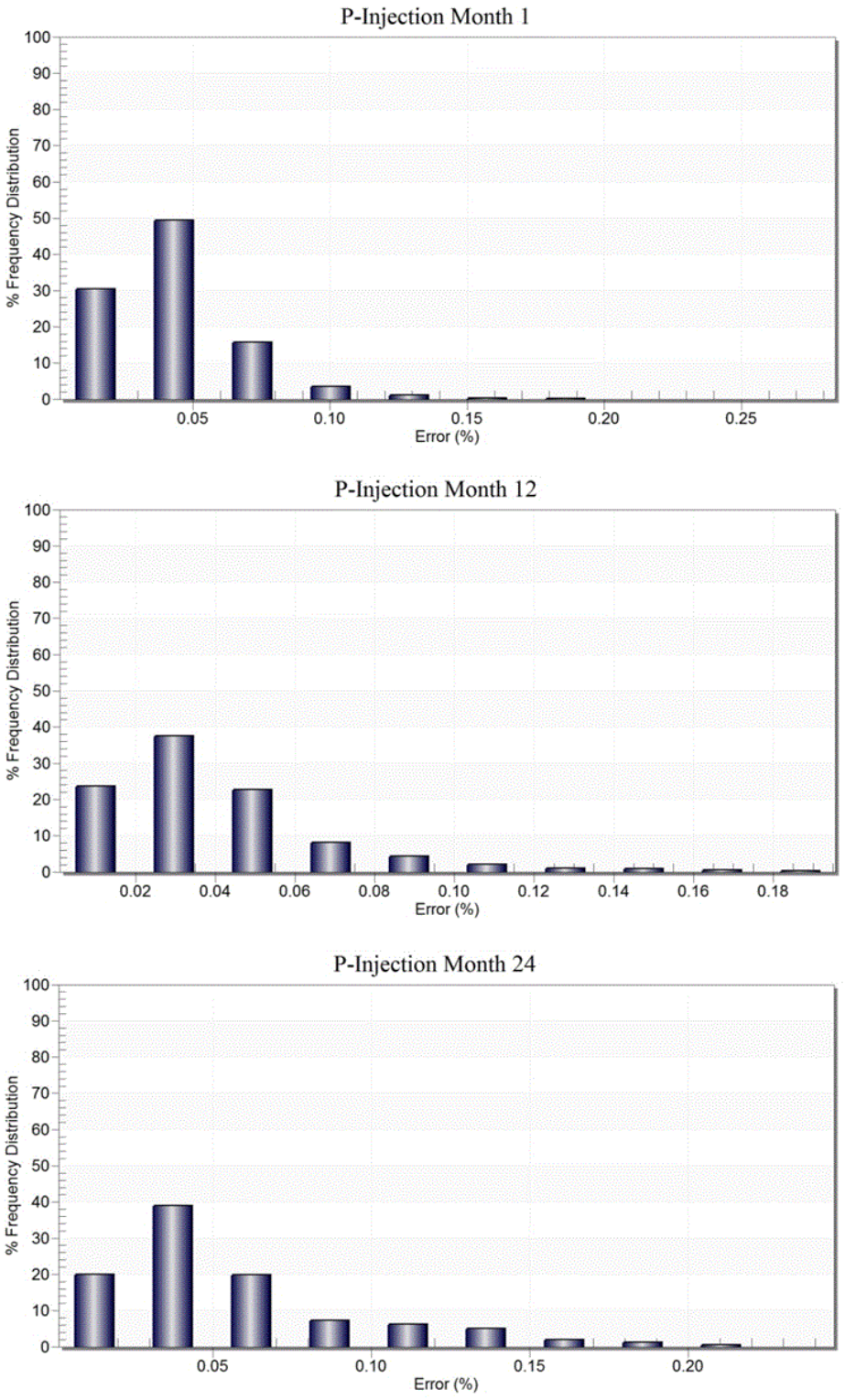

Figure 50. Pressure Error Frequency Distribution for all grid blocks of the reservoir at 3 time steps during the injection-Training case

Pressure Error Frequency Distribution plots-Blind Case

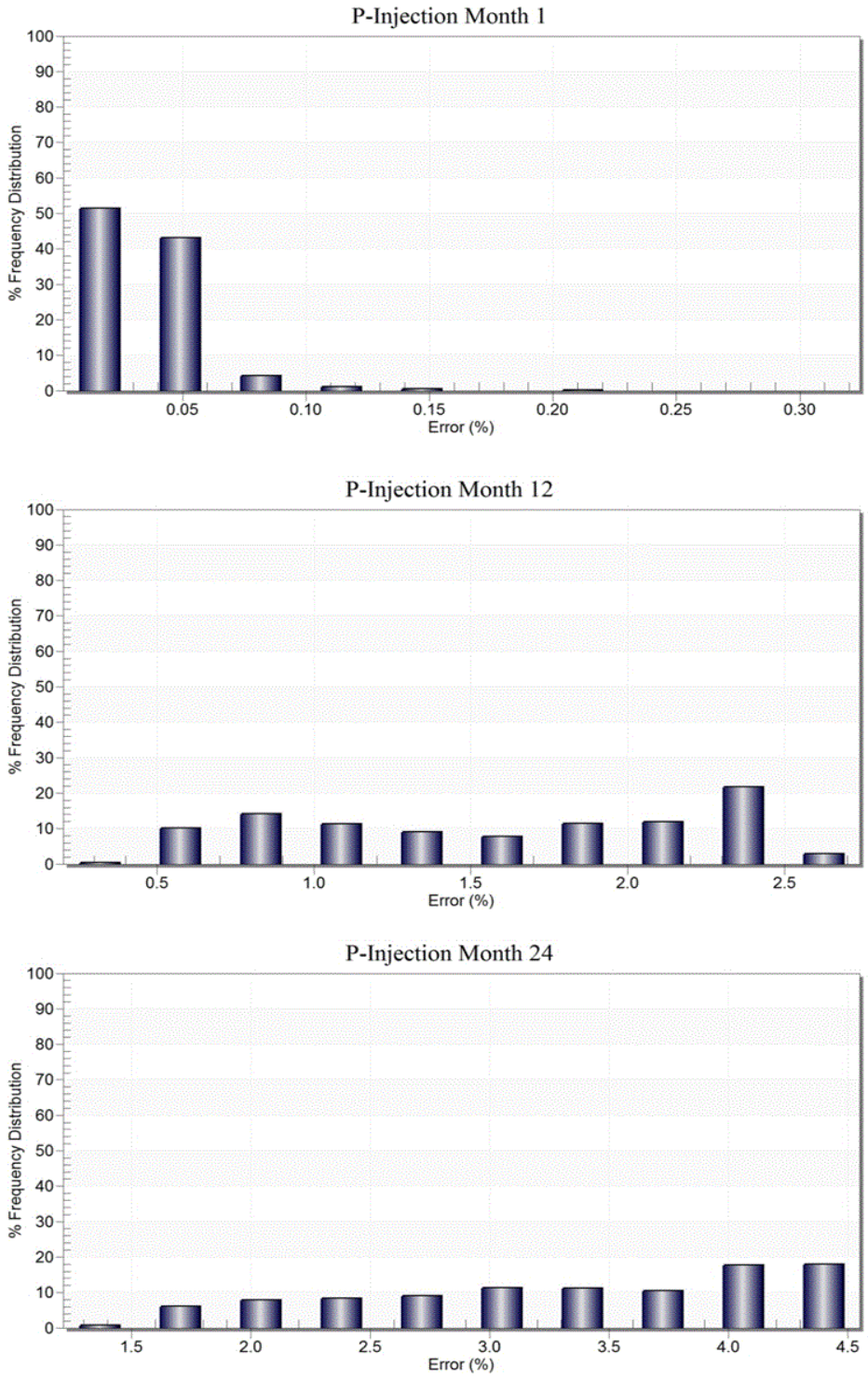

Figure 51. Pressure Error Frequency Distribution for all grid blocks of the reservoir at 3 time steps during the injection-Blind case

Gas Saturation Error Frequency Distribution plots-Training Case

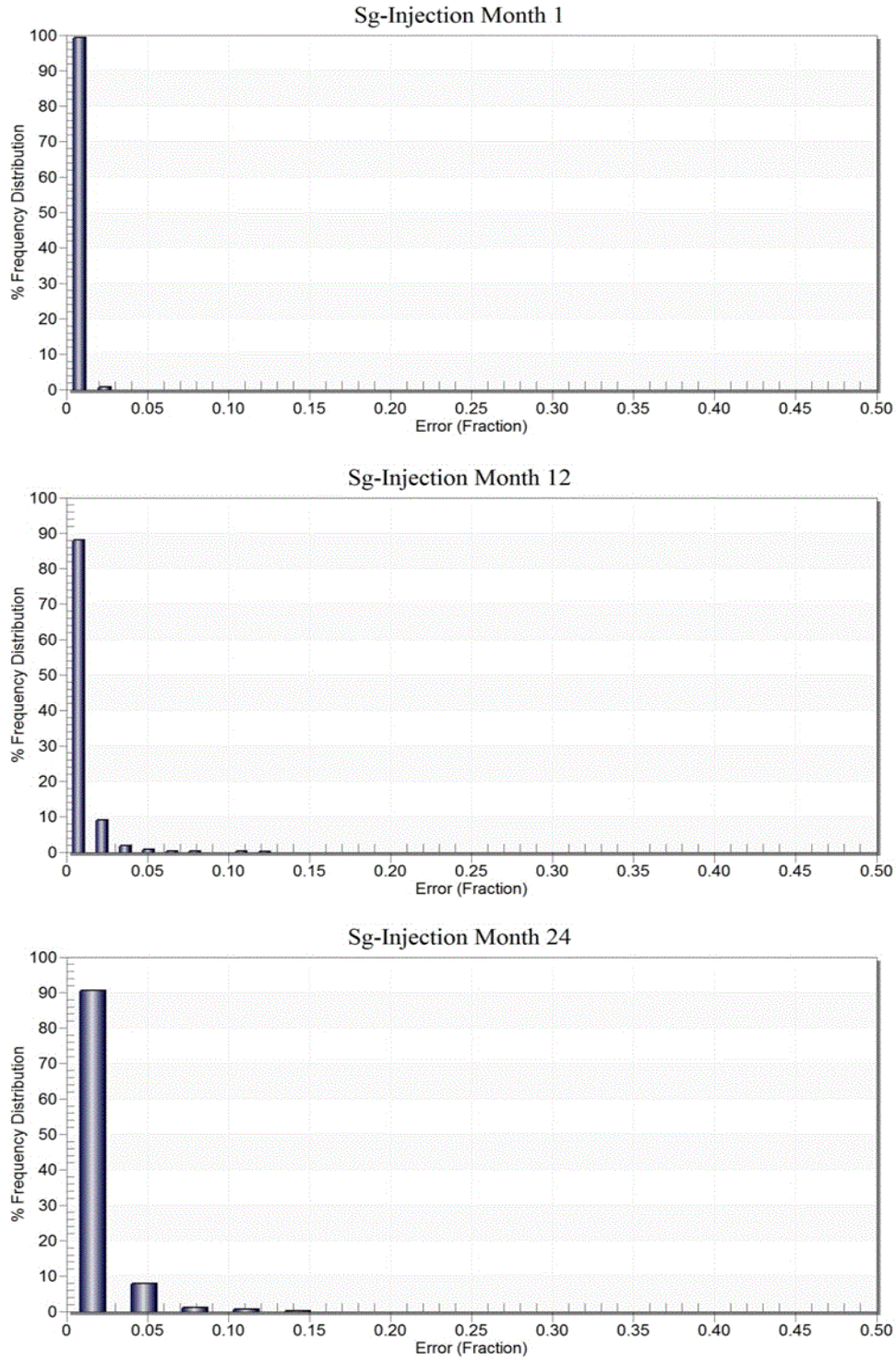

Figure 52. Gas Saturation Error Frequency Distribution for all grid blocks of the reservoir at 3 time steps during the injection-Training case

Gas Saturation Error Frequency Distribution plots-Blind Case

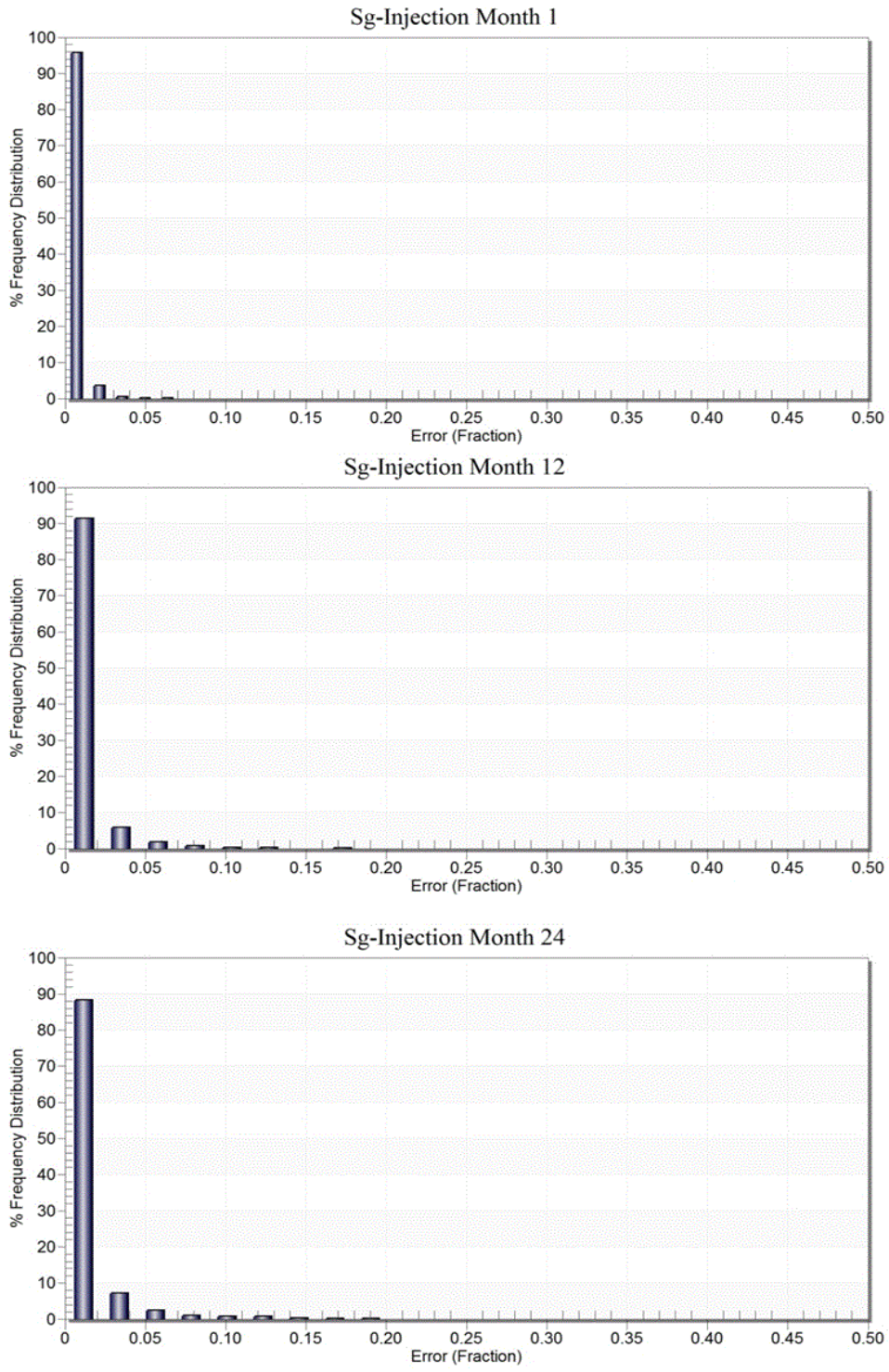

Figure 53. Gas Saturation Error Frequency Distribution for all grid blocks of the reservoir at 3 time steps during the injection-Blind case

CO_2 Mole Fraction Error Frequency Distribution plots-Training Case

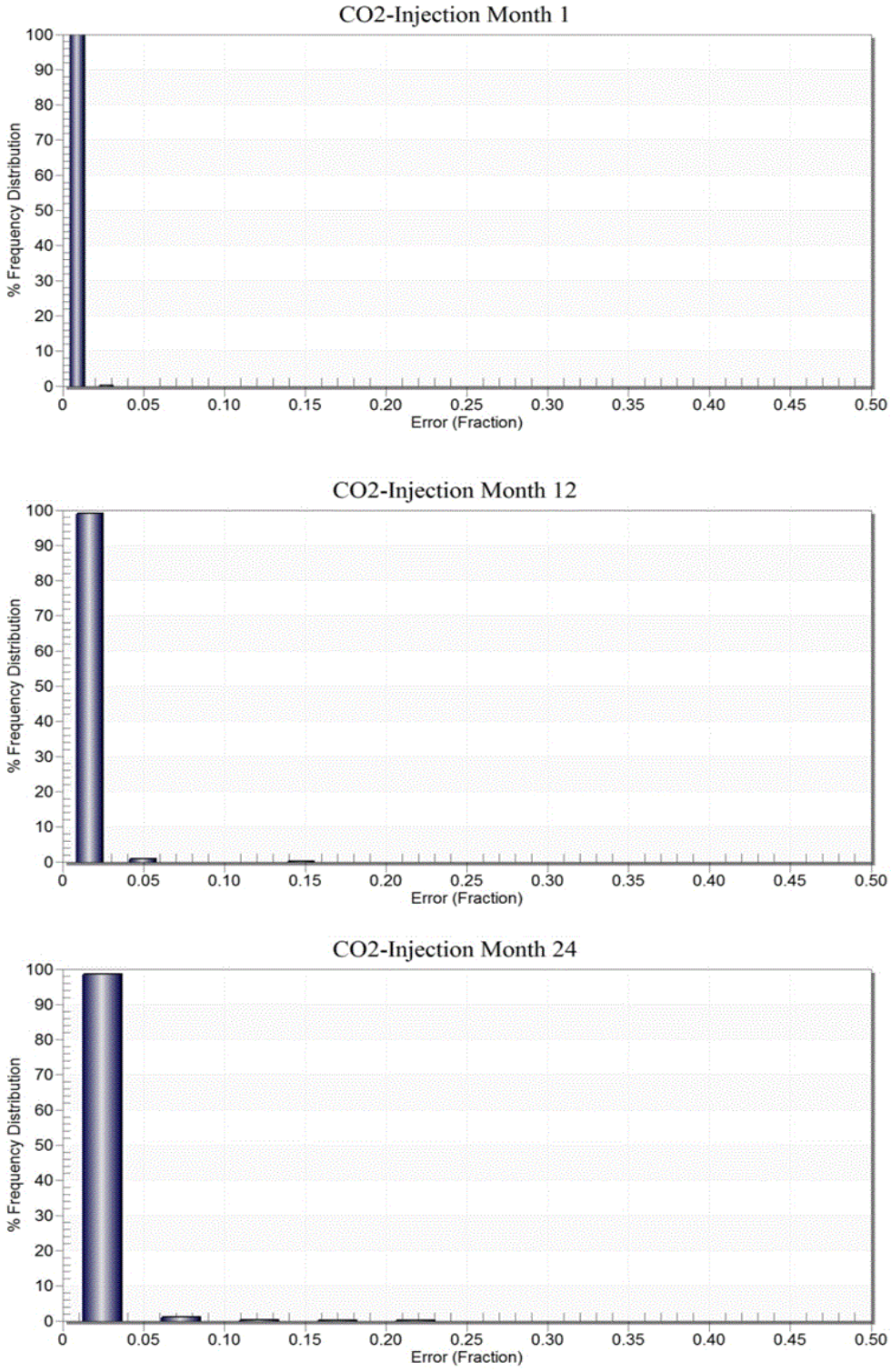

Figure 54. CO_2 mole fraction Error Frequency Distribution for all grid blocks of the reservoir at 3 time steps during the injection-Training case

CO_2 Mole Fraction Error Frequency Distribution plots-Blind Case

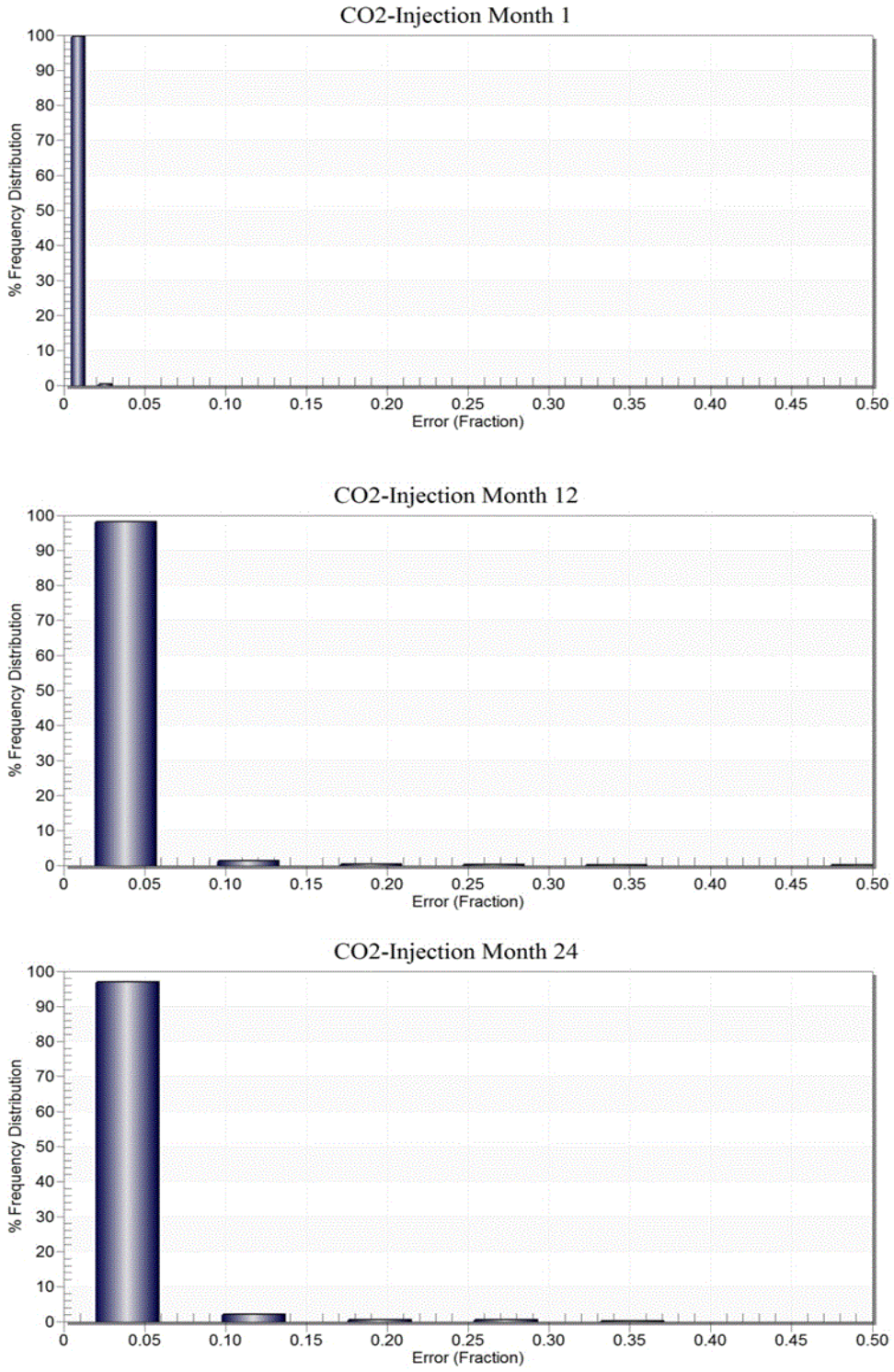

Figure 55. CO_2 mole fraction Error Frequency Distribution for all grid blocks of the reservoir at 3 time steps during the injection-Blind case

7.3 SRM Development for Fine-Grid Model

The fine reservoir model is the original model which consists of 100,000 $(100 \times 100 \times 10)$ grid blocks. The reservoir construction procedure was explained in details in Chapter 4.

For the purpose of SRM development, only the injection phase is the interval of interest. Therefore, three different injection scenarios are designed for 8 months and 24 months of CO_2 injection. Figure 35 and Figure 36 demonstrate the CO_2 injection rate schedule for the two injection intervals.

Two SRMs are developed for the fine-grid reservoir model for the two constant injection intervals of 8 months and 24 months.

As a first trial, SRM was generated for 8 months of CO_2 injection. Three training simulation cases were conducted using CMG simulator which were used as training cases.

To generate a comprehensive spatio-temporal data base, data should be extracted from the three simulation cases for each grid block. Since the reservoir consists of 100,000 grid blocks, the total number of data in the data set adds up to 300,000. This amount of data is much higher than the number of data that can be used in neural network development and training. Therefore, for the fine-grid reservoir, employing sampling to reduce the number of data is inevitable; whereas, in SRM development for the coarse-grid reservoir, the entire data from the training cases were utilized in neural network training process. Since the sampling method is based on the change of parameters at each time step with respect to time 0, sampling is performed individually for pressure, gas saturation, and CO_2 mole fraction for each scenario. At each time step 10% of all data was sampled which mostly includes the grid blocks with the higher amount of change for that specific parameter.

The neural network inputs are generated based on the non-cascading approach in order to avoid error accumulations during the deployment stage.

Having the inputs, for each parameter, at each monthly time step, a single neural network is developed and trained. The total number of networks equals 24 for the SRM related to 8 months of CO_2 injection and 72 for the scenarios with an injection interval of 24 months.

7.3.1 SRM Result for Fine-Grid Model

In order to implement the fine-grid SRM, the previously developed computer code was modified to be able to use a data set of 100,000 rows of input data, corresponding to the all reservoir grids to generate the desired output. At each time step (each month of injection), the specific neural

network related to pressure, gas saturation, and CO_2 mole fraction is applied to a single scenario data file.

The developed SRM were deployed to two simulation cases. The first case is one of the scenarios which was included in the training process (Scenario#2) and the second case is a blind scenario (where 1.5 G of CO_2 is injected into the reservoir) which was not used in neural network training.

The results of the dynamic parameters distribution generated by the developed SRM are presented in the following sections. The error between the generated parameters and the outputs of the numerical reservoir simulation model demonstrates the degree of accuracy of the SRM.

SRM Results for Training Case-8 Months of Injection

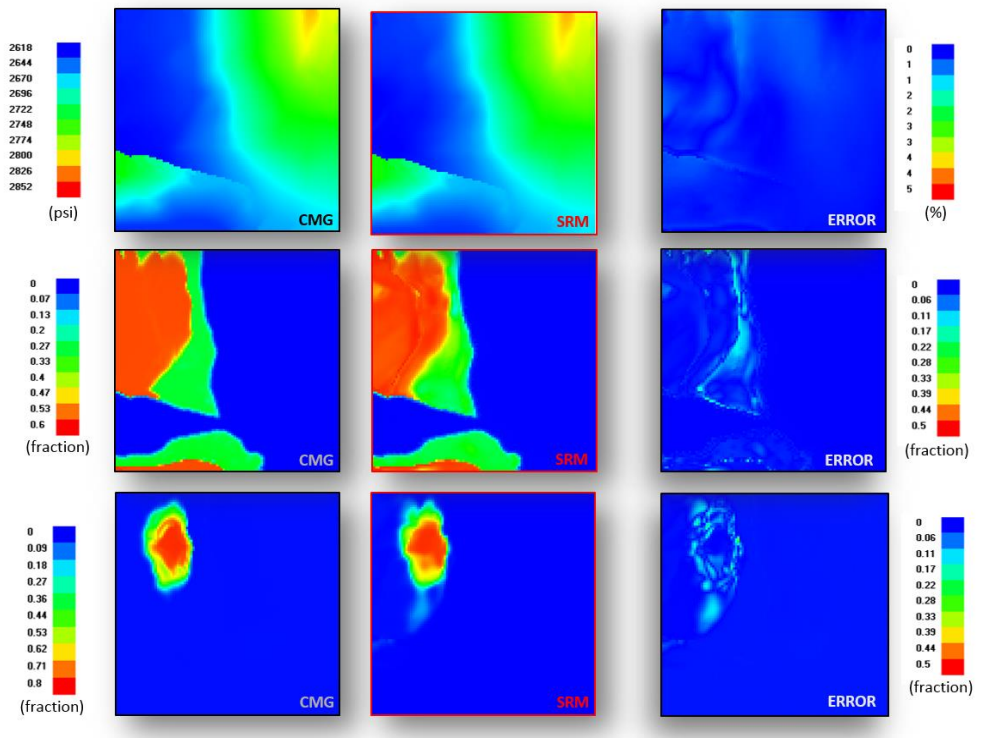

Figure 56. Distribution maps of Pressure, Gas saturation and CO_2 mole fraction in the first layer of the reservoir (from left: CMG output, SRM result and Error) – Training case- 4 Months after injection

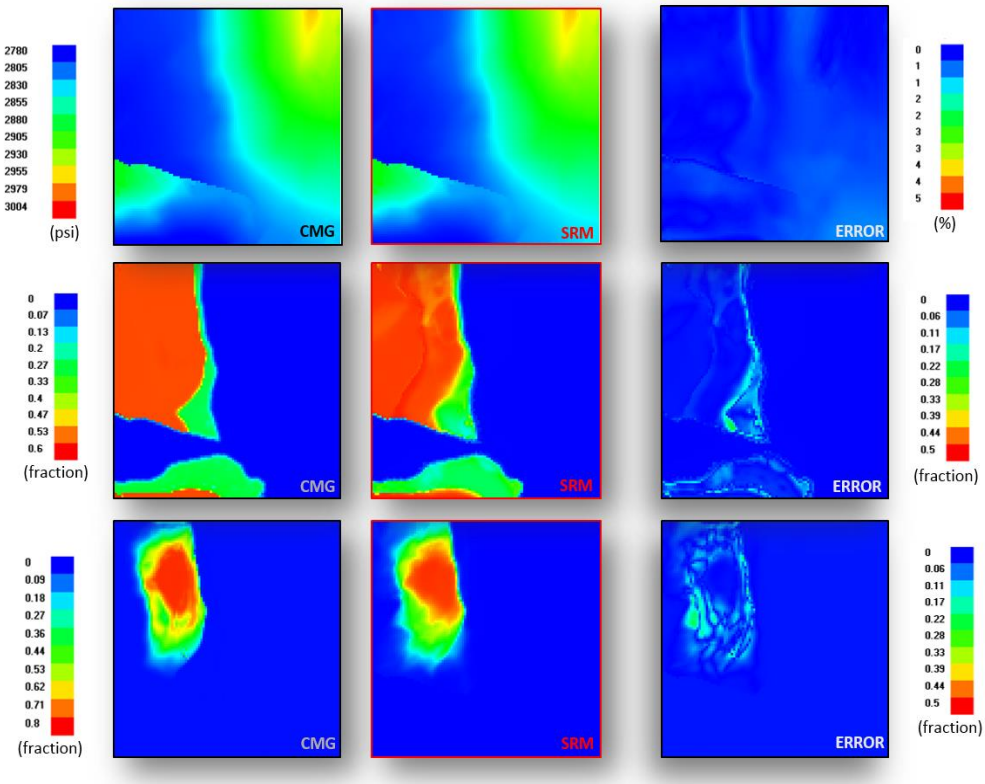

Figure 57. Distribution maps of Pressure, Gas saturation and CO_2 mole fraction in the first layer of the reservoir (from left: CMG output, SRM result and Error) – Training case- 8 Months after injection

SRM Results for Blind Case-8 Months of Injection

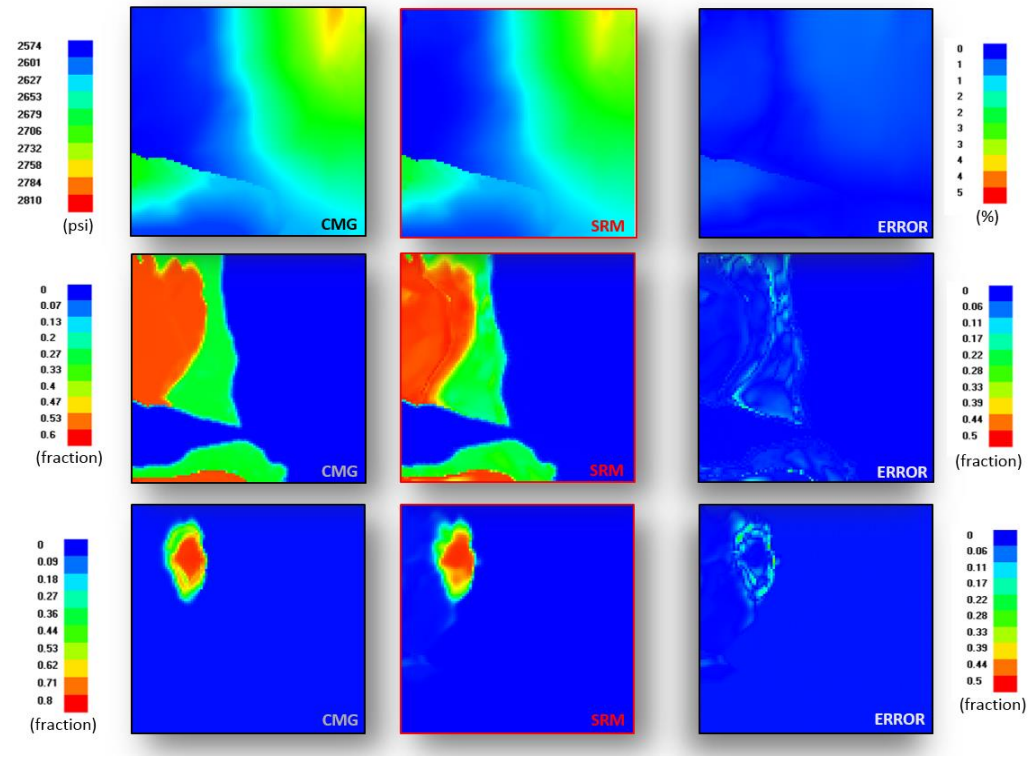

Figure 58. Distribution maps of Pressure, Gas saturation and CO_2 mole fraction in the first layer of the reservoir (from left: CMG output, SRM result and Error) – Blind case- 4 Months after injection

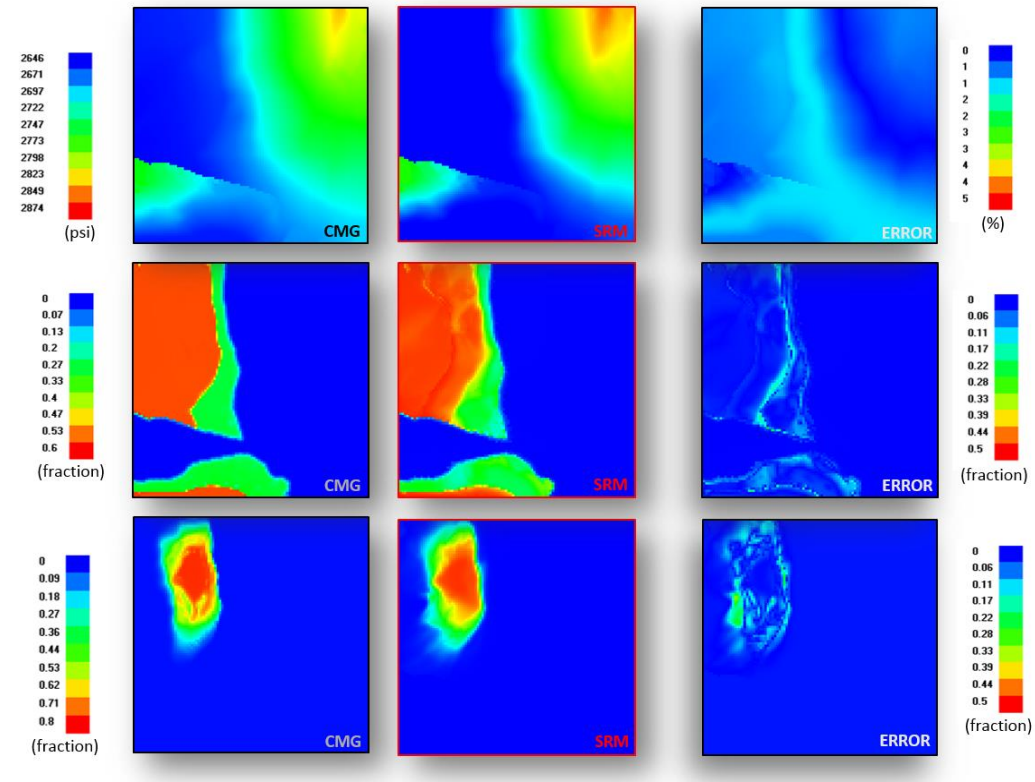

Figure 59. Distribution maps of Pressure, Gas saturation and CO_2 mole fraction in the first layer of the reservoir (from left: CMG output, SRM result and Error) – Blind case- 8 Months after injection

7.3.2 Fine-Grid SRM Discussion

Observing the results which are obtained through the constructed SRM for fine-grid reservoir, the following can be pointed out:

- The results of the fine-grid SRM in generating the pressure field demonstrate higher accuracy, when applied to the blind case, compared to that of the coarse grid. As mentioned in section 7.2.4 the pressure networks could be over-trained for the coarse grid SRM where the pressure data of all grid blocks are included in the training set. Whereas, for the fine grid pressure networks only a portion of the data are considered in the training process which could prevent the networks from being over-trained.

- In general, pressure distribution generated by fine-grid SRM is of very high accuracy (less than 3% of error) compared to gas saturation and CO_2 mole fraction distribution. The reason lies in the fact that the reservoir has a relatively small volume with strong aquifer support and therefore, the entire reservoir is pressurized as a result of CO_2 injection. Consequently, pressure does not have a clear front which needs to be specifically detected. This can be the reason why the changes in pressure can be captured effectively through the sampled data.

- On the contrary, the output generated by fine-grid SRM for gas saturation and CO_2 mole fraction shows higher amounts of error, and therefore the accuracy is less than the coarse-grid SRM. The reason is that both of these two parameters have a sharp front, and therefore in order to be accurately detected, sufficient amount of data is required to be introduced to the network particularly from the areas close to the edge of the plume.
  The problem of having insufficient data comes from two main sources. The first one is that although the sampling methodology is based on selecting the majority of the data from the area with maximum amount of change, it does not guarantee selection of all the data specifically from the edge of the CO_2 plume. The second reason is that the plume always extends more in the simulation cases where more amounts of CO_2 is injected into the reservoir, and therefore the grid blocks that are affected by this maximum amount of CO_2, if selected during the sampling process, are introduced to the network only once. This does not provide enough data for the network to learn from the extended CO_2 plume area.

7.4 Modification to Fine-Grid SRM

Evaluating the errors, especially the gas saturation and CO_2 mole fraction errors, suggests that performing some modifications to the inputs of the neural network might be helpful to better introducing the variability of the system to the neural network which could ultimately improve the SRM accuracy in generating the reservoir model output.

The problem mentioned above can be addressed to some extent by adding more scenarios closer to the desired maximum amount of injection. For instance, if the maximum amount of total CO_2 that is designed to be injected into a reservoir equals to $3 \times G$ (assuming G as the base amount of CO_2 to be injected), some simulation cases in which the amount of total CO_2 is close and larger than this amount can be conducted. Using data related to this higher total CO_2 injection can provide more information from the grid blocks in the edge of the CO_2 plume.

7.4.1 Adding to the Number of Training Cases

Based on the error evaluation of the previously developed SRM for fine-grid reservoir, the decision was made to increase the number of training simulation cases from 3 scenarios to 5. The 5 scenarios include the 3 original training cases, and two other cases in which the amount of CO_2 injection is close to the maximum target of total injected CO_2.

The following plots demonstrate the monthly CO_2 injection schedule for 5 training simulation runs for 8 months and 24 months of injection respectively. In these plots, the CO_2 monthly injection rate curves related to the three initial simulation runs are shown in solid lines and the two injection rate curves related to the new simulation cases are demonstrated by dashed lines.

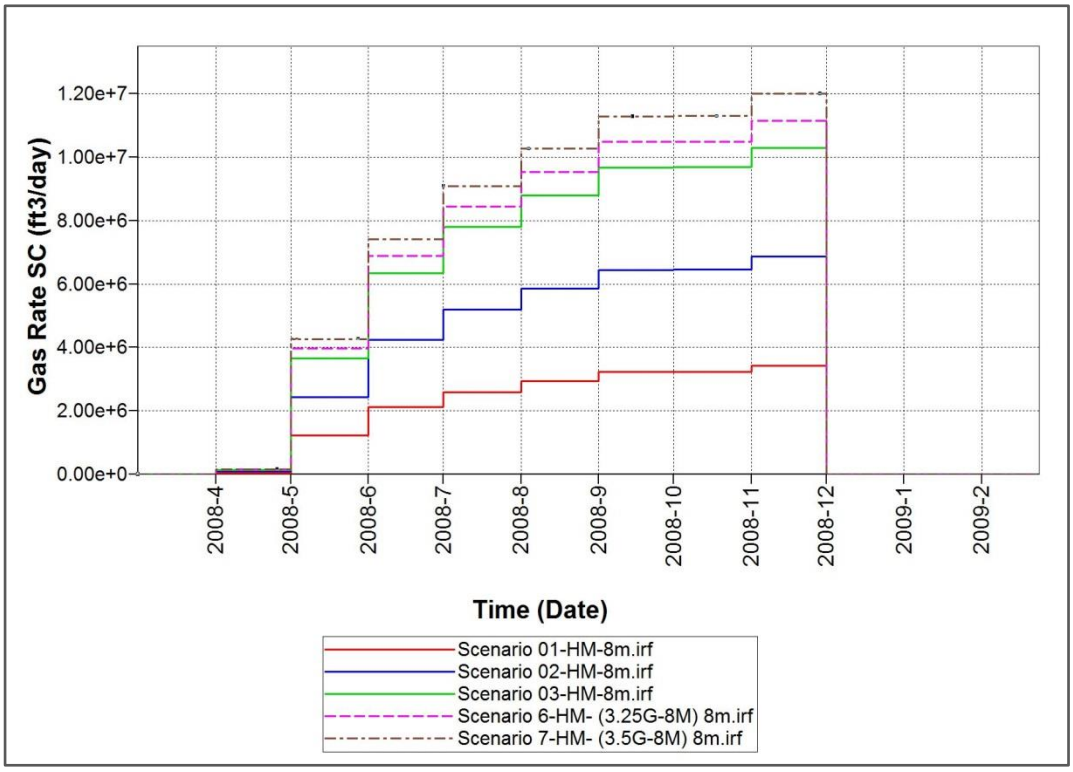

Figure 60. Five CO_2 injection scenarios within 8 months of injection

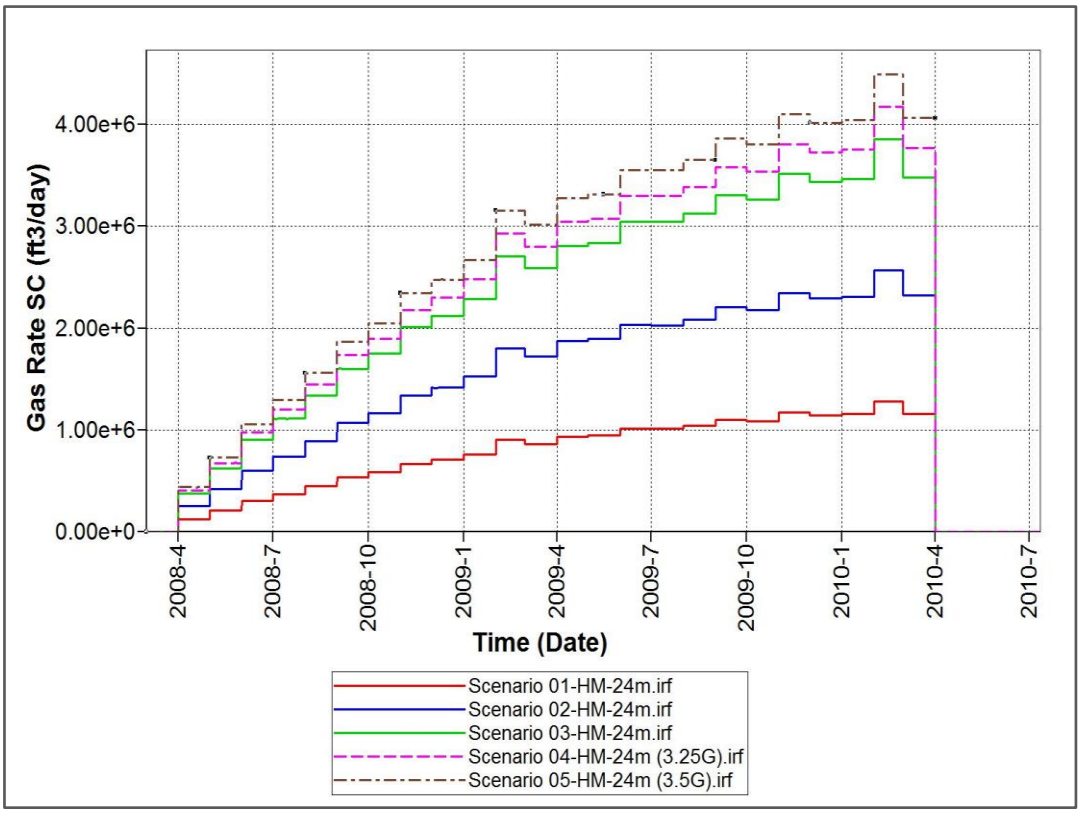

Figure 61. Five CO_2 injection scenarios within 24 months of injection

7.4.2 Modified Fine-Grid Models for 8 Months of injection

A new data set was generated which includes the static, dynamic, and well data pertaining to the new simulation runs in addition to the 3 orginial simulation cases. This data set comprises 500,000 rows of data, which must be reduced in order to be used for neural network trianig.

For reducing the number of data, 10% of the data was decided to be selected. In order to ensure selection of the maximum number of grid blocks, which were affected by CO_2 injection, the sampling procedure was implemented for each simulation case individually.

In the next step, SRM inputs were generated for 8 months and in total 24 neural networks were trained for pressure, gas saturation, and CO_2 mole fraction at each month.

The results of the developed SRM for the first layer of the reservoir are demonstrated in the following section. The results for some other reservoir layers in other time steps are presented in Appendix-C.

Modified SRM Results for Training Case-8 Months of Injection

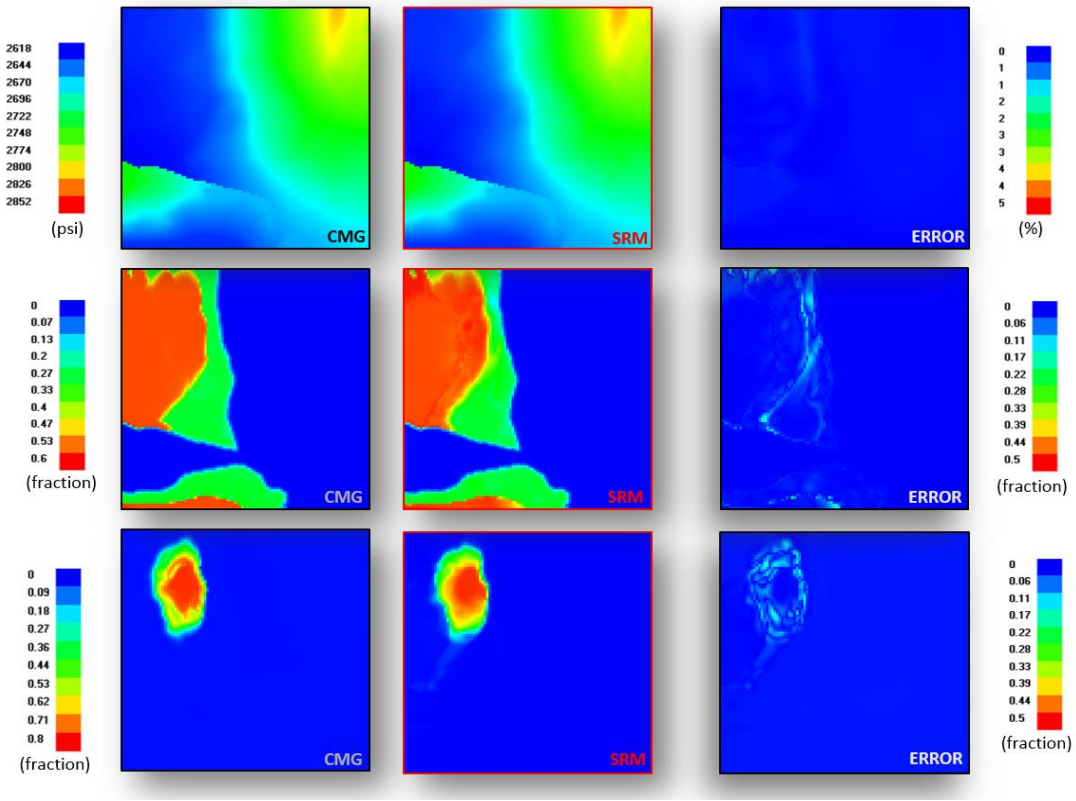

Figure 62. Distribution maps of Pressure, Gas saturation and CO_2 mole fraction in the first layer of the reservoir (from left: CMG output, SRM result and Error) – Training case-4 Months after injection

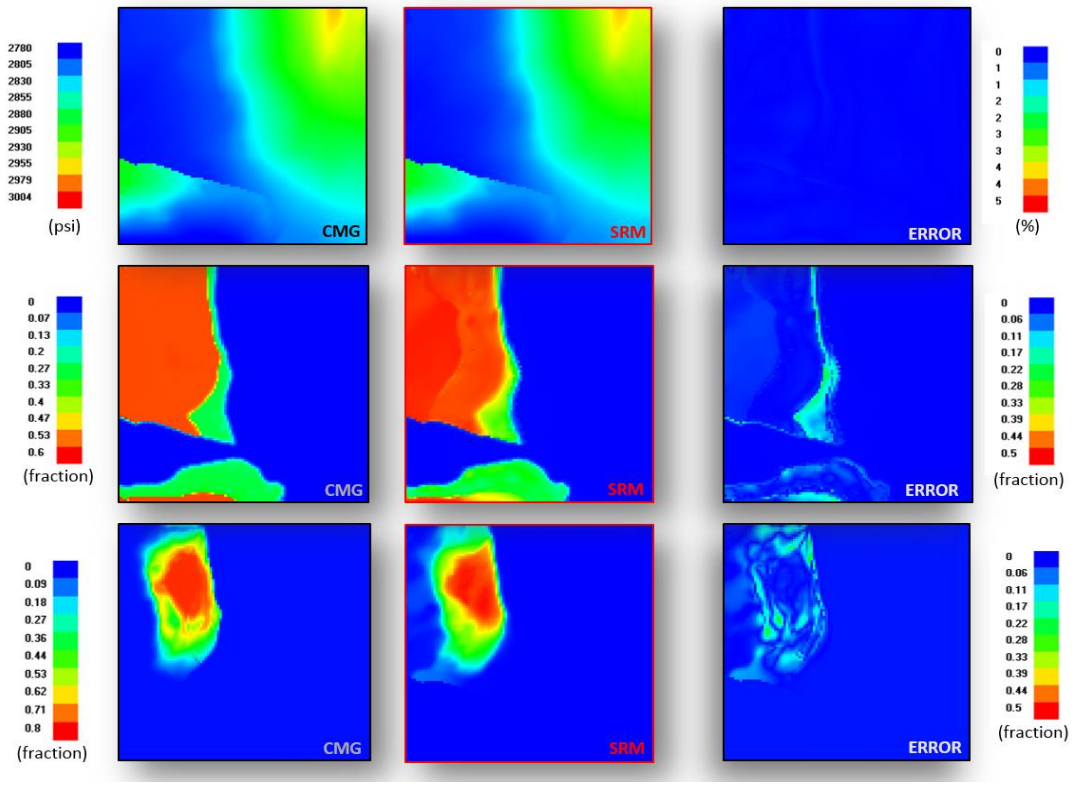

Figure 63. Distribution maps of Pressure, Gas saturation and CO_2 mole fraction in the first layer of the reservoir (from left: CMG output, SRM result and Error) – Training case-8 Months after injection

Modified SRM Results for Blind Case-8 Months of Injection

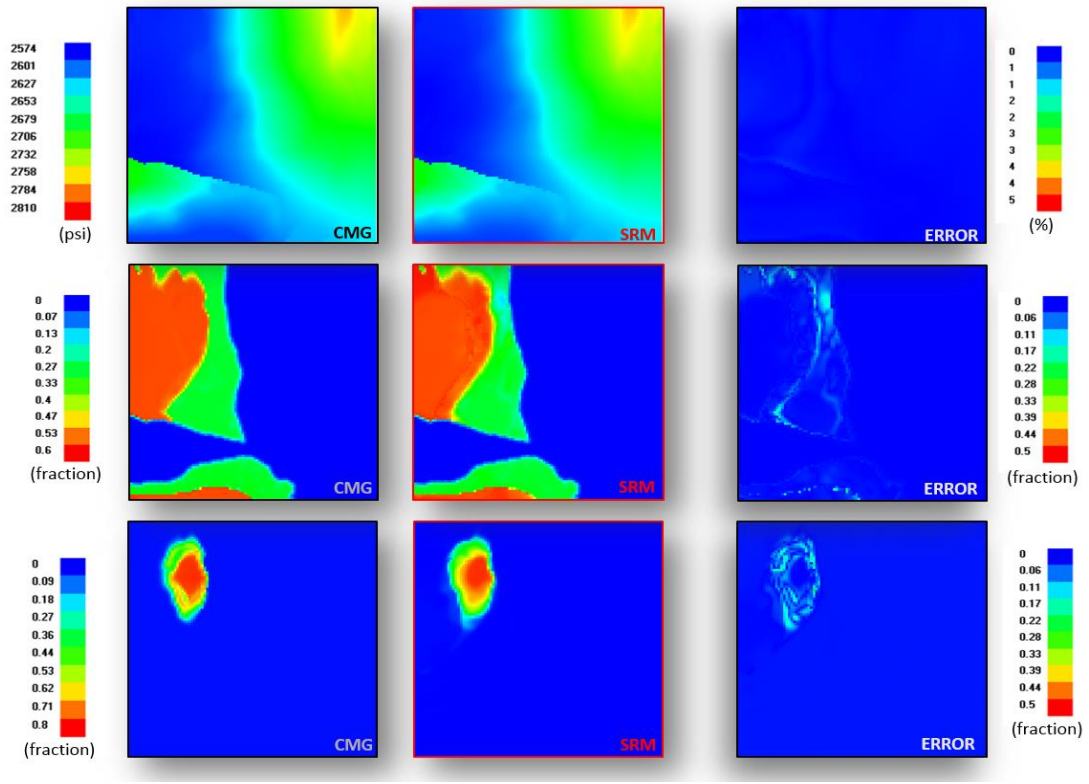

Figure 64. Distribution maps of Pressure, Gas saturation and CO_2 mole fraction in the first layer of the reservoir (from left: CMG output, SRM result and Error) – Blind case-4 Months after injection

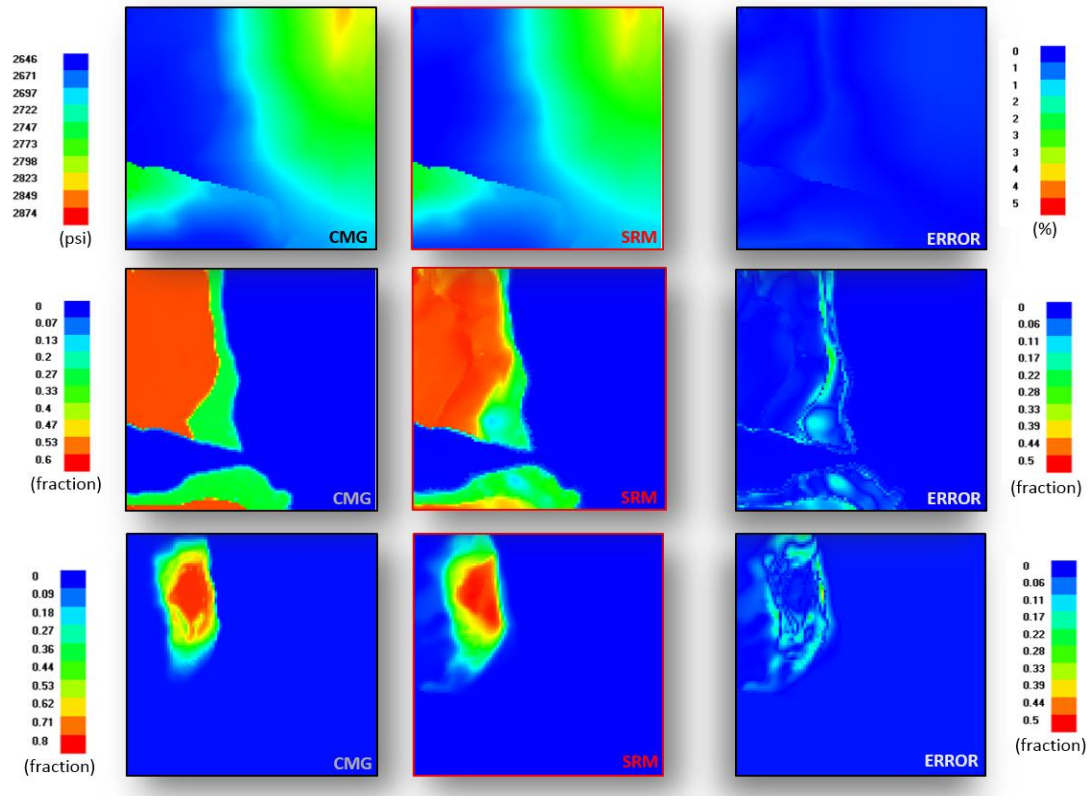

Figure 65. Distribution maps of Pressure, Gas saturation and CO_2 mole fraction in the first layer of the reservoir (from left: CMG output, SRM result and Error) – Blind case-8 Months after injection

7.4.3 Fine-Grid Models for 24 Months of Injection

The results of the SRM for 8 months of injection suggests that including more numbers of training simulation cases leads to an improvement in the accuracy of the output generated by SRM. Therefore, the same strategy was used to develop SRM for the simulation cases with 24 months of CO_2 injection.

The same procedure as described above was followed to generate individual SRM input for pressure, gas saturation, and CO_2 mole fraction for 24 months.

The corresponding neural networks were developed and trained for 24 months. The results when SRM is applied to one training case (Scenario#1) and one Blind case (when 1.5 G of CO_2 is injected into the reservoir) are presented in the following sections.

Modified SRM Results for Training Case-24 Months of Injection

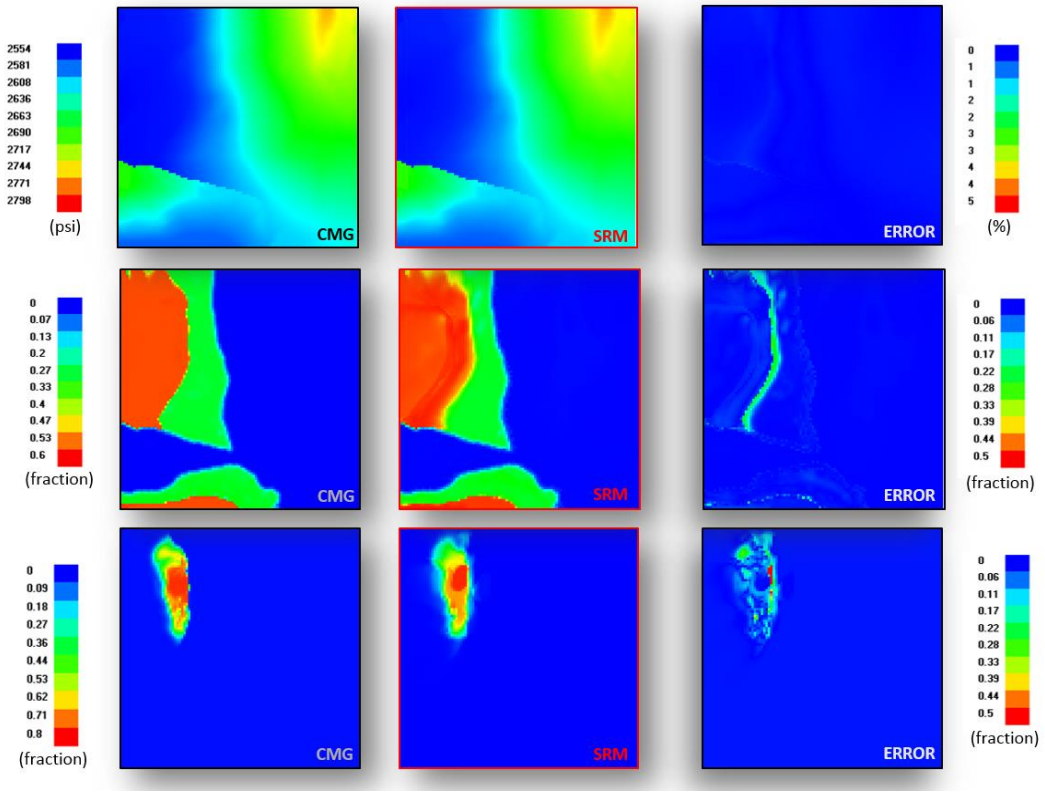

Figure 66. Distribution maps of Pressure, Gas saturation and CO_2 mole fraction in the first layer of the reservoir (from left: CMG output, SRM result and Error) – Training case- 12 Months after injection

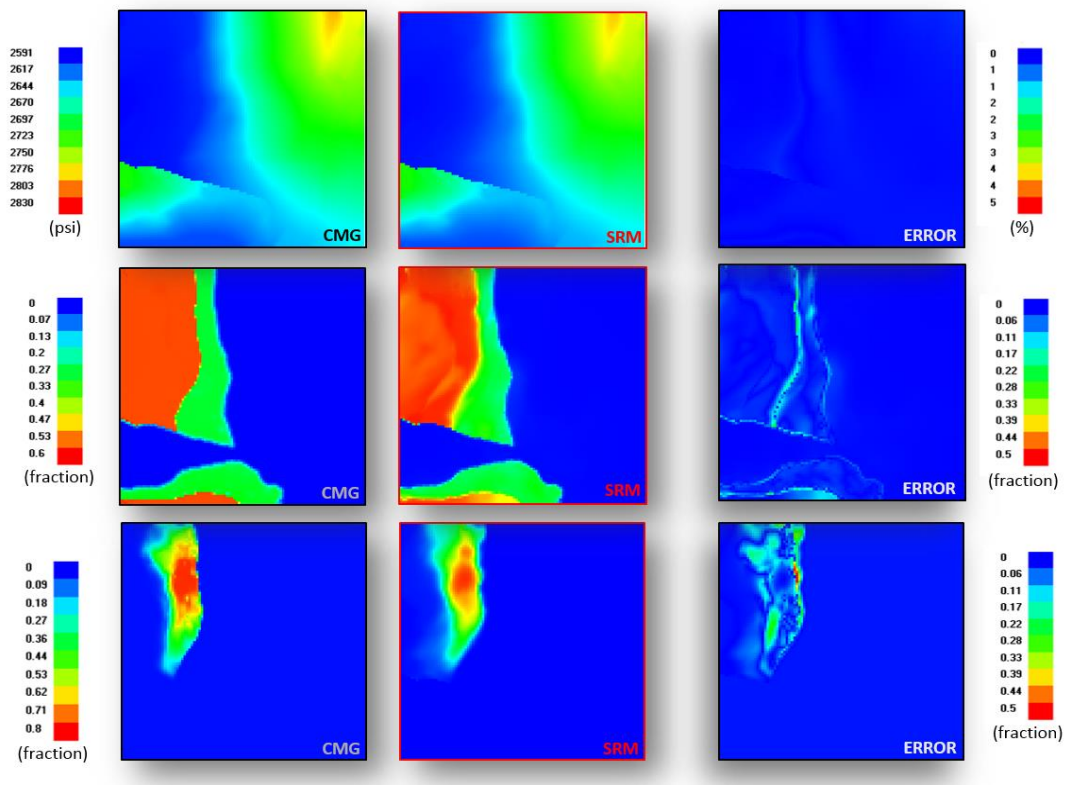

Figure 67. Distribution maps of Pressure, Gas saturation and CO_2 mole fraction in the first layer of the reservoir (from left: CMG output, SRM result and Error) – Training case- 24 Months after injection

Modified SRM Results for Blind Case-24 Months of Injection

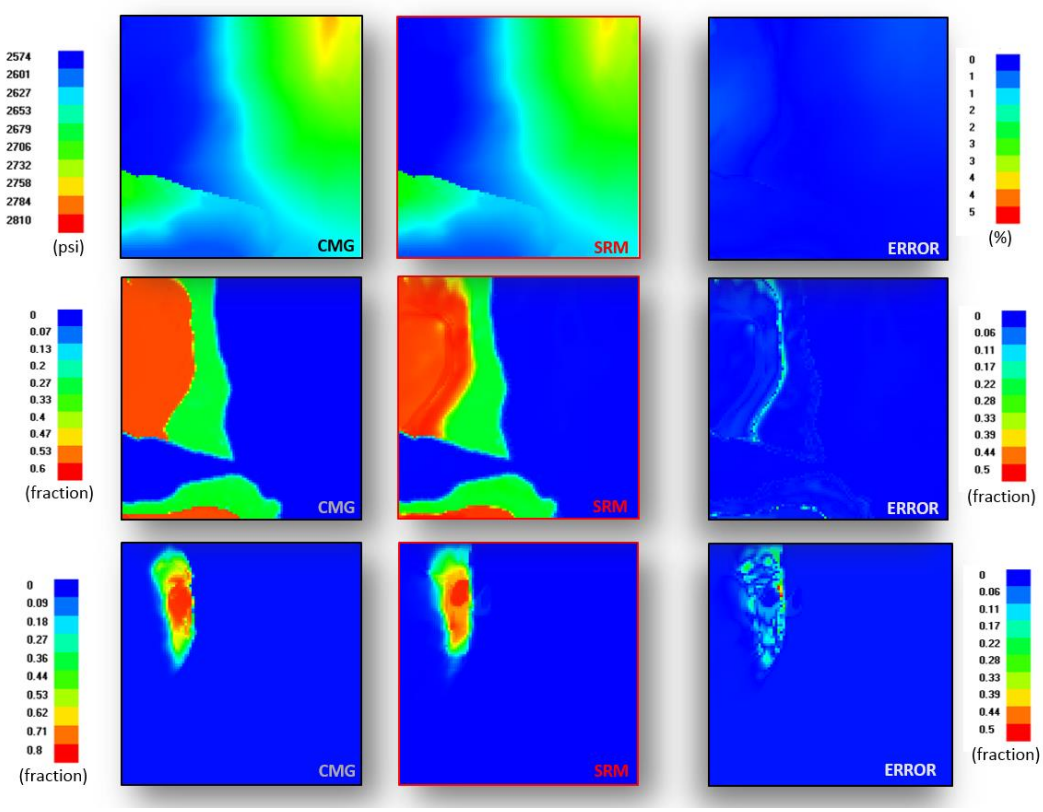

Figure 68. Distribution maps of Pressure, Gas saturation and CO_2 mole fraction in the first layer of the reservoir (from left: CMG output, SRM result and Error) – Blind case- 12 Months after injection

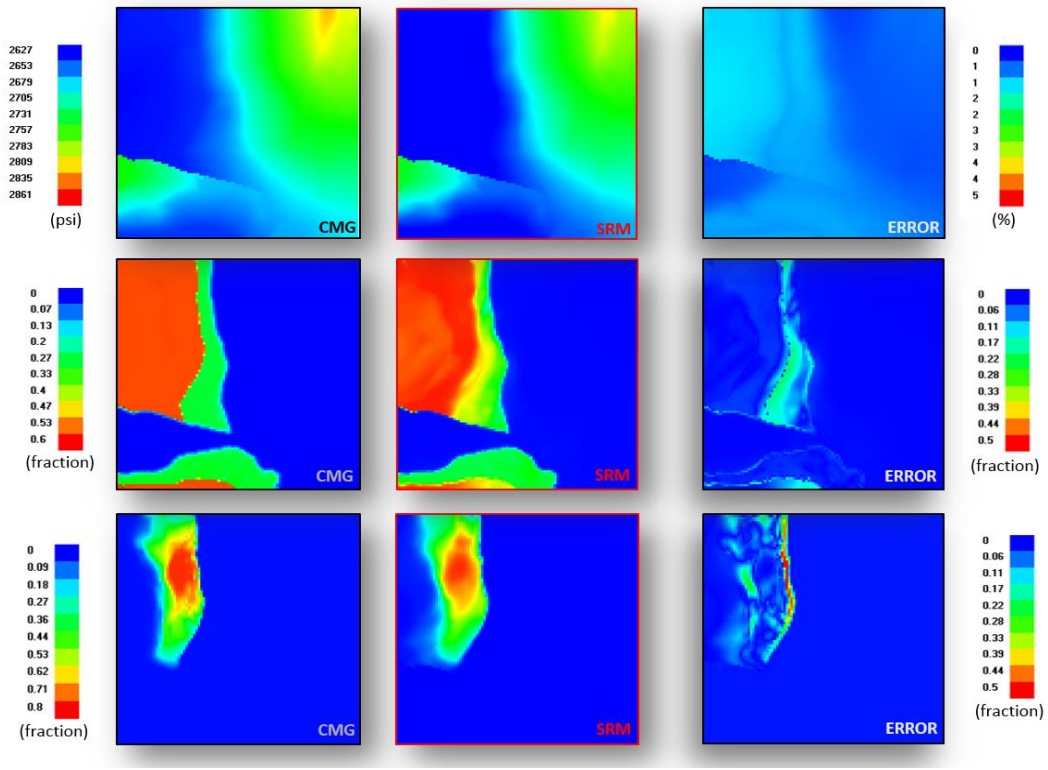

Figure 69. Distribution maps of Pressure, Gas saturation and CO_2 mole fraction in the first layer of the reservoir (from left: CMG output, SRM result and Error) – Blind case- 24 Months after injection

7.4.3.1 Fine-Grid SRM Error Evaluation

The 2D distribution maps, which were presented in the previous sections, visualize the SRM result versus the CMG output for each layer of the reservoir. In this section the frequency error plots is presented in order to demonstrate the frequency distribution of the error for all grid blocks of the reservoir.

The plots presented in Figure 70 to Figure 75 are generated for each parameter of pressure, gas saturation, and CO_2 mole fraction individually when neural networks are applied to two different scenarios with 24 months of injection (the training case and the blind case) at three time steps during the injection (as an example).

Generally, the frequency of the grid blocks with higher amount of error increases when the neural networks are applied to the blind case as opposed to the training case, especially in the later time steps.

The same as the coarse-grid SRM the results show that the pressure networks have the highest acuracy in predicting the pressure distribution since for this parameter the amount of error for the blind case scenario after 24 months of injection does not exceed 2%.
The frequency error plot for gas saturation prediction for the same blind case after 24 months of injection shows that around 85% of the grid blocks have an error of less than 0.02.
The prediction results for the same case for CO_2 mole fraction show that more than 95% of the grid blocks have an error of less than or equal to 0.05.

Observing the amount of error presented in the frequency error plots it can be concluded that the accuracy of the developed fine-grid SRM is comparable to that of the coarse-grid which demonstrates that the SRM is able to generate the outputs of a large numercial reservoir simulation model very effectively even when only 10% of the data are used.

Pressure Error Frequency Distribution plots-Training Case

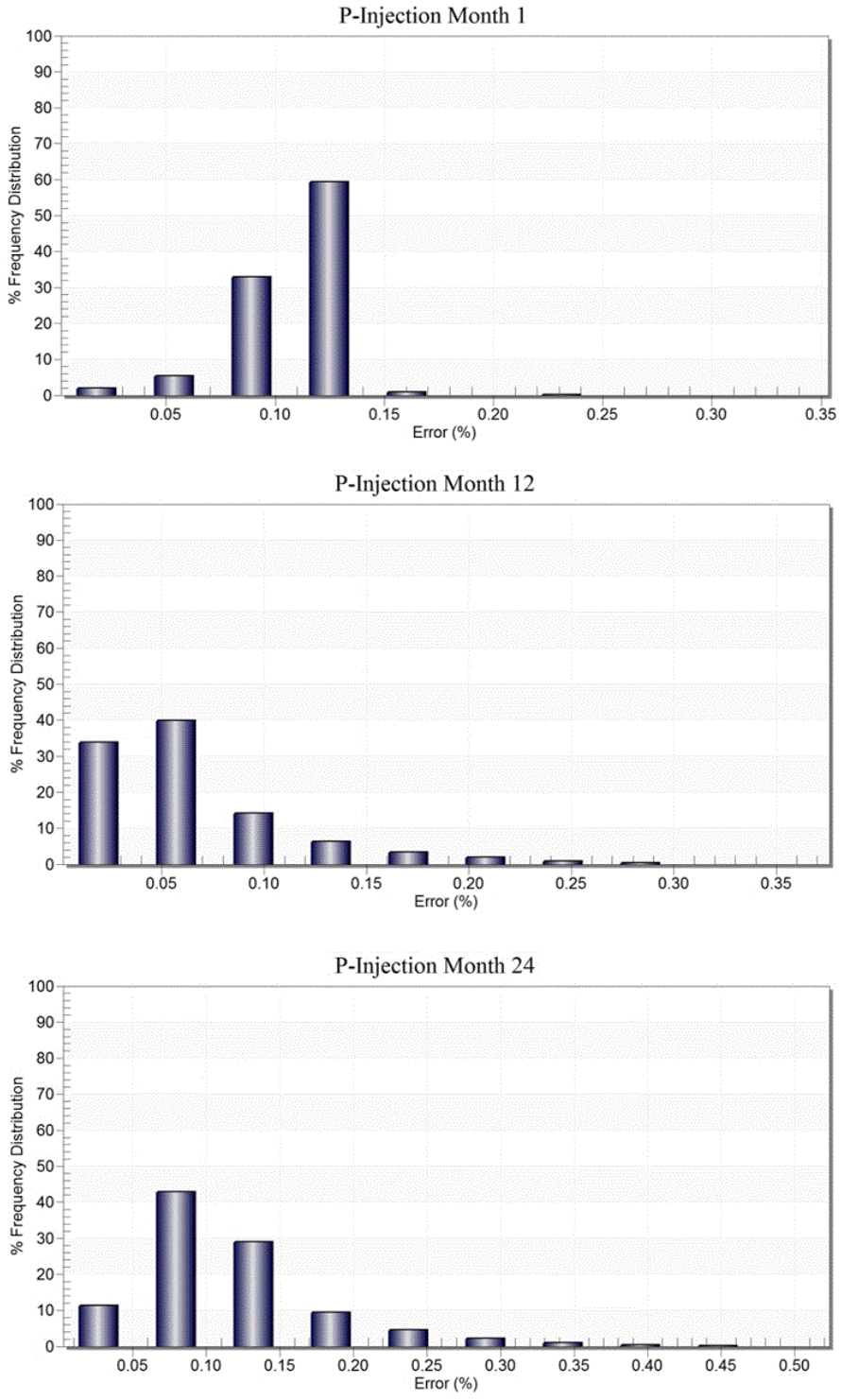

Figure 70. Pressure Error Frequency Distribution for all grid blocks of the reservoir at 3 time steps during the injection-Training case

Pressure Error Frequency Distribution plots-Blind Case

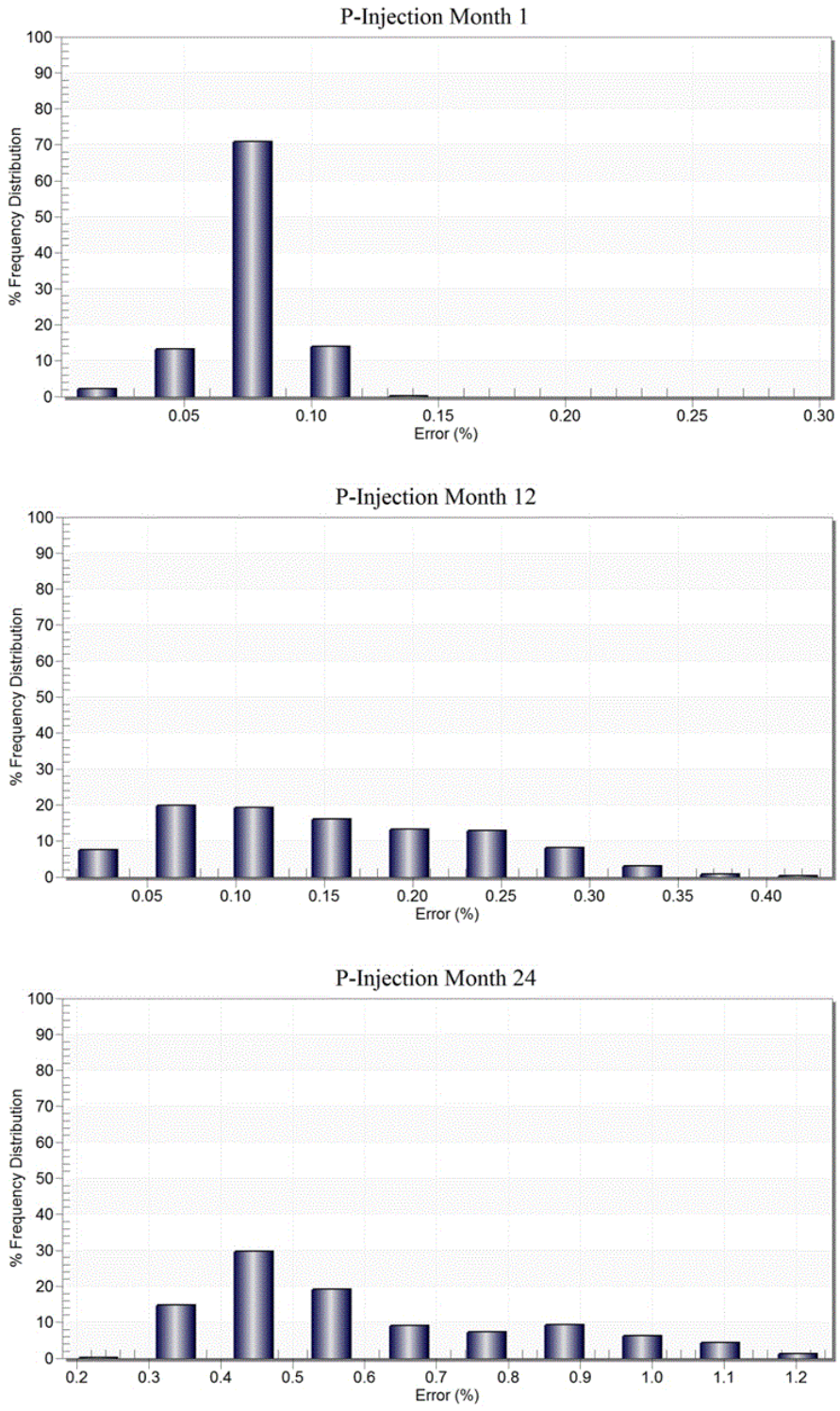

Figure 71. Pressure Error Frequency Distribution for all grid blocks of the reservoir at 3 time steps during the injection-Blind case

Gas Saturation Error Frequency Distribution plots-Training Case

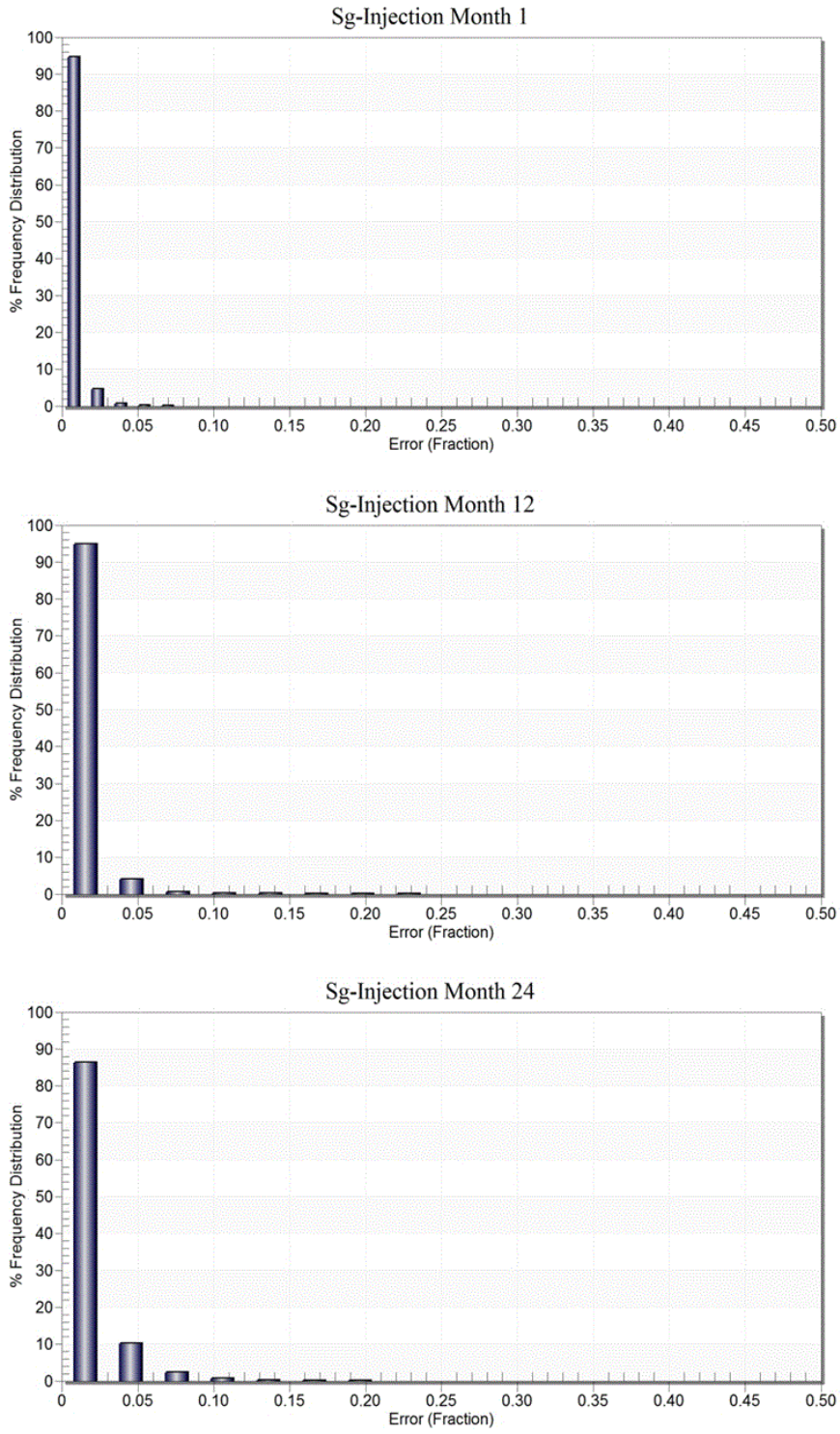

Figure 72. Gas Saturation Error Frequency Distribution for all grid blocks of the reservoir at 3 time steps during the injection-Training case

Gas Saturation Error Frequency Distribution plots-Blind Case

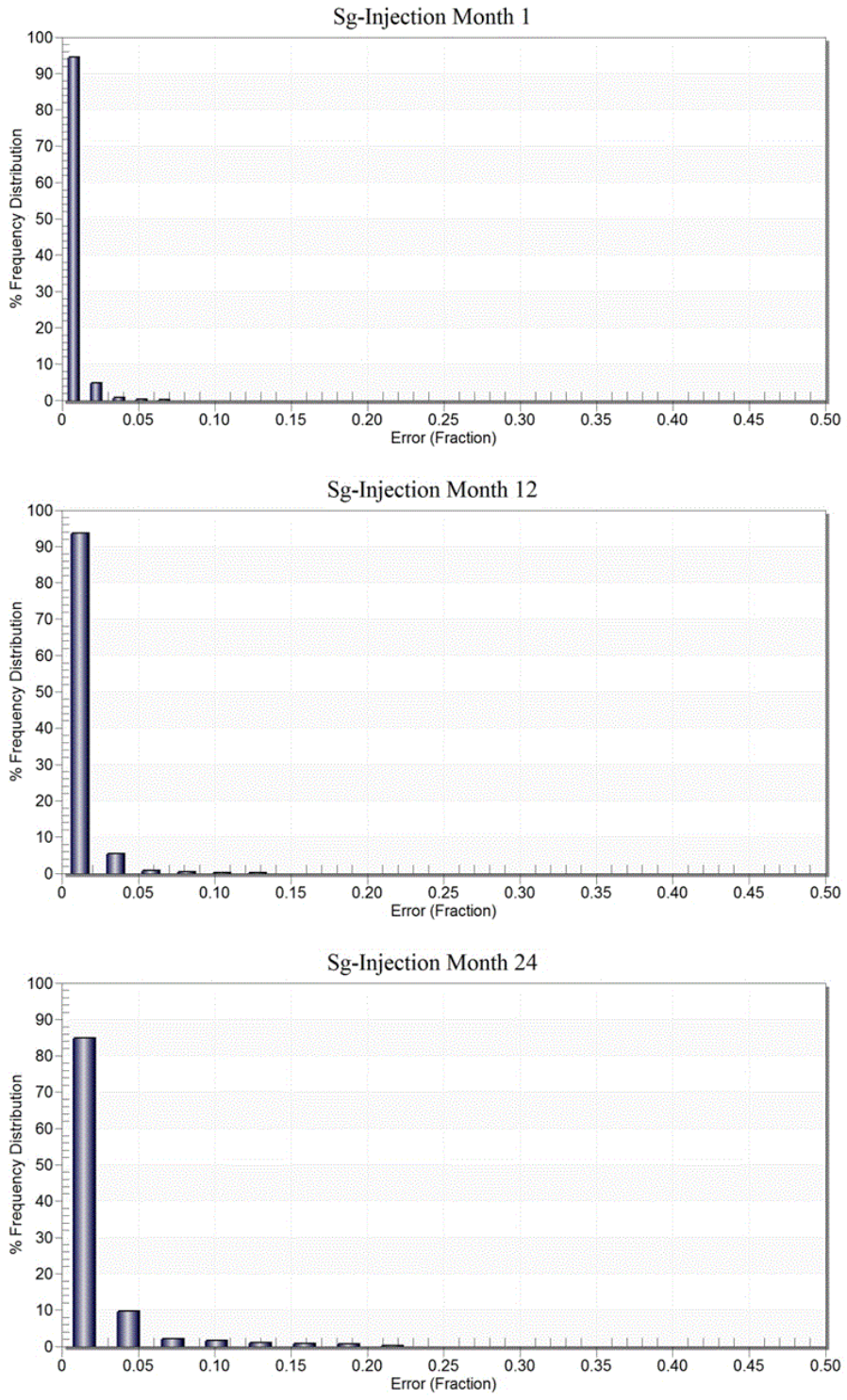

Figure 73. Gas Saturation Error Frequency Distribution for all grid blocks of the reservoir at 3 time steps during the injection-Blind case

CO_2 Mole Fraction Error Frequency Distribution plots-Training Case

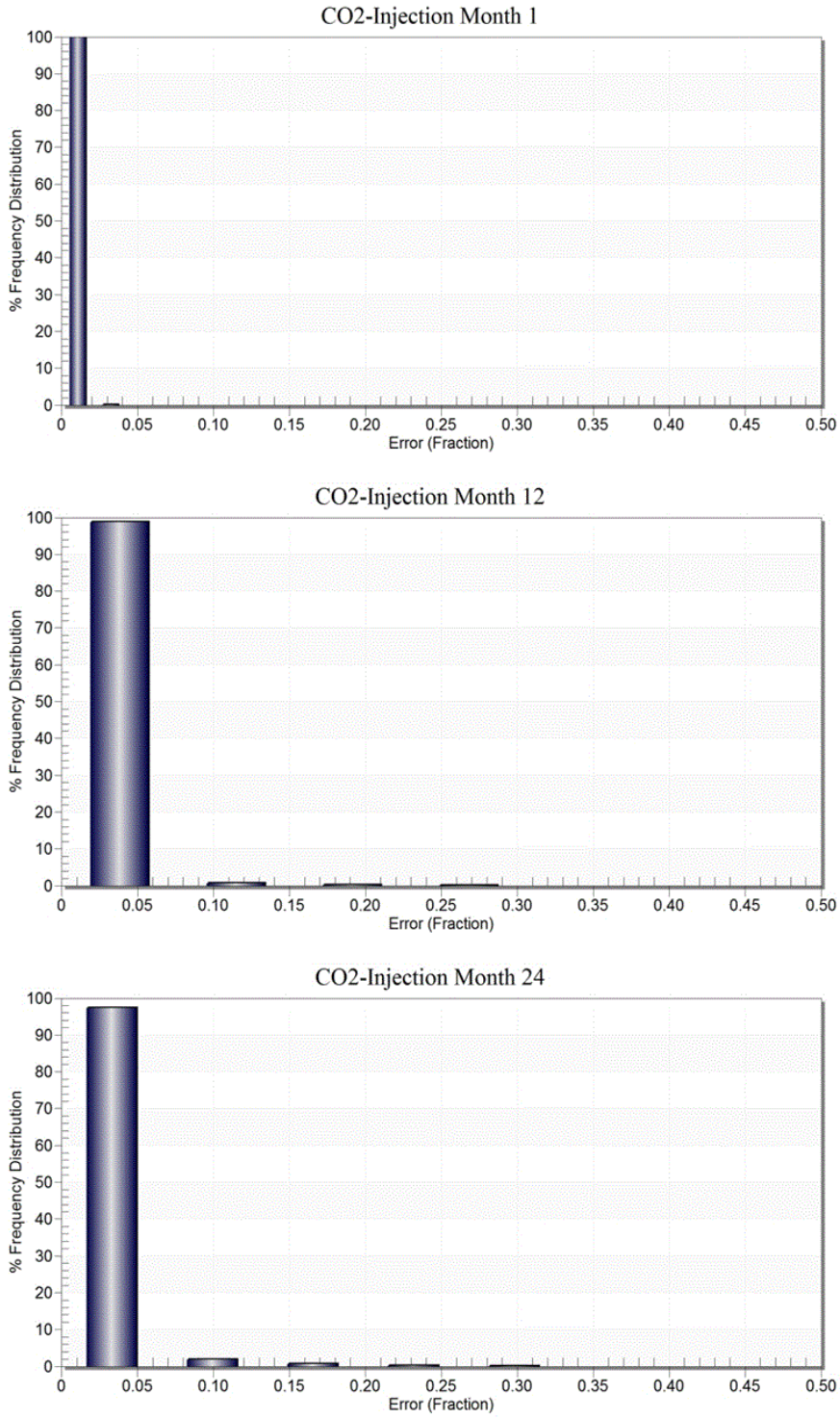

Figure 74. CO_2 mole fraction Error Frequency Distribution for all grid blocks of the reservoir at 3 time steps during the injection-Training case

CO_2 Mole Fraction Error Frequency Distribution plots-Blind Case

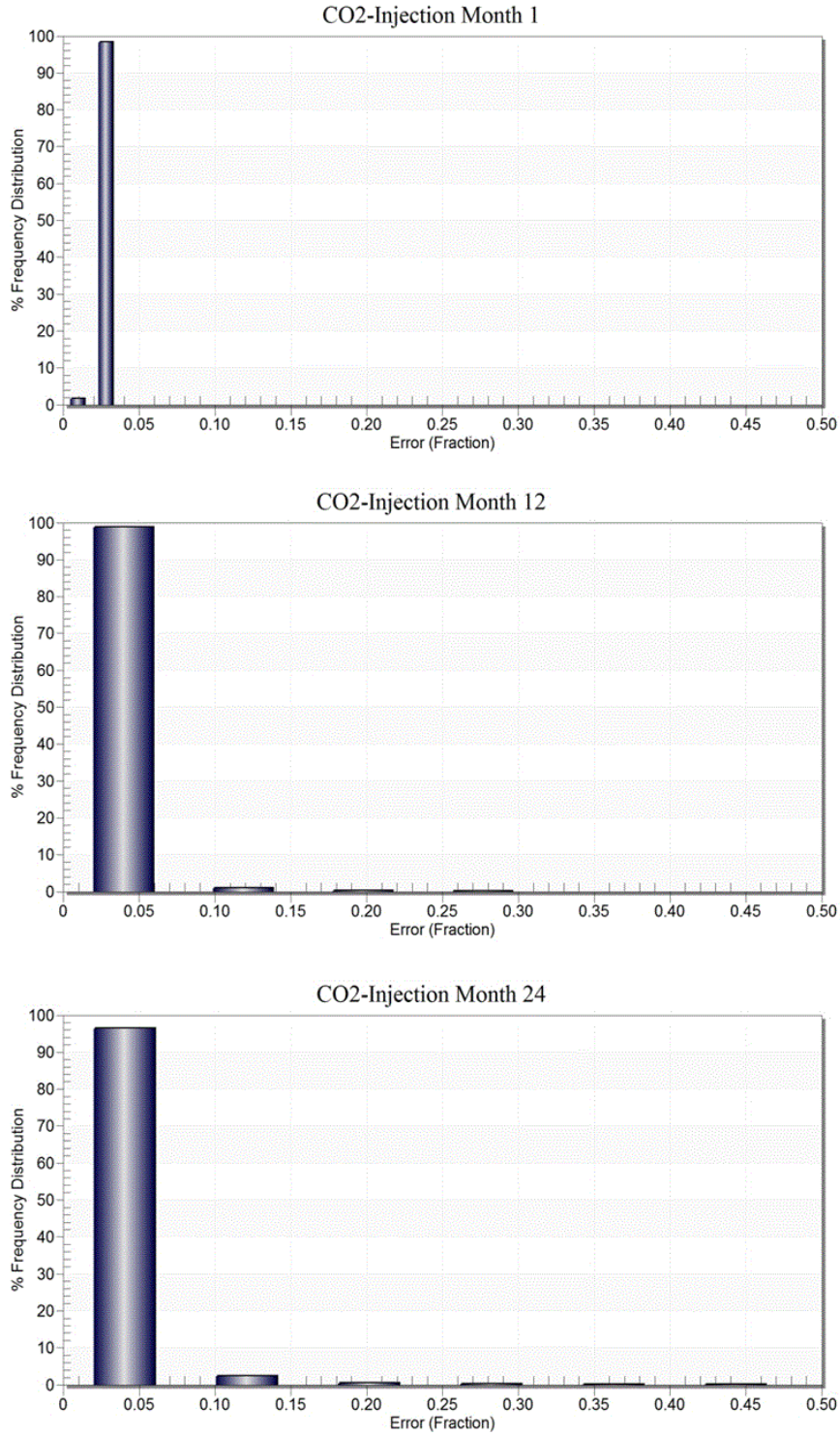

Figure 75. CO_2 mole fraction Error Frequency Distribution for all grid blocks of the reservoir at 3 time steps during the injection-Blind case

CHAPTER 8
LESSONS LEARNED AND CONCLUDING REMARKS

8.1 Lessons Learned

In this work artificial intelligence has been applied as a technique to develop a proxy/surrogate reservoir model to be substituted for a numerical reservoir simulation model. This proxy model generates the outputs of the reservoir simulation model at the grid bock level, or in other words, it is able to calculate the pressure, gas saturation, and CO_2 mole fraction distribution throughout the reservoir under different injection scenarios.

Different stages which were performed toward developing the surrogate reservoir model for this specific CO_2 sequestration study is summarized and presented as a flow chart in Appendix-A.

The following can be pointed out as the most important findings of this study:

1. Neural networks can be considered as an efficient tool which is capable of learning the behavior of a system through the provided data. These data must be collected wisely so that the system behavior can be captured and learned by the network. This is one of the most important aspects of application of a neural network which makes all the difference between employing the neural network as a black box, and changing that to a transparent box. If the amount of data to develop the model is not sufficient, or the collected data cannot represent the system behavior, the constructed network will have a poor performance and that is the reason why many researchers call the neural network a black box that is not a proper tool to be used for modeling different processes.

2. In the cases where a portion of data must be selected due to the high dimensionality of the data set, application of a proper data sampling method is of significant importance. According to this study in the case of the coarse reservoir model, where the data related to all the grid blocks are included in training, the developed SRM is able to generate the outputs with very high accuracy by including only 3 training simulation runs. However, the SRM developed for the fine grid reservoir, in which only 10% of the data are included in the training process, the generated outputs through SRM (using 3 simulation runs) are of lower accuracy. Therefore, in this case more simulation runs are required to be included in the training so that the variability of the system can be properly introduced to the network through sufficient sampled data.

3. The CO_2 sequestration project, which the current research was implemented on, is not the best candidate for developing a SRM which is able to generate the dynamic parameter distribution under different geological realizations. The reason is that in this reservoir there is only a single injection well through which CO_2 is injected into the reservoir. Therefore, the data which should introduce the plume extension and its behavior during CO_2 injection only comes from a single injection point and some grid blocks close to this location in the entire reservoir.

   If the injection process is performed in several locations throughout the reservoir, then the data, which is collected from different locations, carry the information related to the injection process, and therefore they can more efficiently reflect the effect of different geological characteristics of the reservoir. In other words, in case of more injection wells the neural network can be more efficiently trained to capture the effect of variability of the reservoir geology on the model output.

4. Since CO_2 mole fraction and gas saturation both have a sharp front, the maximum error occurs around the edge of the plume or close to the fluid front. Therefore, one of the solutions which can improve the results in these areas is to design the majority of the simulation runs close to the maximum amount of injection and even extend the amount of injection to a higher amount than what is required for a specific study. This can help the training process by providing more data from the fluid front location, which leads to a more accurate prediction of the parameter distribution in those areas.

8.2 Concluding Remarks

Based on the current research, Surrogate Reservoir Modeling (SRM) technique, which uses artificial intelligence and data mining, is a very efficient method for developing a proxy/surrogate reservoir model. The developed SRM is capable of generating the results of a complex reservoir simulation model at the grid block level with reasonable accuracy in a very short amount of time with significantly less computational cost.

The several reasons which make this technique an efficient and practical approach for developing proxy model for any complex numerical reservoir model are listed below.

1. SRM is not limited by the choice of a predefined function and therefore it is very flexible. In all the proxy models developed through statistical approaches, the function that represents the system behavior is solely determined through the relationships between the uncertain parameters and the system outputs. However, in SRM any type of data which influences the output of the model or introduces the under study system can be included in model development, no matter what the parameters of interest are. Therefore, the neural network is trained by providing information related to any component of the system, the relationship between these components, and the effect of each of them on system behavior.

2. SRM can be used to model significantly non-linear behavior of a system. The pattern recognition capability of SRM enables the model to capture the interrelationship between multiple parameters of the system without encountering any instability problems. Therefore, SRM can be developed for a very complex reservoir model with more than 10^6 grid blocks and in existence of maximum number of fluid phases (3 dimensional reservoir, 3 phase fluid flow).

3. In SRM development no simplifying assumption is made. In this approach all the complexity of the reservoir, fluid properties, rock properties, etc. are introduced to the neural network. Instead of generating a model by simplifying the physics of the process, SRM tries to find the complex relationship between the inputs and outputs of the system.

4. Once SRM is developed, the input parameters can be changed (within a range) at any time and the output response to this change at that time is calculated in a fraction of a second. In other words the impact of any input alteration on the output can be obtained regardless of the complexity of the reservoir model in a very short amount of time.

For one of the cases studied in this research which includes 100,000 grid blocks with 8 months of CO_2 injection and 500 years of post-injection, the numerical reservoir model developed in CMG takes about 440 minutes to run, however SRM is able to generate the results in less than 2 minutes on the same machine, which means that the developed proxy model can be run about 150 times faster than the original numerical simulation model. About the same amount of run time speed up can be achieved for the other scenarios for this specific study.

CHAPTER 9
RECOMMENDATIONS FOR FUTURE WORK

The current work is the first comprehensive work with the objective of developing a proxy/surrogate model which is able to mimic a numerical reservoir model's output at the gird block level. Therefore, the results of this research can be further improved and its capabilities can be extended in different aspects. For this purpose the following are proposed:

1. Within the current study, two different techniques of cascading and non-cascading SRM development were employed. In the first approach, the inputs to the neural networks included the dynamic parameters of the last time step. In the second, the only dynamic parameter used was the pressure, gas saturation, and CO_2 mole fraction at the time step zero (before injection starts).

   According to the results, in cascading SRM the accuracy of the prediction is decreased as time passes and that is due to the error accumulation that happens through parameter updating at each time step. In the non-cascading approach, since the dynamic parameters at one time step before is not used in neural network training the error is not accumulated. However, since the pattern of the dynamic parameter distribution, especially gas saturation and CO_2 mole fraction are changing during the time, just providing the dynamic parameter at time zero cannot be as useful for the networks at the later time steps.

   Therefore, it is suggested to use a semi-cascading approach to develop the SRM. In this approach, dynamic parameters of the previous time step are used at every predetermined time interval (not at every single time steps). For instance, if the CO_2 injection duration is 24 months, after each 6 month pressure, gas saturation, and CO_2 mole fraction of the previous time can be included in the in network inputs. This, on one hand, introduces to the network the new pattern of the dynamic parameter distribution, and on the other hand, reduces the error accumulation. Consequently, this approach can help increasing the accuracy of the output generation specifically during the later time steps.

2. The sampling method which was used in this study is a significantly efficient method of data selection for this specific case. However, based on the error evaluation for each individual dynamic parameter more data can be selected and included in the training process from specific areas which still have higher error distribution. This can be used as a local diagnostic approach which can improve the accuracy of the results.

3. The result of the SRM which was developed for different geological realizations of this specific case of CO_2 sequestration was not of acceptable accuracy. This is due to the fact that in this specific project injection takes place in a single location of the reservoir and therefore the data which are gathered from the entire grid blocks of the reservoir does not provide sufficient information about the injection process.

   For this reason, it is suggested to apply the same methodology to a different case with more injection wells throughout the reservoir and observe the performance of the surrogate reservoir model in generating the outputs of numerical reservoir model when the model is run under different porosity and permeability distribution.

4. In this work the SRM was developed for ascending CO_2 injection schedule; however, the application of grid-based SRM can be extended to study the reservoir behavior under varying injection/production schedule.

Appendix-A

A-1. SRM Development procedure in different Stages

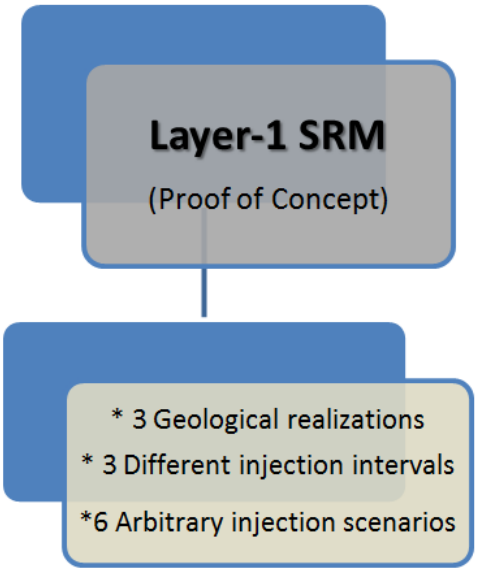

Figure 76. Layer-1 SRM development

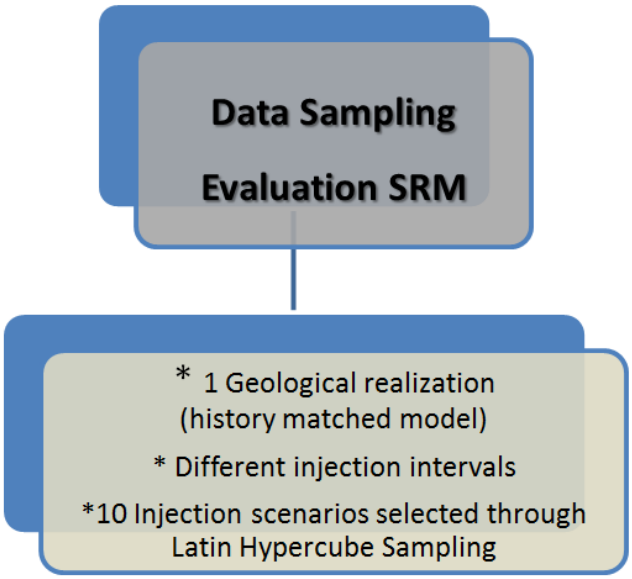

Figure 77. SRM development for data sampling evaluation

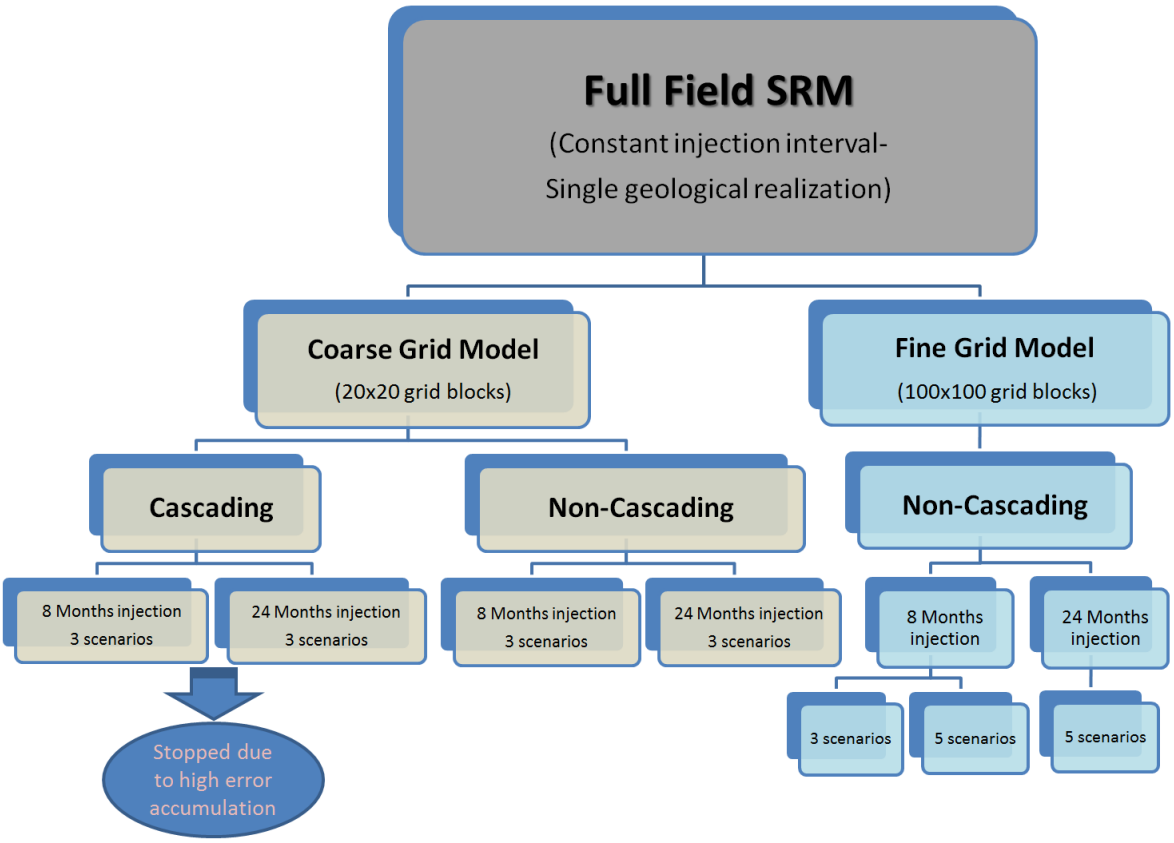

Figure 78. Full field SRM development flow chart

Appendix-B

B-1. Cascading SRM Results for coarse-grid model

The result of cascading SRM for the first layer of the reservoir was presented in Chapter 7 (section 7.2.3). In this section the dynamic parameter distribution maps generated by SRM for layer 2 and layer 4 of the reservoir, in 2 different time steps during the injection interval (in the middle of the injection and at the end of injection), are demonstrated and compared to the corresponding CMG outputs.

B-1.1. Layer 2-Training Case-8 Months of Injection

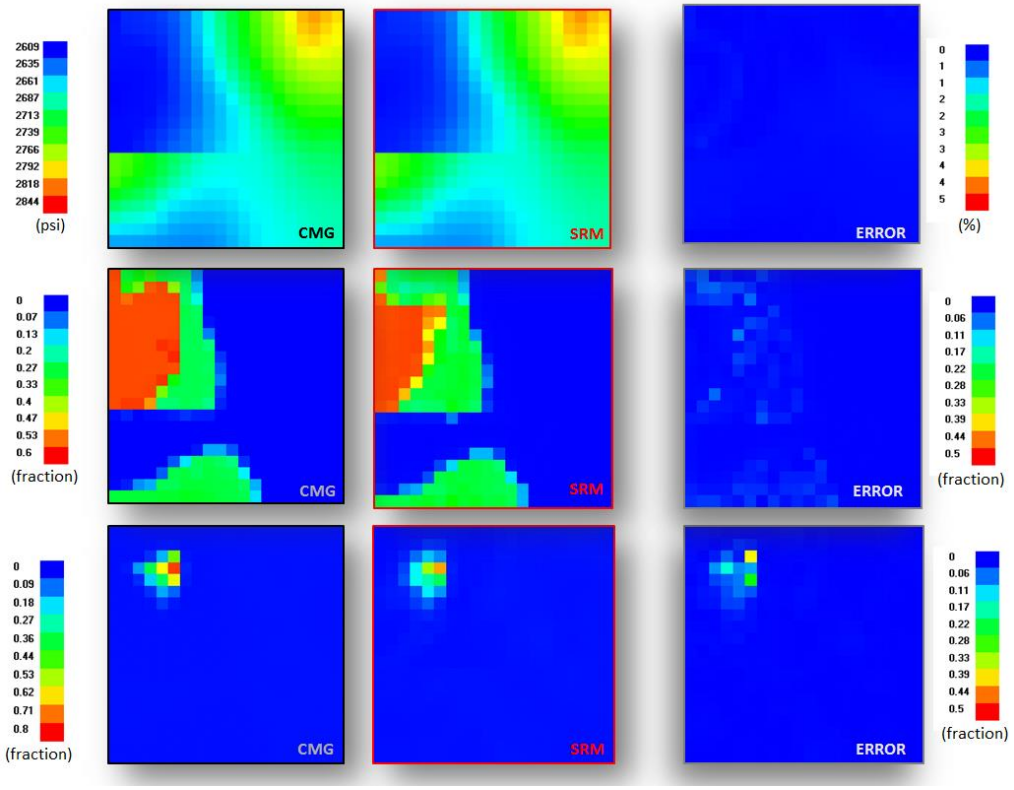

Figure 79. Distribution maps of Pressure, Gas saturation and CO_2 mole fraction in layer 2 of the reservoir (from left: CMG output, SRM result and Error) – Training case- 4 Months after injection

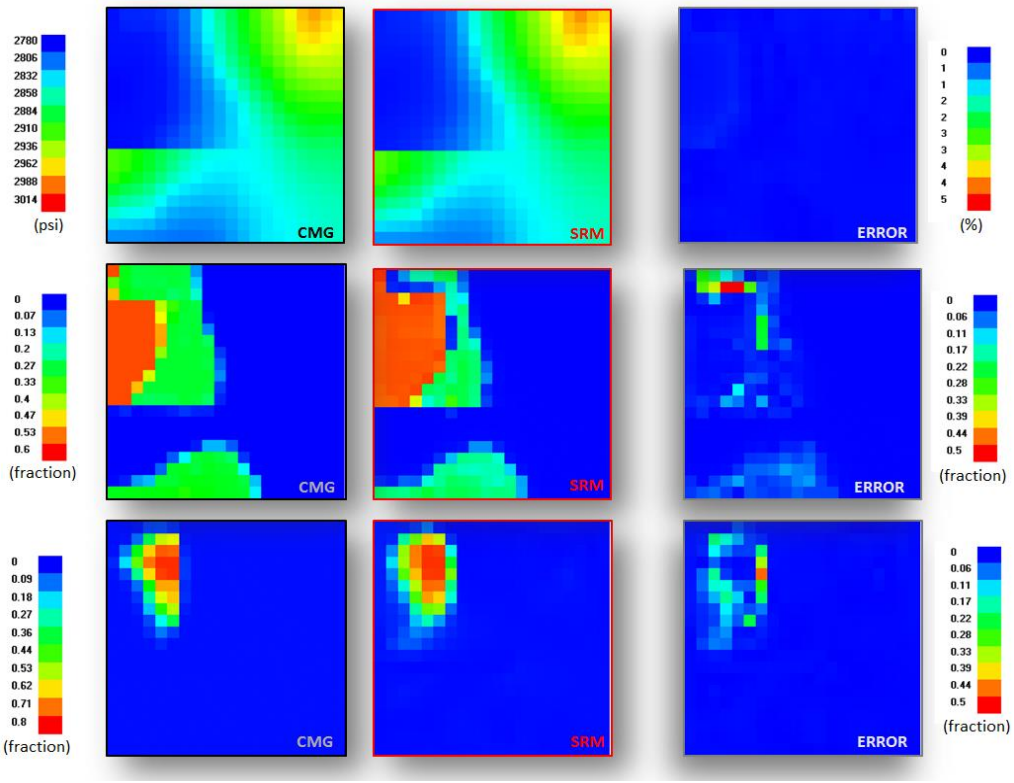

Figure 80. Distribution maps of Pressure, Gas saturation and CO_2 mole fraction in layer 2 of the reservoir (from left: CMG output, SRM result and Error) – Training case- 8 Months after injection

B-1.2. Layer 4-Training Case-8 Months of Injection

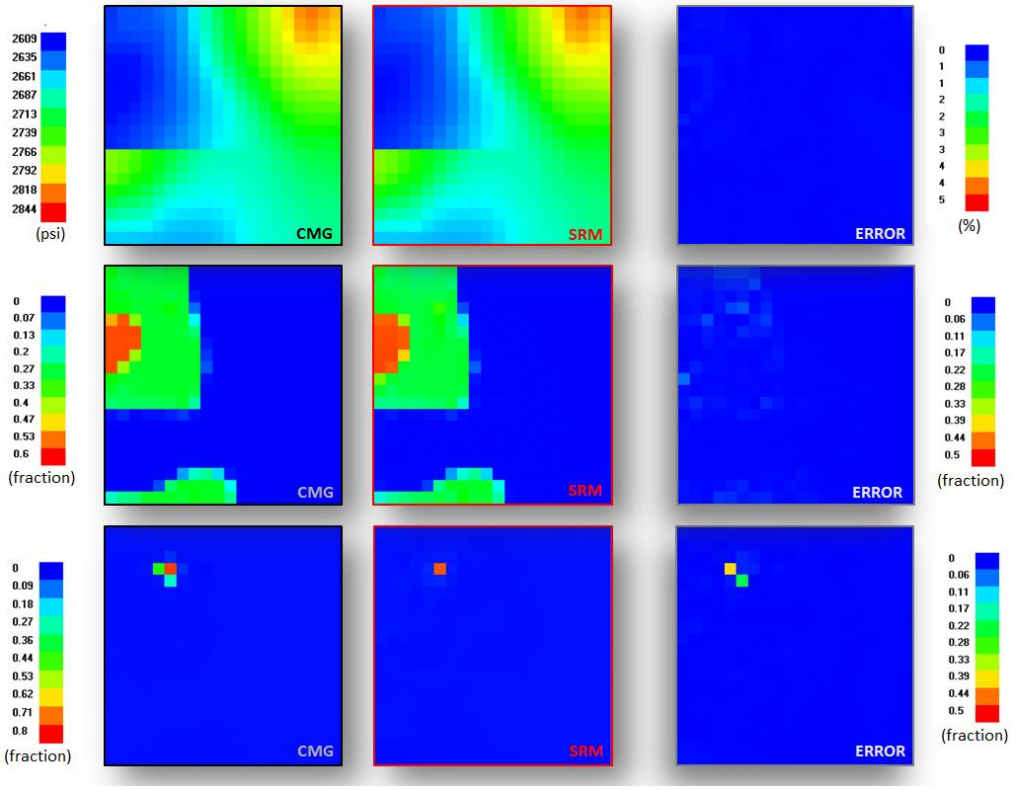

Figure 81. Distribution maps of Pressure, Gas saturation and CO_2 mole fraction in layer 4 of the reservoir (from left: CMG output, SRM result and Error) – Training case- 4 Months after injection

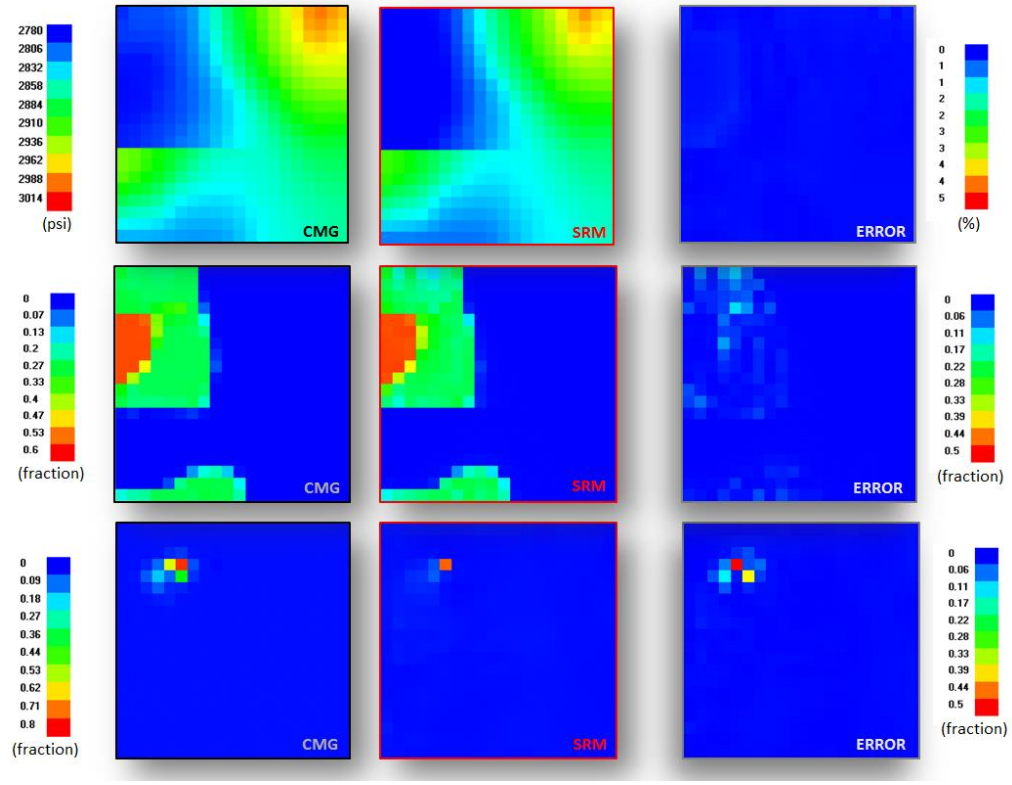

Figure 82. Distribution maps of Pressure, Gas saturation and CO2 mole fraction in layer 4 of the reservoir (from left: CMG output, SRM result and Error) – Training case- 8 Months after injection

B-1.3. Layer 2-Training Case-24 Months of Injection

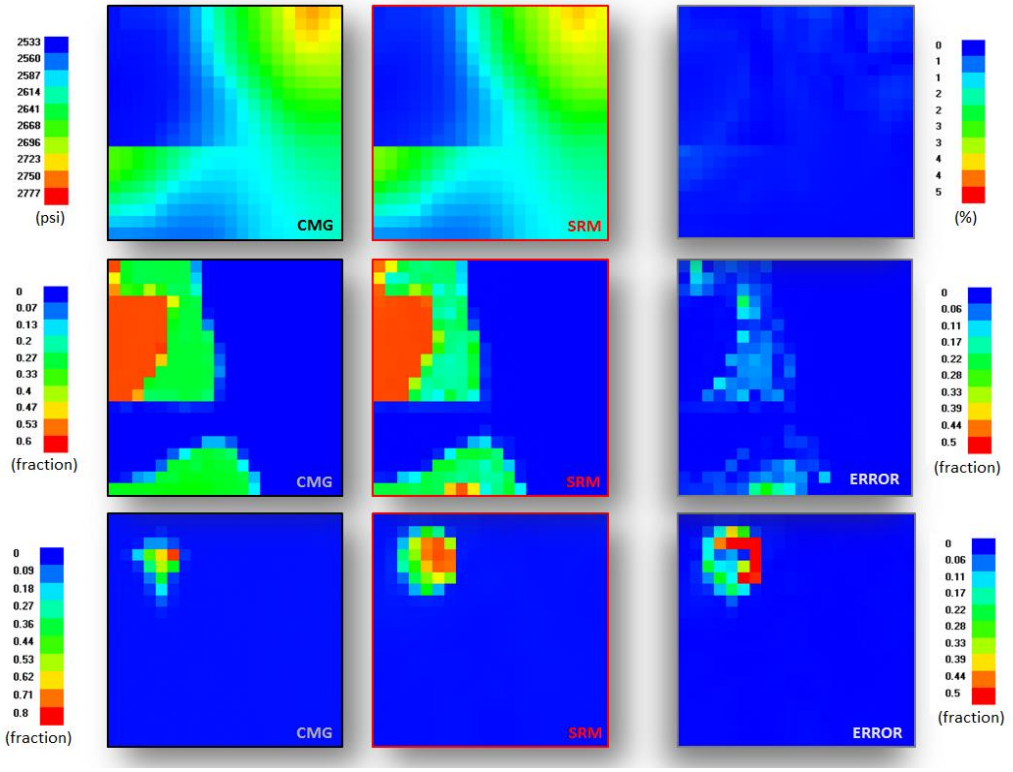

Figure 83. Distribution maps of Pressure, Gas saturation and CO_2 mole fraction in layer 2 of the reservoir (from left: CMG output, SRM result and Error) – Training case- 12 Months after injection

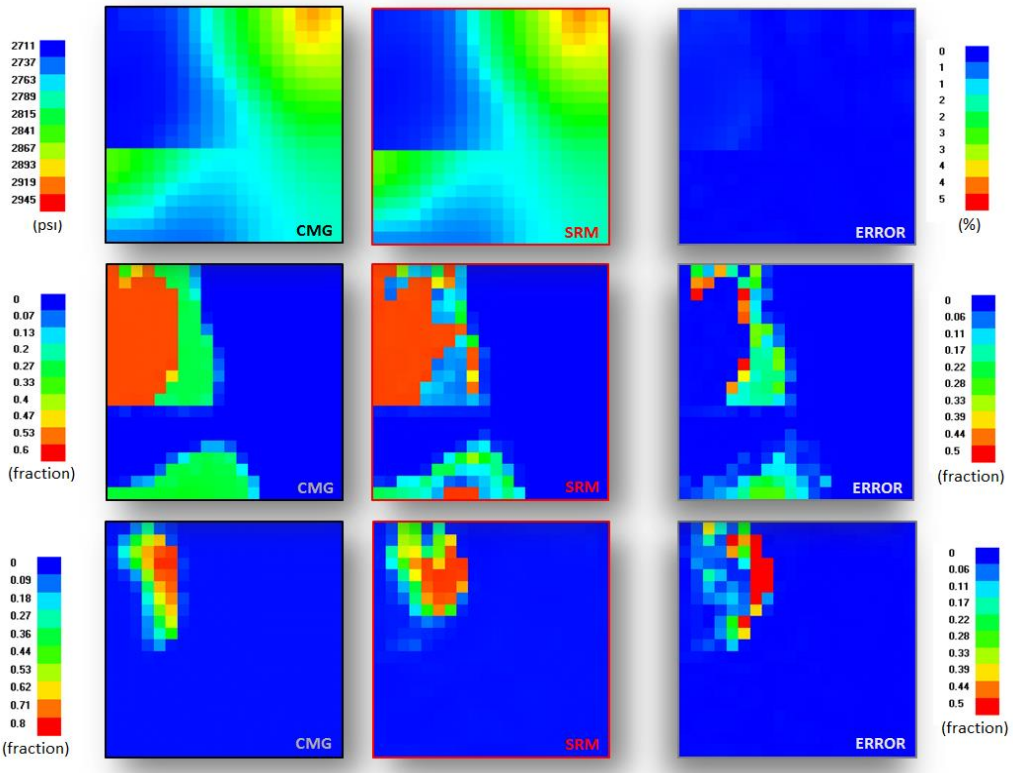

Figure 84. Distribution maps of Pressure, Gas saturation and CO_2 mole fraction in layer 2 of the reservoir (from left: CMG output, SRM result and Error) – Training case- 24 Months after injection

B-1.4. Layer 4-Training Case-24 Months of Injection

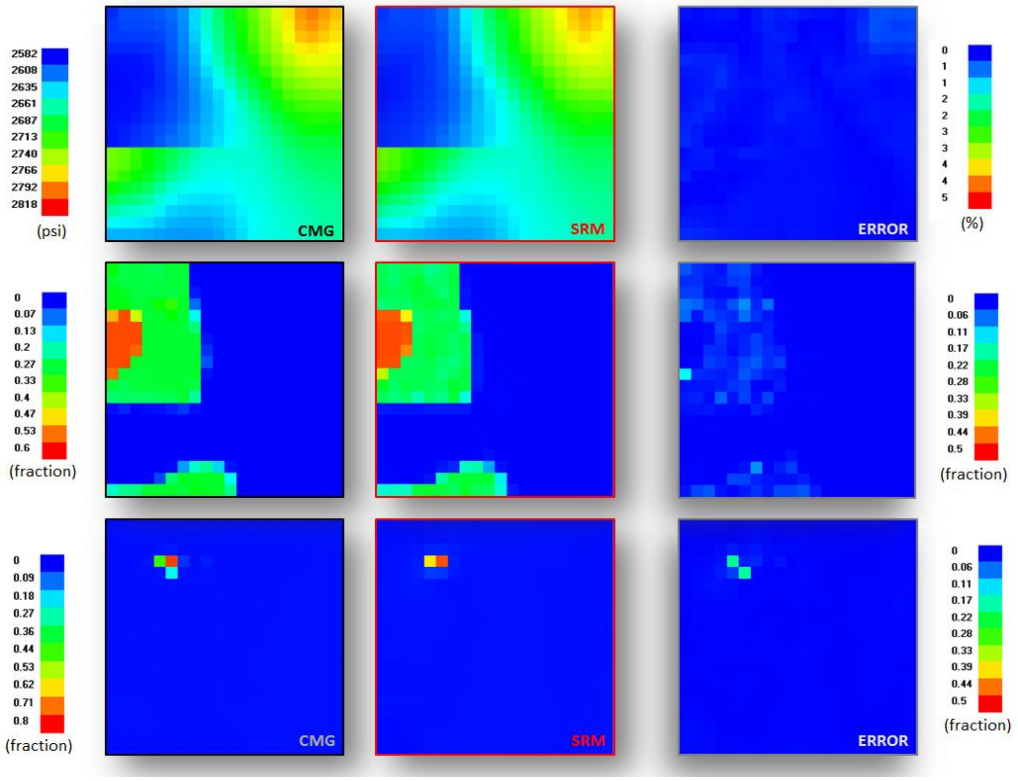

Figure 85. Distribution maps of Pressure, Gas saturation and CO_2 mole fraction in layer 4 of the reservoir (from left: CMG output, SRM result and Error) – Training case- 12 Months after injection

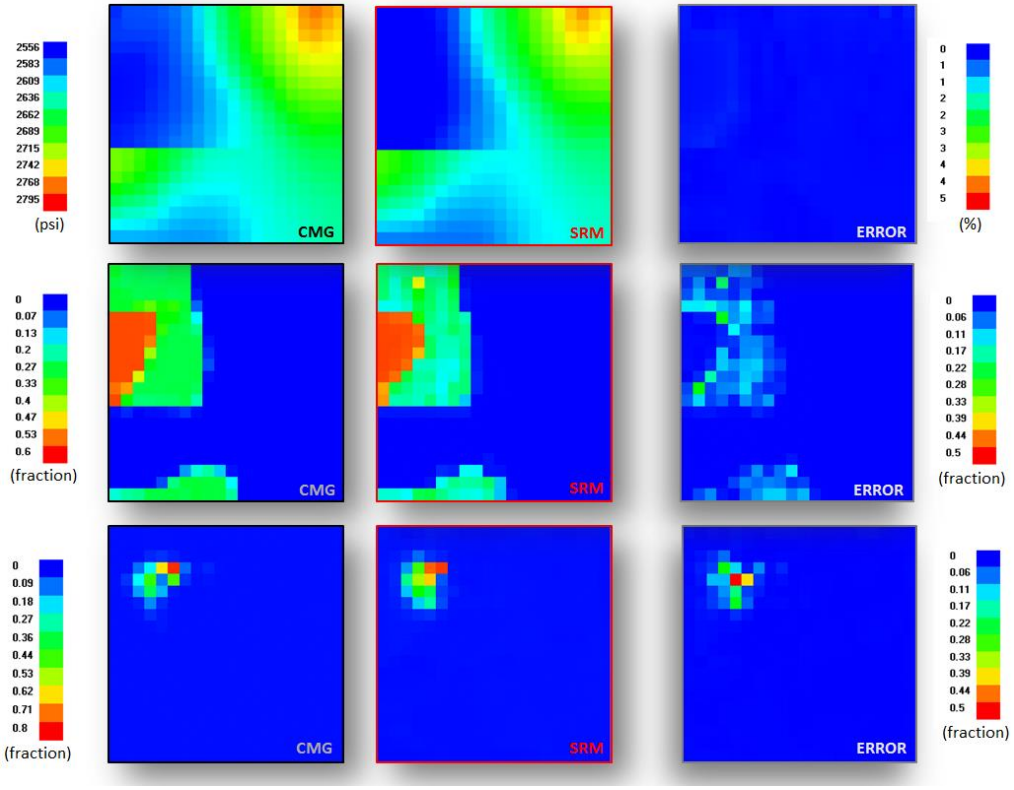

Figure 86. Distribution maps of Pressure, Gas saturation and CO_2 mole fraction in layer 4 of the reservoir (from left: CMG output, SRM result and Error) – Training case- 24 Months after injection

B-2. Cascading Result Evaluation

Based on the cascading SRM results which were presented in chapter 7 (section 7.2.3) it was concluded that in cascading procedure the error accumulation at each time step generates a large amount of errors especially in the latest time steps during the injection. Further study was performed to ensure that the deterioration of the results at later time steps is due to the cascading process.

For this purpose, the SRM results for gas saturation networks are evaluated when the neural networks are applied with and without cascading.

In the first step, the neural networks are applied through cascading process in which the output of the previous time step is used as input of the current time step. Then, the same networks are applied independent of the generated outputs of the previous time step, which means that the inputs of the current time are not updated with the SRM results and the value of the CMG output is used instead.

In the second step, some of the grid blocks with the highest amount of changes of dynamic parameter are selected from each layer of the reservoir. Then, the error between the SRM and the CMG outputs for each selected grid block is calculated both for cascading and non-cascading procedure at each time step during the injection interval. Finally, the amount of error during the injection interval is evaluated and compared for both procedures.

The injection scenario used for this study is scenario#1 with 24 months of CO_2 injection. The error plots for both processes are depicted in the following figures for layer 1, 3 and 5 of the reservoir (as an example).

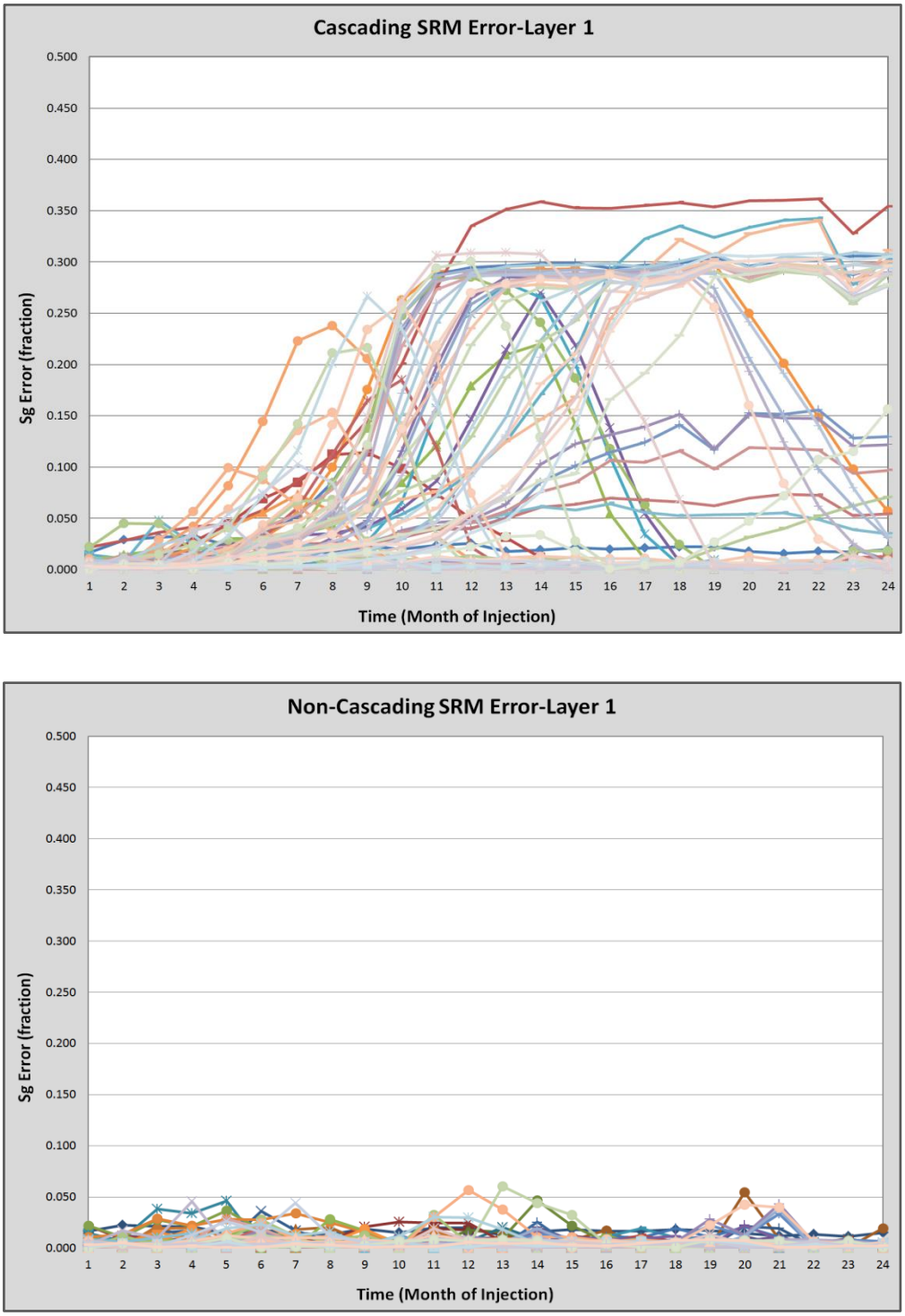

Figure 87. Error comparison between cascading (top) and non-cascading (bottom) results for gas saturation during 24 months of CO_2 injection in Layer 1

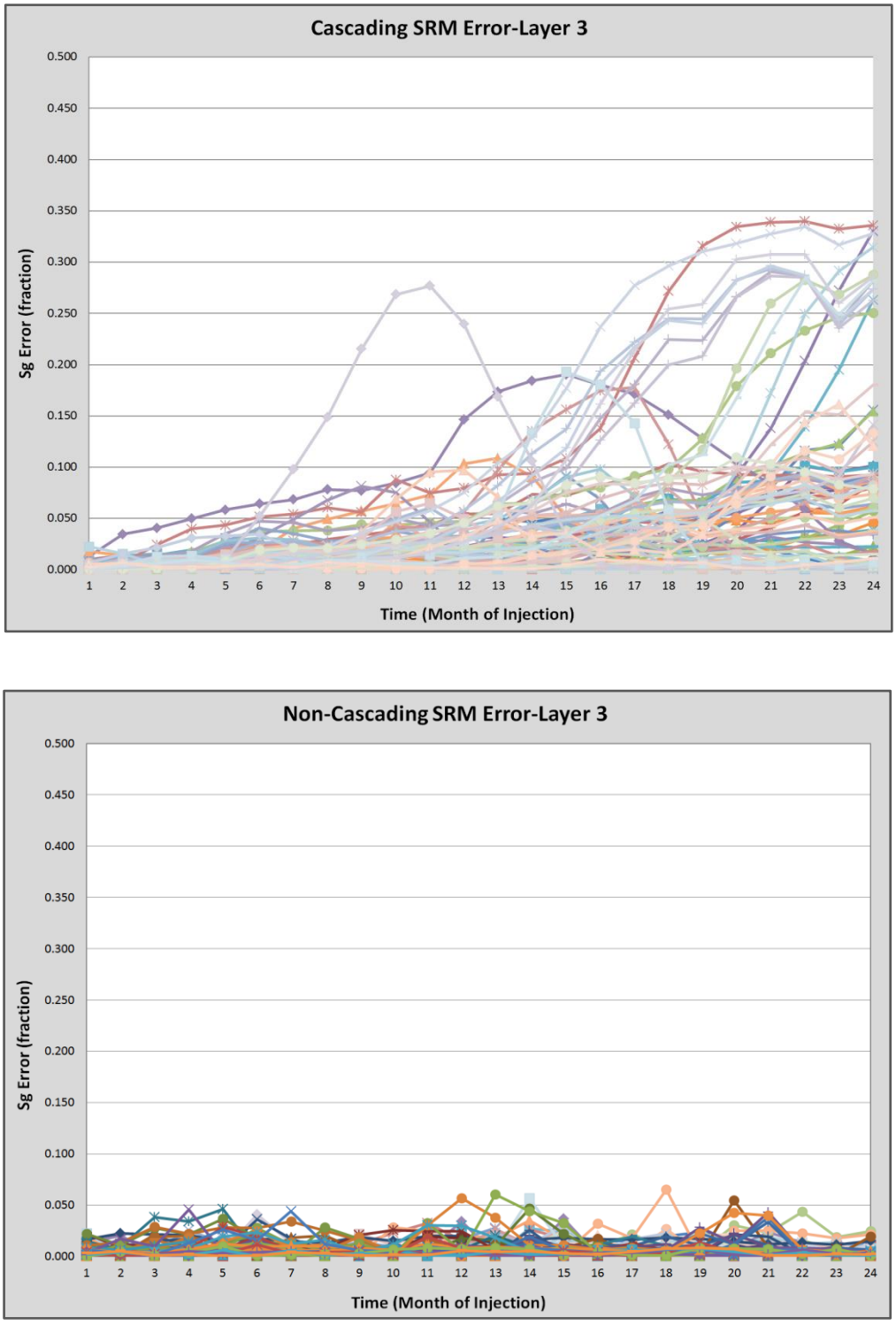

Figure 88. Error comparison between cascading (top) and non-cascading (bottom) results for gas saturation during 24 months of CO_2 injection in Layer 3

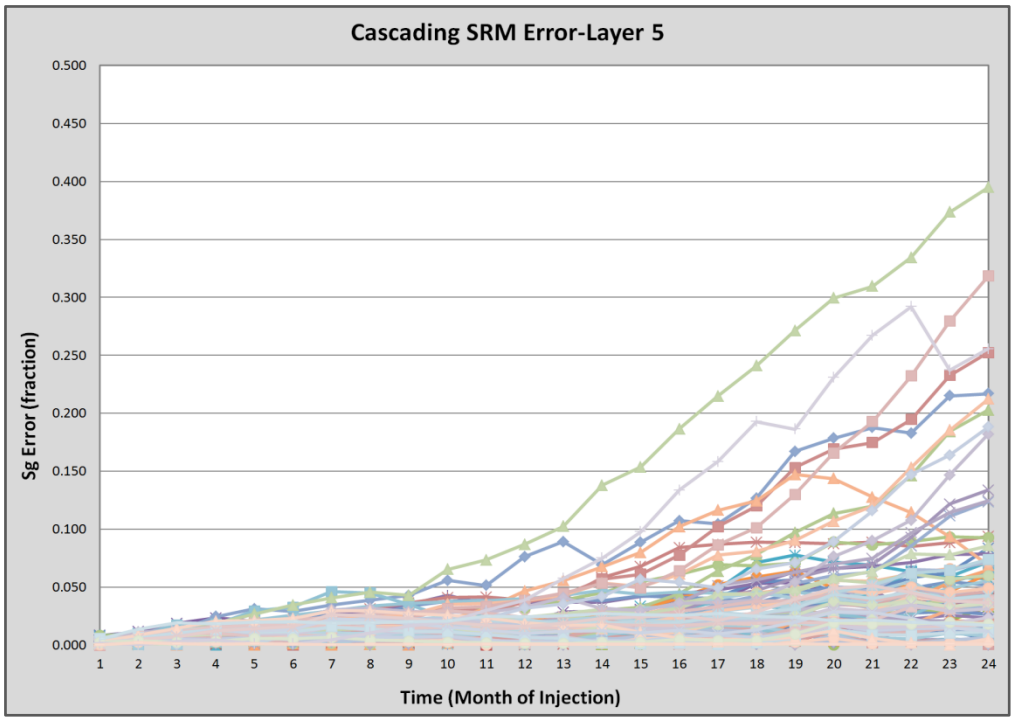

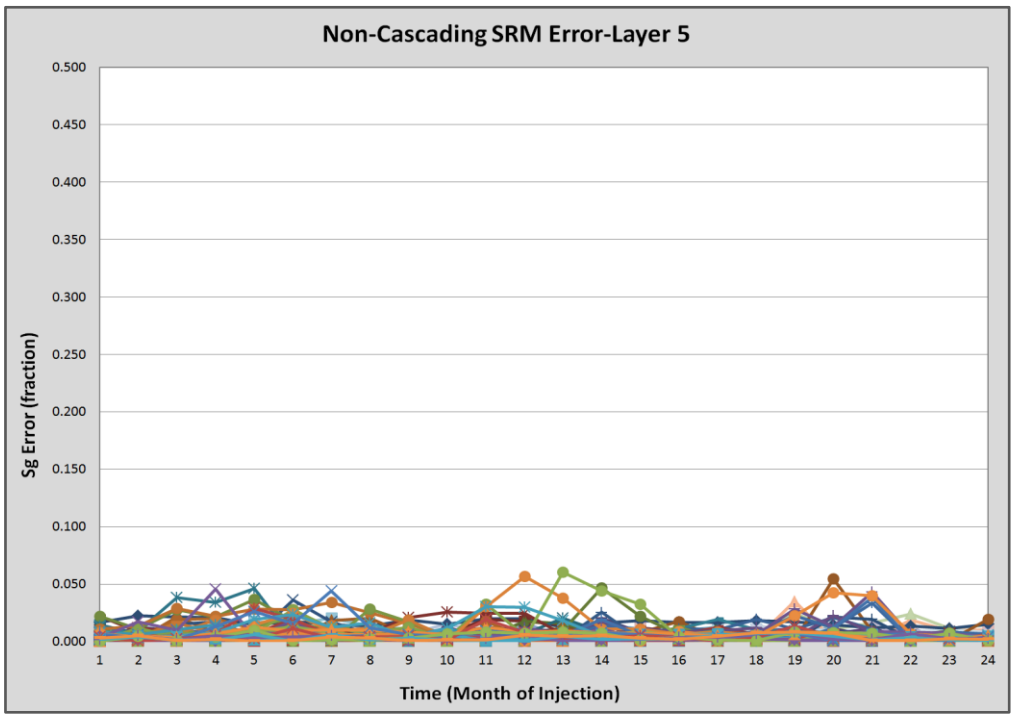

Figure 89. Error comparison between cascading (top) and non-cascading (bottom) results for gas saturation during 24 months of CO_2 injection in Layer 5

Appendix-C

C-1. Non-Cascading SRM Results for Coarse-grid Model

The result of non-cascading coarse-grid SRM for the first layer of the reservoir was presented in Chapter 7 (section 7.2.4). In this section the dynamic parameter distribution maps generated by SRM for layer 2 and layer 4 of the reservoir, in 2 different time steps during the injection interval, are demonstrated and compared to the corresponding CMG outputs. The results are presented in the following sections.

C-1.1. Layer 2-Training Case-8 Months of Injection

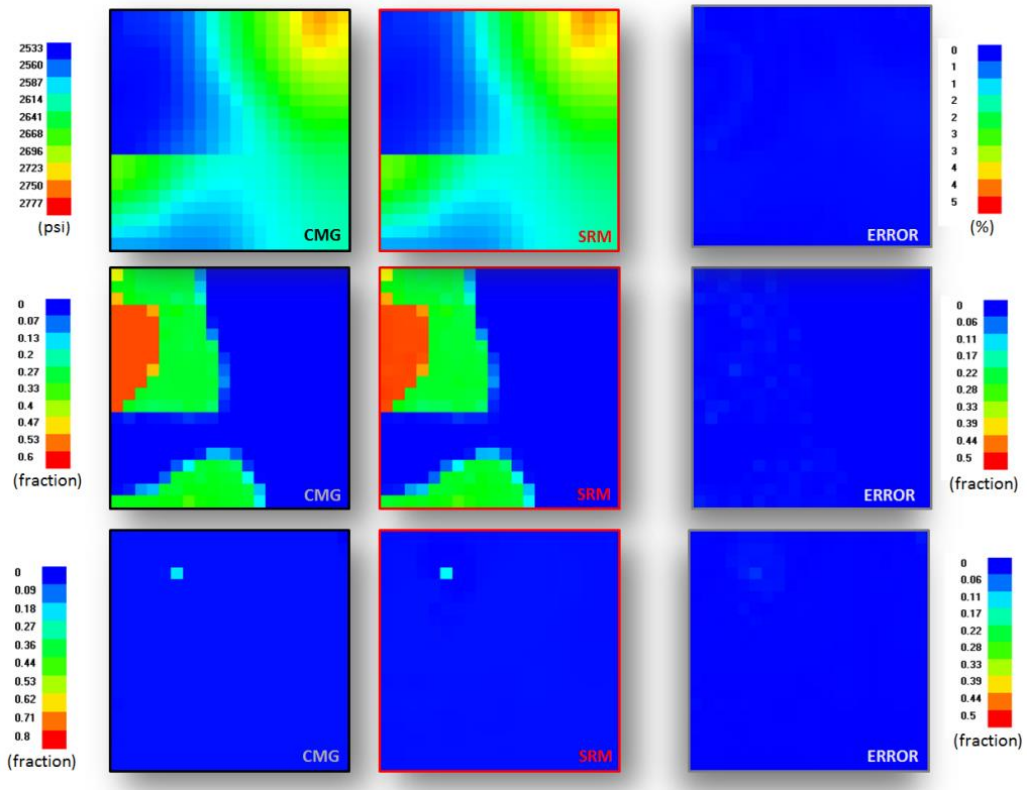

Figure 90. Distribution maps of Pressure, Gas saturation and CO_2 mole fraction in layer 2 of the reservoir (from left: CMG output, SRM result and Error) - Training Case- 4 Months after injection

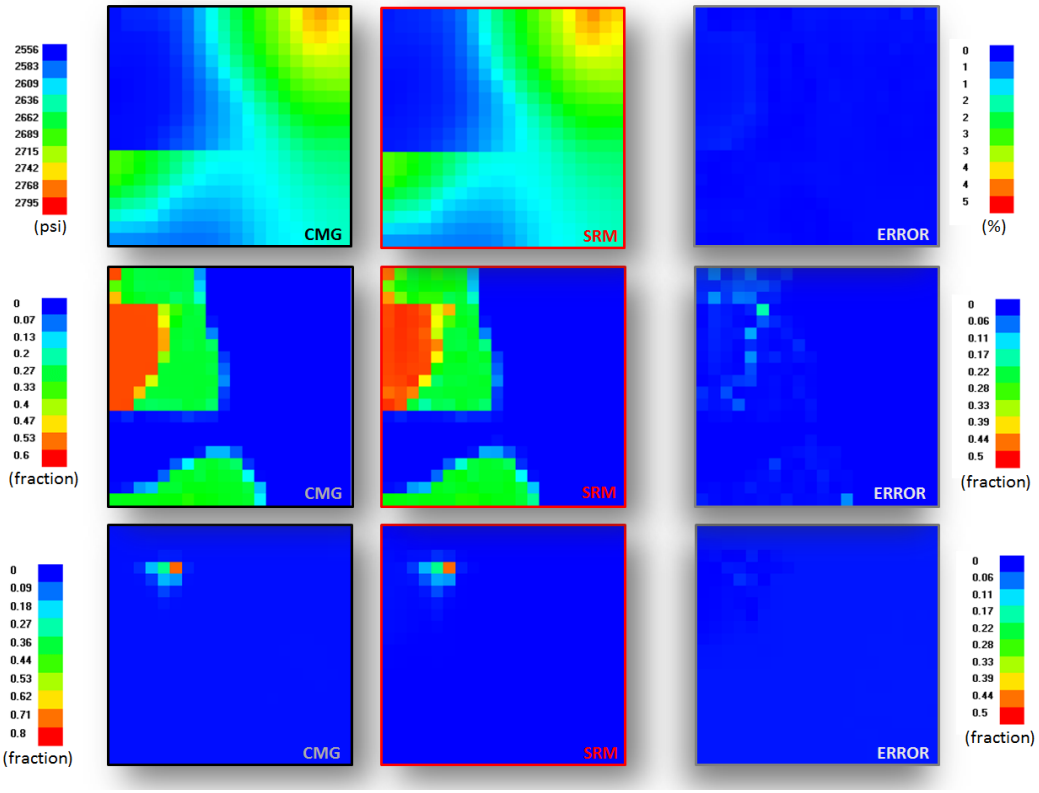

Figure 91. Distribution maps of Pressure, Gas saturation and CO_2 mole fraction in layer 2 of the reservoir (from left: CMG output, SRM result and Error) –Training Case- 8 Months after injection

C-1.2. Layer 4-Training Case-8 Months of Injection

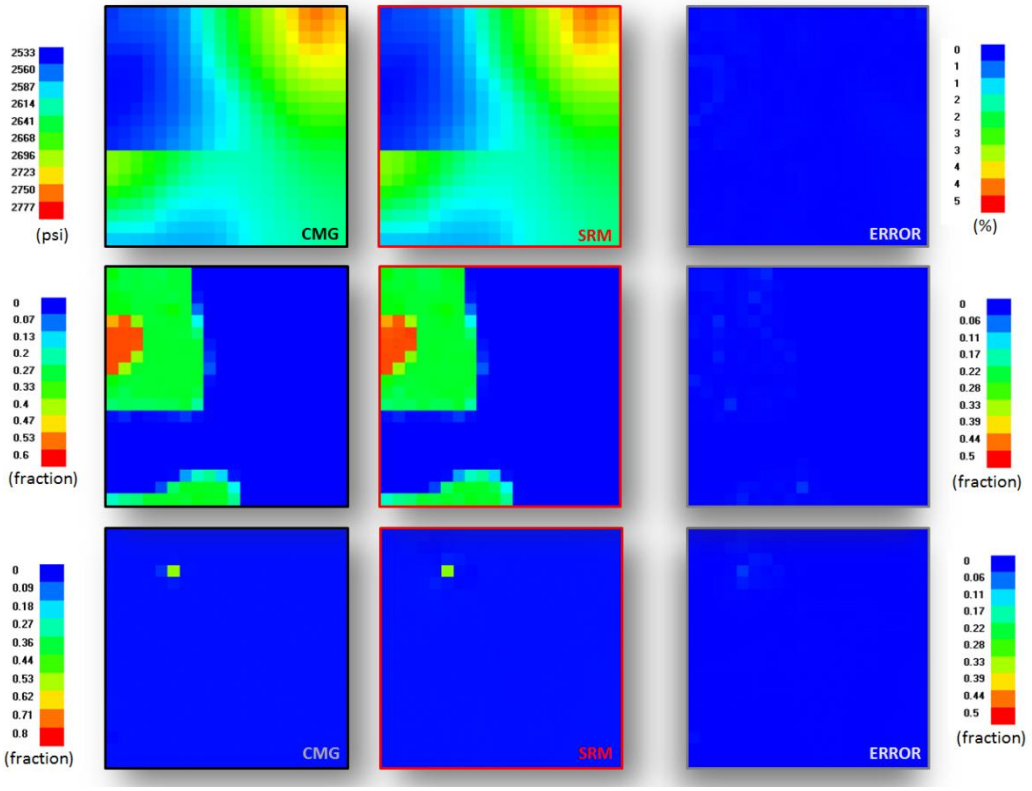

Figure 92. Distribution maps of Pressure, Gas saturation and CO_2 mole fraction in layer 4 of the reservoir (from left: CMG output, SRM result and Error) - Training Case- 4 Months after injection

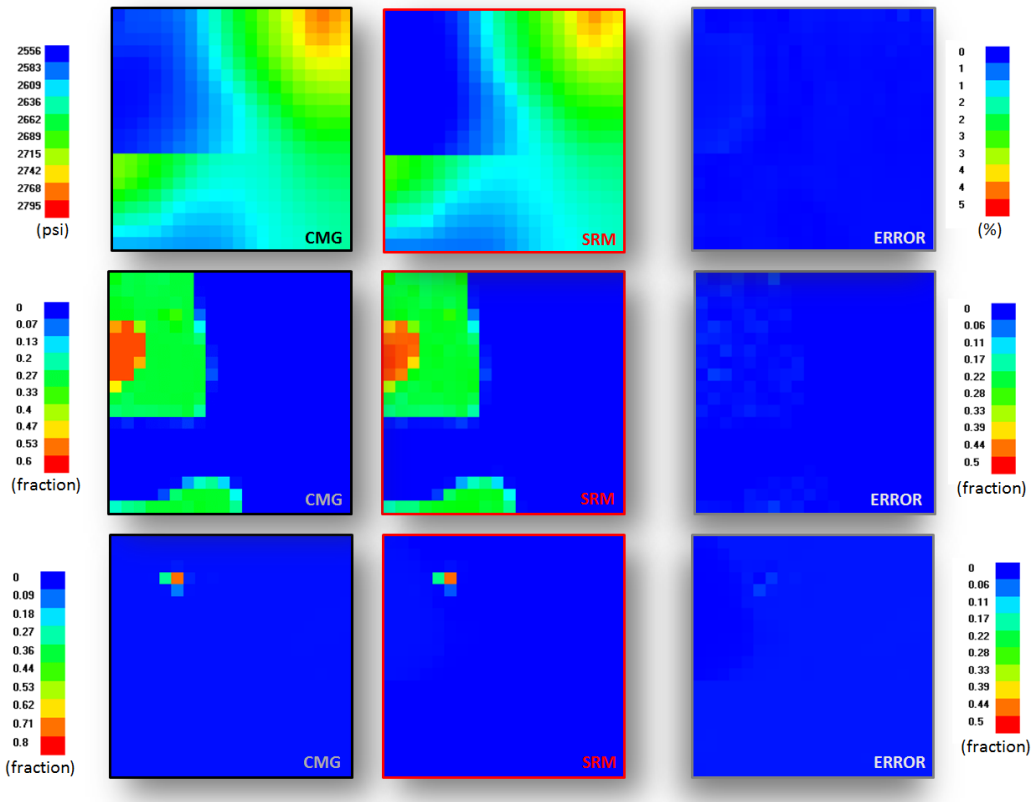

Figure 93. Distribution maps of Pressure, Gas saturation and CO_2 mole fraction in layer 4 of the reservoir (from left: CMG output, SRM result and Error) - Training Case- 8 Months after injection

C-1.3. Layer 2-Blind Case-8 Months of Injection

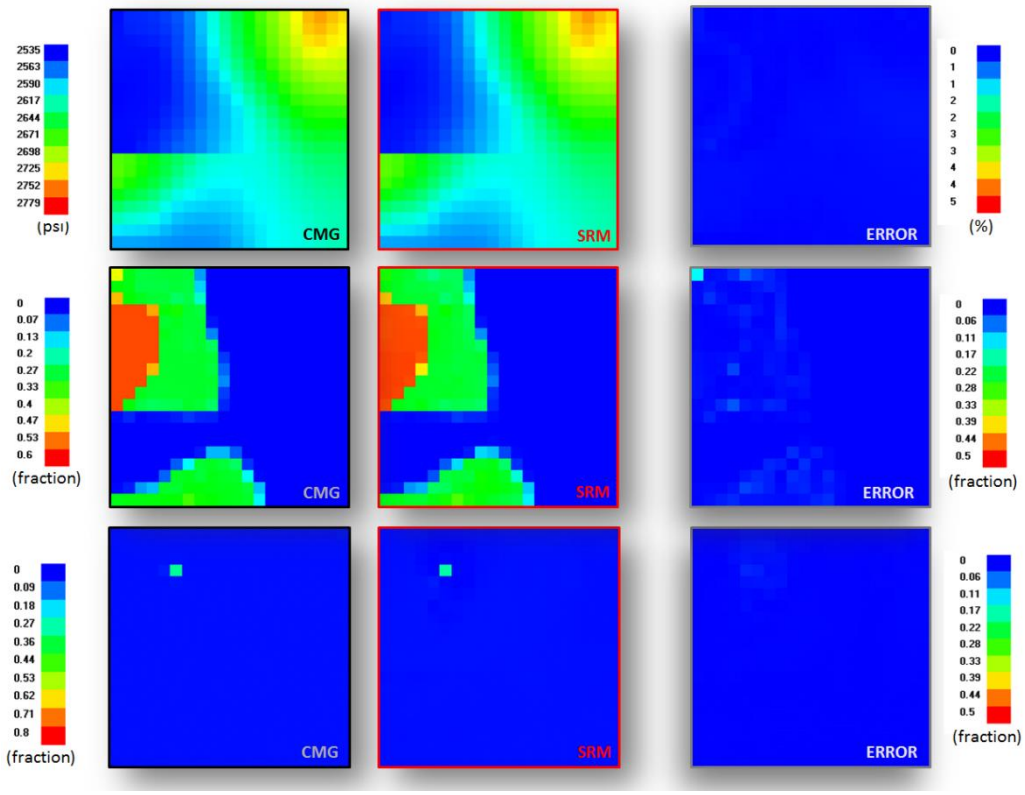

Figure 94. Distribution maps of Pressure, Gas saturation and CO_2 mole fraction in layer 2 of the reservoir (from left: CMG output, SRM result and Error) - Blind Case- 4 Months after injection

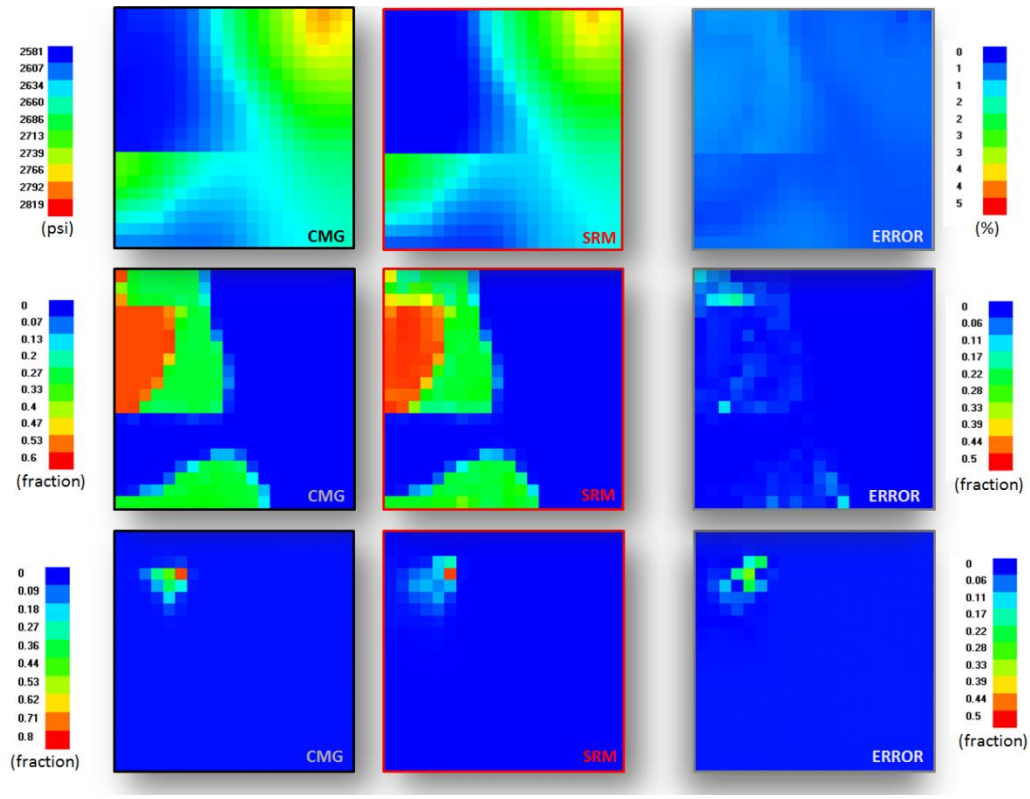

Figure 95. Distribution maps of Pressure, Gas saturation and CO_2 mole fraction in layer 2 of the reservoir (from left: CMG output, SRM result and Error) - Blind Case- 8 Months after injection

C-1.4. Layer 4- Blind Case-8 Months of Injection

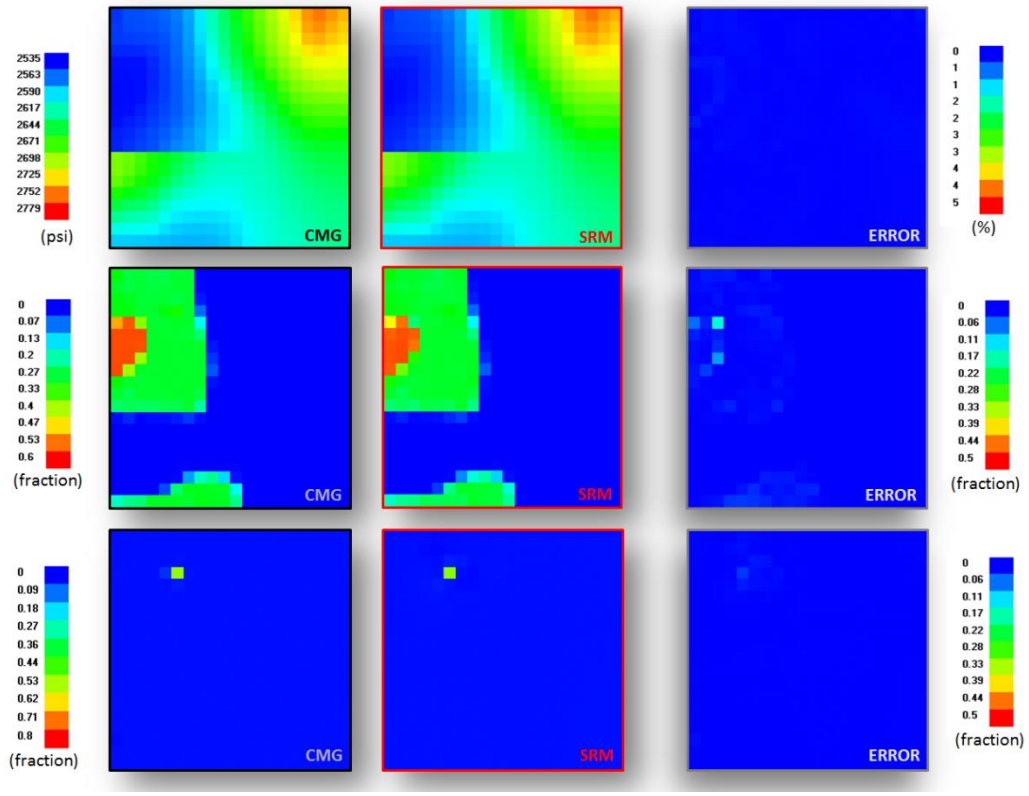

Figure 96. Distribution maps of Pressure, Gas saturation and CO_2 mole fraction in layer 4 of the reservoir (from left: CMG output, SRM result and Error) - Blind Case- 4 Months after injection

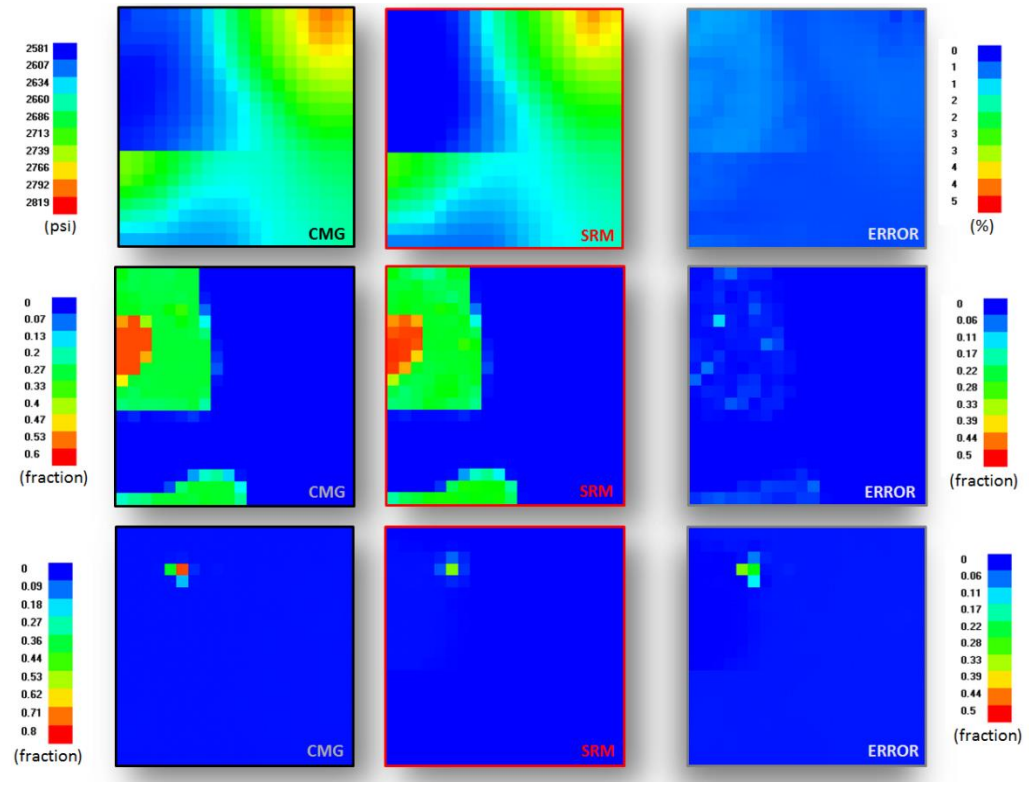

Figure 97. Distribution maps of Pressure, Gas saturation and CO_2 mole fraction in layer 4 of the reservoir (from left: CMG output, SRM result and Error) - Blind Case- 8 Months after injection

C-1.5. Layer 2-Training Case-24 Months of Injection

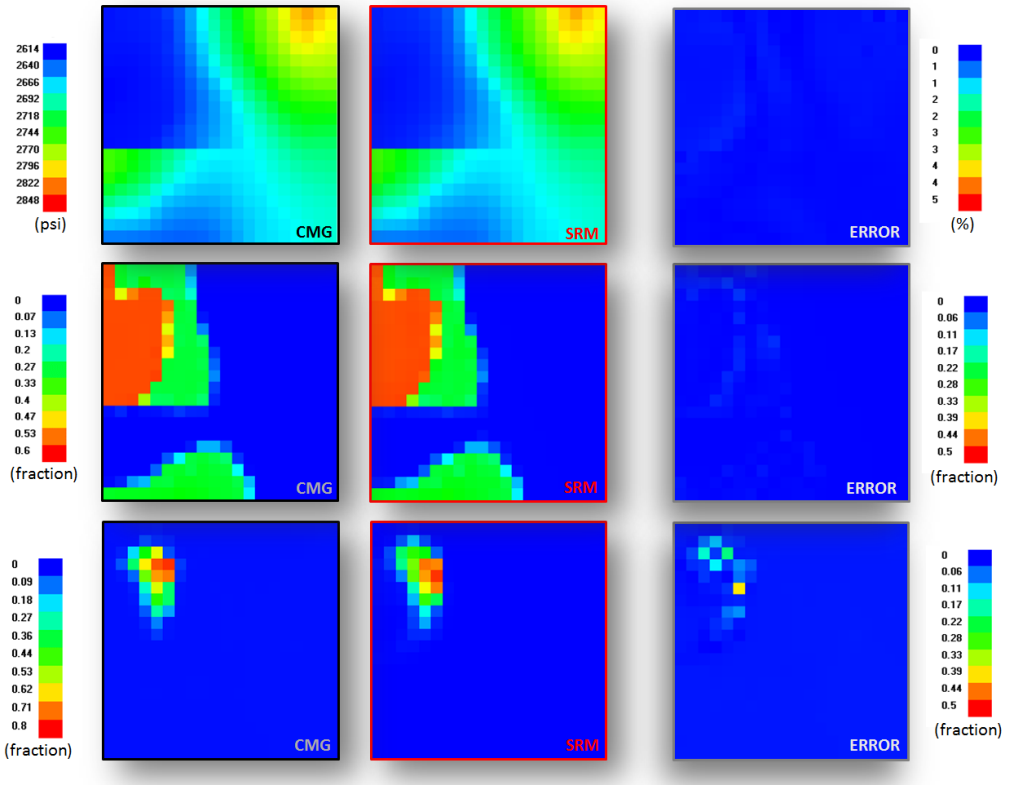

Figure 98. Distribution maps of Pressure, Gas saturation and CO_2 mole fraction in layer 2 of the reservoir (from left: CMG output, SRM result and Error) - Training Case- 16 Months after injection

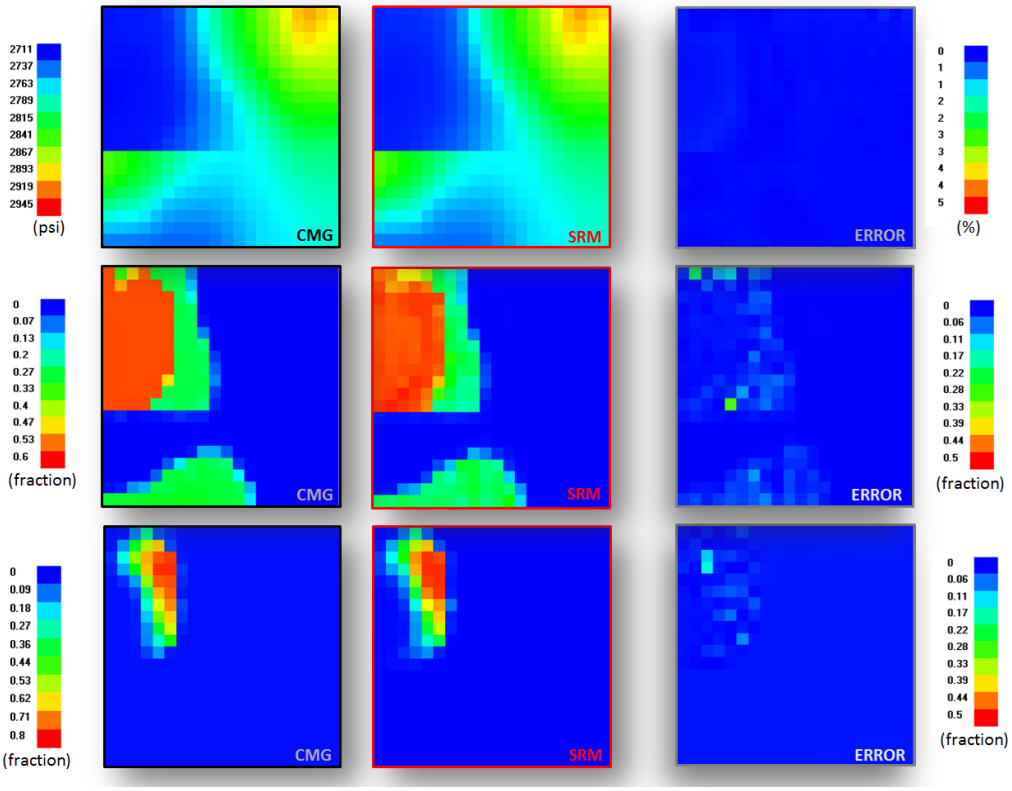

Figure 99. Distribution maps of Pressure, Gas saturation and CO_2 mole fraction in layer 2 of the reservoir (from left: CMG output, SRM result and Error) - Training Case- 24 Months after injection

C-1.6. Layer 4-Training Case-24 Months of Injection

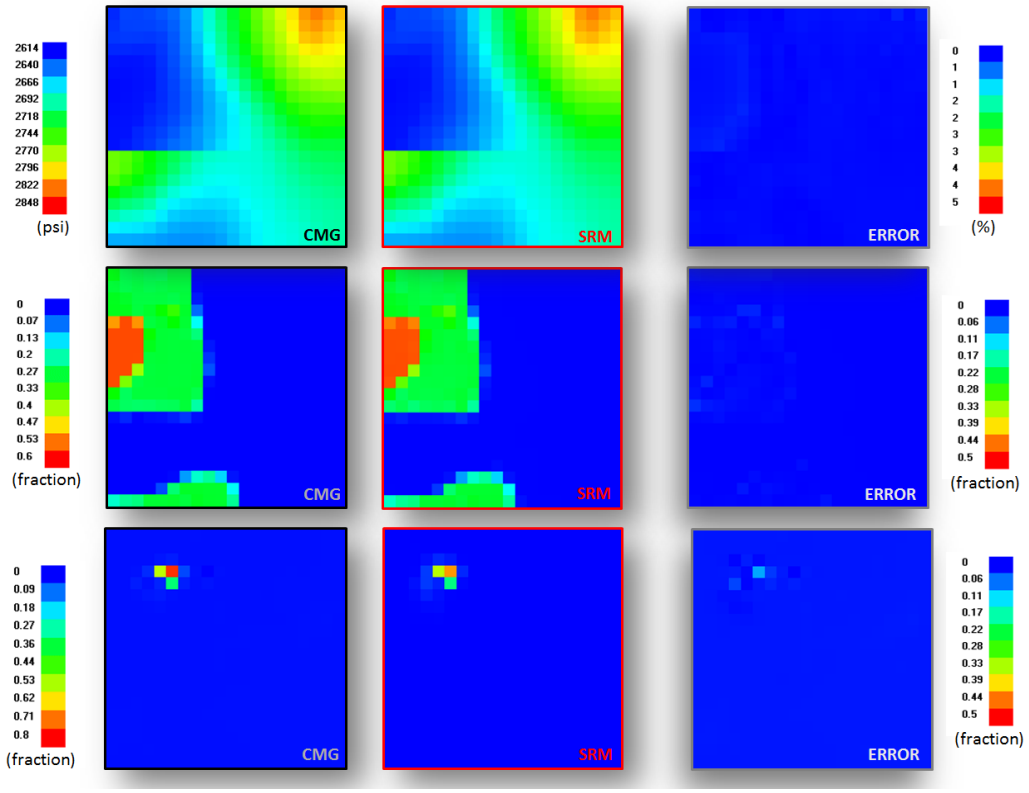

Figure 100. Distribution maps of Pressure, Gas saturation and CO_2 mole fraction in layer 4 of the reservoir (from left: CMG output, SRM result and Error) - Training Case- 16 Months after injection

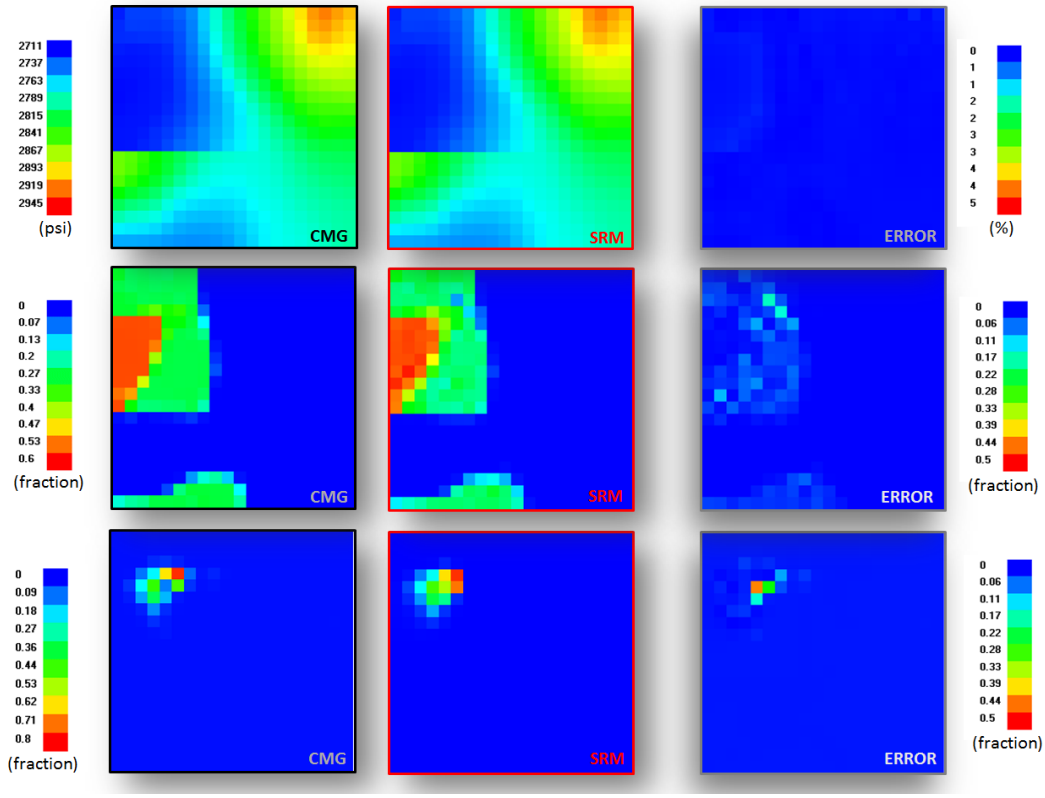

Figure 101. Distribution maps of Pressure, Gas saturation and CO_2 mole fraction in layer 4 of the reservoir (from left: CMG output, SRM result and Error) - Training Case- 24 Months after injection

C-1.7. Layer 2-Blind Case-24 Months of Injection

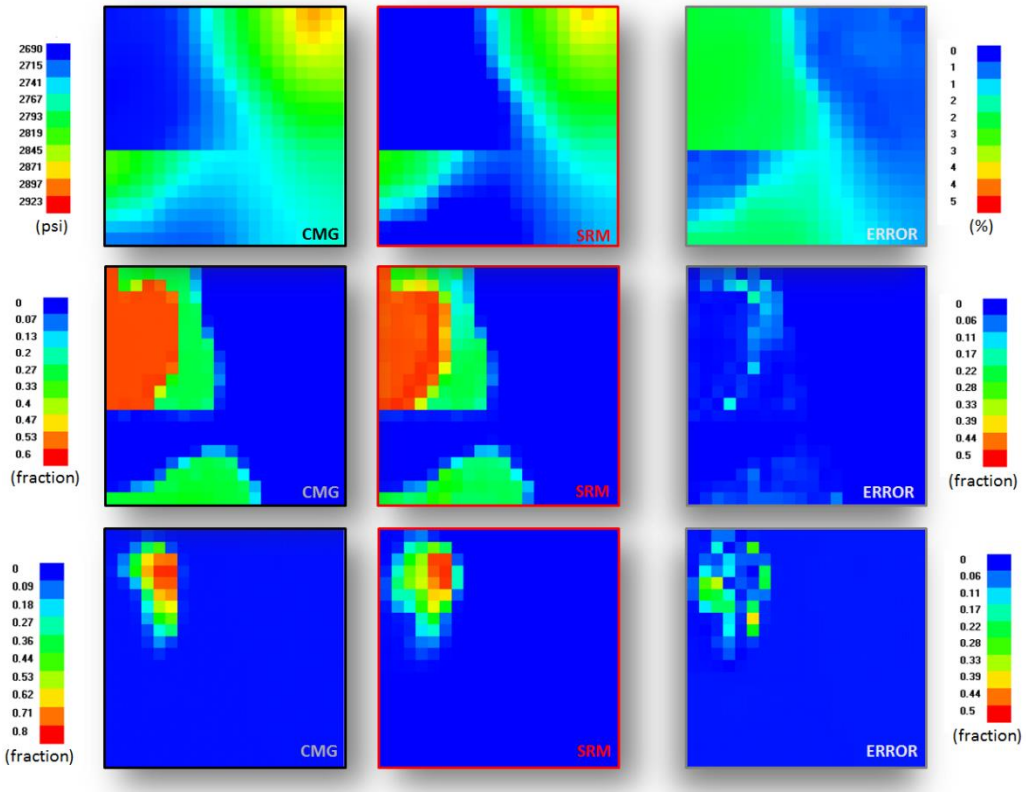

Figure 102. Distribution maps of Pressure, Gas saturation and CO_2 mole fraction in layer 2 of the reservoir (from left: CMG output, SRM result and Error) - Blind Case- 16 Months after injection

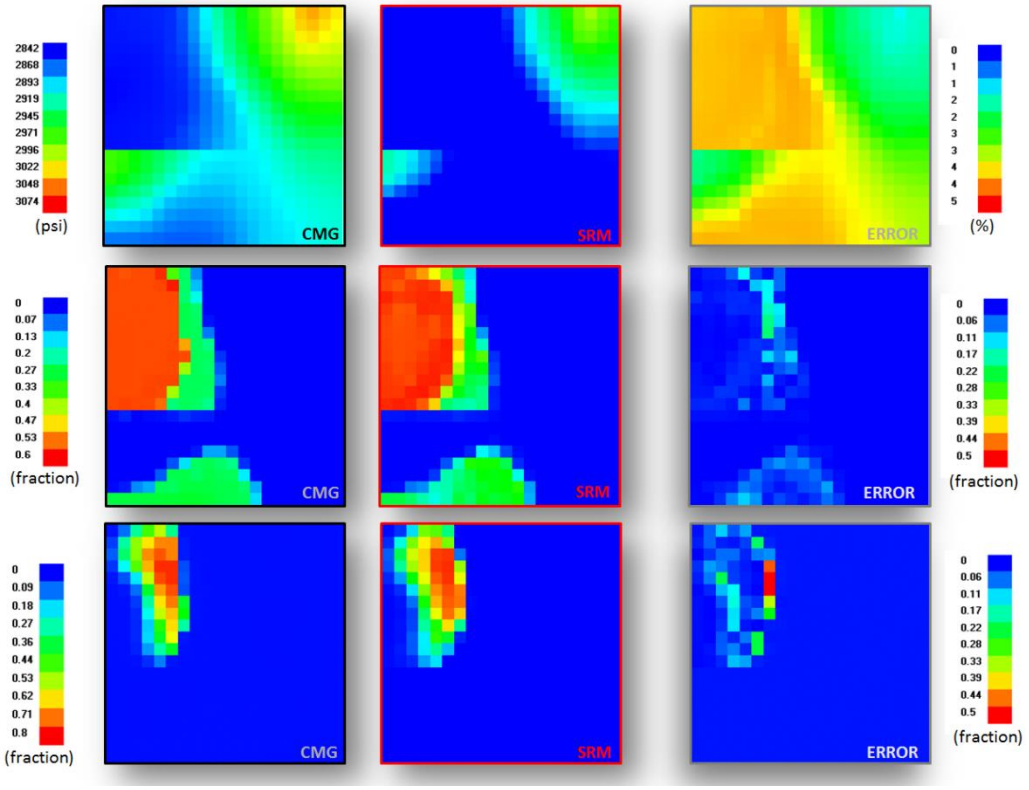

Figure 103. Distribution maps of Pressure, Gas saturation and CO_2 mole fraction in layer 2 of the reservoir (from left: CMG output, SRM result and Error) - Blind Case- 24 Months after injection

C-1.8. Layer 4- Blind Case-24 Months of Injection

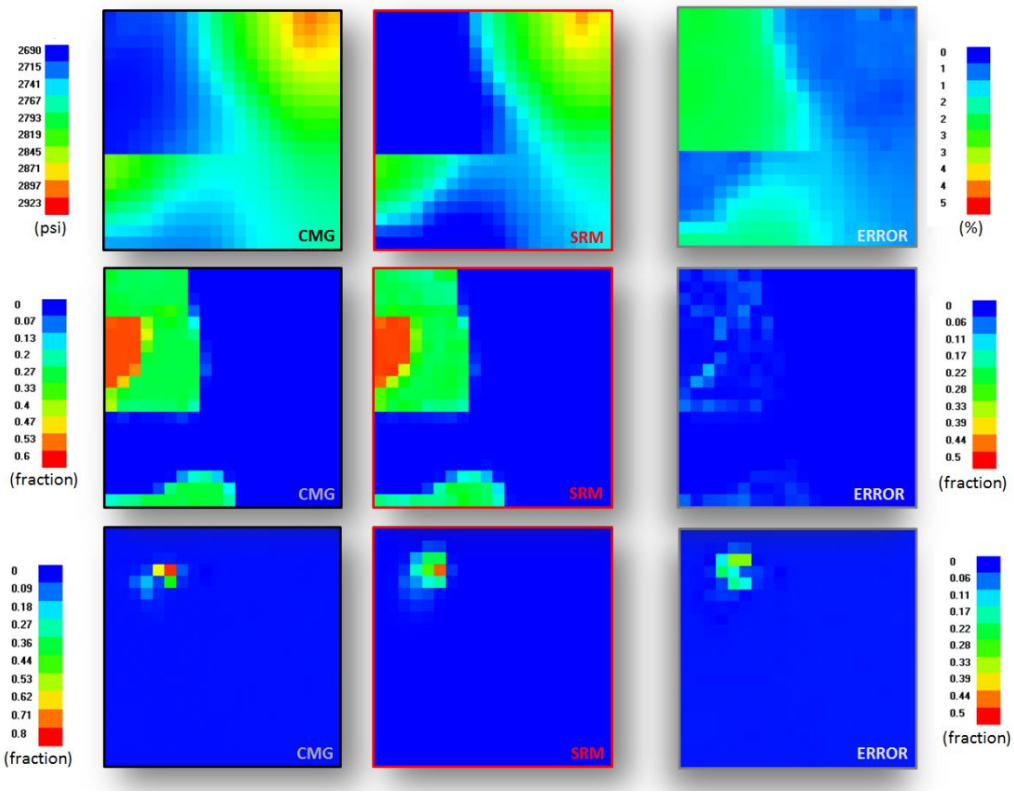

Figure 104. Distribution maps of Pressure, Gas saturation and CO_2 mole fraction in layer 4 of the reservoir (from left: CMG output, SRM result and Error) - Blind Case- 16 Months after injection

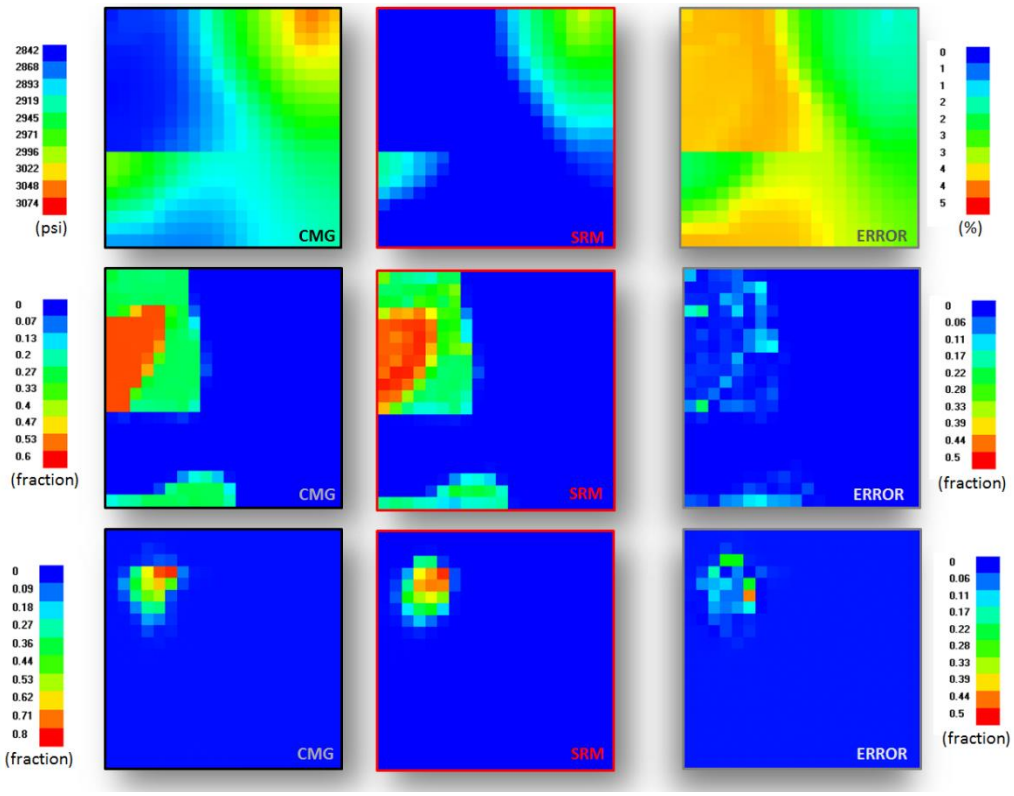

Figure 105. Distribution maps of Pressure, Gas saturation and CO_2 mole fraction in layer 4 of the reservoir (from left: CMG output, SRM result and Error) - Blind Case- 24 Months after injection

C-2. Non-Cascading SRM Results for Fine-grid Model

The result of non-cascading fine-grid SRM for the first layer of the reservoir was presented in Chapter 7 (section 7.4.2 and 7.4.3). In this section the dynamic parameter distribution maps generated by SRM for layer 2 and layer 4 of the reservoir, in 2 different time steps during the injection interval, are demonstrated and compared to the corresponding CMG outputs. The results are presented in the following sections

C-2.1. Layer 2-Training Case-8 Months of Injection

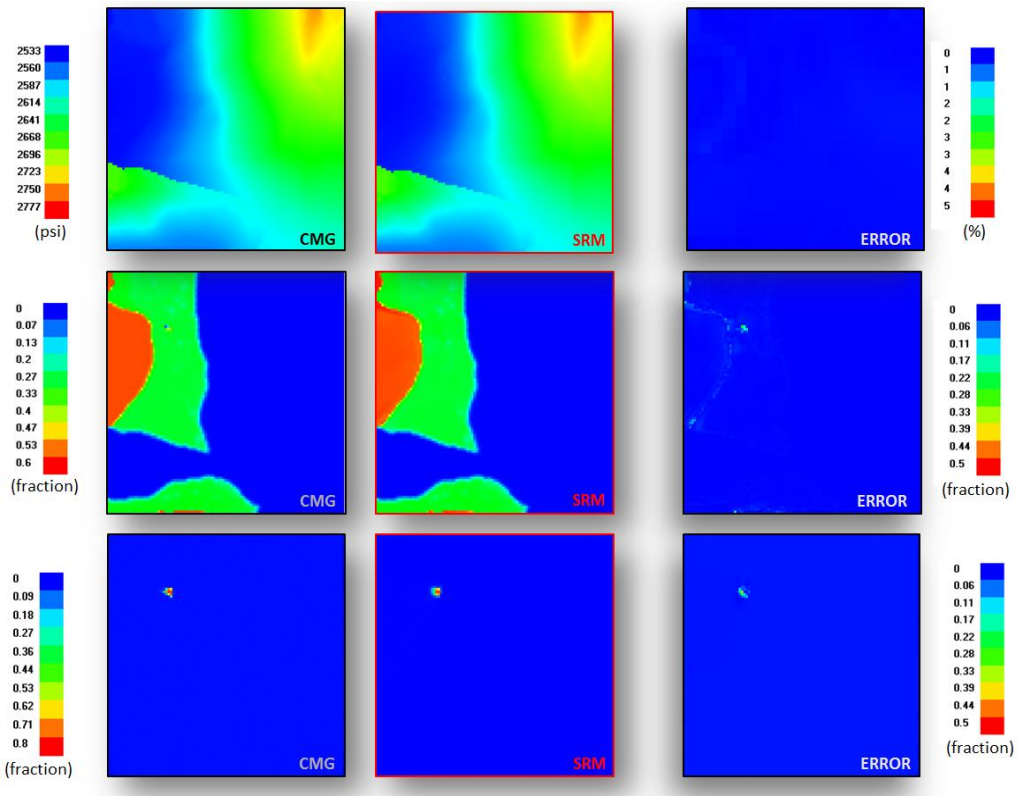

Figure 106. Distribution maps of Pressure, Gas saturation and CO_2 mole fraction in layer 2 of the reservoir (from left: CMG output, SRM result and Error) - Training Case- 4 Months after injection

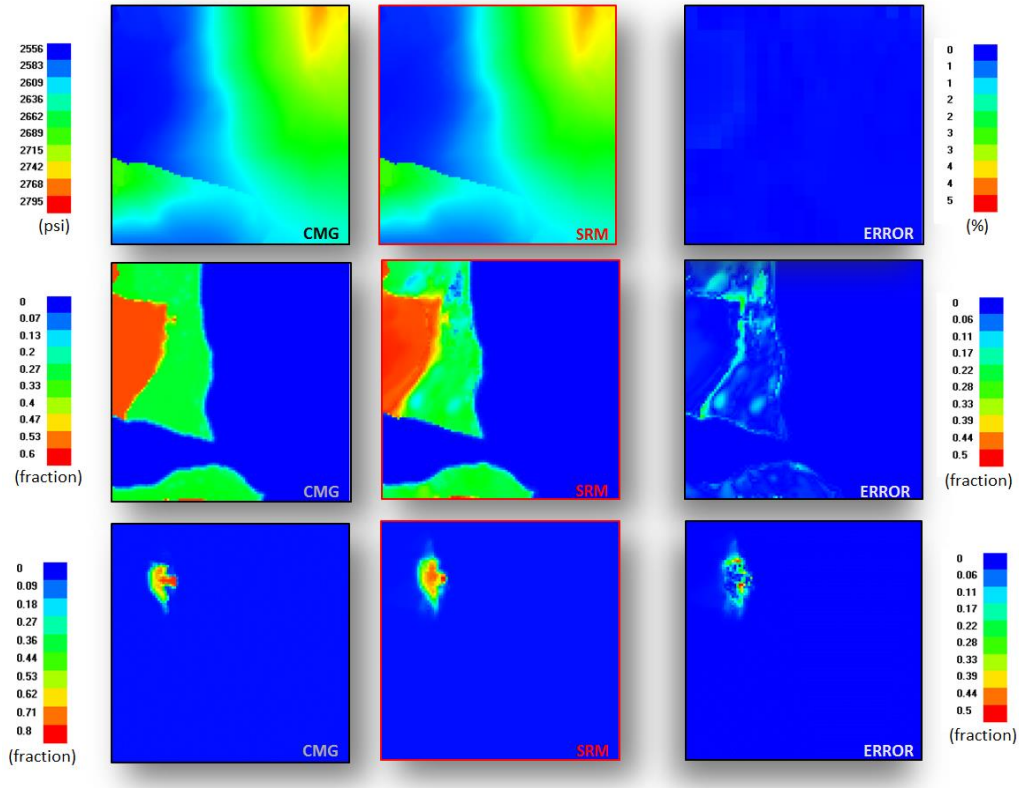

Figure 107. Distribution maps of Pressure, Gas saturation and CO_2 mole fraction in layer 2 of the reservoir (from left: CMG output, SRM result and Error) - Training Case- 8 Months after injection

C-2.2. Layer 4-Training Case-8 Months of Injection

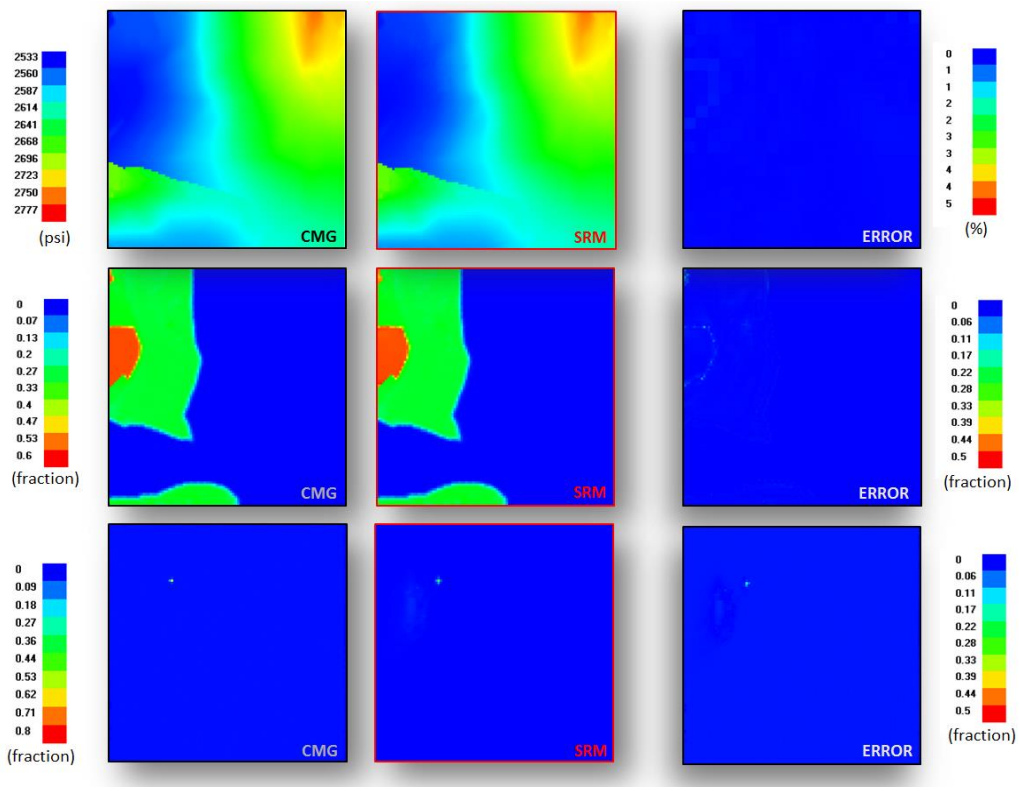

Figure 108. Distribution maps of Pressure, Gas saturation and CO_2 mole fraction in layer 4 of the reservoir (from left: CMG output, SRM result and Error) - Training Case- 4 Months after injection

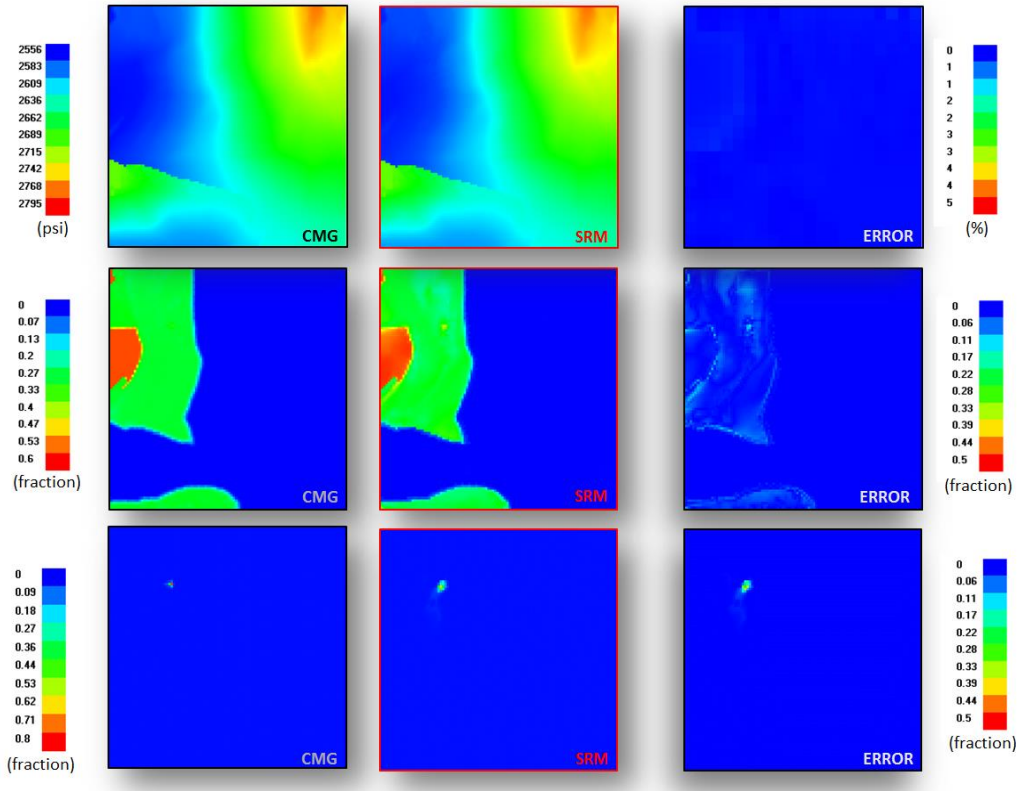

Figure 109. Distribution maps of Pressure, Gas saturation and CO_2 mole fraction in layer 4 of the reservoir (from left: CMG output, SRM result and Error) - Training Case- 8 Months after injection

C-2.3. Layer 2-Blind Case-8 Months of Injection

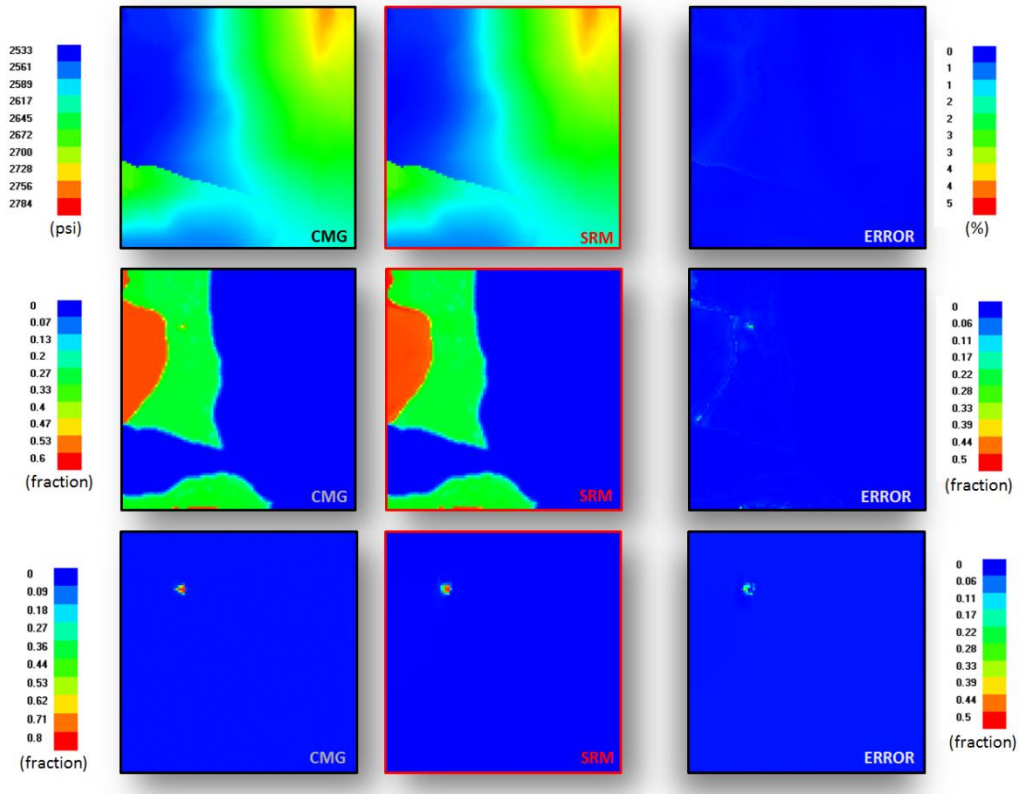

Figure 110. Distribution maps of Pressure, Gas saturation and CO_2 mole fraction in layer 2 of the reservoir (from left: CMG output, SRM result and Error) - Blind Case- 4 Months after injection

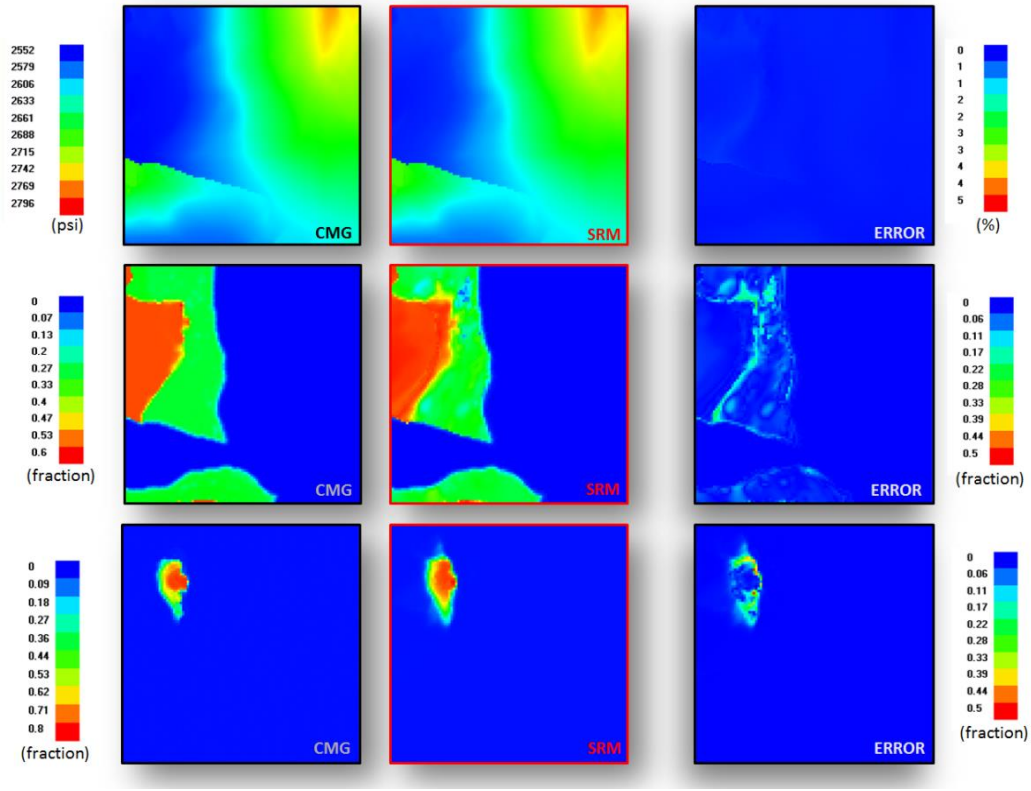

Figure 111. Distribution maps of Pressure, Gas saturation and CO_2 mole fraction in layer 2 of the reservoir (from left: CMG output, SRM result and Error) - Blind Case- 8 Months after injection

C-2.4. Layer 4- Blind Case-8 Months of Injection

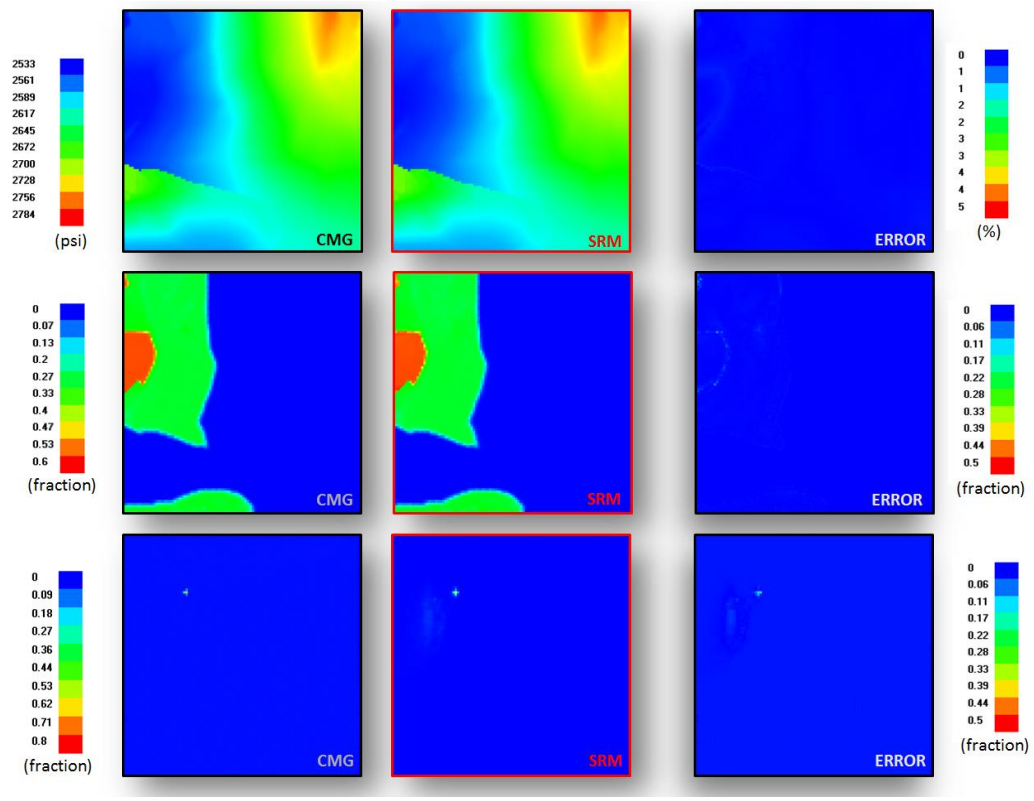

Figure 112. Distribution maps of Pressure, Gas saturation and CO_2 mole fraction in layer 4 of the reservoir (from left: CMG output, SRM result and Error) - Blind Case- 4 Months after injection

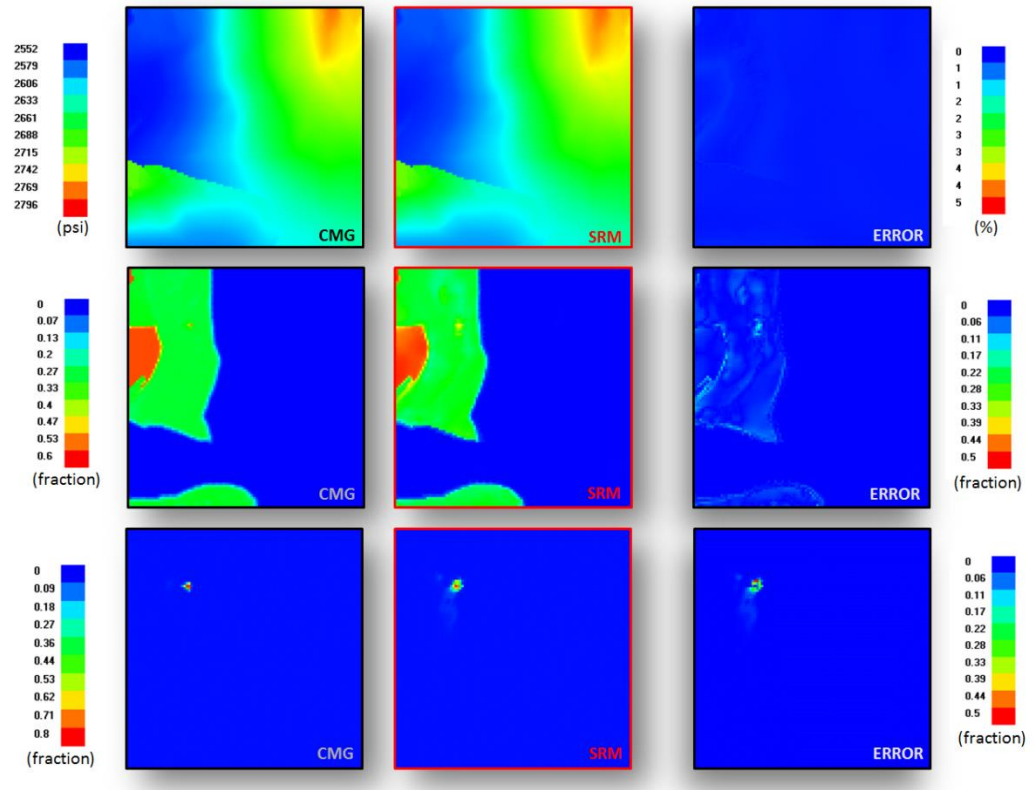

Figure 113. Distribution maps of Pressure, Gas saturation and CO_2 mole fraction in layer 4 of the reservoir (from left: CMG output, SRM result and Error) - Blind Case- 8 Months after injection

C-2.5. Layer 2-Training Case-24 Months of Injection

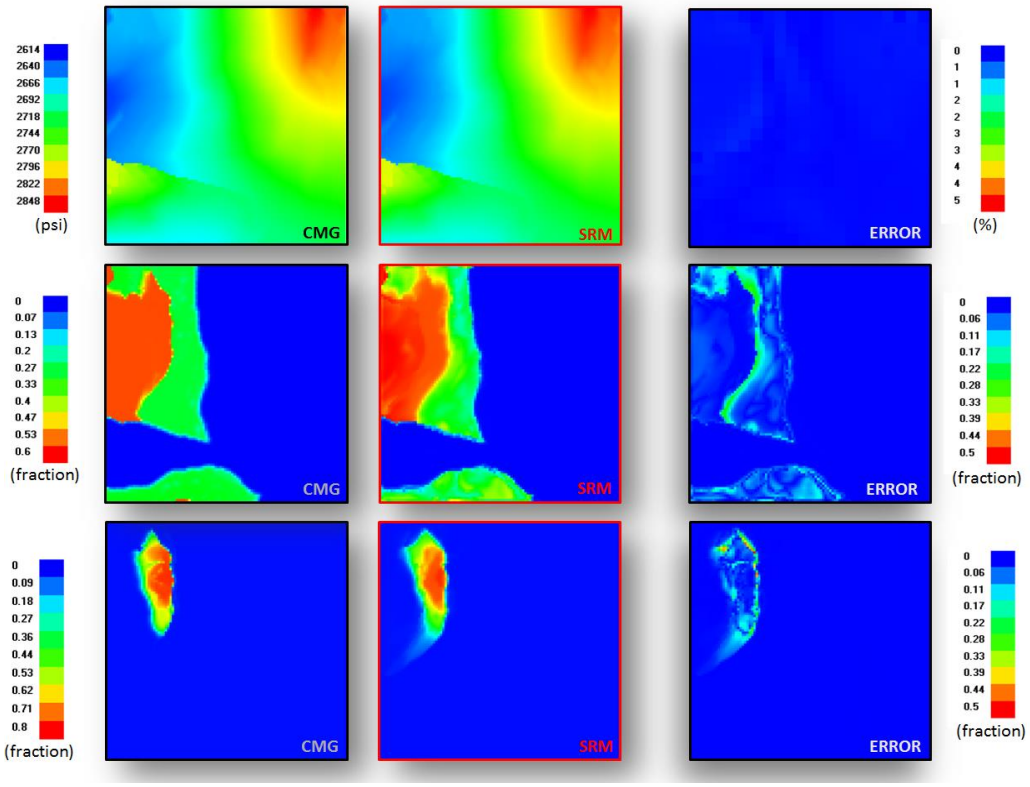

Figure 114. Distribution maps of Pressure, Gas saturation and CO_2 mole fraction in layer 2 of the reservoir (from left: CMG output, SRM result and Error) - Training Case- 16 Months after injection

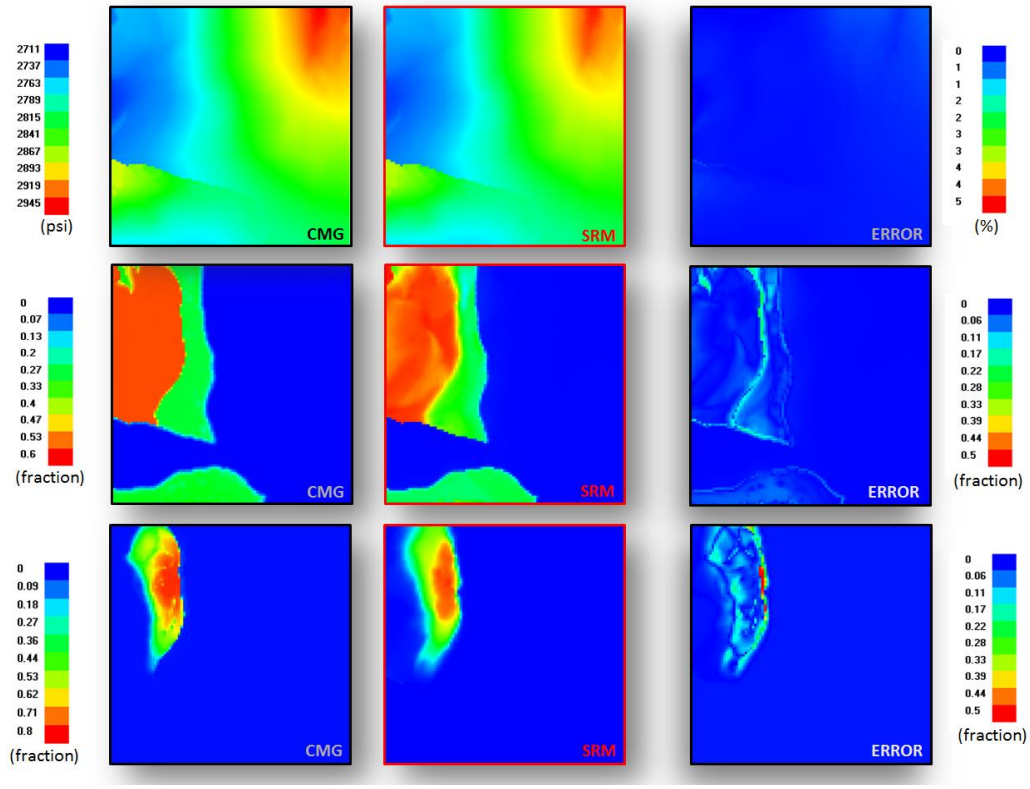

Figure 115. Distribution maps of Pressure, Gas saturation and CO_2 mole fraction in layer 2 of the reservoir (from left: CMG output, SRM result and Error) - Training Case- 24 Months after injection

C-2.6. Layer 4-Training Case-24 Months of Injection

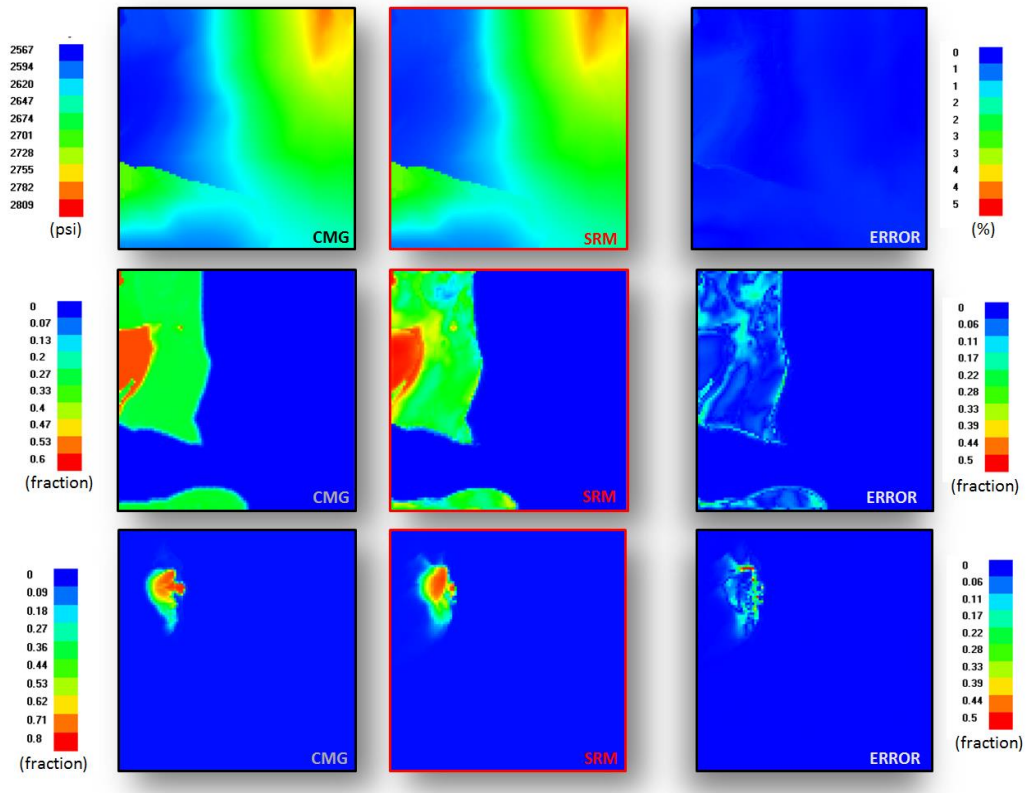

Figure 116. Distribution maps of Pressure, Gas saturation and CO_2 mole fraction in layer 4 of the reservoir (from left: CMG output, SRM result and Error) - Training Case- 16 Months after injection

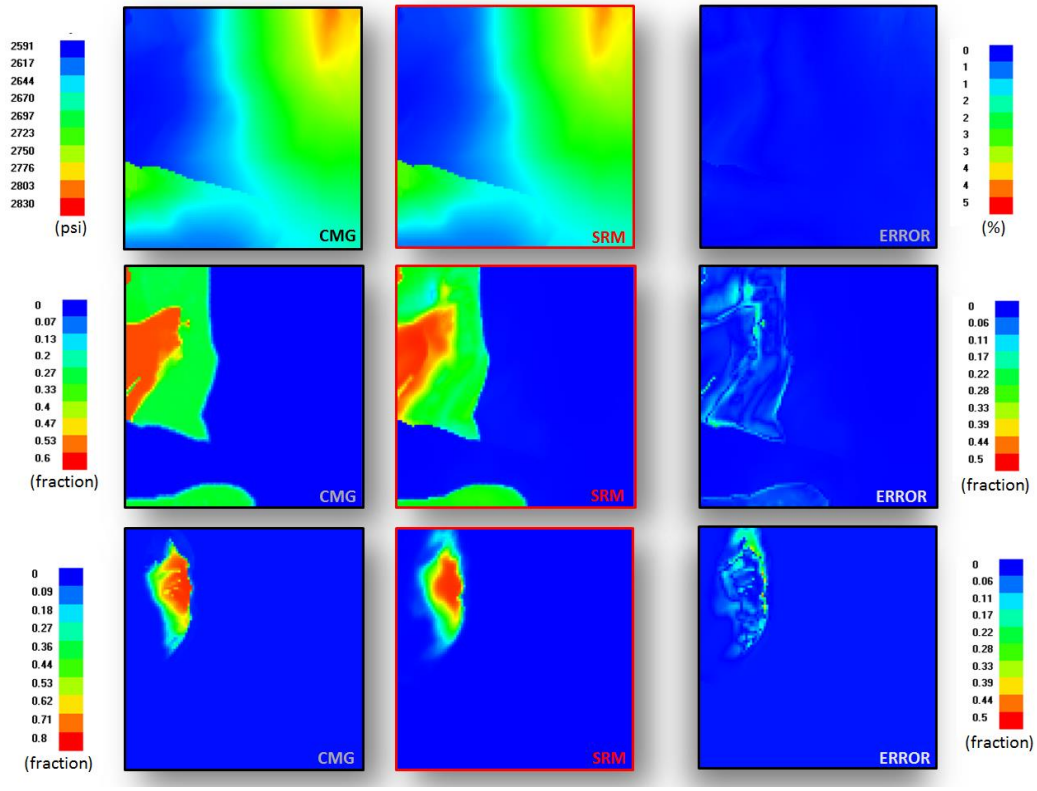

Figure 117. Distribution maps of Pressure, Gas saturation and CO_2 mole fraction in layer 4 of the reservoir (from left: CMG output, SRM result and Error) - Training Case- 24 Months after injection

C-2.7. Layer 2-Blind Case-24 Months of Injection

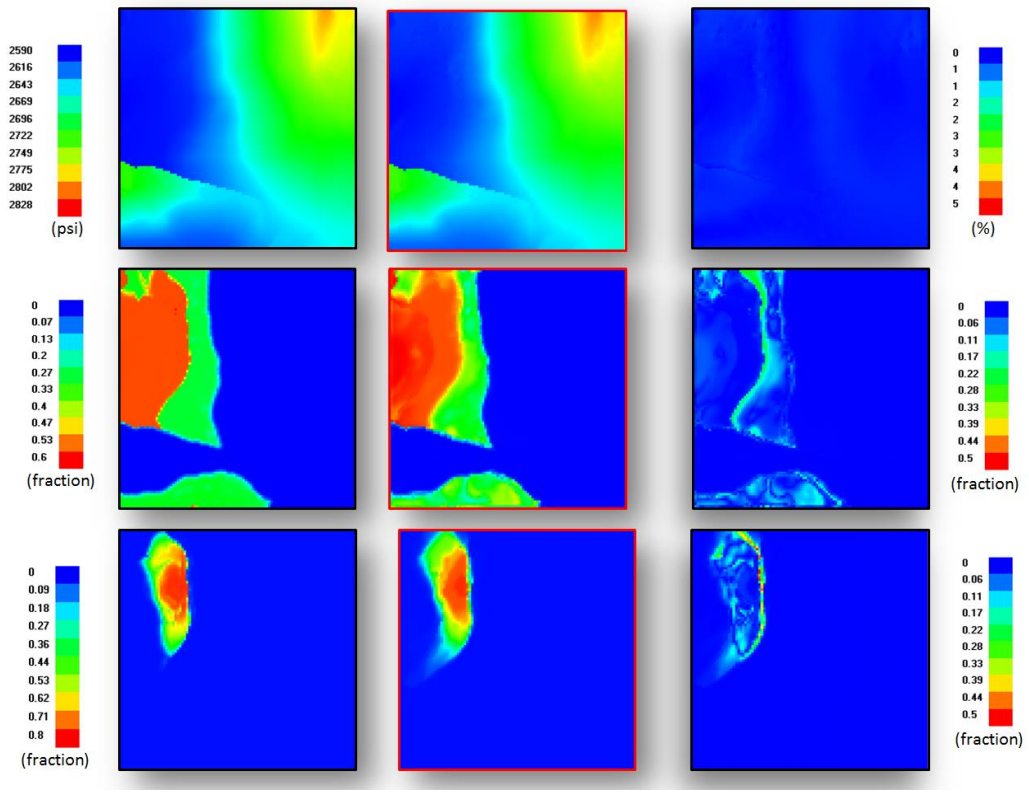

Figure 118. Distribution maps of Pressure, Gas saturation and CO_2 mole fraction in layer 2 of the reservoir (from left: CMG output, SRM result and Error) - Blind Case- 16 Months after injection

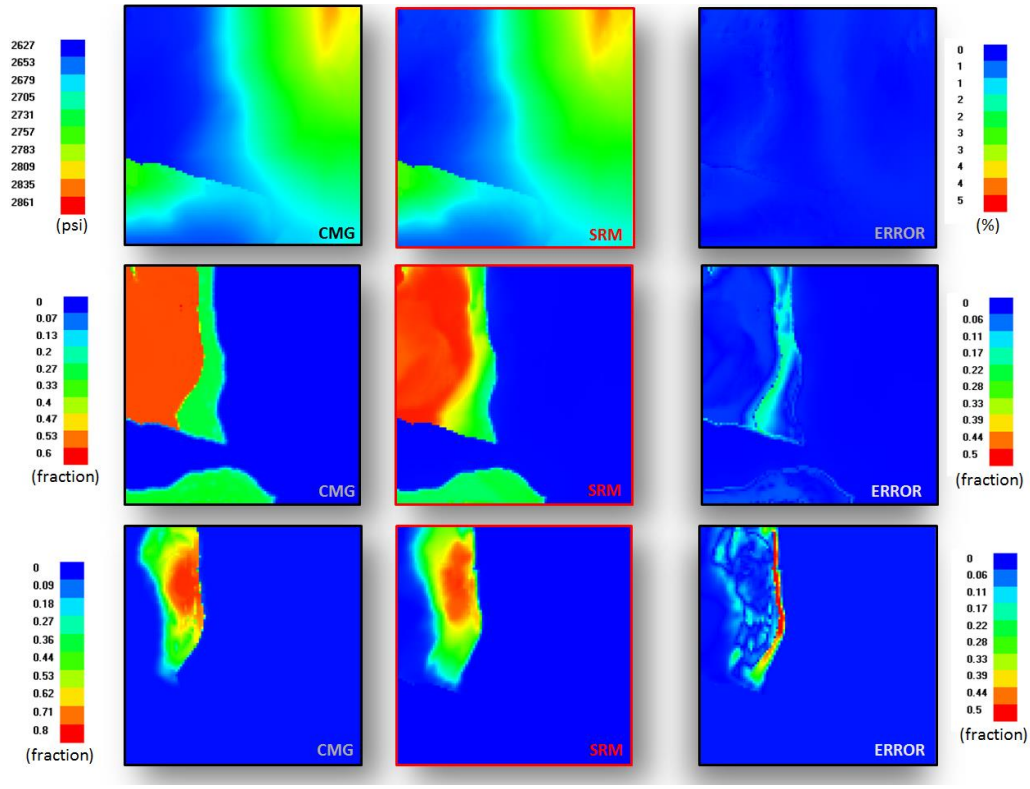

Figure 119. Distribution maps of Pressure, Gas saturation and CO_2 mole fraction in layer 2 of the reservoir (from left: CMG output, SRM result and Error) - Blind Case- 24 Months after injection

C-2.8. Layer 4- Blind Case-24 Months of Injection

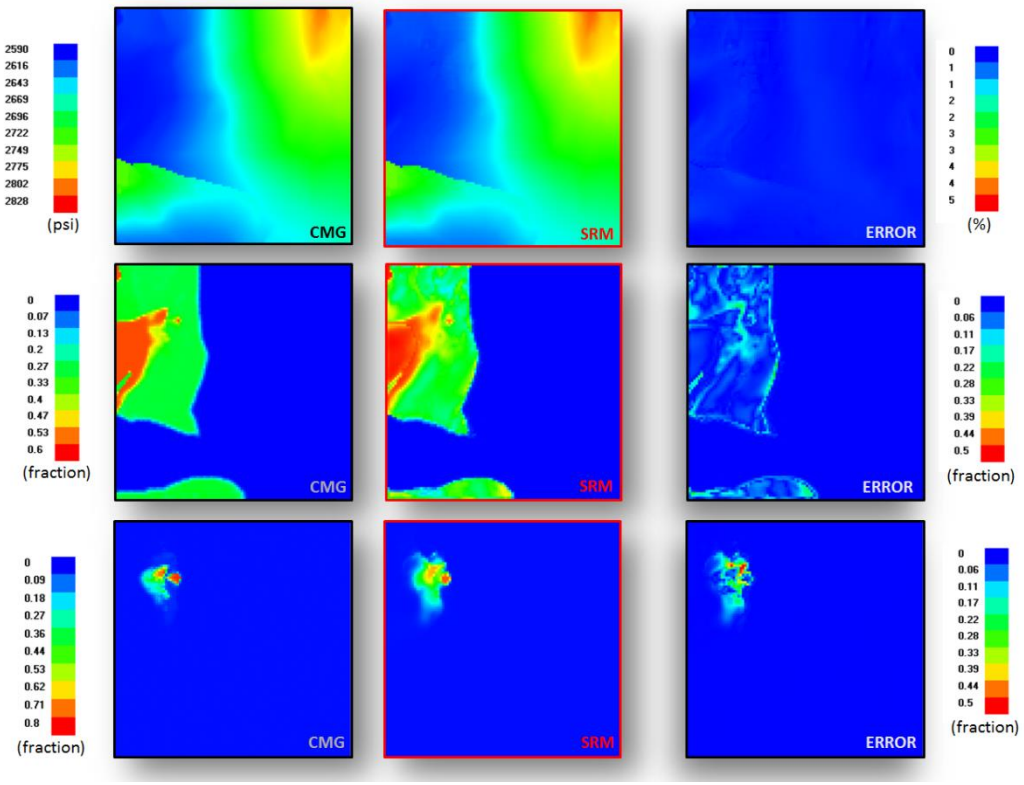

Figure 120. Distribution maps of Pressure, Gas saturation and CO_2 mole fraction in layer 4 of the reservoir (from left: CMG output, SRM result and Error) - Blind Case- 16 Months after injection

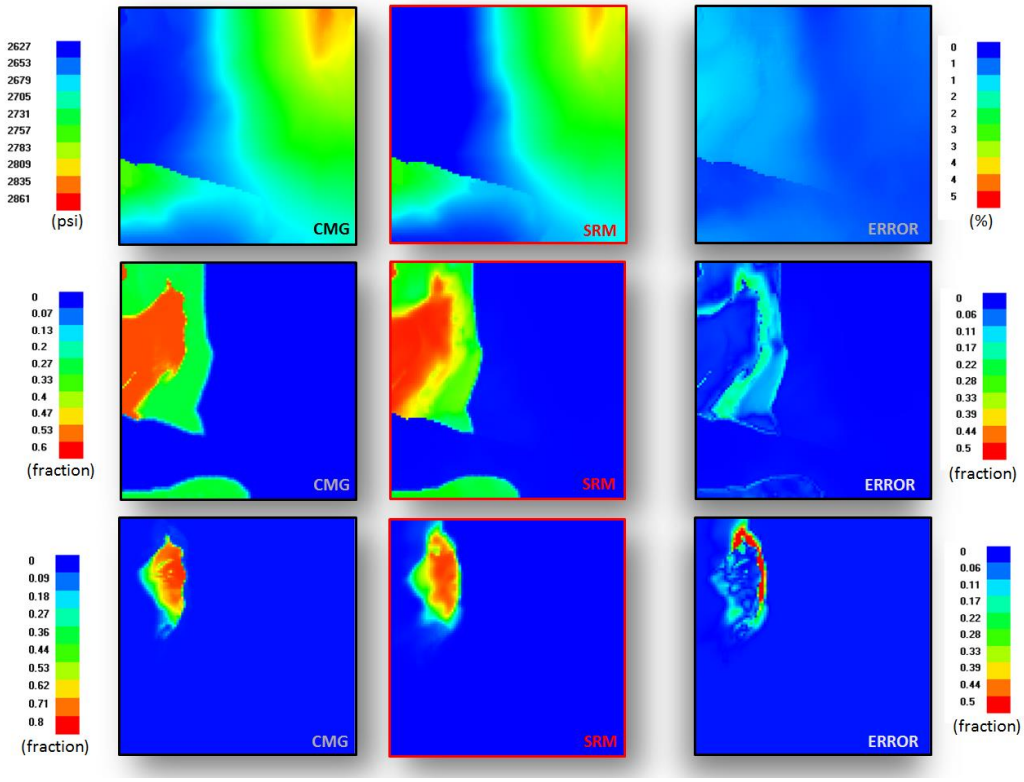

Figure 121. Distribution maps of Pressure, Gas saturation and CO_2 mole fraction in layer 4 of the reservoir (from left: CMG output, SRM result and Error) - Blind Case- 24 Months after injection

Bibliography

Ahmed, Syed Jawwad, Reda Recham, Ali Nozari, Shamsudin Bughio, Ralf Schulze-Riegert, and Ryadh Ben Salem. "Uncertainty Quantification Workflow for Mature Oil Fields: Combining Experimental Design Techniques and Different Response Surface Models." *SPE Middle East Oil and Gas Show and Conference.* Manama, Bahrain, 2013.

Al Salhi, Mohamed Said, Michiel F.J. Van Rijen, Harm Dijk, and Lingli Wei. "Structured Uncertainty Assessment for Fahud Field through the Application of Experimental Design and Response Surface Methods." *SPE Middle East Oil and Gas Show and Conference.* Bahrain, 2005.

Alajmi, M., and T. Ertekin. "Development of an Artificial Neural Network as a Pressure Transient Analysis." *SPE Asia Pacific Oil & Gas Conference.* Jakarta: SPE, 2007.

Al-Kaabi, Abdul-Aziz U., and John W. Lee. "Using Artificial Neural Networks To Identify the Well Test Interpretation Model." *SPE Formation Evaluation* (Society of Petroleum Engineers) 8, no. 3 (1993).

Amini, Shohreh, Shahab Mohaghegh, Razi Gaskari, and Grant Bromhal . "Uncertainty Analysis of a CO2 Sequestration Project Using Surrogate." *SPE Western North American Regional Meeting.* Bakersfield, California: SPE, 2012.

Astrid, P. *Reduction of Process Simulation Models: A Proper Orthogonal Decomposition Approach.* PhD thesis, Eindhoven University of Technology, 2004.

Azad, A., and R. j. Chalaturnyk. "A Mathematical Improvement to SAGD using Geomechanical Modeling." (Journal of Canadian Petroleum Technology) 2010.

Azad, Ali, Rick J. Chalaturnyk, and Sahar Movaghati. "Reservoir Characterization: Application of Extended Kalman Filter and Analytical Physics-Based Proxy Models in Thermal Recovery." *International Association for Mathematical Geosciences.* 2011.

Aziz, K., and A. Settari. *Fundamentals of Reservoir Simulation.* Elsevier Applied Science Publishers, 1986.

Aziz, Khalid, and Antonin Settari. *Petroleum reservoir simulation.* Applied Science Publishers, 1979.

Bachu, Stefan. "Sequestration of CO2 in geological media: criteria and approach for site selection in response to climate change." *Energy Conversion and Management*, 2000: 953-970.

Basu, J. K., D. Bhattacharyya, and T. Kim. "Use of Artificial Neural Network in Pattern Recognition." *International Journal of Software Engineering and Its Applications* 4 (2010).

Bazargan, Hamid, and Mike Christie. "Efficient Polynomial Chaos Proxy-based History Matching and Uncertainty Quantification for Complex Geological Structures." *SPE Kuwait International Petroleum Conference and Exhibition.* Kuwait City, 2012.

Bishop, C. M. "Pattern recognition and machine learning." (Springer) 2006.

Bishop, Christopher M. *Neural Network for Pattern Recognition.* Clarendon Press, 1995.

Butler, R. M. "A New Approach to the Modeling of Steam-Assisted Gravity Drainage." (Journal of Canadian Petroleum Technology (JCPT)) 1987.

Butler, R. M., and I. J. Mokrys. "Solvent Analog Model of Steam Assisted Gravity Drainage." (AOSTRA Journal of Research) 5 (1989).

Cardoso, M. a. *Development and Application of Reduced-Order Modeling Procedures for Reservoir Simulation.* PhD Dissertation, Stanford University , 2009.

Cardoso, M. A., and L. J. Durlofsky. "Linearized Reduced-Order Models for Subsurface Flow Simulation." (Journal of Computational Physics) 2010.

Cardoso, Marco Antonio. "Development And Application Of Reduced-Order Modeling Procedures For Reservoir Simulation." *PhD Dissertation.* Stanford University, 2009.

Carreras, Patricia Elva , Scott Edward Turner, and Gwendolyn Tharp Wilkinson. "Tahiti: Development Strategy Assessment Using Design of Experiments and Response Surface Methods." *SPE Western Regional.* Anchorage, Alaska, 2006.

Chen, Han, Hector Klie, and Qiqi Wang. "A Black-Box Stencil Interpolation Method to Accelerate Reservoir Simulations." *SPE Reservoir Simulation Symposium.* Woodlands, Texas, USA, 2013.

Chu, C. "Prediction of steamflood performance in heavy oil reservoirs using correlations developed by factorial design method." *Proceedings of the 60th SPE California Regional Meeting.* Ventura, California: SPE, 1990.

CSIRO . *Carbon storage trial set to go.* Month 12, 2008. http://www.sciencealert.com.au/features/20081303-17040.html.

Damsleth, E., A. Hage, and R. Volden. "Maximum information at minimum cost: a North Sea field development study with an experimental design." *Journal of Petroleum Technology* (SPE), 1992: 1350-1356.

Dancea, T., L. Spencera, and J. Xua. "What a difference a well makes." *International Conference on Greenhouse Gas Control Technologies (GHGT-9).* Washington DC, 2008.

Eldred, S. E., and J. Burkardt. "Comparison of non-intrusive polynomial chaos and stochastic collocation methods for uncertainty quantification." *47th AIAA Aerospace Sciences Meeting.* Orlando, FL, 2009.

Esmaili, Soodabeh. "Production History Matching and Forecasting of Shale Assets Using Pattern Recognition." 2013.

Fetel, Emmanuel, and Guillaume Caumon. "Reservoir flow uncertainty assessment using response surface constrained by secondary information." *Journal of Petroleum Science and Engineering* (Elsevier) 60, no. 3-4 (2007).

Forrester, Alexander I. J., Andras Sobester, and Andy Keane. *Engineering Design Via Surrogate Modelling: A practical guide.* Wiley, 2008.

Gildin, Eduardo, Mohammadreza Ghasemi, Anastasiya Protasov, and Yalchin Efendiev. "Nonlinear Complexity Reduction for Fast Simulation of Flow in Heterogeneous Porous Media." *SPE Reservoir Simulation Symposium.* Woodlands: Texas, 2013.

Gorucu, F., et al. "A Neurosimulation Tool for Predicting Performance in Enhanced Coalbed Methane and CO2 Sequestration Project." *SPE Annual TEchnical Conference.* Dallas, Texas: SPE, 2005.

Gratton, D., and K. Willcox. "Reduced order trajectory piecewise-linear models for nonlinear computational fluid dynamics." *34th AIAA Fluid Dynamics Conference and Exhibit.* Portland, 2004.

He, Jincong. *Enhanced Linearized Reduced-order Models For Subsurface Flow Simulation.* PhD Dissertation, Stanford University, 2010.

He, Jincong, and Louis J. Durlofsky. "Reduced-Order Modeling for Compositional Simulation by use of Trajectory Piecewise Linearization." *SPE Journal* (Society of Petroleum engineering), 2014.

Heijn, T., R. Markovinovic, and J. D. Jansen. "Generation of Low-Order Reservoir Models Using System-Theoretical Concepts." *Computational Geosciences* 10, no. 1 (2006): 137-158.

Heijn, T., R. Markovinovic, and J. D. Jansen. "Generation of low-order reservoir models using system-theoretical concepts." *SPE Journal* (Society of Petroleum Engineers) 9, no. 2 (2004).

Hejin, T., R. Markovinovic, and J. Jansen. "Generation of Low-Order Reservoir Models Using System-Theoretical Concepts." *SPE Reservoir Simulation Symposium.* Houston, Texas, 2003.

Holdaway, Keith . *Harness Oil and Gas Big Data with Analytics: Optimize Exploration and Production with Data Driven Models.* Wiley, 2014.

Holmes, P., J. L. Lumley, and G. Berkooz. *Turbulence, Coherent Structures, Dynamical Systems and Symmetry.* Cambridge University Press, 1996.

Jansen, J. D., and R. Markovinovic. "System Analysis for Reservoir Management." *Delft University of Technology Lecture Note.* 2004.

Kaldi, J. G., and C. M. Gibson-Poole. *Storage Capacity Estimation, Site Selection and Characterisation for CO2 Storage Projects.* CO2CRC, 2008.

Klie, Hector. "Unlocking Fast Reservoir Predictions via Non-Intrusive Reduced Order Models." *SPE Reservoir Simulation Symposium.* Woodlands, Texas, 2013.

Lumley, J. L. "Atmospheric turbulence and radio wave propagation." *Journal of computational Chemistry* 13, no. 23 (1967).

Ly, H. V., and H. T. Tran. "Modeling and control of physical processes using proper orthogonal decomposition." *Mathematical and Computer Modeling* 33 (2001): 223-236.

Markovinovic, R. *System-Theoretical Model Reduction for Reservoir Simulation and Optimization.* PhD thesis, Delft University of Technology, 2009.

Markovinovic, R., and J. D. Jansen. "Accelerating iterative solution methods using reduced-order models as solution predictors ." (International Journal for Numerical Methods in Engineering) 68, no. 5 (2006).

McCulloch, W. S., and W. Pitts. "A logical calculus of the ideas immament in nervous activity ." *Bulletin of Mathematical Biophysics.* Vol. 5. Reprinted in Anderson and Rosenfeld, 1988.

Mohaghegh, S. D. "Quantifying Uncertainties Associated with Reservoir Simulation Studies Using Surrogate Reservoir Models." *SPE Annual Conference & Exhibition.* San Antonio, Texas: SPE, 2006.

Mohaghegh, S., R. Arefi, and S. Ameri. "Petroleum Reservoir Characterization with the Aid of Artificial Neural Network." *Journal of Petroleum Science and Engineering*, 1996.

Mohaghegh, S., S. Ameri, and R. Arefi. "Virtual Measurement of Heterogeneous Formation Premeability Using Geophysical Well Log Responses." *Log Analyst*, 1996.

Mohaghegh, Shahab D. "Virtual-Intelligence Applications in Petroleum Engineering: Part 1-Artificial Neural Networks." *Journal of Petroleum Technology* (Society of Petroleum Engineers) 52, no. 9 (2000).

Mohaghegh, Shahab D., Abi Modavi, Hafez Hafez , Masoud Haajizadeh, and Srikant Guruswamy. "Development of Surrogate Reservoir Model (SRM) for fast track analysis of a complex reservoir." (Inderscience Publishers) 2009.

Mohaghegh, Shahab. "Reservoir Simulation and Modeling Based on Pattern Recognition." *SPE Digital Energy Conference and Exhibition.* Woodlands, Texas: Society of Petroleum Engineers, 2011.

Mohaghegh, Shahab. "Virtual-Intelligence Applications in Petroleum Engineering: Part 2-Evolutionary Computing." *JPT* (Society of Petroleum Engineers), 2000.

Mohaghegh, Shahab, Reza Arefi, Ilkin Bilgesu, Sam Ameri, and Deanna Rose. "Design and Development of an Artificial Neural Network for Estimation of Formation Permeability." *SPE Computer Applications* (SPE) 7, no. 6 (1995).

Montgomery, Douglas C. *Design and Analysis of Experiments: Response surface method and designs.* New Jerse: John Wiley and Sons, Inc., 2005.

Narayanan, K., C. D. White, J. W. Lake, and B. J. Willis. "Response Surface Methods for Upscaling Heterogeneous Geologic Models." *SPE Reservoir Simulation Symposium.* Houston, Texas, 1999.

Nikravesh, M., A. R. Kovscek, and T. W. Patzek. "Prediction of Formation Damage During Fluid Injection Into Fractured Low-Permeability Reservoirs via Neural Networks." Lafayette, Louisiana: SPE Formation Damage Symposium, 1996.

Oladyshkin, S., H. Class, R. Helmig, and W. Nowak. "An integrative approach to robust design and probabilistic risk assessment for storage in geological formations." *Computational Geoscience* 15 (2011).

Poole, David, Alan Mackworth, and Randy Goebel. *Computational Intelligence: Alogical Approach.* New York: Oxford University Press, 1998.

Purwar, S., C. J. Jablonowski, and Q. P. Nguyen. "A Method for Integrating Response Surfaces into Optimization Models with." *SPE Hydrocarbon Economics and Evaluation Symposium.* Dallas, Texas, 2010.

Reid, Stuart Gordon. *http://www.stuartreid.co.za/misconceptions-about-neural-networks/.* May 8, 2014. (accessed 2014).

Rewienski, M., and J. White. "A trajectory piecewise-linear approach to model order reduction and fast simulation of nonlinear circuits and micromachined devices." *Transactions on Computer-Aided Design of Integrated Circuits and Systems* (IEEE) 22, no. 2 (2003): 155–170.

Rousset, Matthieu A. H., Chung K. Huang, Hector Klie, and Louis J. Durlofsky. "Reduced-order modeling for thermal recovery processes." (Computational Geosciences) 18, no. 3-4 (2013).

Rousset, Matthieu. *Reduced-order Modeling for Thermal Simulation.* PhD Dissertation, Stanford University, 2010.

Russell, Stuart J., and Peter Norvig. *Artificial intelligence: a modern approach.* 2nd. Pearson Education, 2003.

Shahkarami, Alireza. "Assisted History Matching Using Pattern Recognition Technology." 2014.

Shi, Jindong, and Juliana Y. Leung. "Physics-Based Proxy for Vapex Process Modeling in Heterogeneous Reservoirs." *SPE Heavy Oil Conference Canada.* Calgary, 2013.

Sirovich, L. "Turbulence and the Dynamics of Coherent Structures." *Quarterly of applied mathematics* 45, no. 3 (1987): 561-571.

Slotte, Per Arne, and Eivind Smorgrav. "Response Surface Methodology Approach for History Matching and Uncertainty Assessment of Reservoir Simulation Models." *Europec/EAGE Conference and Exhibition.* Rome, Italy, 2008.

Van Doren, J., R. Markovinovic, and J. Jansen. "Use of POD in Control of Flow Through Porous Media." *European Conference on Computational Fluid Dynamics.* 2006.

Vanegas, Walter J., Clayton V. Deutsch, and Luciane B. Cunha. "Uncertainty Assessment of SAGD Performance Using a Proxy Model Based on Butler's Theory." *SPE Annual Technical Conference and Exhibition.* Denver, 2008.

Vermeulen, P. T. M., A. W. Heemink, and C. B. M. Te Stroet. "Reduced models for linear ground water flow models using empirical orthogonal function." (Advances in Water Resources) 27, no. 1 (n.d.).

Vermeulen, P. T. M., A. W. Heemink, and C. B. M. Te Stroet. "Reduced models for linear ground water flow models using empirical orthogonal function." (Advances in Water Resources) 27, no. 1 (2004).

Webster, M., and A. M. Tatang. *Application of the probabilistic collocation method for an uncertainty analysis of a simple ocean model.* MIT Joint Program on the Science and Policy of Global Change, 1996.

Wilson, K. C., and L. J. Durlofsky. "Computational Optimization of Shale Resource Development using Reduced-Physics Surrogate Models." *SPE Western Regional Meeting.* Bakersfield, California: Society of Petroleum Engineers, 2012.

Wilson, Kurt Caylor. *Optimization of Shale Resource Development using Reduced-Physics Surrogate Model.* Master Thesis, Stanford University, 2012.

Yeten, B., A. Castellini, B. Guyaguler, and H. W. Chen. "A comparison study on experimental design and response surface methodology." *Proceedings of the 2005 SPE Reservoir SimulationSymposium.* Houston: SPE, 2005.

Yeten, B., A. Castellini, B. Guyaguler, and W. H. Chen. "A Comparison Study on Experimental Design and Response Surface Methodologies." *SPE Reservoir Simulation Symposium.* The woodlands: SPE, 2005.

Zhang, Yan, and Nikolaos V. Sahinidis. "Uncertainty Quantification in CO2 Sequestration Using Surrogate Models from Polynomial Chaos Expansion." *Industrial & Engineering Chemistry Research* (ACS Publications) 52, no. 9 (2012).

Zhang, Yingqi, and George Pau. *Reduced-Order Model Development for CO2 Storage in Brine Reservoirs.* Berkeley, CA: Earth Sciences Division, Lawrence Berkeley National Lab, Technical Report Series, 2012.